







UNIFORMED SERVICES UNIVERSITY OF THE HEALTH SCIENCES  
F. EDWARD HÉBERT SCHOOL OF MEDICINE  
4301 JONES BRIDGE ROAD  
BETHESDA, MARYLAND 20814-4799



GRADUATE EDUCATION

APPROVAL SHEET

TEACHING HOSPITALS  
WALTER REED ARMY MEDICAL CENTER  
NAVAL HOSPITAL, BETHESDA  
MALCOLM GROW AIR FORCE MEDICAL CENTER  
WILFORD HALL AIR FORCE MEDICAL CENTER

Title of Dissertation: "The Effect of Cholesterol on the Binding  
and Insertion of Cytochrome  $b_5$  into  
Liposomes of Phosphatidylcholines"

Name of Candidate: Kenneth M.P. Taylor  
Doctor of Philosophy Degree  
September 30, 1993

Dissertation and Abstract Approved:

H. M. Heine  
Committee Chairperson

9/30/93  
Date

Mark A. Voreman  
Committee Member

9/30/93  
Date

Eva Beck  
Committee Member

9/30/93  
Date

Michael S. Paruty  
Committee Member

9/30/93  
Date



The author hereby certifies that the use of any copyrighted material in the dissertation manuscript entitled:

"The Effect of Cholesterol on the Binding and Insertion of  
Cytochrome  $b_5$  into Liposomes of Phosphatidylcholines"

beyond brief excerpts is with the permission of the copyright owner, and will save and hold harmless the Uniformed Services University of the Health Sciences from any damage which may arise from such copyright violations.

A handwritten signature in black ink, reading "Kenneth M. P. Taylor". The signature is written in a cursive style with a large, sweeping initial 'K' and a long, trailing flourish at the end.

Kenneth M. P. Taylor  
Department of Biochemistry  
Uniformed Services University  
of the Health Sciences



## ABSTRACT

Title of Dissertation: The Effect of Cholesterol on the Binding and Insertion of Cytochrome  $b_5$  into Liposomes of Phosphatidylcholines.

Kenneth Michael-Paul Taylor, Doctor of Philosophy, 1993.

Dissertation directed by: Mark A. Roseman, Ph.D.

Associate Professor

Department of Biochemistry

Cholesterol regulates the physical properties of lipid bilayers. But despite its extensively characterized effects on phospholipid motional freedom, surface areas, and phase transitions, the effect of cholesterol on protein solubility in lipid bilayers has not been established. To examine if cholesterol affects the solvent properties of lipid bilayers with respect to integral membrane proteins, the spontaneous binding and insertion of cytochrome  $b_5$  (cyt  $b_5$ ) into phosphatidylcholine liposomes containing cholesterol has been investigated as an archetypical system for lipid-protein interactions. The results indicate that:

(1) The cyt  $b_5$  saturation levels of small unilamellar vesicles (SUVs) are significantly greater than those of large unilamellar vesicles (LUVs). The saturation limits of LUVs are so low that there appear to be many vacant sites for the binding of additional protein.

(2) The overall cyt  $b_5$  binding equilibrium with SUVs that are prepared from natural phospholipids mixtures is greater than that for SUVs of a single phospholipid component. Cyt  $b_5$  has a lower affinity for SUVs



with a 1:1 phospholipid/cholesterol composition than for SUVs of pure phospholipids.

(3) The cyt  $b_5$ /surface area ratio decreases in cholesterol-containing bilayers, indicating that cholesterol reduces cyt  $b_5$  binding to all liposomes. The extent of inhibition significantly increases with phospholipid condensibility.

(4) Cholesterol inhibition is significantly more pronounced in LUVs than in SUVs.

(5) Within the 0-50 mole percent range of cholesterol compositions, the saturation level of cyt  $b_5$  binding to POPC LUVs as a function of cholesterol concentration appears triphasic, similar to a titration curve, with inflection points at 20 and 33 mole percent cholesterol.

(6) The rate of cyt  $b_5$  tight insertion is maximal at 20-25% percent cholesterol.

The results can be explained by assuming that cyt  $b_5$  binding to liposomes depends upon phospholipid motional freedom. Cholesterol inhibits cyt  $b_5$  binding by restricting phospholipids from forming complimentary annuli. The inhibitory effect correlates with reductions in bilayer free volume, suggesting that cholesterol reduces the solvent efficacy of lipid bilayers by synergistic interactions with phospholipids. At low compositions, cholesterol facilitates tight insertion because of defective molecular packing. Accordingly, cholesterol may regulate the protein/lipid composition and protein lateral organization in biological membranes.



THE EFFECT OF CHOLESTEROL ON THE BINDING AND INSERTION OF  
CYTOCHROME  $b_5$  INTO LIPOSOMES OF PHOSPHATIDYLCHOLINES

By

Kenneth Michael-Paul Taylor

Dissertation submitted to the Faculty of the  
Department of Biochemistry Graduate Program  
of the Uniformed Services University of  
the Health Sciences  
in partial fulfillment of the requirements  
for the degree of  
Doctor of Philosophy, 1993



DEDICATION

To

my Mother, Father and Sister

...for their encouragement and for persisting with me through  
a very long process.

## ACKNOWLEDGEMENTS

Dr. Mark A. Roseman: I wish to express my sincerest appreciation for your expert and positive guidance and assistance throughout the course of this research. I have not only had a competent mentor who has taught me scientific excellence and competitiveness which I hope to emulate throughout my professional career; but it has been my good fortune to also have a friend. Thank you for taking a personal interest in me. Your patience with my approach to completing this project not only enabled me to develop independent scholarship, but also gave me an optimistic outlook when times were less than optimal. I will miss the many conversations that we have shared...scientific and otherwise.

Dr. Andrew M. Holmes: Thank you for serving on my committee. Only an enthusiastic biochemist as yourself could effectively contribute to the scientific quality of research that is remote from your own general interests. Your critical suggestions of the initial set of experiments provided me with direction for completing this research. I am also grateful for the opportunity to have taught with you during the 1988 Medical Biochemistry Course.

Dr. Troy J. Beeler: I wish to thank you for serving on my committee. I have always respected your incisive, practical intellect, which has improved the quality of this manuscript.

Dr. Muriel S. Prouty: Thank you for setting aside time to serve on my committee. Your expertise in cytochrome  $b_5$  chemistry and suggestions have been most helpful and appreciated.

Dr. Robert W. Williams: I wish to thank you for the opportunity to do a rotation in your laboratory and the many hours of expertise that you shared with me concerning Raman Spectroscopy. I enjoyed those very late evenings during the Summer of 1988, when you worked side by side with me, teaching me everything from operating a sophisticated Raman instrument to the analysis and interpretation of the obtained spectra. I am privileged to share a manuscript with you.

Mrs. Susan F. Greenhut: I sincerely thank you for providing me with expert technical assistance when I was first learning how to prepare liposomes according to various procedures. You definitely provided me with a solid foundation to understanding the operations of Dr. Roseman's laboratory, which eventually enabled me to pursue this research. Most importantly, I thank you for your unconditional friendship and support. I am grateful for the opportunity to publish a manuscript with you and Dr. Roseman.

Mr. Kenneth Gable: I thank you for your willingness to always provide me with technical advice during the course of this project.



## CONTENTS

Approval Sheet . . . . .	i
Copyright Statement . . . . .	ii
Abstract . . . . .	iii
Title Page . . . . .	v
Dedication . . . . .	vi
Acknowledgements . . . . .	vii
Contents . . . . .	viii
Abbreviations . . . . .	x
List of Figures . . . . .	xiii
List of Tables . . . . .	xvii
Introduction . . . . .	1
A. Effect of cholesterol on the segmental motion of phospholipids . . . . .	16
B. Cholesterol Affects Membrane Permeability . . . . .	17
C. Cholesterol "decreases" phospholipid surface areas: The Condensing Effect . . . . .	18
D. Cholesterol reduces the cooperative phase transitions of phospholipids . . . . .	20
E. Structural requirements for modulating the physical properties of membranes . . . . .	24
F. Models of cholesterol/phospholipid interactions . . . . .	24
G. Effect of cholesterol on membrane proteins . . . . .	33
Experimental Procedures . . . . .	63
A. Materials . . . . .	63
B. Buffer Solutions . . . . .	63
C. Preparation of Large Unilamellar Vesicles (LUVs) . . . . .	64
D. Preparation of Small Unilamellar Vesicles (SUVs) . . . . .	64
E. Determination of Outside to Inside Lipid Mass Ratios of Reverse-phase Liposomes . . . . .	65
F. Cytochrome $b_5$ Saturation of Large Unilamellar Vesicles . . . . .	66
G. Cytochrome $b_5$ Saturation of Small Unilamellar Vesicles . . . . .	67
H. Analysis of Cytochrome $b_5$ Binding Isotherms . . . . .	68
I. Cytochrome $b_5$ Binding Affinity for Reverse-phase Liposomes Containing Cholesterol . . . . .	73
J. Transfer Studies of Cytochrome $b_5$ between Liposome Populations . . . . .	74
Results . . . . .	75

A. Characterization of Reverse-phase Liposomes . . . . .	75
B. The Effect of Cholesterol on the Binding of Cytochrome $b_5$ to Large Reverse-phase Liposomes of Various Phosphatidylcholines . . . . .	82
C. Effect of Cholesterol on the Binding of Cytochrome $b_5$ to Small Unilamellar Vesicles (SUVs) prepared from various Phosphatidylcholines . . . . .	97
D. Cytochrome $b_5$ binding and insertion into 1-palmitoyl-2- oleoyl- <i>sn</i> -glycero-3-phosphorylcholine LUVs . . . . .	176
(A.) Effect of cholesterol on cytochrome $b_5$ binding to POPC LUVs . . . . .	176
(B.) Effect of cholesterol on the tight insertion of cytochrome $b_5$ . . . . .	210
E. Effect of cytochrome $b_5$ tight insertion on the saturation level of liposomes . . . . .	232
Discussion . . . . .	234
References . . . . .	260

## ABBREVIATIONS

DLPC;	1,2-dilinoleoyl- <i>sn</i> -glycero-3-phosphorylcholine
DMPC;	1,2-dimyristoyl- <i>sn</i> -glycero-3-phosphorylcholine
DPPC;	1,2-dipalmitoyl- <i>sn</i> -glycero-3-phosphorylcholine
DSPC;	1,2-stearoyl- <i>sn</i> -glycero-3-phosphorylcholine
DOPC;	1,2-dioleoyl- <i>sn</i> -glycero-3-phosphorylcholine
OSPC;	1-oleoyl-2-stearoyl- <i>sn</i> -glycero-3-phosphorylcholine
PLPC;	1-palmitoyl-2-linoleoyl- <i>sn</i> -glycero-3-phosphorylcholine
POPC;	1-palmitoyl-2-oleoyl- <i>sn</i> -glycero-3-phosphorylcholine
SLPC;	1-stearoyl-2-linoleoyl- <i>sn</i> -glycero-3-phosphorylcholine
SOPC;	1-stearoyl-2-oleoyl- <i>sn</i> -glycero-3-phosphorylcholine
egg PC;	egg L- $\alpha$ -phosphatidylcholine
liver PC;	bovine liver L- $\alpha$ -phosphatidylcholine
SPH;	bovine brain sphingomyelin
egg PE	egg phosphatidylethanolamine (Transphosphatidylated egg PC)
PC;	phosphatidylcholine (lecithin)
[ <sup>14</sup> C]-POPC;	L- $\alpha$ -1-palmitoyl-2-oleoyl-[oleoyl-1- <sup>14</sup> C] phosphatidylcholine
[ <sup>3</sup> H]-triolein;	[9,10- <sup>3</sup> H(N)] triolein
cyt b <sub>5</sub> ;	cytochrome b <sub>5</sub>



LUV;	large unilamellar vesicle
SUV;	small unilamellar vesicle
Bicine;	N,N-bis[2-hydroxyethyl]-glycine
EDTA;	ethylenediaminetetraacetic acid
NaCl;	sodium chloride
TNBS;	2,4,6-trinitrobenzenesulfonic acid
Tris;	Tris(hydroxymethyl)aminomethane
$C_A$ ;	concentration of unbound ligand
$C_i$ ;	curie
CPK;	Cory-Pauling-Koltun
dpm;	disintegrations per minute
$f_v$ ;	free volume
$h$ ;	hour(s)
$K_{eff}$ ;	effective binding constant
$K_{(c+p)}$ ;	effective binding constant corrected for total effective lipid
min;	minute(s)
$n$ ;	minimum phospholipid molecules constituting a ligand adsorption site
PL;	phospholipid
$r$ ;	$[\text{bound cyt } b_5]/[\text{phospholipid}]$
rpm;	revolutions per minute
$z$ ;	coordination number
$\alpha$ ;	alpha; excluded area factor
$\beta$ ;	beta

$\gamma$ ;        gamma; general ligand shape factor  
 $\Delta$ ;        delta; *cis* carbon-carbon double bond  
 $\eta$ ;        eta; cooperativity parameter  
 $\lambda$ ;        lambda; binding lattice geometry factor  
 $\phi$ ;        phi; cholesterol inhibitory parameter

## LIST OF FIGURES

1. Chemical Structure of Phospholipids . . . . .	2
2. Chemical Structures of Common Sterols . . . . .	5
3. Chemical Structure of Cholesterol . . . . .	8
4. Corey-Pauling-Koltun Model of Cholesterol . . . . .	10
5. Corey-Pauling-Koltun Model of Cholesterol . . . . .	12
6. Interaction of cholesterol with phospholipids . . . . .	14
7. Structure of Cytochrome $b_5$ . . . . .	49
8. Cytochrome $b_5$ Binding to Preformed Liposomes . . . . .	52
9. Loose Binding of Cytochrome $b_5$ . . . . .	54
10. Tight Binding of Cytochrome $b_5$ . . . . .	56
11. Model of stretched hexagonal lattice for cytochrome $b_5$ adsorption to liposome surfaces . . . . .	71
12. External:Total PE Determination by Trinitrophenylation for POPC reverse-phase liposomes; 0% cholesterol . . . . .	76
13. External:Total PE Determination by Trinitrophenylation for POPC reverse-phase liposomes; 50% cholesterol . . . . .	78
14. Effect of cholesterol on the saturation level of cytochrome $b_5$ binding to DMPC LUVs . . . . .	83
15. Effect of cholesterol on the saturation level of cytochrome $b_5$ binding to DOPC LUVs . . . . .	85
16. Effect of cholesterol on the saturation level of cytochrome $b_5$ binding to DLPC LUVs . . . . .	87
17. Effect of cholesterol on the saturation level of cytochrome $b_5$ binding to POPC LUVs . . . . .	89
18. Effect of cholesterol on the saturation level of cytochrome $b_5$ binding to PLPC LUVs . . . . .	91
19. Effect of cholesterol on the saturation level of cytochrome $b_5$ binding to egg PC LUVs . . . . .	93
20. Fluorescence of cytochrome $b_5$ . . . . .	99
21. Treatment of cytochrome $b_5$ fluorescence spectra . . . . .	101



22. Cytochrome $b_5$ binding to egg PC SUVs; 0% cholesterol . . . . .	106
23. Cytochrome $b_5$ binding to bovine liver PC/bovine brain SPH (1:1) SUVs; 0% cholesterol . . . . .	108
24. Cytochrome $b_5$ binding to egg PC SUVs; 50% cholesterol . . . . .	110
25. Cytochrome $b_5$ binding to bovine liver PC/bovine brain SPH (1:1) SUVs; 50% cholesterol . . . . .	112
26. Cytochrome $b_5$ binding to DMPC SUVs; 0% cholesterol . . . . .	114
27. Cytochrome $b_5$ binding to DMPC SUVs; 50% cholesterol . . . . .	116
28. Cytochrome $b_5$ binding to DOPC SUVs; 0% cholesterol . . . . .	118
29. Cytochrome $b_5$ binding to DOPC SUVs; 50% cholesterol . . . . .	120
30. Cytochrome $b_5$ binding to POPC SUVs; 0% cholesterol . . . . .	122
31. Cytochrome $b_5$ binding to POPC SUVs; 50% cholesterol . . . . .	124
32. Cytochrome $b_5$ binding to SOPC SUVs; 0% cholesterol . . . . .	126
33. Cytochrome $b_5$ binding to SOPC SUVs; 50% cholesterol . . . . .	128
34. Cytochrome $b_5$ binding to SLPC SUVs; 0% cholesterol . . . . .	130
35. Cytochrome $b_5$ binding to SLPC SUVs; 50% cholesterol . . . . .	132
36. Theoretical Scatchard plots for the adsorption of hexagonal ligands with different affinity constants . . . . .	136
37. Theoretical Scatchard plots for the adsorption of hexagonal ligands to membrane lattices of different sizes . . . . .	138
38. Theoretical Scatchard plots for the adsorption of hexagonal ligands exhibiting different cooperativities . . . . .	140
39. Scatchard plot of cytochrome $b_5$ binding to egg PC SUVs containing 50 mole percent cholesterol . . . . .	143
40. Scatchard plot of cytochrome $b_5$ binding to bovine liver PC/bovine brain SPH (1:1) SUVs containing 50 mole percent cholesterol .	145
41. Scatchard plot of cytochrome $b_5$ binding to DMPC SUVs . . . . .	147
42. Scatchard plot of cytochrome $b_5$ binding to DMPC SUVs containing 50 mole percent cholesterol . . . . .	149
43. Scatchard plot of cytochrome $b_5$ binding to DOPC SUVs . . . . .	151

44. Scatchard plot of cytochrome $b_5$ binding to DOPC SUVs containing 50 mole percent cholesterol . . . . .	153
45. Scatchard plot of cytochrome $b_5$ binding to POPC SUVs . . . . .	155
46. Scatchard plot of cytochrome $b_5$ binding to POPC SUVs containing 50 mole percent cholesterol . . . . .	157
47. Scatchard plot of cytochrome $b_5$ binding to SOPC SUVs . . . . .	159
48. Scatchard plot of cytochrome $b_5$ binding to SOPC SUVs containing 50 mole percent cholesterol . . . . .	161
49. Scatchard plot of cytochrome $b_5$ binding to SLPC SUVs . . . . .	163
50. Scatchard plot of cytochrome $b_5$ binding to SLPC SUVs containing 50 mole percent cholesterol . . . . .	165
51. Cytochrome $b_5$ binding to POPC LUVs containing cholesterol . . . . .	178
52. Inhibition of cyt $b_5$ binding to POPC LUVs as a function of cholesterol mole percent . . . . .	180
53. Cytochrome $b_5$ binding to POPC LUVs; 0% cholesterol . . . . .	183
54. Cytochrome $b_5$ binding to POPC LUVs; 10% cholesterol . . . . .	185
55. Cytochrome $b_5$ binding to POPC LUVs; 20% cholesterol . . . . .	187
56. Cytochrome $b_5$ binding to POPC LUVs; 40% cholesterol . . . . .	189
57. Model of cytochrome $b_5$ binding lattice for POPC LUVs without cholesterol . . . . .	192
58. Model of cytochrome $b_5$ binding lattice for POPC LUVs with 10% cholesterol . . . . .	194
59. Model of cytochrome $b_5$ binding lattice for POPC LUVs with 20% cholesterol . . . . .	196
60. Model of cytochrome $b_5$ binding lattice for POPC LUVs with 40% cholesterol . . . . .	198
61. Scatchard plot of cytochrome $b_5$ binding to POPC LUVs; 0% cholesterol . . . . .	201
62. Scatchard plot of cytochrome $b_5$ binding to POPC LUVs; 10% cholesterol . . . . .	203
63. Scatchard plot of cytochrome $b_5$ binding to POPC LUVs; 20% cholesterol . . . . .	205

64. Scatchard plot of cytochrome $b_5$ binding to POPC LUVs; 40% cholesterol . . . . .	207
65. Cytochrome $b_5$ Transfer among donor POPC LUVs and acceptor POPC SUVs . . . . .	212
66. Cytochrome $b_5$ Transfer among donor POPC LUVs and acceptor POPC SUVs . . . . .	214
67. Cytochrome $b_5$ Transfer among donor POPC LUVs and acceptor POPC SUVs . . . . .	216
68. Cytochrome $b_5$ tight insertion into POPC LUVs within 24 hours as a function of cholesterol mole percent . . . . .	218
69. Cytochrome $b_5$ transfer from POPC reverse-phase donor liposomes to acceptor POPC SUVs . . . . .	222
70. Cytochrome $b_5$ tight insertion into POPC LUVs within 2 hours as a function of cholesterol mole percent . . . . .	226
71. Kinetics of cytochrome $b_5$ tight insertion into POPC reverse-phase liposomes . . . . .	230
72. Structure of the cyt $b_5$ membrane binding domain in a bilayer .	236
73. Proximity of cytochrome $b_5$ molecules in LUVs and SUVs . . . . .	239
74. Correlation of cholesterol-mediated inhibition of cytochrome $b_5$ to LUVs with the Condensing Effect and Free Volume . . . . .	243
75. "Bimolecular mesomorphic lattice" model; 20 mole percent cholesterol . . . . .	249
76. "Bimolecular mesomorphic lattice" model; 33 mole percent cholesterol . . . . .	251
77. "Bimolecular mesomorphic lattice" model; 50 mole percent cholesterol . . . . .	253



## LIST OF TABLES

I. Effect of Cholesterol on the Lamellar Parameter of Reverse-phase Liposomes . . . . .	81
II. Effect of Cholesterol on Cytochrome $b_5$ Binding to Reverse-phase Liposomes of Phosphatidylcholines . . . . .	95
III. Scatchard Analysis Summary of Cytochrome $b_5$ Binding to Small Unilamellar Vesicles Prepared from various Phosphatidylcholines and Cholesterol . . . . .	167
IV. Effect of Cholesterol on the Saturation Levels of Cytochrome $b_5$ Binding to Phosphatidylcholine Small Unilamellar Vesicles . . .	169
V. Effect of Cholesterol on Cytochrome $b_5$ Binding Equilibrium for Phosphatidylcholine Small Unilamellar Vesicles . . . . .	173
VI. Effect of Cholesterol on Cytochrome $b_5$ Binding to POPC-LUVs . .	209

## INTRODUCTION

A distinctive characteristic of biological membranes is their complex lipid composition. Yet the basis for such compositional heterogeneity is not understood. The predominant types of lipids are glycerophospholipids, sphingolipids, glycolipids, and sterols. The 1,2-diacyl-*sn*-phosphoglycerides, or phospholipids, are the most abundant. Typically these lipids have a hydrophilic phosphoryl head group linked to a glycerol hydroxyl by a phosphate ester bond. In sphingolipids, which are derived from ceramide, sphingosine forms the backbone of the phospholipid instead of glycerol. As shown in Figure 1, the polar head groups consist of phosphate linked to alcohols such as choline, ethanolamine, serine, glycerol, or inositol. Two hydrophobic polymethylene chains are esterified to the other glycerol hydroxyls. Together, the polar head group and the hydrocarbon chains make phospholipids amphipathic molecules.

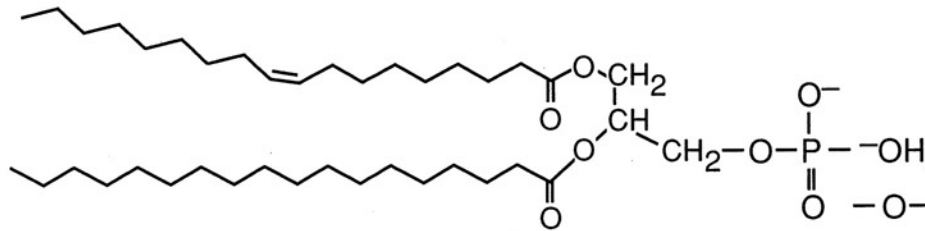
Phosphatidylcholine (PC) is the predominant phospholipid species, comprising 40-60% of the total phospholipid in rat liver mitochondria, ER, lysosomes, plasma membranes, nuclear membranes, and Golgi, and 25-66% of the total lipid in human erythrocyte, bovine disk, and rabbit sarcoplasmic reticulum [see Gennis (1989a) and references therein].

In addition to the diversity of polar head groups, phospholipids exhibit a broad range of fatty acyl compositions. Although the fatty acyl chains vary from 14 to 24 carbons, most are 16, 18, and 20 carbon atoms in length. Double bonds on the hydrocarbon chains typically occur at positions 9-, 9,12-, 6,9,12-, and 5,8,11,14- and are always in a *cis* configuration (Jain, 1988a). Usually, the saturated and unsaturated fatty

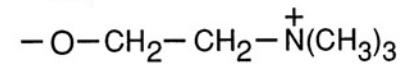
**Figure 1.**

**Chemical Structure of Phospholipids.**

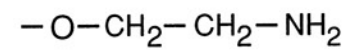
## Phospholipids



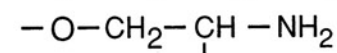
phosphatidic acid



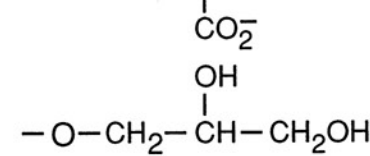
phosphatidylcholine



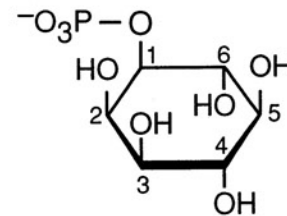
phosphatidylethanolamine



phosphatidylserine



phosphatidylglycerol



phosphatidylinositol



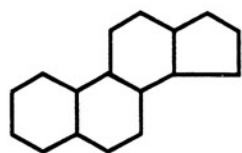
acyl chains are esterified at the first (*sn*-1) and second (*sn*-2) glycerol carbons, respectively. Like the various phospholipid classes, the hydrocarbon chain composition varies among the different cellular membranes. A typical biological membrane usually has 3-4 phospholipid classes and approximately 10 types of fatty acyl chains.

Sterols represent the second most predominant class of lipids in biological membranes. The structural motif of sterols is a *trans*-fused perhydrocyclopentanophenanthrene ring system with a hydroxyl group and an aliphatic chain of 6 to 10 carbon atoms (Figure 2). Various sterols are found in plant, mammalian, and microbial membranes, with differences among individual sterols arising from substitutions of the aliphatic side chain and methyl groups on the  $\beta$ -face. For example, the principal sterols in the membranes of higher plants are stigmasterol and  $\beta$ -sitosterol, while ergosterol and diplopterol are sterols found in *Saccharomyces cerevisiae* (yeast) and *Tetrahymena*, respectively. Similarly, dinosterol and fucosterol are sterols that occur in the marine organisms *Gonyaulax tamarensis* (a toxic dinoflagellate) and *Phaeophyceae* (marine brown algae) (Gennis 1989b; Jain, 1988b; The Merck Index, 10<sup>th</sup> ed., 1983). Figure 2 depicts the chemical structures of these sterols. Unlike phospholipids, sterols do not form a stable bilayer by themselves. However, as components of biological membranes, sterols have a substantial affect on the physical properties of lipid bilayers.

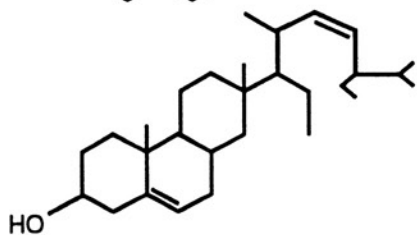
Cholesterol is the sterol found in mammalian membranes. It is disproportionately distributed among intracellular membranes, comprising approximately 3, 7, 33, and 29-43 mole percent of the total lipid of rat liver mitochondrial, endoplasmic reticulum, lysosomal, and plasma

**Figure 2.**

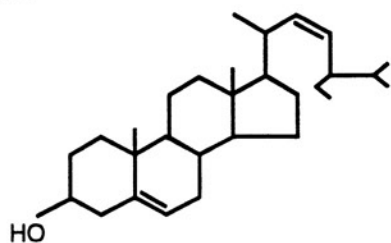
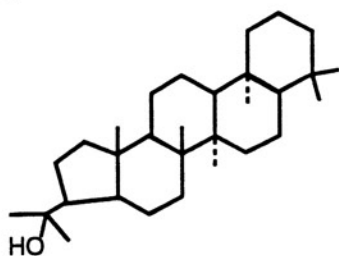
**Chemical Structures of Common Sterols.**



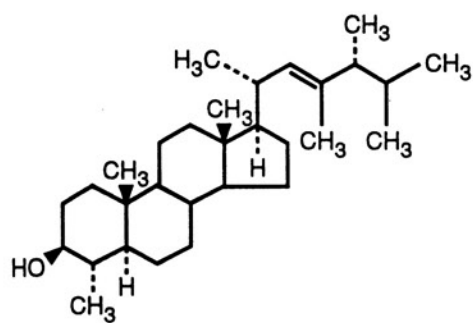
Perhydrocyclopentanophenanthrene



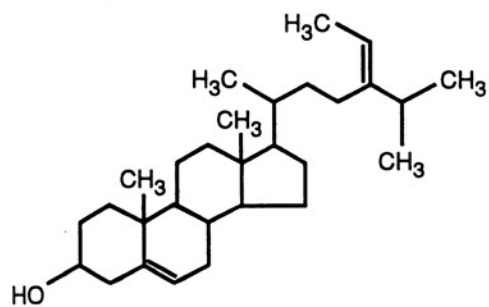
Stigmasterol

 $\beta$  – Sitosterol

Diplopterol



Dinosterol



Fucosterol

membranes, respectively (van Meer, 1989). Typically, the cholesterol concentration in plasma membranes is much higher (30-50 mole percent) than in intracellular membranes (less than 20%) (Jain, 1988c).

Structural models of cholesterol (Figures 3, 4 and 5) show that it consists of the fused perhydrocyclopentanophenanthrene ring system with a  $\beta$ -hydroxyl ( $\beta$ -OH) group at one end and a branched, flexible hydrocarbon chain of 8 carbon atoms at the other. Although the two-dimensional depiction of cholesterol makes it difficult to visualize just how cholesterol can be incorporated into membranes, CPK models show that it resembles a long hydrocarbon chain (Figure 4). The rigid steroid nucleus exhibits an essentially planar  $\alpha$  surface, and a bulky  $\beta$  side (Figure 5). Together, these features impart stereochemical properties that enable cholesterol to fit between phospholipids in bilayers. Electron density profiles obtained by X-ray diffraction of hydrated egg phosphatidylcholine and cholesterol bilayers show that cholesterol is oriented with its long axis normal to the plane of the bilayer, with the  $\beta$ -OH group toward the ester carbonyl region of the phospholipids and the hydrocarbon tail extending toward the center of the bilayer (Figure 6) (Worcester, D. L. and Franks, N. P., 1976).

Cholesterol has been extensively investigated in model lipid bilayers to elucidate its importance in biological membranes. As a membrane component, cholesterol significantly affects the physical properties of lipid bilayers, most notably the membrane "fluidity." By intercalating between phospholipid molecules and preventing optimal interactions among the fatty acyl chains, cholesterol stabilizes the liquid-crystalline state in phospholipids that would normally form a rigid

**Figure 3.**

**Chemical structure of cholesterol.**

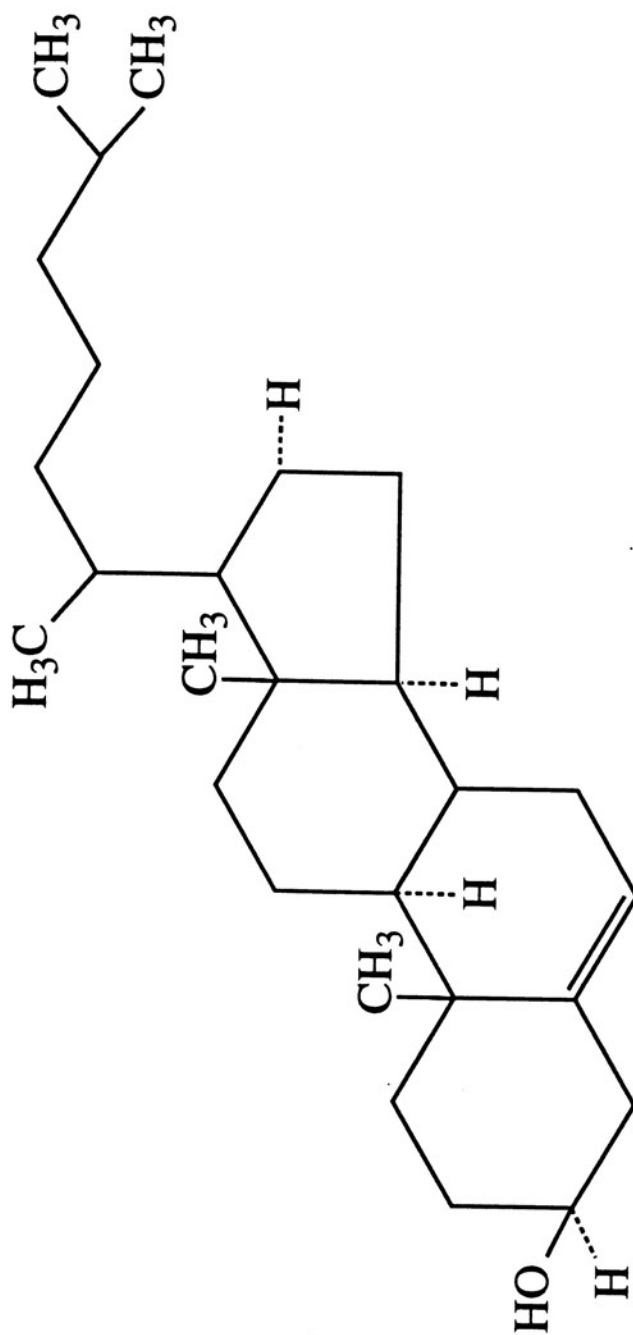
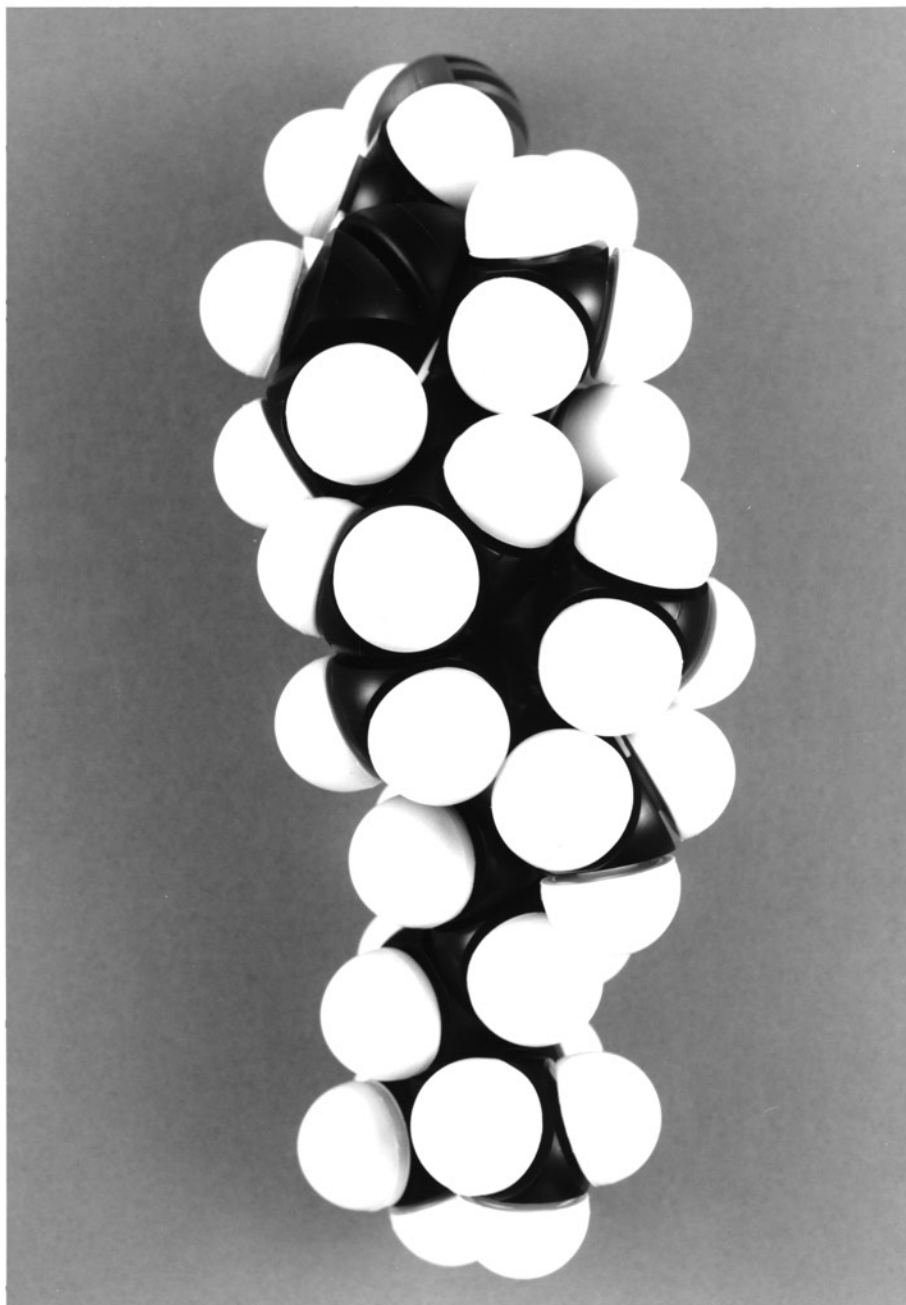




Figure 4.

CPK space-filling model of cholesterol.



**Figure 5.**

CPK space-filling model of cholesterol, side view. The molecule has been rotated 90° from the original position in Figure 4. The left side is the planar  $\alpha$  surface of cholesterol, while the  $\beta$  side is on the right.

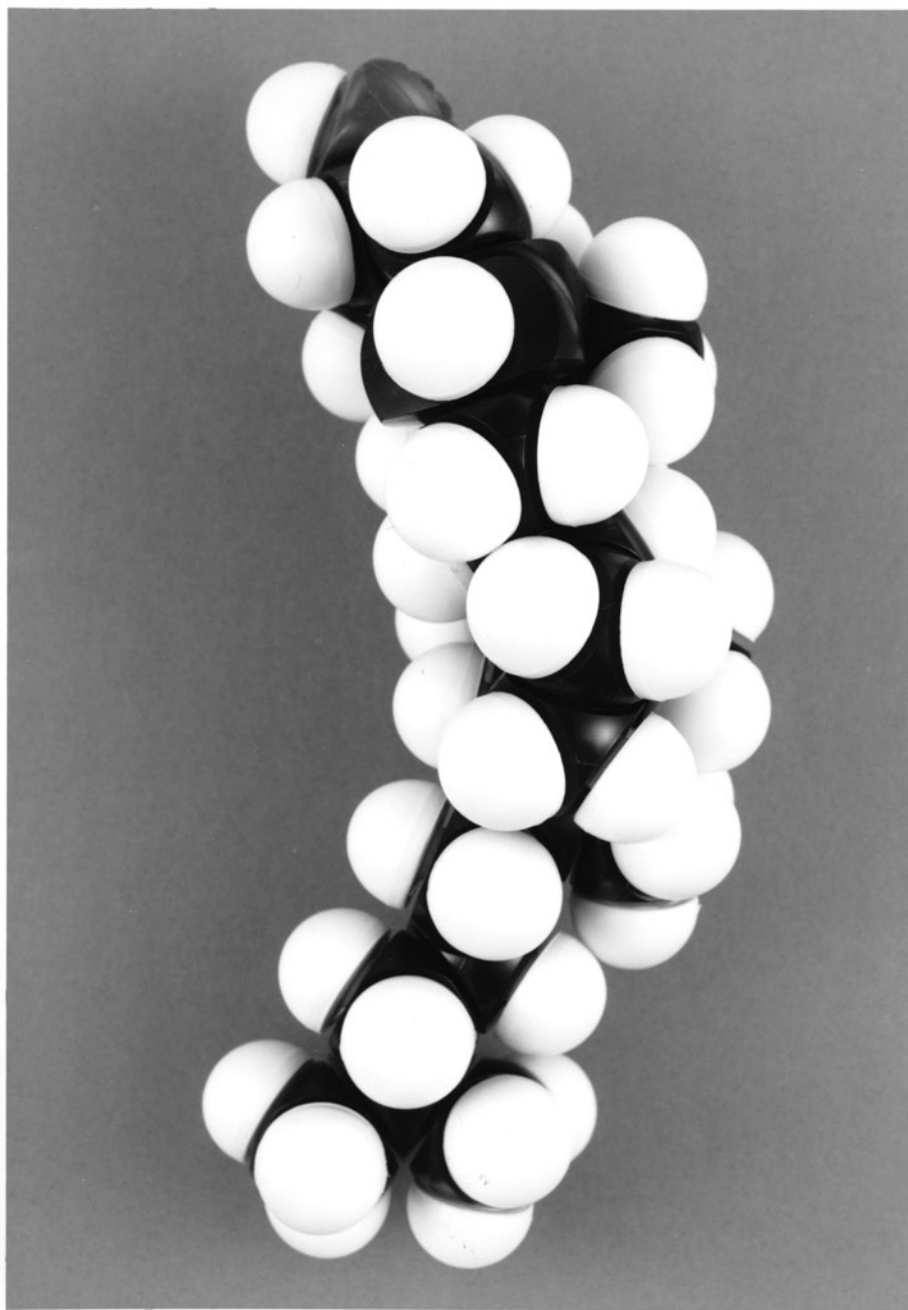
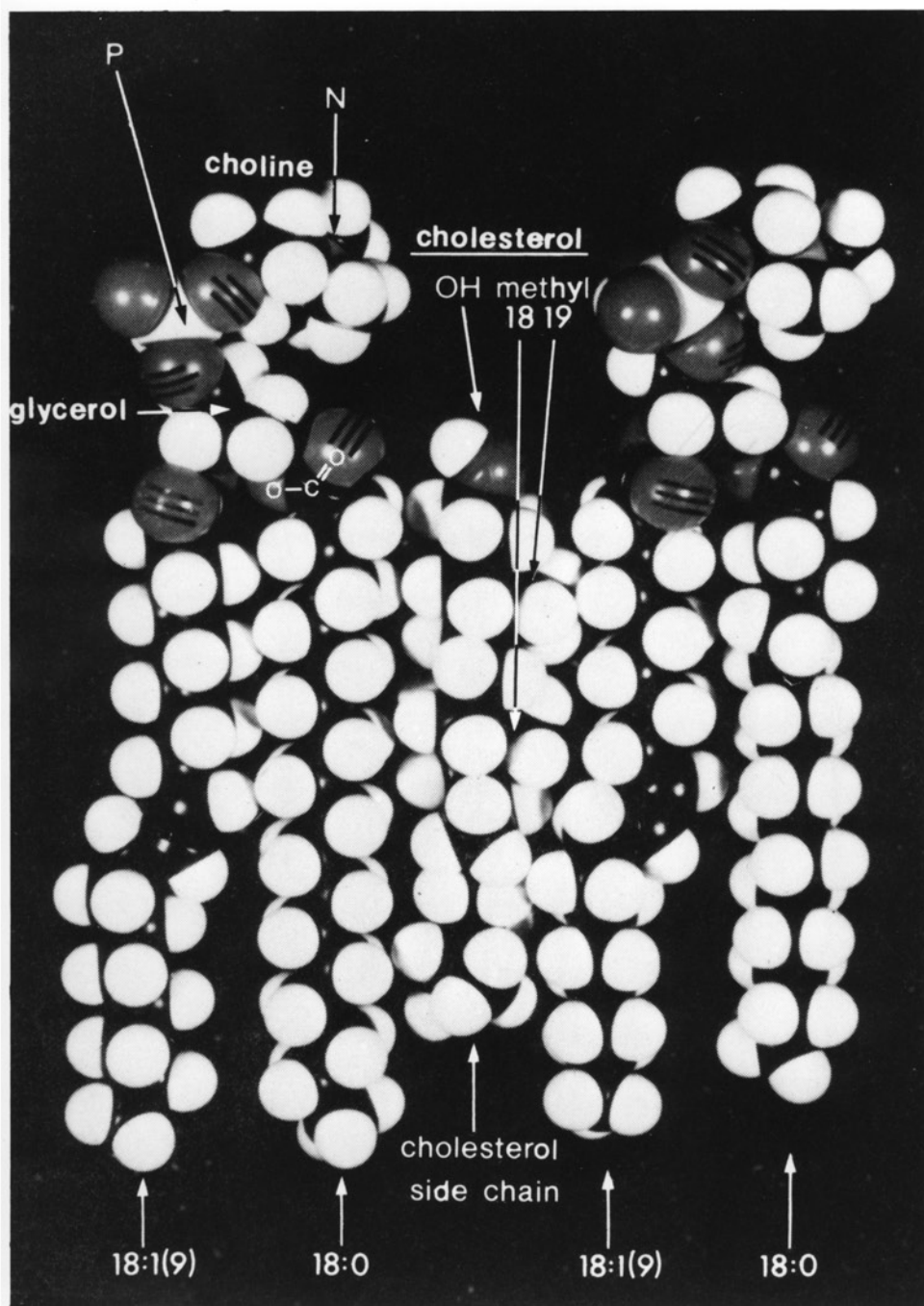


**Figure 6.**

**Interaction of cholesterol with phospholipids.**





gel state below transition temperatures ( $T_c$ ). Simultaneously, cholesterol exhibits a unique "ordering effect" in bilayers by reducing the motional degrees of movement for phospholipids. Because it orders the liquid-crystalline phase and disorders the gel state, cholesterol modulates membrane "fluidity." Some of the related physical effects of cholesterol [reviewed by Yeagle (1985)] include ordering phospholipid sequential motion, decreasing membrane permeability, decreasing phospholipid surface areas, and perturbing cooperative phospholipid phase transitions.

A. *Effect of cholesterol on the segmental motion of phospholipids.*

Cholesterol "orders" phospholipids by restricting the segmental motion, i.e. *trans-gauche* isomerizations of fatty acyl chains. In the liquid-crystalline or fluid state, phospholipid acyl chains exhibit relatively unhindered motional freedom, with nearly isotropic motion in the center of the bilayer. Free rotation occurs about each carbon-carbon bond, with *trans-gauche* isomerizations in the acyl chains occurring on a time scale of 0.01-1 nsec (Jain, 1988d). The *trans* configuration is thermodynamically favored, since the overall free energy necessary to rotate into the *gauche* conformation is approximately +3.5 kcal/mole (Gennis, 1989c). Because the hydrocarbon chains are maximally extended, the all-*trans* conformation reflects increased membrane order. In contrast, *gauche* conformations introduce bends in the acyl chains, which weaken hydrophobic interactions among neighboring molecules and cause long-range disorder in membranes.

Cholesterol orders phospholipids by stabilizing or inducing the *trans* conformation of acyl chains. This conclusion comes mainly from

studies in which cholesterol was observed to increase the thickness of bilayers prepared from phospholipids with acyl chains up to 16 carbon atoms (McIntosh, T. J., 1978). Additionally,  $^2\text{H}$ -NMR shows that the average molecular order of deuterated stearic acid probes in egg phosphatidylcholine bilayers increases as the cholesterol composition also increases from 0-33 mole percent (Stockton, G. W. and Smith, I. C. P., 1976). However, the most significant ordering occurs near to the glycerol moiety (between the first and tenth methyl groups). Cholesterol exhibits minimal acyl chain ordering in the center of membranes. Similarly, Monte Carlo studies of the interactions between cholesterol and lipid chains of 14-18 carbon atoms also indicate that cholesterol most significantly affects the upper portion of the chains (Scott and Kalaskar, 1989). Specifically, cholesterol slows (but does not completely prevent) *gauche* rotations and rotameric disordering in phospholipids that are nearest neighbors. According to the calculations, cholesterol significantly inhibits about six neighboring acyl chains from changing rotameric conformations. Therefore, at low cholesterol:phospholipid ratios cholesterol prevents about 3 phospholipid molecules from participating in cooperative interactions. The significance of this 3:1 phospholipid to cholesterol ratio will be discussed later.

#### **B. Cholesterol Affects Membrane Permeability.**

In addition to ordering phospholipid acyl chains, cholesterol decreases membrane permeability to glucose (Papahadjopoulos *et al.*, 1971, Demel *et al.*, 1972a, Yeagle *et al.*, 1977, and Jain, 1988d), water (Jain, 1988e), and ions (Papahadjopoulos *et al.*, 1971, Demel *et al.*, 1972a).

*C. Cholesterol "decreases" phospholipid surface areas: The Condensing Effect.*

Cholesterol exhibits a unique "condensing effect" on phospholipids. This phenomenon, observed in monolayer studies of cholesterol/phospholipid mixtures, describes how cholesterol decreases mean molecular surface areas. Typically, the method involves spreading a lipid mixture in a volatile solvent at an air/water interface. As the solvent evaporates, the lipids form an oriented monolayer, with polar groups in contact with the aqueous phase and the hydrophobic portions extending above. A Langmuir film balance permits measurement of the surface area (A) and lateral pressure ( $\pi$ ) required to maintain the monolayer. The  $\pi$ -A isotherms provide the molecular area of lipids.

In mixed monolayers containing cholesterol, the total surface area is not a simple additive function of individual molecular areas, but demonstrates negative deviation from linearity (Zatz, 1974). This has been termed the Condensing Effect. However, the extent of phospholipid surface area reduction depends upon the number and position of double bonds in the acyl chains (Demel et al., 1972b). Cholesterol exhibits the largest condensing effect on 1-stearoyl-2-oleoyl-*sn*-glycero-3-phosphorylcholine (18:0, 18:1), and to a smaller extent on 1-palmitoyl-2-linoleoyl-*sn*-glycero-3-phosphorylcholine (16:0, 18:2) and 1-palmitoyl-2-linolenoyl-*sn*-glycero-3-phosphorylcholine (16:0, 18:3). In contrast, cholesterol shows no condensing effect on 1,2-dilinoleoyl-*sn*-glycero-3-phosphorylcholine (18:2, 18:2) and 1,2-distearoyl-*sn*-glycero-3-phosphorylcholine (18:0, 18:0) (Demel et al., 1972b).

The condensing effect reflects the extent of interaction between

cholesterol and phospholipids. The monolayer studies suggest effective lateral packing of cholesterol with mixed-chain phospholipids (SOPC and PLPC) but not with disaturated (DSPC) and polyunsaturated (DLPC) species. Indeed, the overall interaction between phospholipids and cholesterol may significantly depend upon the extent of acyl chain unsaturation. In fluorescence polarization studies of cholesterol in bilayers of various unsaturated phosphatidylcholines, van Blitterswijk *et al.* (1987) observed that increasing acyl chain unsaturation causes a weaker phospholipid association with cholesterol. Although fluorescence polarization, which is a measure of the "microviscosity" of the membrane, exponentially increases with cholesterol content, the extent of the increase at a given cholesterol/phospholipid mole ratio depends upon the phospholipid. With different phospholipids, variations in the degree of cholesterol-induced polarization are described by a cholesterol-ordering coefficient,  $\alpha$ , which reflects cholesterol/phospholipid interaction. For POPC, PLPC, egg PC, DOPC, and DLPC, the values of  $\alpha$  are 2.45, 1.84, 1.93, 1.76, and 1.33, respectively (van Blitterswijk *et al.* 1987), indicating weaker interactions of cholesterol with highly unsaturated phospholipids.

To explain why cholesterol has a large condensing effect on mixed-chain phosphatidylcholines (SOPC, PLPC, and SLPC) but not on disaturated or di-unsaturated phospholipids (DSPC and DLPC), Huang (1977) has suggested that the  $\beta$  surface of cholesterol fills the hydrophobic "pocket" above a  $\Delta^{9,10}$ -*cis* double bond-*trans-gauche* kink, while the  $\alpha$  side preferentially interacts with saturated chains. The  $\Delta^{9,10}$ -*cis* double bond lowers the energy barrier of *trans-gauche* isomerizations from +3.5 to +2 Kcal mol<sup>-1</sup> at adjacent C-C single bonds. A  $\Delta^{9,10}$ -*cis* double bond-*trans-*

*gauche* kink linearizes the acyl chain overall, but displaces it laterally, creating an abscess that can accomodate the rigid steroid nucleus.

More recently, the condensing effect has been postulated to arise from "poor solvent" effects of cholesterol. Hyslop *et al.* (1990), by examining the theoretical molar attraction constants of the various fatty acyl chain and sterol structural groups, conclude that the interactions between adjacent fatty acyl chains are greater than the interactions between cholesterol and a fatty acyl chain. Hence, phospholipid condensing may originate from increased acyl chain interpenetration.

In summary, the condensing effect indicates that cholesterol interacts differently with specific phospholipids. Although this phenomenon is observed in mixed monolayers of cholesterol and phospholipids, fluorescence polarization studies indicate similar behavior of cholesterol with phospholipids in bilayers. The latter studies seem to have more relevant application to understanding cholesterol/phospholipid interactions in biological membranes, since measurements are made using true lipid bilayers (liposomes) under equilibrium conditions. If so, further systematic investigation with model lipid bilayers will be beneficial in discerning how different interactions between cholesterol and phospholipids may affect other membrane related phenomena.

***D. Cholesterol reduces the cooperative phase transitions of phospholipids.***

The effect of cholesterol on the thermodynamic properties of phospholipids is perhaps most significant to understanding its role as a membrane component. Pure phospholipid bilayers exhibit two predominant

physical states: a highly ordered rigid gel state and a fluid, disordered liquid-crystalline state. The transition temperature,  $T_c$ , which indicates the beginning of the "gel to liquid-crystalline" endothermic phase transitions, is determined by the phospholipid acyl chain length and extent of unsaturation. Increasing chain length results in greater  $T_c$  values, whereas unsaturation lowers phospholipid transition temperatures.

The phase behavior of phospholipids is studied by differential scanning calorimetry (DSC). Calorimetry measures the differential heat required to maintain identical temperatures in an independent phospholipid sample undergoing the gel/liquid-crystalline phase transition with the temperature of an inert reference.

For bilayers of pure phospholipids, the phase transition is usually represented by a sharp endothermic peak in the heat capacity within a narrow temperature range. The transition midpoint ( $T_m$ ), or melting temperature, indicates when the phase change is 50% complete.

Additionally, the transition width indicates phospholipid cooperativity. Acute calorimetry profiles indicate a large cooperative unit of phospholipids participating in the phase transition, whereas a greater transition breadth corresponds to reduced intermolecular cooperativity, or the number of phospholipids that have been removed from participating in the transition.

Cholesterol reduces the sharp endothermic transitions starting at approximately 20 mole percent, and completely eliminates it between 32 and 50 mole percent in multilamellar vesicles of DPPC (Ladbroke *et al.*, 1968, Estep *et al.*, 1978), DMPC (Mabrey *et al.*, 1978), and DSPC (Davis and Keough, 1983). Similar results are seen for the mixed-chain phospholipids:



SOPC and OSPC, except that the endothermic phase transition broadens at about 15% cholesterol, with complete disappearance at 30% (Davis and Keough, 1983). With multilamellar vesicles of PLPC and SLPC, low cholesterol compositions dramatically affect the calorimetric profiles: the sharp transitions broaden at just 5 mole percent cholesterol, with complete phospholipid cooperativity eliminated at only 17% (Keough *et al.*, 1989). However, cholesterol reduces and broadens, but does not completely eliminate, the phase transition of DOPC (Davis and Keough, 1983) and shows essentially no effect on the phase behaviors of the di-polyenoic phospholipids: DLPC, DAPC, and 1,2-didocosahexaenoyl-*sn*-glycero-3-phosphorylcholine (Kariel *et al.*, 1991).

The reduction/broadening of phospholipid phase transitions indicates that cholesterol introduces disorder into phospholipid bilayers and inhibits formation of the rigid gel state by preventing cooperative hydrophobic interactions among acyl chains. Cholesterol minimally effects the phase transitions of highly unsaturated phospholipids, most likely because polyenoic acyl chains already exhibit little intermolecular cooperativity.

The presence of double bonds in phospholipids, which decrease  $T_c$  and introduce disorder in membranes, does influence the cholesterol affect on cooperative phase transitions. In systematic calorimetric studies of three synthetic long chain phosphatidylcholines (24:1, 24:1) with different double bond positions at  $\Delta^5$ ,  $\Delta^9$ , and  $\Delta^{15}$ , cholesterol eliminated the transition enthalpy in  $\Delta^{15}$ -PC(24:1, 24:1), but exhibited a significantly lesser effect on the phase transitions of  $\Delta^5$ - or  $\Delta^9$ -PC(24:1, 24:1) (Ayanoglu *et al.*, 1990). Cholesterol does not affect the phase transition

in both  $\Delta^5$ - and  $\Delta^9$ -(24:1, 24:1) PC's because the location of double bonds in the upper portion of the acyl chain significantly disrupts cooperative interactions. In contrast, the  $\Delta^{15}$  double bond is located toward the disordered bilayer center, where its entropic effects are less significant. Hence, cholesterol most significantly affects the phase transition of this particular PC because it disrupts the cooperative interactions in the acyl chain upper segments, which are typically more ordered.

To review, differential scanning calorimetry shows that cholesterol introduces disorder into gel-state bilayers by disrupting the cooperative interactions of phospholipids. However, the extent to which cholesterol affects phospholipid phase transitions depends on the number and position of double bonds in the acyl chains. Double bonds introduce bilayer disorder when located in the upper segments of the hydrocarbon chains, where they most significantly disrupt cooperative interactions. In such cases, cholesterol does not appreciably affect the phase transitions because of significant disorder (reduced cooperativity) in the acyl chains themselves.

The effect of cholesterol on phospholipid phase behaviors demonstrate the effectiveness of cholesterol as a modulator of membrane fluidity. The "disordering" effect of cholesterol is relevant to regulating membrane fluidity for gel-state phospholipids (phospholipids with a high  $T_c$ ), whereas the "ordering effect" is important at modulating fluidity in phospholipid bilayers that are in a liquid-crystalline state.

***E. Structural requirements for modulating the physical properties of membranes.***

The planar  $\alpha$  surface and  $\beta$ -OH seem to be essential for cholesterol to exhibit its unique effects on the physical properties of phospholipids. To illustrate, lanosterol, which does not have a planar  $\alpha$  side due to an axial methyl group at carbon-14, is less effective than cholesterol at immobilizing phospholipid acyl chains and reducing bilayer permeability (Yeagle *et al.*, 1977). Space-filling models indicate that this methyl group sterically hinders interactions between lanosterol and the phospholipid acyl chains (Bloch, 1976). Similarly, epicholesterol, which has an  $\alpha$ -OH instead of the  $\beta$ -OH, does not demonstrate a condensing effect or a reduction in phospholipid phase transition enthalpy (DeKruyff *et al.*, 1973) as cholesterol.

***F. Models of cholesterol/phospholipid interactions.***

Molecular models of cholesterol organization in lipid bilayers have been proposed to account for the effects of cholesterol on the physical properties of membranes. More importantly, understanding the lateral arrangement of cholesterol in membranes is essential to elucidating its role as a component of biological membranes.

Perhaps the most comprehensive model of cholesterol-phospholipid interactions proposes a nonrandom lateral distribution of cholesterol in lipid bilayers (Presti *et al.*, 1982). This model in particular accounts for the vast physico-chemical data that has been obtained with calorimetry, freeze-fracture electron microscopy, fluorescence photobleaching, dilatometry, x-ray diffraction, and nuclear magnetic

resonance spectroscopy. The model proposes that as cholesterol is incorporated into phospholipid bilayers from 0-20 mole percent, each cholesterol molecule forms a tight stoichiometric complex with one phospholipid molecule, which in turn is loosely associated with a second phospholipid. These 1:2 cholesterol-phospholipid complexes are not, however, randomly distributed throughout the bilayer. Cholesterol-enriched regions segregate from regions of pure phospholipid, with interfacial boundary phospholipid separating the two phases. Between 0-20 mole percent cholesterol, the high-cholesterol phase and boundary phospholipid areas increase as the pure-phospholipid domain concomitantly decreases. At approximately 20 mole percent cholesterol, the domains of pure phospholipid disappear, with interfacial boundary phospholipids remaining among 1:2 cholesterol-enriched domains. The interfacial area is maximal at about 20-22% cholesterol and it is postulated to be a region of bilayer instability, a consequence of lipid packing defects. Between 20-33%, the area of boundary phospholipid decreases until there exists only a single phase of the 1:2 cholesterol-phospholipid complexes at 33 mole percent cholesterol. At higher cholesterol compositions (33-50 mole percent cholesterol), the loosely associated phospholipids are depleted until only 1:1 cholesterol-phospholipid complexes are present. Within the cholesterol-enriched phase, 1:1 cholesterol-phospholipid pairs are organized in antiparallel linear arrays, with loosely associated phospholipids intercalating in between. The loosely associated phospholipids arrange in a quasi-hexagonal order that is almost identical to the pure lipid gel-state. The arrangement gives minimal intermolecular void and provides maximum van der Waals contact in the acyl chain region

of the bilayer. At 50 mole percent cholesterol the loosely associated phospholipids are depleted, leaving only 1:1 cholesterol-phospholipid complexes that are also organized in antiparallel linear arrays. The 1:1 complexes are a tight interaction between cholesterol and phospholipid molecules through combined hydrogen bonding and van der Waals attraction.

A number of physical studies correlate with nonideal mixing of cholesterol and phospholipids in bilayers. For example, calorimetry studies show that at 20 mole percent, cholesterol decreases and broadens the sharp endothermic phase transition in multilamellar vesicles of DPPC (Estep *et al.*, 1978), DMPC (Mabrey *et al.*, 1978), and DSPC (Davis and Keough, 1983). This shows that as the cholesterol content in lipid bilayers increases, it removes phospholipids from participating in the cooperative gel-to-liquid-crystalline transitions. This suggests lateral phase separation below 20 mole percent cholesterol and the existence of a single phase from 20-50 mole percent. According to the Presti model (1982), the pure phospholipid phase disappears at about 20% cholesterol which is manifested by a change in the phospholipid endotherms. Additionally, freeze-fracture studies show evidence of distinct phases. Between the pretransition and gel/liquid-crystalline phase transition temperatures, a "ripple effect" is observed in DMPC and DPPC multilamellar vesicles (Copeland and McConnel, 1980). The "ripples" are putative areas of pure phospholipid. As cholesterol content increases, the frequency of linear "ripples" decreases; with complete disappearance of pure phospholipid ripples at 20 mole percent cholesterol.

At about 20-22 mole percent cholesterol, the area of interfacial phospholipid is proposed to be maximal and accounts for discontinuities in

the permeability properties of the bilayer. For example, Tsong (1975) has observed that the transport rate of 8-anilino-1-naphthalenesulfonate across DMPC bilayers is maximal at 17% cholesterol. Similarly, photobleaching studies show that lateral diffusion of the fluorescent probe phosphatidyl-N-(4-nitrobenzo-2-oxa-1,3-diazole)ethanolamine increases by 10 fold at 20 mole percent cholesterol in DMPC and DPPC vesicles that are below the lipid transition temperature (Rubenstein *et al.*, 1979).

In further support of a model in which cholesterol is nonrandomly distributed, other studies have revealed two cholesterol-associated events. Dilatometry shows that below "gel to liquid-crystalline" transition temperatures, the partial specific volume of DPPC MLVs increases with cholesterol composition, but exhibits three distinct segments: the rate of bilayer expansion is constant up to 20% cholesterol, becomes maximal between 20-29%, and then decreases beyond 29% cholesterol (Melchior *et al.*, 1980). Additionally, X-ray diffraction of DPPC-cholesterol bilayers has demonstrated two cholesterol events. A distinct 4.15-Å band due to ordered gel-state phospholipid, observed alone at 0% cholesterol, becomes accompanied by a broad 4.7-Å band at 20%. As cholesterol composition increases, the diffracted energy in the 4.7-Å band increases while the 4.15-Å line decreases, with complete disappearance of the 4.15-Å band at 33 mole percent cholesterol (Engelman and Rothman, 1972). Finally, nuclear magnetic resonance spectroscopy shows that at cholesterol compositions up to 30% cholesterol, the phosphatidylcholine hydration signal gives a sharp, symmetric band with a half-height line width of 120-150 Hz. This signal broadens (half-height widths

approximately 300-1000 Hz) and becomes asymmetric at 35% cholesterol (Taylor *et al.*, 1977). Collectively, these studies suggest the existence of two cholesterol titration points in membranes, one at 20 mole percent and the other between 30-35%.

Finally, the 1:1 complexes represent an intimate association between cholesterol and phospholipids, arising from a combination of hydrogen bonding and van der Waals attraction. Proton NMR studies of the stereospecific isomers, *sn*-3 and *sn*-1 dipalmitoylphosphatidylcholine, indicate that cholesterol interacts with phospholipids near the second glycerol carbon (Chatterjee and Brockerhoff, 1978). Additionally, studies described earlier (page 6) show that lanosterol (Yeagle *et al.*, 1977) and epicholesterol (DeKruyff *et al.*, 1973) exhibit different effects than cholesterol on lipid bilayers, suggesting that the planar  $\alpha$  surface and  $\beta$ -OH give cholesterol the proper molecular geometry for interaction with phospholipids. In the 1:1 complexes cholesterol tightly associates with phospholipids by hydrogen bonding between its  $\beta$ -OH and the second glycerol oxygen, which is esterified to the *sn*-2 fatty acyl chain. The planar  $\alpha$  surface maximizes van der Waals forces by interacting with the second fatty acyl chain.

Many of the observed phenomena that support the cholesterol phase separation model occur in lipid bilayers that are below the  $T_c$  of phospholipids. Accordingly, the nonrandom model seems to most appropriately apply to gel-state lipid bilayers; it probably has indeterminate relevance to cholesterol organization in liquid-crystalline biological membranes. More recent studies of cholesterol lateral organization have been performed to include lipid bilayers that are above



phospholipid phase transitions.

The complete phase diagrams of DPPC/cholesterol (Vist and Davis, 1990; Sankaram and Thompson, 1991) and DMPC/cholesterol (Almeida *et al.*, 1992) mixtures indicate in-plane immiscibility of cholesterol-enriched regions in both gel-state and liquid-crystalline bilayers. Below the transition temperature (23.9°C) in the DMPC/cholesterol system, a single gel-phase (S) exists at cholesterol compositions less than 6 mole percent. Between 6 and 28-30 mole percent cholesterol, the S phase coexists with a laterally separated liquid-ordered phase ( $L_o$ ) of high-cholesterol content. Only the  $L_o$  region remains at cholesterol compositions that are above 30 mole percent. (For the gel-state DPPC/cholesterol system, the region of S and  $L_o$  phase coexistence occurs from 7.5 to 22 mole percent cholesterol.) Above the  $T_c$ , these systems similarly exist either as a fluid liquid-disordered ( $L_d$ ) phase at low cholesterol compositions, as the liquid-ordered ( $L_o$ ) gel-like phase at high cholesterol compositions, or as a mixture of the two separate phases. Therefore, as similarly observed in gel-state bilayers, addition of cholesterol to the bilayer induces transition from the  $L_d$  phase to the  $L_o$  phase in liquid-crystalline lipid bilayers. However, above  $T_c$  the boundary lines for either the  $L_d$  or  $L_o$  phases significantly depend upon temperature in addition to cholesterol content. As temperature increases above  $T_c$  the  $L_d$  region predominates within a greater range of cholesterol composition. To illustrate, the DMPC phase diagram indicates that at 25°C only the  $L_d$  region exists up to about 6 mole percent cholesterol before the  $L_o$  region initially forms at greater cholesterol compositions, whereas at 50°C, the  $L_d$  phase is exclusively present up to cholesterol compositions of 20 mole percent. Although to a

significantly lesser extent, temperature elevation similarly shifts the boundary line of the  $L_o$  region to greater cholesterol compositions in the DMPC/cholesterol phase diagram; the boundary line of the  $L_o$  phase shifts from approximately 30 mole percent cholesterol at 25°C to about 33 mole percent at 55°C. In liquid-crystalline DMPC/cholesterol and DPPC/cholesterol mixtures, the boundary lines of the  $L_d$  and  $L_o$  phases converge as the temperature increases. As a result, the  $L_d+L_o$  coexistence region occurs within an increasingly narrow range of cholesterol composition as the temperature becomes elevated.

The molecular arrangement of cholesterol with phospholipids is proposed to differ between the two liquid phases of the DMPC/cholesterol and DPPC/cholesterol phase diagrams (Sankaram and Thompson, 1991). In the  $L_d$  phase, cholesterol localizes toward the bilayer median so that it partially spans the hydrophobic region of each monolayer, whereas in the  $L_o$  phase it aligns with phospholipids in either monolayer.

Consequently, the two liquid-liquid immiscible phases exhibit different physical properties. The characteristics of the low-cholesterol  $L_d$  and high-cholesterol  $L_o$  phases have been summarily compared as: (1) lateral diffusion is similar in the  $L_o$  and the  $L_d$  phases; (2) axial rotational rates of lipid molecules are essentially the same in both  $L_d$  and  $L_o$  phases; (3) phospholipid acyl chains are highly ordered in the  $L_o$  domain; (4) bilayer thickness increases in the cholesterol-enriched domains relative to the  $L_d$  phase, but remains less than the depth observed in the rigid gel-state (S); and (5) bilayer elasticity is less in the  $L_o$  phase than in the  $L_d$  phase (Vist and Davis, 1990). Additionally, the  $L_d$  phase is a region with broad fluctuations of total free volume ( $f_v$ ), and

the  $L_o$  phase is a region with a narrow distribution of reduced total free volume (Almeida *et al.*, 1992).

As already noted, the phase diagrams indicate separation of high cholesterol ( $L_o$ ) and low cholesterol ( $L_d$ ) phases in liquid-crystalline DMPC/cholesterol and DPPC/cholesterol mixtures. However, the liquid-liquid phase immiscibility region occurs within increasingly narrow ranges of cholesterol composition as temperature increases. The behavior of lipid molecules in these systems indicates that the  $L_d$  and  $L_o$  phases probably become miscible at temperatures that are sufficiently greater than  $T_c$ .

Although inhomogeneity of cholesterol-enriched domains occurs in liquid-crystalline DMPC and DPPC bilayers, similar phase diagrams of physiologically relevant phospholipids and cholesterol should be more appropriate to understanding the lateral organization of cholesterol in biological membranes. However, a complete phase diagram for a synthetic phospholipid as POPC with cholesterol has not yet been obtained. But if the phase diagram of a POPC/cholesterol mixture is at least qualitatively similar to the DMPC/cholesterol phase diagram, then separation of a cholesterol-enriched region likely occurs in both gel and liquid-crystalline states. More importantly, the  $L_d$  and  $L_o$  boundaries may similarly converge (i.e. the  $L_d+L_o$  immiscibility region narrows) above  $T_c$  in the POPC/cholesterol system. In the DMPC/cholesterol phase diagram, the  $L_d$  and  $L_o$  boundary lines appear to intersect at approximately 65°C, suggesting that at higher temperatures the  $L_d$  and  $L_o$  phases are miscible. Similarly, any surmised phase inhomogeneity in the POPC/cholesterol system may also disappear at 40° above the POPC transition temperature (-4°C).

Investigation of POPC/cholesterol mixtures at 37°C indicates that

the lateral organization of cholesterol and phospholipids in liquid-crystalline bilayers can involve a random molecular arrangement, suggesting that the  $L_d$  and  $L_o$  phases do become miscible at temperatures that are significantly above  $T_c$ . Steady-state fluorescence depolarization studies of cholesta-5,7,9-trien-3 $\beta$ -ol (cholestatrienol) in POPC multilamellar liposomes show that at 1:1 cholesterol/phospholipid ratios, the distance between cholesterol molecules is approximately 10.6 Å. This observation suggests infrequent cholesterol-cholesterol contacts in liquid-crystalline POPC bilayers and no lateral separation of cholesterol-enriched phases at cholesterol compositions less than 50 mole percent. Instead, the lipid matrix is arranged as an "ordered bimolecular mesomorphic lattice" (Hyslop *et al.*, 1990). This regular lattice has alternating linear arrays of cholesterol and phospholipid molecules that occur two-dimensionally. Since cholesterol molecules are separated by an average distance of 11 Å, each cholesterol molecule must be surrounded by four phospholipids as nearest neighbors. This particular model is consistent with Monte Carlo studies, which show that each cholesterol molecule immobilizes about 3 neighboring phospholipids (Scott and Kalaskar, 1989).

The reviewed observations indicate that cholesterol lateral organization probably depends upon the actual physical state of lipid bilayers. Separate cholesterol-enriched phases occur in gel-state bilayers. The recently obtained phase diagrams of DMPC/cholesterol and DPPC/cholesterol mixtures especially indicate such lipid inhomogeneity. The phase behavior of these same phospholipid/cholesterol mixtures also demonstrate immiscible cholesterol-containing regions in liquid-

crystalline bilayers. However, as temperatures of phospholipid/cholesterol mixtures are continually increased above  $T_c$ , the regions of liquid-liquid phase immiscibility concomitantly decrease. The converging boundary lines indicate that the high- and low-cholesterol content domains probably become miscible at specific temperatures that are significantly above  $T_c$ . However, the temperature at which cholesterol becomes randomly distributed in liquid-crystalline bilayers may depend upon the individual phospholipid.

#### G. *Effect of cholesterol on membrane proteins.*

The extensive studies of cholesterol/phospholipid interactions have contributed to our understanding the effects of cholesterol on the physical properties of lipid bilayers. However, these approaches do not necessarily elucidate the functional roles of cholesterol in biological membranes, which contain proteins. Therefore, investigating cholesterol in lipid bilayers that also contain associated proteins should significantly advance understanding cholesterol as a membrane component. Such studies examine the physical properties of more valid model membrane systems.

Similar to its effect on phospholipids, cholesterol also influences the physical properties of integral membrane proteins. As discussed earlier, cholesterol regulates phospholipid conformations. It may also affect the conformations of membrane-associated proteins.

A recent study shows that bilayer cholesterol participates in regulating the metarhodopsin I  $\leftrightarrow$  metarhodopsin II conformational equilibrium (Mitchell *et al.*, 1990). Both meta I and meta II are consecutive intermediates in the photolysis reaction cascade of the visual

pigment protein, rhodopsin. The packing properties of the surrounding lipid bilayer modulate the conversion of meta I to meta II: The meta I  $\leftrightarrow$  meta II equilibrium constant,  $K_{eq}$  increases linearly with  $f_v$ . Since a 179 Å<sup>3</sup> increase in the protein volume accompanies meta II formation, it is suggested that an increase in the bilayer  $f_v$  facilitates expansion of the protein and induces the formation of the meta II conformation. At 37°C, egg PC liposomes with a 30 mole percent cholesterol composition have a 35-62% less total free volume than liposomes that are devoid of cholesterol (Straume and Litman, 1987). Similarly, the equilibrium constant of the meta I to meta II conversion is reduced approximately 50% in egg PC liposomes with 30% cholesterol (Mitchell *et al.*, 1990).

Protein conformation appears to be one parameter that cholesterol can affect. However, perhaps the most fundamental of the physical properties that cholesterol might influence is the solubility of a protein in the bilayer matrix, which may be defined as the highest attainable protein to lipid ratio before the individual components form separate phases. Formally, it is the chemical potential of each component of the mixture which determines the overall composition and distribution of components within a membrane, and among intracellular membranes.

The concept that cholesterol may affect protein affinity for or solubility in lipid bilayers is a distinct possibility. Not only does the cholesterol composition vary among intracellular membranes, the overall protein per total lipid content differs extensively also. For example, in rat liver inner mitochondrial-, rough endoplasmic reticulum-, nuclear-, Golgi-, lysosomal-, and plasma membranes the relative ratios are 3-4, 2-5, 2-5, 0.7, 3-4, and 1-2 protein:lipid (w/w) respectively (Jain, 1988e).

Additionally, if cholesterol significantly affects the overall protein/lipid ratio in a given membrane, it probably regulates the lateral organization of proteins within biological membranes. The arrangement of integral membrane proteins has particular relevance to processes such as the electron transport cascades in mitochondria and ER or the signal transduction pathway of the plasma membrane, which involve effective interactions among multiple protein components. Therefore, an assessment if cholesterol affects protein solubility in lipid bilayers should indicate if an important function of cholesterol is regulation of the content and lateral organization of proteins in biological membranes.

An initial approach to exploring these possibilities is to ascertain whether cholesterol/protein interactions are thermodynamically stable. A number of studies have investigated if integral membrane proteins associate with bilayer cholesterol.

Morphological examination of membrane systems that contain both proteins and cholesterol has been one approach to determine if cholesterol affects the lateral distribution of proteins. In one study, Hochli *et al.* (1980) altered the lipid composition of mitoplasts (liposomes prepared from inner mitochondrial membranes) by fusion with cholesterol-containing liposomes. Freeze-fracture electron micrographs of these modified membranes show dispersed intramembrane particles up to cholesterol compositions of 30 mole percent at 22°C. However, aggregation of the intramembrane particles became evident at higher cholesterol/phospholipid ratios. The results suggest that proteins become immiscible in cholesterol-phospholipid domains above 30 mole percent cholesterol. Freeze-fracture electron microscopy shows similar results with

bacteriorhodopsin that has been reconstituted in liquid-crystalline DMPC liposomes. At a 136:1 phospholipid to protein mole ratio, bacteriorhodopsin is randomly distributed in the absence of cholesterol, but then becomes segregated into noticeably distinct regions in liposomes that have the relatively low composition of 10 mole percent cholesterol (Cherry *et al.*, 1980). Additionally, flash-induced transient circular dichroism shows a decrease in the rotational mobility of bacteriorhodopsin, which provides further evidence of protein aggregation. From these results it was suggested that cholesterol affects the lateral distribution of membrane proteins because protein/cholesterol interactions are thermodynamically unfavorable.

If cholesterol-protein interactions are unfavorable, then variations in protein:lipid ratios should affect the equilibrium distribution of cholesterol among biological membranes. However, an *in vitro* study of spontaneous cholesterol equilibration between liposomes and intact membrane fractions (plasma, ER, and mitochondria) suggests that the cholesterol content (up to approximately 20 mole percent) of membranes does not appear to be related to the content of integral proteins. The partition coefficients of cholesterol between egg PC liposomes and liposomes that are prepared from extracted membrane phospholipids are identical to the partition coefficients for cholesterol transfer between egg PC liposomes and the intact membranes (Wattenberg and Silbert, 1983). The results indicate that phospholipids alone determine equilibrium cholesterol compositions, even though the protein concentrations of these membranes varies substantially.

The cholesterol equilibration studies appear to be inconsistent with



the observations that adding cholesterol to mitoplasts or to DMPC liposomes induces protein aggregation (Hochli *et al.*, 1980 and Cherry *et al.*, 1980), since the aggregation of proteins to produce phase separation reflects unfavorable protein-cholesterol interactions. However, it is difficult to compare the results among these studies because of the differences in important parameters such as the nature and ratios of lipid and protein components. For example, the behavior of membrane components in lipid bilayers containing a single short-chain saturated phospholipid may not be the same as with membranes of a natural mixture of lipids. An attempt to reconcile these results is suggested later in this review.

Although morphological investigations have attempted to indirectly ascertain whether proteins and cholesterol associate in lipid bilayers, alternative biophysical approaches examine if cholesterol integrates into the lipid annulus of membrane proteins.

By reconstituting glycophorin into liposomes containing cholesterol, Yeagle (1984) has examined cholesterol behavior in terms of annular lipid. Recombinant liposomes could be formed from initially solubilized mixtures of glycophorin and egg PC with 0 to 60 mole percent cholesterol. Freeze-fracture electron microscopy revealed recombinant 1000-5000 Å diameter liposomes with intramembrane particles and the reconstituted glycophorin was nonsusceptible to extensive trypsin hydrolysis. From  $^{31}\text{P}$  NMR, the number of annular phospholipids per glycophorin molecule was observed to vary inversely with cholesterol composition. As the cholesterol composition increased from 0 to 60 mole percent the number of immobilized phospholipids decreased from 30 to 10. Assuming that glycophorin is an archetypical membrane protein, these reconstitution studies were suggested

to indicate thermodynamically stable cholesterol-protein interactions because cholesterol apparently replaces annular phospholipids as the cholesterol/phospholipid ratio increases.

Several inconsistencies with the glycophorin study seemingly indicate that cholesterol cannot simply exchange with phospholipids in the annulus. The decrease in the number of annular phospholipids may not necessarily be the result of cholesterol substitution of phospholipids, but a reduction in the annular protein surface area instead. Assuming that glycophorin can only associate with phospholipids, protein aggregation may occur to avoid interactions with cholesterol. Because the *total* annular surface area is reduced when the protein is aggregated, fewer annular phospholipids are required per protein molecule. In addition to this alternative interpretation, the observation that the number of annular phospholipids decreasing from 30 to 10 as cholesterol content increases from 0 to 60 mole percent has inconsistencies. Since the cholesterol saturation limit of PC is 50 mole percent, approximately 17% of the total cholesterol in a lipid mixture containing 60 mole percent cholesterol must form a separate crystalline domain. Then if only 10 phospholipid molecules comprise a glycophorin annulus in a 50 mole percent cholesterol liposome, cholesterol must be present in the annulus in excess of 2:1 cholesterol/phospholipid, since it has a smaller surface area than phospholipids. However, an annulus probably cannot contain a cholesterol composition that is greater than the saturation limitation of phospholipids. Therefore, whether cholesterol can simply exchange with phospholipids in the annulus of glycophorin is rather uncertain, and these studies fail to conclusively establish if proteins have favorable

interactions with cholesterol.

Similar to the glycophorin investigation, biophysical studies of the  $\text{Ca}^{+2}$  ATPase have tried to determine if cholesterol directly interacts with proteins in lipid bilayers. In one instance, the effect of cholesterol composition on collisional quenchers of the  $\text{Ca}^{+2}$  ATPase intrinsic tryptophan fluorescence was examined (Simmonds *et al.*, 1982). Increasing cholesterol compositions did not relieve the fluorescence quenching of brominated PC, yet increasing levels of brominated cholesterol quenched the  $\text{Ca}^{+2}$  ATPase fluorescence as effectively as brominated PC. These "noncompetitive" results suggest that cholesterol is excluded from annular sites that are normally occupied by phospholipids, but that it does interact at alternative, non-annular sites (speculated to be approximately 3 sites per ATPase monomer) from which phospholipids are excluded. The non-annular sites were suggested to be either regions where protein monomers normally contact, or regions in between the helical loops of the protein. The maximum cholesterol/phospholipid ratio associated with a single  $\text{Ca}^{+2}$  ATPase molecule was estimated to be 0.1. However, this model fails to explain why these putative regions for direct interaction of cholesterol should exclude phospholipids.

Electron spin resonance (ESR) of spin-labelled PC and spin-labelled cholesterol was also used to determine if cholesterol directly interacts with the  $\text{Ca}^{+2}$  ATPase. Silvius *et al.* (1984) found that PC exhibits no greater affinity for the annulus than it does for the bulk lipid phase, whereas cholesterol, in the presence of excess phospholipid, prefers the bulk phase over the annulus by a modest factor of approximately 1.54. As these authors suggest, the results indicate either that: (1) cholesterol

binds to 65% of the number of annular sites with equal affinity as phospholipids, or (2) cholesterol integrates into all of the annular sites with only about 65% of the affinity as a phospholipid.

The  $\text{Ca}^{+2}$  ATPase studies suggest that either cholesterol binds to different high affinity sites (Simmonds *et al.*, 1982) or that it exhibits a comparable affinity as phospholipids for this protein (Silvius *et al.*, 1984). But the results of these two studies are difficult to compare because the cholesterol-binding experiments were performed at vastly different cholesterol compositions. The lowest cholesterol/phospholipid ratio in the fluorescence study was about 0.3, whereas it was only 0.007 for the ESR investigations. These ratios imply that the respective compositions of the reconstituted liposomes were 28 and less than 1 mole percent cholesterol.

Both studies suggest that cholesterol, to a very limited extent, directly interacts with  $\text{Ca}^{+2}$  ATPase. For lipid molecules that are in direct contact with the  $\text{Ca}^{+2}$  ATPase, the purported 0.1 cholesterol/phospholipid ratio (Simmonds *et al.*, 1982) is consistent with the observation that cholesterol and phospholipids have comparable affinities for the  $\text{Ca}^{+2}$  ATPase at the cholesterol/phospholipid ratio of 0.007 (Silvius *et al.*, 1984). Therefore, an increase in the total bilayer cholesterol composition does not necessarily enhance protein-associated cholesterol, because the protein can intrinsically interact with only a few cholesterol molecules. This novel explanation is plausible since cholesterol has the unique ability to "condense" phospholipids. Even at very insignificant compositions (less than 1 mole percent cholesterol), cholesterol may become incorporated into the annulus without replacing any of the

phospholipids. The circumference of the annulus would remain essentially constant by a net reduction in the average molecular surface area. Since annular incorporation of phospholipids and cholesterol should not be a competitive process, cholesterol does not necessarily have to replace phospholipids in the annulus. The  $\text{Ca}^{+2}$  ATPase studies indicate that perhaps a few cholesterol molecules can integrate into the protein annulus independently of the total bilayer cholesterol composition.

The model which describes very limited cholesterol interactions with  $\text{Ca}^{+2}$  ATPase cannot explain the observation that brominated cholesterol quenches the fluorescence as effectively as brominated PC. This result suggests that cholesterol and phospholipids equally incorporate into the protein annulus. For this observation to be consistent with the model proposed herein, brominated cholesterol must be an intrinsically better quencher of tryptophan fluorescence than brominated PC. If so, then a relatively small number of brominated cholesterol derivatives in the protein annulus would quantitatively mimic the effect of a greater amount of brominated phospholipid molecules.

The above model suggests that the limited interaction of cholesterol with the  $\text{Ca}^{+2}$  ATPase does not primarily function in forming a stable annulus. Instead of integrating into the lipid-protein interface, cholesterol apparently interacts with the  $\text{Ca}^{+2}$  ATPase at nonannular sites to essentially modulate the enzymatic activity: Increasing cholesterol composition from 0 to 50 mole percent in dimyristoleoylphosphatidylcholine liposomes significantly enhances  $\text{Ca}^{+2}$  ATPase activity approximately 7-fold (Michelangeli *et al.*, 1990). This increase in enzymatic activity is achieved at cholesterol compositions of at least 30 mole percent. The

rather significant bilayer cholesterol composition is suggested to be required in order to negate phospholipid competition with the  $\text{Ca}^{+2}$  ATPase for cholesterol. At 30 mole percent, cholesterol is suggested to completely saturate all of the  $\text{Ca}^{+2}$  ATPase nonannular binding sites.

As can be seen from the review of various investigations, compared to the extensive studies of cholesterol/phospholipid interactions, the effect of cholesterol on the physical properties of integral membrane proteins is only very rudimentary. Many of the investigations have been limited to determining whether membrane associated proteins can directly interact with cholesterol. Based upon the various integral membrane proteins reviewed herein, cholesterol/protein interactions may possibly depend upon the overall cholesterol composition of the membrane and the intrinsic characteristics of the protein.

The significance of cholesterol composition is evident from the behaviors of bacteriorhodopsin and mitochondrial protein in model membrane systems. Below specific cholesterol compositions, the protein molecules were randomly dispersed, but then became aggregated above the "critical" cholesterol/phospholipid ratios (Hochli *et al.*, 1980 and Cherry *et al.*, 1980). Phase separation, however, may not necessarily preclude cholesterol from directly interacting with the protein. A small percentage of the total bilayer cholesterol might possibly interact directly with either bacteriorhodopsin or the mitochondrial proteins. Indeed, the  $\text{Ca}^{+2}$  ATPase investigations support the concept that a very limited amount of cholesterol associates with some integral membrane proteins, even when cholesterol is present at significant bilayer compositions (Simmonds *et al.*, 1982 and Silvius *et al.*, 1984). Additionally, the aggregation of

bacteriorhodopsin and mitochondrial proteins may simply be a manifestation of the coexistence of binary lipid phases. The phase diagrams of DMPC/cholesterol (Almeida *et al.*, 1992) and DPPC/cholesterol (Vist and Davis, 1990; Sankaram and Thompson, 1991) mixtures indicate that above  $T_c$ , the lateral distribution of cholesterol in bilayers is composition and temperature dependent. Particularly, the DMPC/cholesterol phase diagram shows that at about 37°C a single liquid-disordered phase exists in liquid-crystalline DMPC liposomes at compositions less than 10 mole percent cholesterol. However, lateral inhomogeneity of a liquid-ordered phase occurs beyond this cholesterol/phospholipid ratio. As indicated earlier, the disordered phase is characterized as having a relatively low cholesterol content whereas the ordered phase has a greater cholesterol composition. Assuming that bacteriorhodopsin can only be located in the liquid-disordered region, the formation of the liquid-ordered domain may actually induce the observed aggregation of bacteriorhodopsin in liquid-crystalline DMPC liposomes at 10 mole percent cholesterol. Since some of the total bilayer cholesterol is randomly located throughout the liquid-disordered phase, direct interactions between cholesterol and bacteriorhodopsin seem plausible. Lipid inhomogeneities may similarly affect the lateral distribution of the mitochondrial proteins, however insufficient data on the phase behaviors of multicomponent systems makes additional assertions highly speculative. Therefore, aggregation of integral membrane proteins may not be necessarily indicate unfavorable interactions with cholesterol.

Although cholesterol composition probably affects the lateral distribution of proteins in lipid bilayers, the extent of interaction

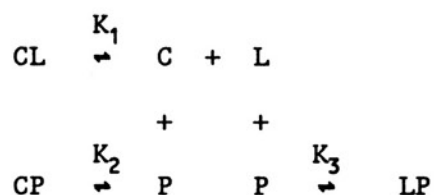
between cholesterol and integral membrane proteins may depend upon the intrinsic properties of the protein itself. If in fact cholesterol can equally replace phospholipids in the annulus of glycophorin (Yeagle, 1984), but it can interact with the  $\text{Ca}^{+2}$  ATPase only to a very minimal extent (Simmonds *et al.*, 1982 and Silvius *et al.*, 1984), the topologies of integral membrane proteins may determine if cholesterol can be included in the annulus.

As previously indicated, it is difficult to formulate definite conclusions about cholesterol-protein interactions from the present results because of the disparities in experimental conditions. Nevertheless, the results that are observed with mitochondrial proteins, bacteriorhodopsin, and  $\text{Ca}^{+2}$  ATPase indicate that integral membrane proteins prefer associations with phospholipids rather than with cholesterol. Because cholesterol interacts to a very limited extent with some integral membrane proteins, it might be useful as a secondary membrane component to phospholipids for creating a stable integral protein annulus or regulating enzymatic activities. The extent to which cholesterol is used as an annular lipid may ultimately depend upon the requirements for maintaining a stable protein conformation in the lipid bilayer matrix.

The biophysical studies which determine the relative affinities of cholesterol and phospholipids for a protein annulus have a rather serious limitation. No matter what results are obtained, the data cannot be used to calculate the effect of cholesterol on the affinity of the protein for the phospholipid-cholesterol mixture, i.e. the affinity of the protein for the bilayer itself. The following hypothetical equilibrium scheme indicates that a protein with equal affinity for cholesterol and



phospholipids does not necessarily have to exhibit equivalent affinities for pure phospholipid bilayers and membranes that contain cholesterol:



In the above scheme C represents cholesterol, L signifies phospholipid, and P is protein. The three equilibria show the interaction of C with L, ( $K_1$ ), the interaction between C and P ( $K_2$ ), and the interaction of L and P ( $K_3$ ). Even if a protein has equal affinity for either phospholipid or cholesterol ( $K_2=K_3$ ), it will have a reduced affinity for the cholesterol/phospholipid mixture (CL) if C preferentially interacts with L rather than with P ( $K_1>K_2$ ). In this instance, formation of the CL mixture is favored instead of the LP and CP complexes. Accordingly, the complex of C and L must have a lower affinity for P, or alternatively, P must have less affinity for a cholesterol/phospholipid mixture than for pure phospholipid.

The reaction scheme indicates that cholesterol can reduce the affinities of integral proteins for lipid bilayers, even if cholesterol and phospholipids individually have comparable affinities for the protein. Apparently, cholesterol "competes" with proteins for phospholipids in membranes. The cholesterol effect of decreasing protein solubility in membranes may be better understood by assuming that lipid molecules must have sufficient intrinsic flexibility to accommodate the irregular shapes of proteins and to maintain the hydrophobic integrity of the bilayer.

Similarly, the second layer of lipid molecules should be rather flexible in order to accomodate the unusual configurations of the annular lipids. Since cholesterol is a rigid molecule it cannot form a complementary interaction with the irregular shapes of integral membrane proteins. In contrast, phospholipids are flexible molecules; segmental motion in the acyl chains enables phospholipids to assume appropriate conformations for effective packing against asymmetric proteins. Accordingly, cholesterol should be essentially excluded from the annuli of proteins. Even if it does not directly contact a protein, cholesterol in the second shell could still restrict the motional freedom of the annular phospholipids. As a result, annular phospholipids would be hindered from adjusting to protein shapes. If so, then cholesterol may decrease the overall affinities of integral proteins for membranes by reducing the solvent effectiveness of phospholipids.

Only the previously discussed morphological studies examine directly the effect of cholesterol on the solubility of a protein in a membrane, and the results of these studies are necessarily semi-quantitative at best.

To obtain quantitative information about the effect of cholesterol on membrane-protein interactions, a study should be designed that is similar to the approach that has been taken to examine the interaction of anesthetics with liposomes. Since these molecules readily partition between the aqueous phase and preformed liposomes, it has been possible to experimentally determine binding isotherms as a function of lipid composition. From the binding data, affinity constants and the saturation level of binding (lipid molecules per site) can be determined. Generally,

such investigations are not possible with integral membrane proteins because they do not readily partition between the aqueous phase and the lipid bilayer. However, cytochrome  $b_5$  is a notable exception. The unusual property of spontaneous binding has been exploited to attempt, for the first time, a systematic study of the interaction of an integral membrane protein with lipid bilayers of different composition and curvature.

Cyt  $b_5$  is an electron transfer protein participating in cholesterol and plasmalogen biosynthesis, cytochrome P-450 reduction, and desaturation of fatty acids [Reviewed by Strittmatter and Dailey, 1982]. Schematically depicted in Figure 7, cyt  $b_5$  is a single polypeptide chain of 133 amino acids with a molecular weight of approximately 16,000. It consists of two independent domains: a highly negatively charged aqueous-soluble catalytic subunit containing a heme prosthetic group at the amino terminus, and a nonpolar membrane anchoring tail at the carboxy-terminus. The entire primary structures have been determined for monkey, rat, rabbit, porcine, bovine, human, equine, and chicken forms of microsomal cyt  $b_5$  (Ozols, 1989, and references therein). The three-dimensional structure of the globular catalytic domain shows that it is a prolate ellipsoid with approximate dimensions of  $25 \text{ \AA} \times 25 \text{ \AA} \times 32 \text{ \AA}$  (Matthews, F. S. *et al.*, 1971; Matthews, F. S. *et al.*, 1972). The heme is held by hydrogen bonding between serine 68 and a heme propionate group, while the heme iron is coordinated by histine residues 43 and 67. Cyt  $b_5$  readily accepts and donates electrons because the oxidized and reduced states of the protein are stabilized by the negatively charged heme propionate and electron-withdrawing heme vinylic moieties, respectively (Reid *et al.*, 1984; Reid *et al.*, 1986). The hydrophobic membrane binding domain, or nonpolar peptide, of cyt  $b_5$  has

been implicated as a signal for spontaneous membrane insertion (George *et al.*, 1989a). This membrane associative property has been studied by genetically constructing a fusion protein of the hydrophobic domain of cyt  $b_5$  and *Escherichia coli*  $\beta$ -galactosidase, a cytoplasmic protein. The hybrid enzyme has been found to bind to *E. coli* membranes (George *et al.*, 1989b) and preformed sonicated vesicles (George *et al.*, 1990).

Cyt  $b_5$  is an excellent protein for studying lipid-protein interactions for several reasons. It can be purified to >99% homogeneity in 100+ mg quantities (Fleming *et al.*, 1978; Greenhut and Roseman, 1985). The purified, detergent-free protein is aqueous soluble, existing either as an octameric complex in high salt (100 mM), or a monomer in low salt (Calabro *et al.*, 1976). Perhaps most important, cyt  $b_5$  spontaneously binds to most membranes and preformed liposomes (Figure 8) (Strittmatter, *et al.*, 1972; Enomoto and Sato, 1973; Dufourcq *et al.*, 1974; Sullivan *et al.*, 1974; Holloway and Katz, 1975; Rogers and Strittmatter, 1975; Remacle, 1978). Not only does the property of spontaneous binding enable the preparation of highly uniformed size vesicles with vectorially oriented protein, it also simulates events *in vivo*, since cyt  $b_5$  is synthesized cytosolically by soluble ribosomes and inserts post-translationally into intracellular membranes (Rachubinski *et al.*, 1978; Okada *et al.*, 1979) without a signal sequence, signal recognition particle, membrane receptors, or ATP hydrolysis (Bendzko *et al.*, 1982; Anderson *et al.*, 1983). Kinetic studies have shown that monomeric cyt  $b_5$  binds to liposomes, and that the dissociation of the octamer is the rate-limiting step in binding (Leto and Holloway, 1979). The protein is conveniently assayed

**Figure 7.**

**The structure of cytochrome  $b_5$ .**



spectrophotometrically from the Soret band at 413 nm. Additionally, the interaction of cyt  $b_5$  with liposomes can be monitored from the enhancement of intrinsic tryptophan fluorescence (Dufourcq *et al.*, 1975; Leto and Holloway, 1979).

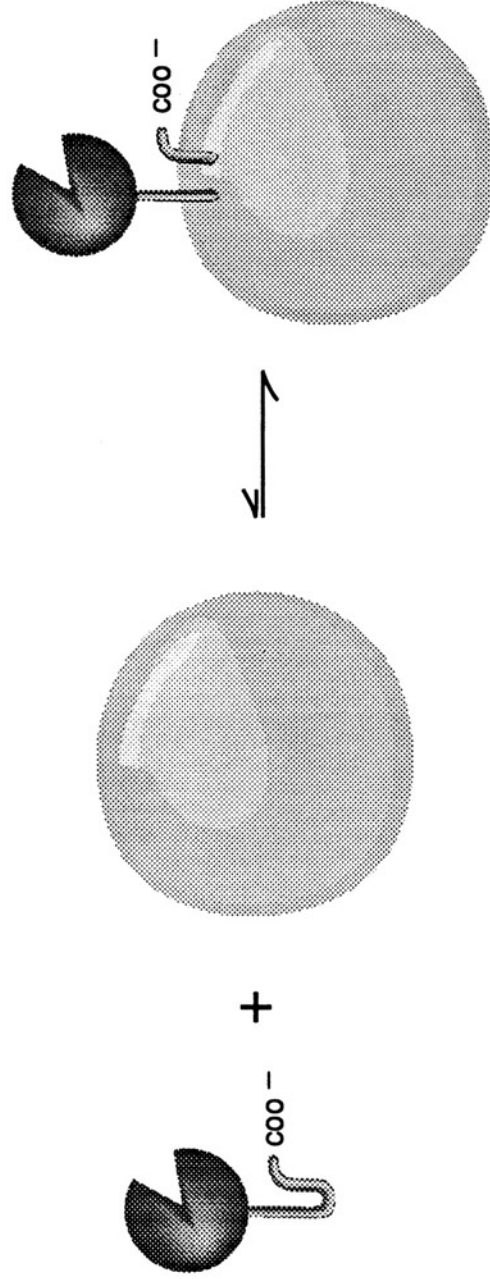
When added to preformed liposomes or isolated membrane fractions, cyt  $b_5$  exhibits one of two binding forms, designated "loose" and "tight." Only the tight form is endogenous to cell membranes. In the "loose" binding form, the hydrophobic tail of cyt  $b_5$  forms a hairpin structure, which purportedly extends to about the middle of the bilayer before looping back to the external aqueous phase (Takagaki *et al.*, 1983a). Hence, the carboxyl-terminal residues remain on the same side (i.e. *cis*) of the membrane with the catalytic domain. The term "loose" insertion describes this binding configuration because cyt  $b_5$  readily transfers between liposome populations (Figure 9) (Roseman *et al.*, 1977; Enoch *et al.*, 1979). Additionally, the "loose" binding form of cyt  $b_5$  is susceptible to carboxypeptidase Y proteolysis at the exposed C-terminus (Enoch *et al.*, 1979). In contrast, tightly inserted cyt  $b_5$  is non-transferable (Figure 10) and is not degraded by carboxypeptidase Y. The topology of the tight binding form has been extensively investigated. Yet the results have led to contradictory conclusions. Hydrophobic photolabelling studies by Khorana's group (Takagaki *et al.*, 1983b) and neutron scattering studies by Gogol and Engelman (1984) suggest that the tight binding form may span the bilayer. However, chemical labelling studies between cyt  $b_5$  and entrapped taurine, a membrane-impermeable nucleophile, indicate that C-terminus is *cis* in the tight configuration (Arinc *et al.*, 1987). More recently, Ozols (1989) has found that externally added trypsin cleaves the C-terminus of

Figure 8.

Cytochrome  $b_5$  Binding to Liposomes.



## Binding to preformed liposomes

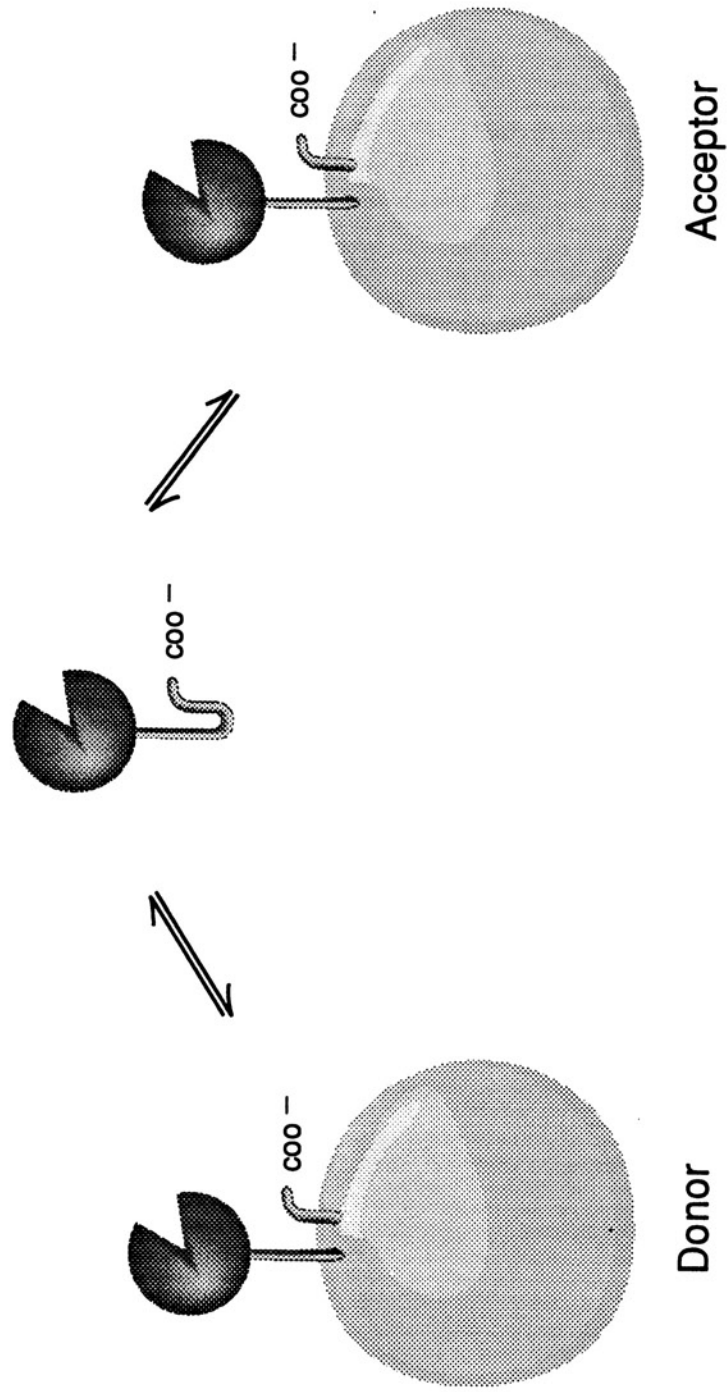


Purified detergent – free cyt b5 is water – soluble and spontaneously binds to most preformed liposomes.

**Figure 9.**

**Loose binding of cytochrome  $b_5$  to liposomes.**

### Loose Binding:

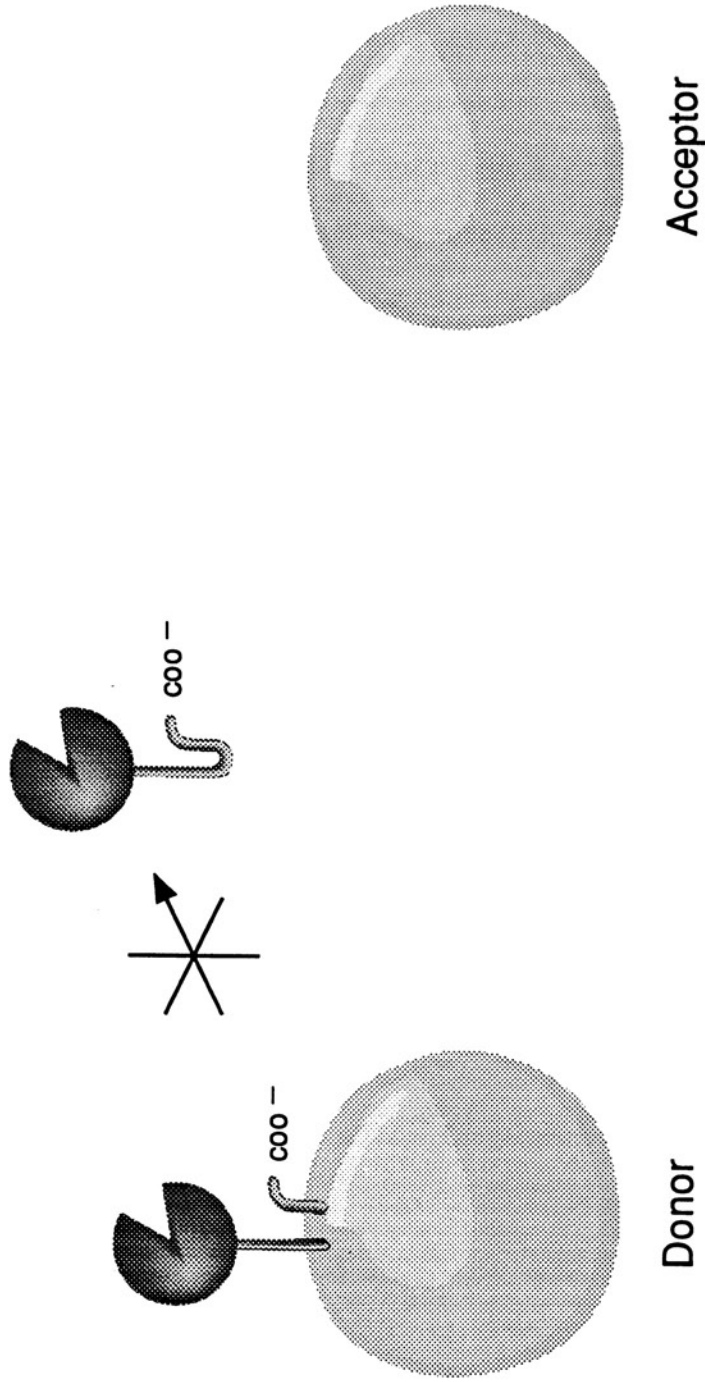


cyt b5 is transferable between liposome populations.

**Figure 10.**

**Tight binding of cytochrome  $b_5$  to liposomes.**

## Tight Binding:



cyt b<sub>5</sub> is nontransferable

Tight insertion is the physiological binding form

endogenous microsomal cyt  $b_5$ , which, in my opinion, rather convincingly indicates that the membrane binding domain is not transmembranal.

Although the topologies of both the loose and tight configuration appear to be helical hairpins, the depth to which the membrane anchoring domain penetrates into the bilayer remains uncertain. Resonance energy transfer between the fluorescent tryptophan of cyt  $b_5$  and *n*-(9-anthroyloxy) fatty acid probes indicate that the tryptophan is located approximately 20 Å below the surface of DMPC liposomes, suggesting that the tail does extend to about the bilayer median (Kleinfeld and Lukacovic, 1985). In contrast, fluorescence quenching studies with various *sn*-2-dibrominated phosphatidylcholines indicate that cyt  $b_5$  is not embedded deeply into membranes. Whether cyt  $b_5$  was either in the loose or tight configuration, the most effective quenching of tryptophan fluorescence was observed in liposomes that were prepared from 1-palmitoyl-2-[(6,7)-dibromo]-stearyl phosphatidylcholine. This result indicates that the quenchable tryptophan is only 7 Å below the liposome surface (Tennyson and Holloway, 1986).

As previously mentioned, endogenous cyt  $b_5$  in liver microsomes invariably exhibits tight insertion (Enoch *et al.*, 1979; Christiansen and Carlsen, 1986; Poensgen and Ullrich, 1980). Exogenously added cyt  $b_5$  also demonstrates relatively high efficiency of spontaneous tight insertion into liver microsomes, which ranges from about 70% (Poensgen and Ullrich, 1980) to 100% (Enoch *et al.*, 1979). In contrast, when cyt  $b_5$  is added to preformed liposomes, the tight insertion is generally inefficient: only 10-20% of the protein becomes tightly bound within 2 hr (Greenhut *et al.*, 1986), followed by a significantly slower phase of tight insertion with a half-time of approximately 9 days (Greenhut *et al.*, 1993). However,

several significant exceptions on cyt  $b_5$  insertion into preformed liposomes have been observed. Cyt  $b_5$  demonstrates 100% tight insertion when added to DMPC vesicles, or to vesicles of egg PC that contain the reconstituted integral membrane protein, stearyl-CoA desaturase (Enoch *et al.*, 1979). The findings suggest that destabilized bilayers may facilitate cyt  $b_5$  tight insertion. Indeed, there is additional precedence for this presumption. For example two other integral membrane proteins, bacteriorhodopsin and cytochrome c oxidase, spontaneously insert into preformed DMPC liposomes that contain small amounts of either myristate or cholesterol as impurities [Reviewed by Jain and Zakim, 1987]. Finally, artificial methods such as detergent-dialysis (Poensgen and Ullrich, 1980) or co-sonication (Enoch *et al.*, 1979) enable cyt  $b_5$  to reconstitute into liposomes in the tight binding form.

As previously noted, cyt  $b_5$  spontaneously binds to membranes and isolated membrane fractions. A notable exception is the plasma membrane; studies with erythrocytes showed that the binding was less than 1 cyt  $b_5$  per 8000 PL (Strittmatter *et al.*, 1972). Enomoto and Sato (1977) hypothesized that the high concentration of cholesterol in the plasma membrane was responsible for the inefficient binding, and designed several experiments to test this possibility. Pretreatment of the membranes with proteases (trypsin) and glycosidases (neuraminidase) failed to significantly enhance cyt  $b_5$  binding, indicating that neither protein nor carbohydrate on the cell surface was preventing binding. However, these authors found an approximate 3 fold increase in cyt  $b_5$  binding to resealed erythrocytes if the plasma membranes were first partially depleted of about 43% cholesterol by transfer to egg phosphatidylcholine multilamellar

liposomes. Similarly, they observed that increasing the cholesterol content in egg PC multilamellar liposomes reduced cyt  $b_5$  binding, from about 1  $b_5$ :636 phospholipids at 0% cholesterol, to 1:1590 at 50 mole percent. Based upon these results the authors concluded that the high cholesterol composition prevents cyt  $b_5$  from binding to plasma membranes. In a subsequent study, Roseman *et al.* (1978) questioned this conclusion for the following reasons: (1) Multilamellar vesicles are heterogeneous with respect to size and surface area, typically with only about 10% of the total lipid exposed to the external medium; (2) approximately 1-2% of the lipid in multilamellar vesicle preparations cannot be sedimented, suggesting that such liposome preparations contain contaminating small vesicles that can amount to 20% of the available surface area. Since these smaller vesicles along with any bound protein would not sediment under Enomoto and Sato's experimental conditions, the protein in the supernatant would have been considered unbound. (3) The cholesterol-depleted erythrocyte membranes became highly permeable during the high temperature incubation with cyt  $b_5$ . Roseman *et al.* (1978) subsequently demonstrated that at a 1 cyt  $b_5$ :1000 egg PC ratio cyt  $b_5$  completely binds to SUVs containing 44 mole percent cholesterol. Since this level of binding was significantly greater than what was observed with erythrocyte membranes, it was concluded that even if cholesterol can reduce the saturation level of cyt  $b_5$  binding, the extent of the inhibition is not sufficient to account for the results that are observed with plasma membranes.

The basis for the present research investigation comes from a preliminary observation that I made to determine if the relatively significant amount of cyt  $b_5$  binding to cholesterol-containing liposomes



is primarily attributable to the curvature effects of SUVs. Cyt  $b_5$  partitioning into large and small unilamellar vesicles of POPC containing 50 mole percent cholesterol was examined (Taylor and Roseman, 1990). In direct binding mixtures of 1 cyt  $b_5$  : 400 POPC, >91% of cyt  $b_5$  binds to LUVs and SUVs that are devoid of cholesterol. However, for liposomes that have a 1:1 cholesterol to phospholipid mole ratio, 94% of the cyt  $b_5$  binds to SUVs, whereas <5% binds to LUVs.

These results indicate that lipid composition and membrane curvature can have profound effects on the binding of integral membrane proteins, and suggest that a systematic investigation of cyt  $b_5$  interactions with liposomes of different curvature and cholesterol content would provide some significant insights into the biophysical chemistry of lipid-protein interactions.

The specific aim of this research is to investigate in detail the effect of cholesterol on the binding and insertion of cytochrome  $b_5$  into liposomes of various phosphatidylcholines. The phospholipids that were selected, specifically disaturated, diunsaturated, polyunsaturated, and mixed acyl chain phospholipids, are representative of those used in a variety of previous biophysical investigations that examine cholesterol in lipid bilayers. In the first part of this work, the saturation level of cyt  $b_5$  binding to LUVs and SUVs prepared from a variety of natural and synthetic phosphatidylcholines is determined by gel-filtration and fluorescence spectroscopy, respectively. Next, cyt  $b_5$  binding and insertion is systematically studied over the 0-50 mole percent range of cholesterol compositions. Finally, the effect of cholesterol on the binding affinity of cyt  $b_5$  is determined. The results are interpreted in terms of a

unifying model that is based upon cholesterol-mediated reduction in bilayer free-volume and the physico-chemical model for cholesterol-phospholipid interactions in liquid-crystalline bilayers (Hyslop, *et al.* 1990).

By studying in detail the binding and insertion in model systems, cyt  $b_5$  also functions as a probe molecule that ultimately provides insight to the physical chemistry of membranes. I hope that this research will not only help further elucidate the role of cholesterol in lipid-protein interactions, but will also contribute to the general understanding of cholesterol-phospholipid interactions.

A preliminary report of this investigation has been presented (Taylor and Roseman, 1993).

## EXPERIMENTAL PROCEDURES

### A. *Materials.*

Synthetic and natural phospholipids: 1,2-dimyristoyl-*sn*-glycero-3-phosphorylcholine (DMPC), 1,2-dioleoyl-*sn*-glycero-3-phosphorylcholine (DOPC), 1,2-dilinoleoyl-*sn*-glycero-3-phosphorylcholine (DLPC), 1-palmitoyl-2-oleoyl-*sn*-glycero-3-phosphorylcholine (POPC), 1-stearoyl-2-oleoyl-*sn*-glycero-3-phosphorylcholine (SOPC), 1-palmitoyl-2-linoleoyl-*sn*-glycero-3-phosphorylcholine (PLPC), 1-stearoyl-2-linoleoyl-*sn*-glycero-3-phosphorylcholine (SLPC), egg L- $\alpha$ -phosphatidylcholine (egg PC), bovine liver L- $\alpha$ -phosphatidylcholine (liver PC), transphosphatidylated phosphatidylethanolamine, prepared from egg PC (PE), and bovine brain sphingomyelin (SPM), >99% purity were purchased from Avanti Polar Lipids (Alabaster, Alabama). Highly purified (>99%) cholesterol was from Calbiochem Corporation (La Jolla, California). Lipids were used without further purification. [ $^{14}\text{C}$ ]-POPC (specific activity, 58.0  $\mu\text{Ci}/\mu\text{mole}$ ) and [ $^3\text{H}$ ]-triolein (specific activity,  $2.68 \times 10^4$   $\mu\text{Ci}/\mu\text{mole}$ ) were from New England Nuclear. TNBS was obtained from Fluka Chemika-BioChemika.

Cytochrome  $b_5$ , from bovine liver, was purified to homogeneity as described by Greenhut and Roseman (1985).

### B. *Buffer Solutions.*

The following buffers were used in this investigation: 20 mM Tris, 100 mM NaCl, 0.1 mM EDTA, pH 8.1 (Tris-acetate buffer); 40 mM Bicine, 10 mM NaCl, 0.1 mM EDTA, pH 8.5 (Bicine buffer).

**C. Preparation of Large Unilamellar Vesicles (LUVs).**

Large unilamellar vesicles were prepared by the reverse-phase evaporation method of Düzgünes *et al.* (1983), using either Tris-acetate or Bicine buffer as the aqueous phase. Phospholipids and cholesterol (100-200  $\mu$ moles total lipid) were incorporated into liposomes by first co-dissolving the lyophilized lipids in 5-10 ml of chloroform. 1.0  $\mu$ Ci of [ $^{14}$ C]-POPC or [ $^3$ H]-triolein was included to radioactively label the vesicles. Chloroform was removed by rotary evaporation followed by lyophilization from benzene under high vacuum. Liposome dispersions were formed by the controlled evaporation of ether (Büchi Rotavapor) from lipid emulsions, maintained above  $T_c$ . The initially formed liposomes were then extruded through successive polycarbonate membranes (Nuclepore) of 0.4, 0.2, 0.1, and 0.08  $\mu$ m pore size. For vesicles having a high cholesterol content, ( $\geq 30$  mole percent cholesterol), extrusion was facilitated using a model HPVE-10 high pressure extrusion apparatus (Sciema Technical Ltd., Vancouver, Canada). Contaminating small and intermediate size vesicles were removed by gel-filtration on a Pharmacia Sepharose 2B-CL column (1.6 x 55 cm); only the peak void-volume fractions were used (Greenhut *et al.*, 1986). Lipid phosphorous was determined by the method of Bartlett (1959).

**D. Preparation of Small Unilamellar Vesicles (SUVs).**

Preparations of homogeneous limit-size small unilamellar vesicles were produced by ultrasonication of lipid dispersions in Tris-acetate buffer (Greenhut and Roseman, 1985). Approximately 100-200  $\mu$ mole of total lipid (phospholipid  $\pm$  cholesterol) were dissolved in chloroform with or without 1-2  $\mu$ Ci of [ $^{14}$ C]-POPC. Solvent was removed by rotary evaporation

followed by lyophilization from 5 ml benzene under high vacuum for a minimum of 12 hours. The dried lipid was subsequently suspended in 11 ml of Tris-acetate buffer pH 8.1, transferred to a 15-ml Corex tube, and sonicated under argon to constant clarity (W-375 Heat Systems-Ultrasonics sonicator, 0.5-in. probe, 50% pulsed duty cycle). Constant temperature was maintained above the gel-to-liquid crystalline phase transition during sonication using a water bath. Contaminating larger vesicles were removed by differential ultracentrifugation (Ti50 fixed-angle rotor, 45,000 rpm, 60 min) as described by Barenholz *et al.* (1977).

***E. Determination of Outside to Inside Lipid Mass Ratios of Reverse-Phase Liposomes.***

The fraction of the total lipid on the exterior liposome surfaces was determined by chemical labelling with TNBS (Greenhut and Roseman, 1985 and Roseman *et al.*, 1975). Liposomes doped with phosphatidylethanolamine (10 mole percent of total phospholipid) were prepared by the reverse-phase evaporation protocol that is described in Part C, using Bicine buffer for the aqueous phase.

(A) *Determination of Lipid on the Outer Liposome Surface.* Aliquots of the liposome preparations that contained a maximum of 0.1  $\mu$ mole of PE were diluted to 400  $\mu$ l with Bicine buffer. The labelling reaction was initiated by the addition with vortexing of 10  $\mu$ l 1.5% TNBS in distilled H<sub>2</sub>O. The TNBS solution was prepared immediately prior to use. Samples were incubated in the dark for 10-60 minutes at 25°C. The reaction was terminated at 10 minute intervals by the rapid addition and vortexing of 600  $\mu$ l 1.06% Triton X-100/1.5 N HCl. The 410 nm absorbance was obtained

immediately in a Gilford Response spectrophotometer. The detection of the trinitrophenyl-PE derivative was adjusted for background by subtracting the  $A_{410}$  for separate blanks of LUVs and TNBS alone at each time interval, using Bicine buffer as a reference. Each derivative sample and blank were assayed in triplicate. Leakage of TNBS into liposomes was corrected by extrapolating the kinetically linear slow phase back to zero time and using the ordinate intercept as the true measure of external PE.

(B) *Determination of Total Lipid.* Equal aliquots of the liposome preparation that were used to determine external lipid were also used for the total lipid assay. After diluting the samples to 300  $\mu$ l with Bicine buffer, the liposomes were solubilized by addition of 100  $\mu$ l of 1.6% Triton X-100, 40 mM Bicine, 10 mM NaCl, 0.1 mM EDTA, pH 8.5. The TNBS reagent (10  $\mu$ l) was then added, and the samples were mixed and incubated at 25°C for 15 minutes. An additional 200  $\mu$ l of 1.6% Triton X-100 solution was added, and the reaction was incubated for an additional 15 minutes. The reaction was terminated by the addition of 400  $\mu$ l 0.4% Triton X-100/1.5 N HCl. As for the external assay, the absorbance of the trinitrophenyl-PE derivative was corrected by subtracting the absorbancies of separate blanks of only LUVs and TNBS. All assays were performed in triplicate.

The lamellarity of liposomes was determined from the ratio of the external to internal PE.

#### **F. *Cytochrome $b_5$ Saturation of Large Unilamellar Vesicles.***

Detergent-free cyt  $b_5$  and preformed LUVs were incubated above  $T_c$  (30 or 37°C) in Tris-acetate buffer for prolonged periods of 24-48 h under

argon. The initial cyt  $b_5$  to phospholipid ratio was varied from 1:40 to 1:417. The extent of cyt  $b_5$  binding was determined by separating the proteoliposomes from unbound protein by gel-filtration on a Pharmacia Sepharose 2B-CL column ( $0.9 \times 28.5$  cm if 2  $\mu$ moles phospholipid were used, or  $1.6 \times 55$  cm if 5-20  $\mu$ moles of phospholipid were used). Cyt  $b_5$  was assayed according to the method of Greenhut *et al.* (1986): to fraction samples in 900  $\mu$ l Tris-acetate buffer, 100  $\mu$ l 10% (w/w) deoxycholate was added (in order to eliminate light scattering by the liposomes) and the absorption spectra were obtained over the range 350 to 500 nm using an SLM-Aminco DW-2C spectrophotometer. The concentration of cyt  $b_5$  was calculated using a molar extinction coefficient of  $1.17 \times 10^5 \text{ M}^{-1} \text{ cm}^{-1}$  at 413 nm (Spatz and Strittmatter, 1971). Elution profiles of  $^{14}\text{C}$ - or  $^3\text{H}$ -labelled liposomes were determined by scintillation counting (60 s) of fraction samples using Beckman HP liquid scintillation cocktail. The extent of binding was determined from the amount of cyt  $b_5$  eluting with the liposomes in the initial incubation mix.

#### G. *Cytochrome $b_5$ Saturation of Small Unilamellar Vesicles.*

The cyt  $b_5$  saturation limit of SUVs was determined from the enhancement in the intrinsic tryptophan fluorescence of cyt  $b_5$  upon binding to vesicles (Dufourcq *et al.*, 1975). Separate samples of cyt  $b_5$  (1.56  $\mu\text{M}$ ) with variable lipid concentration (0-0.624 mM phospholipid) were incubated for 2 h at 25°C or 37°C, depending on the  $T_c$  of the lipids. Fluorescence spectra were obtained in a magnetically stirred cuvette using an SLM-Aminco SPF-500 spectrofluorimeter operating in the ratio mode. Constant temperature of the sample was maintained using a cuvette holder

thermostatted at either 25°C or 37°C. Excitation and emission wavelengths were 280 and 338 nm; bandwidths were 2.5 and 5 nm, respectively. Where appropriate, cyt  $b_5$  fluorescence spectra were adjusted for light scattering by subtracting the scattering spectral intensities of vesicles alone at the corresponding concentrations. The maximum total lipid concentration (1.248 mM) used in these studies was not sufficient to significantly attenuate the incident light beam (Leto and Holloway, 1979 and references therein). The fraction of cyt  $b_5$  bound to vesicles was quantitated using an equation derived by Leto and Holloway (1979):

$$X_{BD} = 1 - (F_{BD} - F_{OBS}) / (F_{BD} - F_{UBD}) \quad (1)$$

where  $X_{BD}$  is the fraction of bound protein,  $F_{BD}$  is the endpoint fluorescence of cyt  $b_5$  obtained in the presence of excess lipid,  $F_{UBD}$  is cyt  $b_5$  fluorescence in the absence of liposomes, and  $F_{OBS}$  is the fluorescence of cyt  $b_5$  during the titration course of increasing lipid concentration. Binding data was evaluated in terms of a nonlinear Scatchard model as described in the following section.

#### H. *Analysis of Cytochrome $b_5$ Binding Isotherms.*

Binding data for cyt  $b_5$  interaction with SUVs was replotted according to the conventional Scatchard method ( $[\text{bound cyt } b_5] / [\text{PL}] [\text{unbound cyt } b_5]$  vs.  $[\text{bound cyt } b_5] / [\text{PL}]$ ). The plots were then analyzed by an iterative curve-fitting routine of a 2-dimensional model which considers the membrane surface as a lattice for large ligand interaction. The general Scatchard equation which accounts for statistical factors as membrane



lattice geometry (Stankowski, 1983a), ligand shape (Stankowski, 1983b), and cooperativity (Stankowski, 1984) has been formulated as:

$$r/C_A = K_{eff}(1-nr) \left[ 1 - \frac{\lambda nr}{1+nr(\lambda-1)} \cdot \frac{2}{\lambda+1} \right]^\gamma \quad (2)$$

with

$$\lambda = [1 + 4(\eta-1)\lambda nr(1-nr) / (1-(1-\lambda)nr)^2]^{1/2} \quad (3)$$

where  $r$  is the solution concentration mole ratio of bound protein to total phospholipid;  $C_A$  is the concentration of free ligand;  $K_{eff}$  is the effective or apparent binding constant,  $n$  is the number of lipid molecules that constitute an adsorption site or the number of lipid molecules that are excluded from further ligand adsorption;  $\lambda$  is a parameter that accounts for lattice geometry or structure (which is based on  $n$  and the ligand shape);  $\gamma$  describes the ligand shape; and the parameter  $\eta$  indicates the type and extent of cooperativity. In a Scatchard plot of  $r/[free\ ligand]$  vs.  $r$ , Eqn. 2 generates a negatively curved function with ordinate and abscissa intercepts  $K_{eff}$  and  $1/n$ , respectively.

A specific equation that could be directly applied to cyt  $b_5$  interaction with liposomes was obtained by determining the limiting values for the binding parameters (i.e. the minimum stoichiometric number of phospholipid per protein). The interaction of cyt  $b_5$  monomers with a binding lattice on the liposome surface was modeled upon the following assumptions: (1) Since the three-dimensional structure of the cyt  $b_5$  catalytic domain is a prolate ellipsoid of dimensions  $25\text{\AA} \times 25\text{\AA} \times 32\text{\AA}$  (Mathews, et al., 1972), the catalytic domain was determined to cover approximately  $491 - 628\text{\AA}^2$  on the bilayer surface, depending upon its

rotational orientation. For simplicity, the greater surface area was selected for the binding lattice model so that the precise domain alignment could be disregarded. (2) The average phospholipid molecular area is approximately  $77\text{\AA}^2$ . Since a cyt  $b_5$  adsorption site apparently requires at least 8 phospholipids, the liposome surface was modeled as a stretched hexagon.

The stretched hexagonal matrix was assumed to have a molecular arrangement of a single contour shell ( $p=1$ ) of eight phospholipids that surrounds a linear sequence of two additional phospholipid molecules (length  $k=2$ ) (Figure 11). This minimum binding surface has an overall length of  $a=4$  phospholipids (where  $a=k+2p$ ) and breadth of  $b=3$  phospholipids (where  $b=2p+1$ ). The geometrical parameter  $\lambda$  for a stretched hexagonal arrangement of phospholipid molecules has been mathematically derived (Stankowski, 1984):

$$n\lambda = [2(a + p) + 1]/3 \quad (4)$$

The excluded area  $\alpha$ , or the total number of lipid subunits that are effectively inhibited from additional ligand adsorption (including the membrane contacts that are actually covered by a bound ligand), has also been similarly formulated for a stretched hexagonal lattice (Stankowski, 1984):

$$n\alpha = [2a^2 - p^2 + 10ap - 7p - a - 1]/3 \quad (5)$$

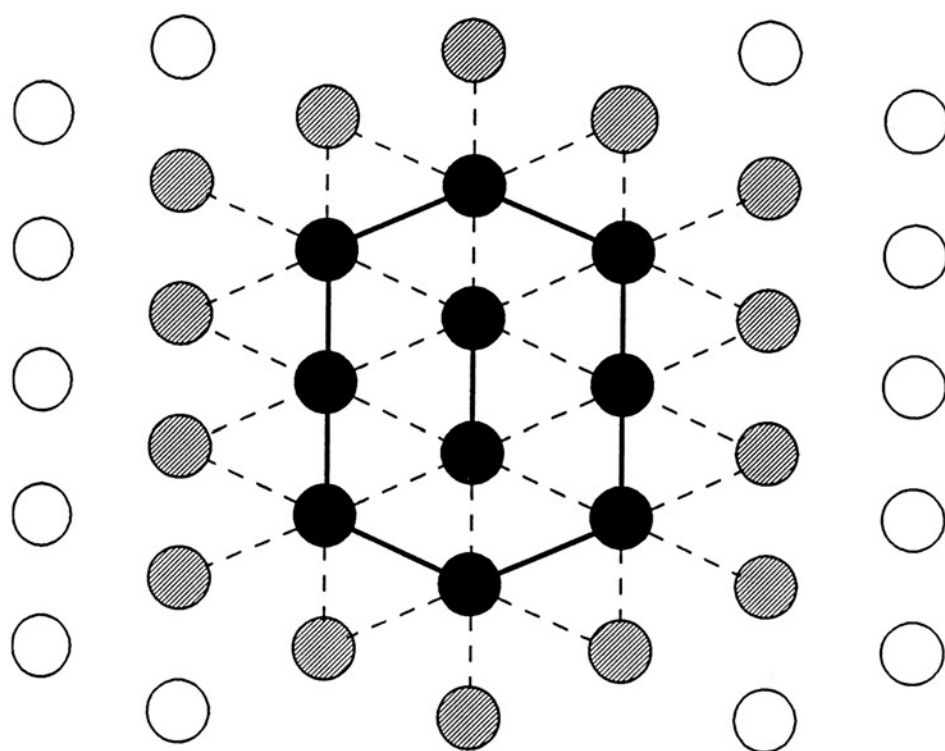
Inserting  $a=4$ ,  $b=3$ , and  $p=1$  into Eqns. 4 and 5 and solving for  $\lambda$  and  $\alpha$  respectively gives:

$$\begin{aligned} \lambda &= 3.7/n \\ \alpha &= 19.7/n \end{aligned} \quad (6a,b)$$

Additionally, the general ligand shape parameter  $\gamma$  has been defined in

Figure 11.

Model of stretched hexagonal lattice for cytochrome  $b_5$  adsorption to liposome surfaces. Circles represent individual phospholipid subunits on the liposome surface. The minimal adsorption surface area, a stretched hexagonal lattice (filled circles connected by solid lines) consists of 10 subunits: 8 phospholipids circumscribing a linear sequence of 2 additional molecules. The hatched circles are subunits of the nearest neighbor shell. Subunit pair contacts are depicted as bond lines (solid & dashed lines). Each lattice subunit has six pair contacts, giving a coordination number of  $z=6$ . The number of subunit pair contacts with the nearest neighbor shell ( $i=22$ ) is similarly indicated.



terms of lattice geometry and excluded area (Stankowski, 1984):

$$\gamma = \alpha/\lambda \quad (7)$$

Substituting Eqns. 6a,b, and 7 for  $\lambda$ ,  $\alpha$ , and  $\gamma$  in Eqns. 2 and 3 and simplifying gives an expression that describes cyt  $b_5$  binding to liposomes:

$$r/C_A = K_{eff}(1-nr) \left[ 1 - \frac{3.7r}{1+3.7r-nr} \cdot \frac{2}{\sqrt{1+14.8(\eta-1)r(1-nr)/(1-nr+3.7r)^2}} \right]^{5.3} \quad (8)$$

with

$$\sqrt{1+14.8(\eta-1)r(1-nr)/(1-nr+3.7r)^2} \quad (9)$$

Fitting of Eqn. 8 to experimental data was performed by an iterative process in which  $K_{eff}$ ,  $n$  and  $\eta$  were varied as free parameters. The set of parameters which gave the best curve-fit to the data were assumed to be the solutions of the binding function.

#### ***I. Cytochrome $b_5$ Binding Affinity for Reverse-phase Liposomes Containing Cholesterol.***

Individual samples of cyt  $b_5$  (1.56  $\mu$ M) were incubated with variable amounts of LUVs (0-2.028 mM POPC) for 2 h at 25°C. The extent of cyt  $b_5$  binding at different POPC: $b_5$  ratios was determined by fluorometry as described in Part G. Fluorescence spectra were adjusted for liposome light scattering as described for the SUV saturation studies; additional correction for excitation beam attenuation in the turbid samples was performed by multiplying the baseline-adjusted fluorescence spectra by a factor of  $\text{Antilog } A_{280}/2$  (Leto and Holloway, 1979), in which  $A_{280}$  is the 280 nm absorbance of LUVs alone at the appropriate concentrations. The cyt  $b_5$  binding isotherms were evaluated by replotting the data in Scatchard form and applying the analytical methods of Stankowski (1984). Assuming a

prolate ellipsoid shape for the cyt  $b_5$  catalytic domain, the liposome surface was modeled as a stretched hexagon. Relative binding lattice sizes and the corresponding geometrical parameters  $\lambda$ ,  $\alpha$ , and  $\gamma$ , were determined from saturation studies of direct binding mixtures of cyt  $b_5$  and LUVs.

*J. Transfer Studies of Cytochrome  $b_5$  between Liposome Populations.*

Cytochrome  $b_5$  transfer between cholesterol-containing liposome populations was investigated to distinguish fractions of "loosely" and "tightly" bound cyt  $b_5$ . LUVs (labelled with  $^3\text{H}$ -triolein) and SUVs (containing  $^{14}\text{C}$ -POPC) were prepared from common stock solutions of 1-palmitoyl-2-oleoyl-*sn*-glycero-3-phosphorylcholine (POPC) and cholesterol. Proteoliposome complexes were formed by incubating purified detergent-free cyt  $b_5$  with LUVs for 2 or 24 h at 30°C, under argon in Tris-acetate buffer. Transfer experiments were performed by incubating LUVs, having completely bound cyt  $b_5$  (no unassociated protein), with a 3-fold (2 h binding incubation) or 4-fold (24 h binding incubation) lipid (mole/mole) excess of SUV acceptors for 2-8 h at 30°C under argon in the same buffer. Donor and acceptor liposome populations were separated by either gel-filtration on a Pharmacia Sepharose 2B-CL column (0.9 × 28.5 cm if 4  $\mu\text{moles}$  POPC were used; or 1.6 × 55 cm if 20  $\mu\text{moles}$  POPC was used) or sedimentation through glycerol step gradients (0.6 ml sample at the top, then 1.3 ml 1% glycerol, 20 mM Tris-acetate, 100 mM NaCl, 0.1 mM EDTA, pH 8.1, and finally, a 0.1 ml 60% glycerol pad) at 45K rpm, 1 hr at 25°C in Ti-50 fixed-angle rotor. (Additional details are described in the text.)

## RESULTS

### *Characterization of Reverse-Phase Liposomes.*

To investigate if the incorporation of cholesterol into reverse-phase liposomes significantly affects vesicle properties with respect to the number of lamellae, as well as to ascertain the amount of exposed surface area available for cyt  $b_5$  interaction, the outside:inside lipid mass ratios was determined by chemical labelling with TNBS for all of the studied phospholipid systems.

The results of two representative TNBS experiments are shown in Figures 12 and 13 for reverse-phase liposomes of POPC  $\pm$  50% cholesterol. For intact vesicles, the trinitrophenylation reaction displays an initial rapid phase during the first 10-20 minutes, followed by a significantly slower, linear phase. In Bicine buffer, the external phosphatidylethanolamine amino groups were completely labelled with the TNBS reagent within 20-30 minutes, as previously observed by Greenhut and Roseman (1985). The slow phase beyond the endpoint of the external reaction results from leakage of TNBS into the liposomes. External PE is therefore determined by extrapolating the slow phase back to  $t=0$ , as shown. The horizontal lines above the kinetic curves in Figures 7 and 8, represent the total PE values, obtained when the liposomes are disrupted by Triton X-100.

Table I lists the average outside:inside lipid mass ratios of reverse-phase liposomes prepared from the various phosphatidylcholines and cholesterol. The qualifying term "average" is used here to indicate that liposomes prepared by this procedure are not necessarily homogeneous with respect to size and the number of lamellae, and the out:in ratio is a mean

Figure 12.

External:Total PE Determination by Trinitrophenylation for POPC Reverse-phase Liposomes; 0% cholesterol. POPC/PE (9:1) liposomes, prepared in Bicine buffer were labelled with TNBS as described in Experimental Procedures. The percentage of external PE was determined kinetically by assaying samples for the trinitrophenyl derivative at 10 minute intervals (●). Leakage was corrected by extrapolating the linear slow phase back to zero time. The dotted horizontal line indicates the result for the trinitrophenylation assay of total PE (○).



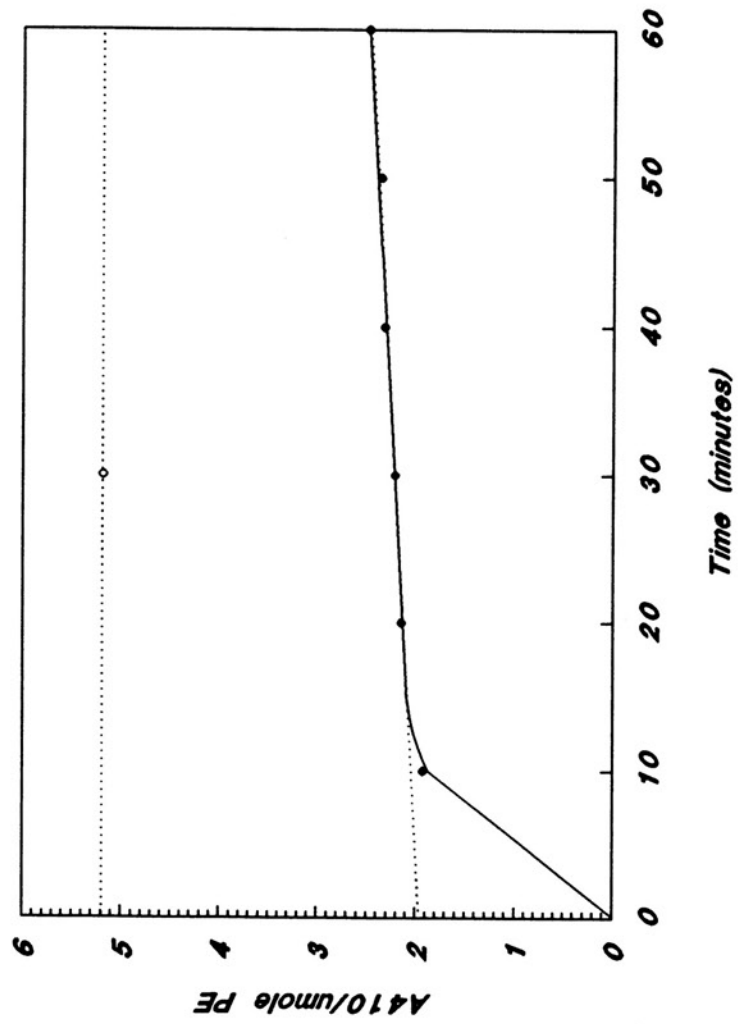
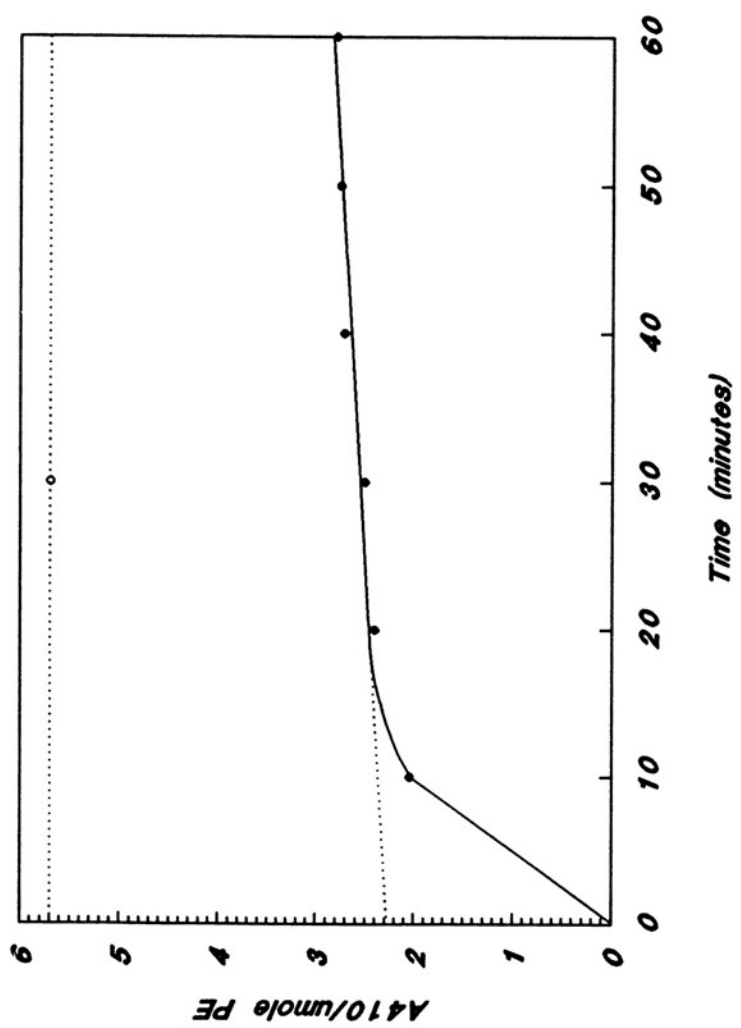


Figure 13.

External:Total PE Determination by Trinitrophenylation for POPC Reverse-phase Liposomes; 50% cholesterol. Same as in Figure 12, except that POPC/PE (9:1) liposomes have a 1:1 phospholipid/cholesterol mole ratio.



value representative of a narrow size distribution. Lichtenberg and Barenholz (1988) recommend that liposome dispersions that have out:in ratios of 1.0-1.2 be classified as large unilamellar vesicles, whereas preparations that exhibit ratios less than 1.0 should be described as oligolamellar and multilamellar vesicles.

In most cases, the out:in ratio for reverse-phase liposomes used in this study is less than 1.0. Approximately 40% of the lipid is located on the outer monolayer. Hence about 80% of the total lipid forms bilayers that can interact with cyt  $b_5$ , with 20% of the lipid sequestered within larger vesicles. Therefore, the liposomes used in this study are probably a mixture of predominantly unilamellar and oligolamellar vesicles. Perhaps most important, there is essentially no change in the out:in ratios of reverse-phase liposomes with incorporation of 50 mole percent cholesterol, indicating that cholesterol does not significantly affect liposome properties with respect to the number of lamellae. Determination of the liposomal surface areas available for cyt  $b_5$  binding will become significant in explaining the results in terms of a molecular model.

Table I: Effect of Cholesterol on the Lamellar Parameter of Reverse-Phase Liposomes<sup>a</sup>

Phospholipid	<u>0% Cholesterol</u>			<u>50% Cholesterol</u>		
	% Out	% In	Out:In	% Out	% In	Out:In
DMPC	52.4	47.6	1.10	48.0	52.0	0.92
DOPC	44.1	55.9	0.79	42.1	57.9	0.73
DLPC	54.1	45.9	1.18	48.8	51.2	0.95
POPC	37.9	62.1	0.61	40.0	60.0	0.67
SOPC	33.6	66.4	0.51	30.2	69.8	0.43
PLPC	37.9	62.1	0.61	39.7	60.3	0.66
SLPC	37.8	62.2	0.61	32.6	67.4	0.48
egg PC	35.8	64.2	0.56	38.3	61.7	0.62
liver PC	42.2	57.8	0.73	46.9	53.1	0.88
PC/SPH (1:1)	45.9	54.1	0.85	45.8	54.2	0.85

<sup>a</sup>The lamellarity of reverse-phase liposomes was determined by trinitrophenylation as described under Experimental Procedures.

*The Effect of Cholesterol on the Binding of Cytochrome  $b_5$  to Large Reverse-Phase Liposomes of Various Phosphatidylcholines.*

Cytochrome  $b_5$ -liposome complexes form spontaneously from the simple mixing of protein with preformed vesicles. The extent of cyt  $b_5$  binding to reverse-phase liposomes can then be conveniently determined by gel-filtration on a Sepharose 2B-CL column. Figures 14-19 show some of the typical results when saturating amounts of cyt  $b_5$  are added to preformed liposomes of DMPC, DOPC, DLPC, POPC, PLPC, and egg PC with and without 50 mole percent cholesterol. In all cases, LUVs and associated cyt  $b_5$  co-elute in the void volume, whereas unbound cyt  $b_5$  elutes from the included volume. As shown, the gel-filtration method gives essentially complete resolution of cyt  $b_5$ -liposome complexes and unbound protein.

Figures 14-19 explicitly show that cholesterol has a significant inhibitory effect with some phospholipids, and a relatively minor effect with others. Additionally, cholesterol does not enhance cyt  $b_5$  binding to liposomes prepared from any of the examined phospholipids. Table II summarizes the cyt  $b_5$  saturation levels of LUVs that are prepared from a variety of natural and synthetic phosphatidylcholines with and without 50 mole percent cholesterol. In order to quantitate and compare this effect among phospholipids, a cholesterol inhibitory parameter  $\phi$  is defined as:

$$\phi = \frac{[\text{cyt } b_5 / 1000 \text{ phospholipids}]_{\text{No cholesterol}}}{[\text{cyt } b_5 / 1000 \text{ phospholipids}]_{50\% \text{ cholesterol}}}$$

Figure 14.

Effect of cholesterol on the saturation level of cytochrome  $b_5$  binding to DMPC LUVs. (A) 0% cholesterol. Cyt  $b_5$  (0.1  $\mu$ moles) and DMPC liposomes (5  $\mu$ moles DMPC doped with  $7.3 \times 10^4$  dpm [ $^{14}\text{C}$ ]-POPC/ $\mu$ mole DMPC) were incubated in a total volume of 1.52 ml Tris-acetate buffer for 24 h at 37°C under argon. 1.4 ml of the incubation mixture was then applied to a Sepharose 2B-CL column (1.6  $\times$  55cm) equilibrated in Tris-acetate buffer and thermostatted at 37°C. Aliquots of 1.7 ml fractions were assayed for DMPC (●) from the dpm of  $^{14}\text{C}$  and cyt  $b_5$  (○) from the absorption spectra as described in Experimental Procedures. (B) 50% cholesterol. Cyt  $b_5$  (0.024  $\mu$ moles) was incubated with liposomes containing 10  $\mu$ moles each of DMPC and cholesterol (doped with  $8.6 \times 10^4$  dpm [ $^{14}\text{C}$ ]-POPC/ $\mu$ mole DMPC) in a total volume of 1.81 ml. 1.66 ml of the incubation mixture was then applied to the Sepharose 2B-CL column. Otherwise, the protocol was the same as in A.

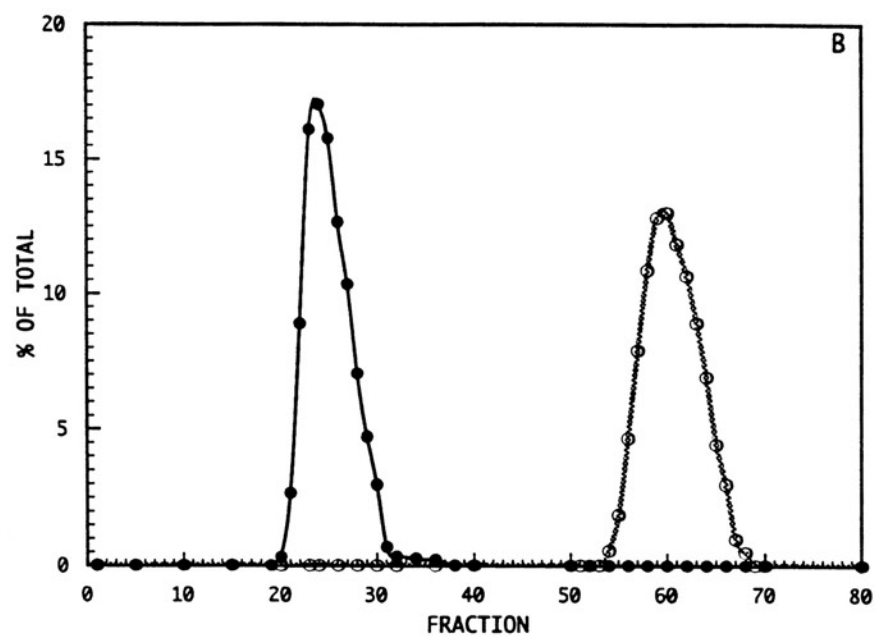
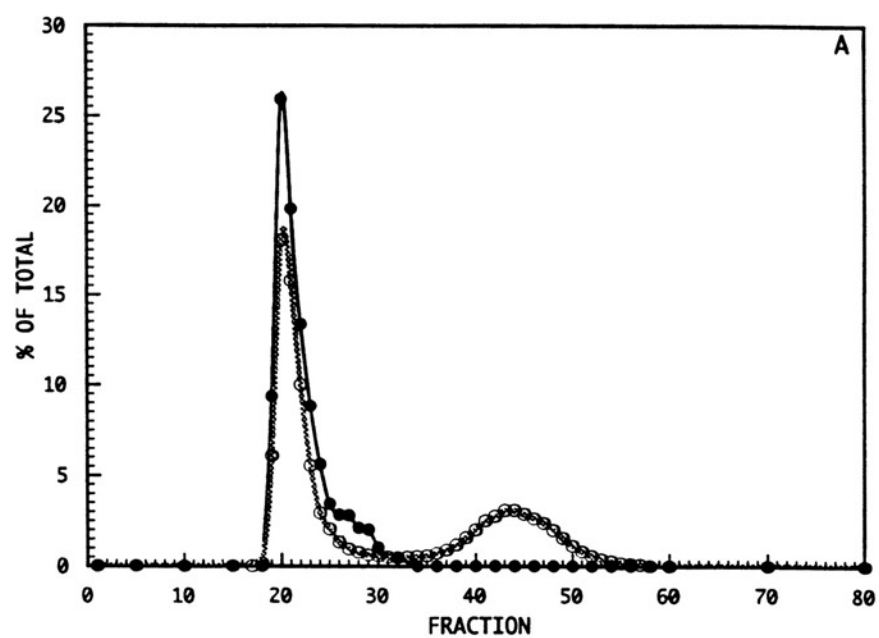




**Figure 15.**

**Effect of cholesterol on the saturation level of cytochrome  $b_5$  binding to DOPC LUVs.** (A) *0% cholesterol.* Cyt  $b_5$  (0.04  $\mu$ moles) and DOPC liposomes (2  $\mu$ moles DOPC doped with  $8.6 \times 10^4$  dpm [ $^{14}\text{C}$ ]-POPC/ $\mu$ mole DOPC) were incubated in a total volume of 558  $\mu$ l Tris-acetate buffer for 24 h at 30°C under argon. 500  $\mu$ l of the incubation mixture was then applied to a Sepharose 2B-CL column (0.9  $\times$  28.5cm) equilibrated in Tris-acetate buffer and thermostatted at 25°C. Aliquots of 320  $\mu$ l fractions were assayed for DOPC (●) from the dpm of  $^{14}\text{C}$  and cyt  $b_5$  (○) from the absorption spectra as described in Experimental Procedures. (B) *50% cholesterol.* Cyt  $b_5$  (0.04  $\mu$ moles) was incubated with liposomes containing 2  $\mu$ moles each of DOPC and cholesterol (doped with  $1.1 \times 10^5$  dpm [ $^{14}\text{C}$ ]-POPC/ $\mu$ mole DOPC) in a total volume of 716  $\mu$ l. 650  $\mu$ l of the incubation mixture was then applied to the Sepharose 2B-CL column. Otherwise, the protocol was the same as in A.

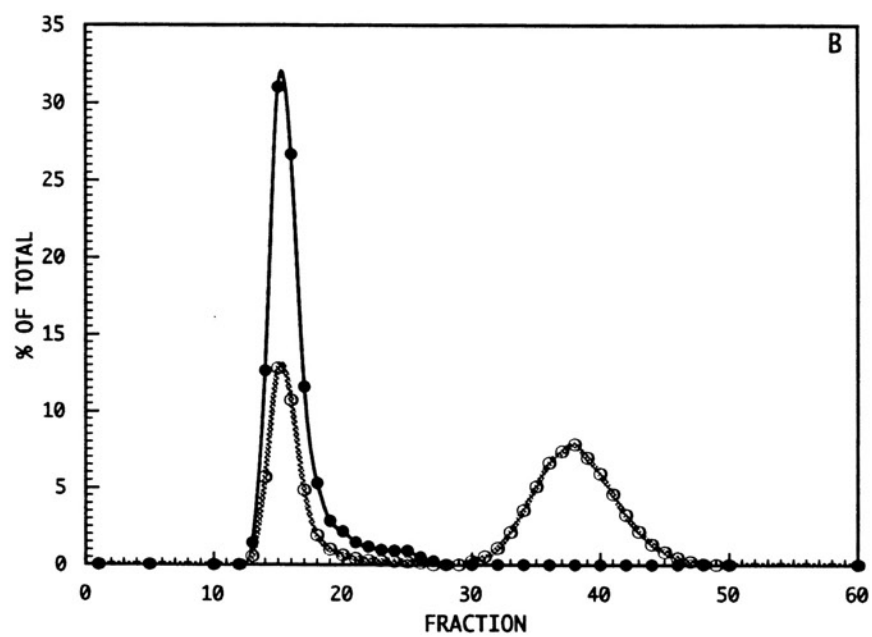
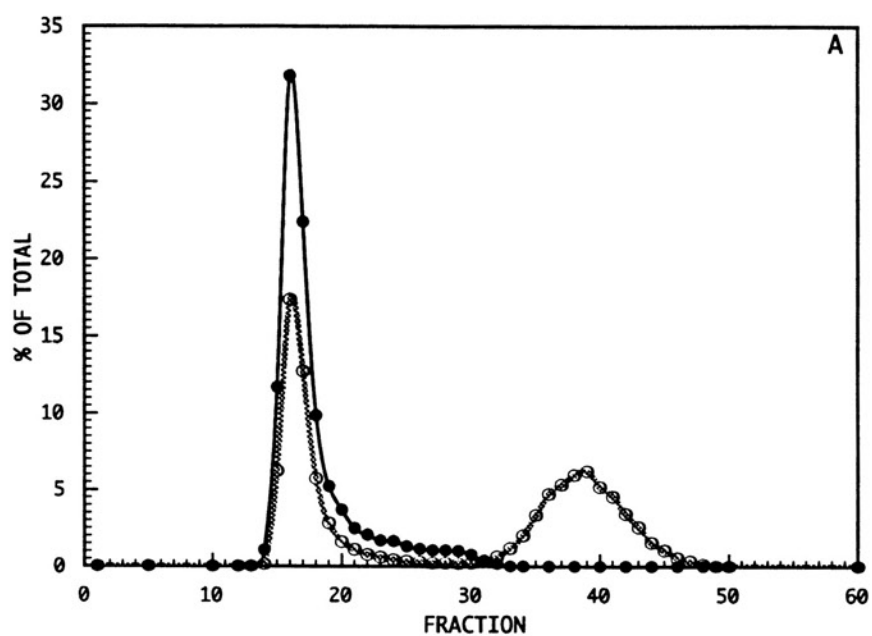


Figure 16.

Effect of cholesterol on the saturation level of cytochrome  $b_5$  binding to DLPC LUVs. (A) 0% cholesterol. Cyt  $b_5$  (0.05  $\mu$ moles) and DLPC liposomes (2  $\mu$ moles DLPC doped with  $9.3 \times 10^4$  dpm [ $^{14}$ C]-POPC/ $\mu$ mole DLPC) were incubated in a total volume of 566  $\mu$ l Tris-acetate buffer for 24 h at 30°C under argon. 500  $\mu$ l of the incubation mixture was then applied to a Sepharose 2B-CL column (0.9  $\times$  28.5cm) equilibrated in Tris-acetate buffer and thermostatted at 25°C. Aliquots of 320  $\mu$ l fractions were assayed for DLPC (●) from the dpm of  $^{14}$ C and cyt  $b_5$  (○) from the absorption spectra as described in Experimental Procedures. (B) 50% cholesterol. Cyt  $b_5$  (0.05  $\mu$ moles) was incubated with liposomes containing 2  $\mu$ moles each of DLPC and cholesterol (doped with  $1.7 \times 10^5$  dpm [ $^{14}$ C]-POPC/ $\mu$ mole DLPC) in a total volume of 1.10 ml. 1.0 ml of the incubation mixture was then applied to the Sepharose 2B-CL column. Otherwise, the protocol was the same as in A.

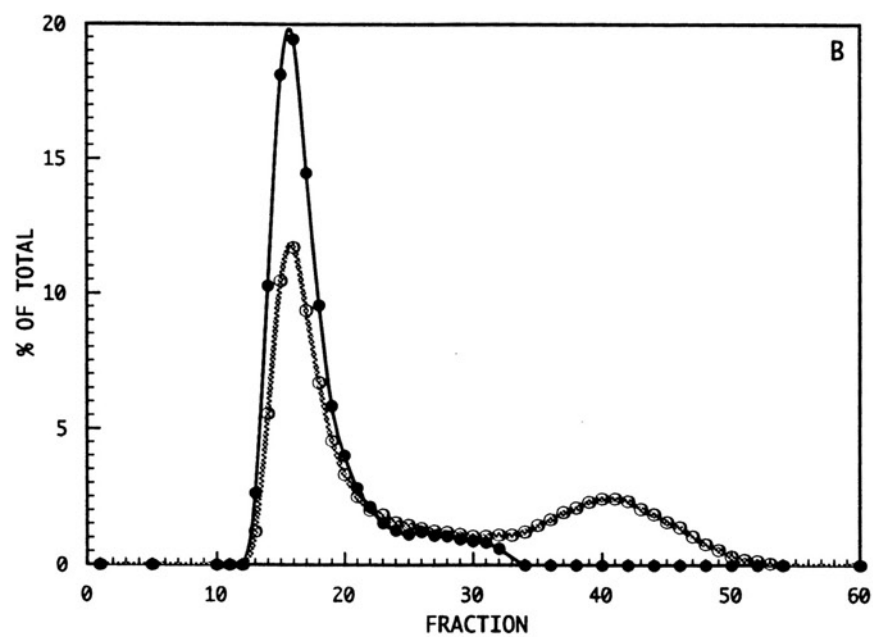
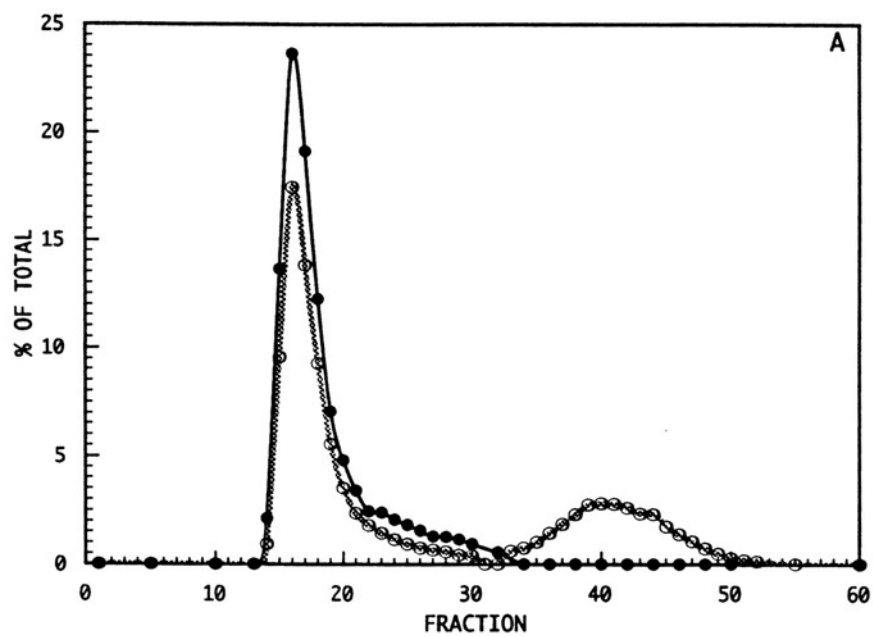


Figure 17.

Effect of cholesterol on the saturation level of cytochrome  $b_5$  binding to POPC LUVs. (A) 0% cholesterol. Cyt  $b_5$  (0.04  $\mu$ moles) and POPC liposomes (2  $\mu$ moles POPC doped with  $6.7 \times 10^4$  dpm [ $^{14}$ C]-POPC/ $\mu$ mole POPC) were incubated in a total volume of 422  $\mu$ l Tris-acetate buffer for 24 h at 30°C under argon. 390  $\mu$ l of the incubation mixture was then applied to a Sepharose 2B-CL column (0.9  $\times$  28.5cm) equilibrated in Tris-acetate buffer, pH 8.1 and thermostatted at 25°C. Aliquots of 320  $\mu$ l fractions were assayed for POPC (●) from the dpm of  $^{14}$ C and cyt  $b_5$  (○) from the absorption spectra as described in Experimental Procedures. (B) 50% cholesterol. Cyt  $b_5$  (0.024  $\mu$ moles) was incubated with liposomes containing 10  $\mu$ moles each of POPC and cholesterol (doped with  $9.8 \times 10^4$  dpm [ $^{14}$ C]-POPC/ $\mu$ mole POPC) in a total volume of 1.76 ml. 1.60 ml of the incubation mixture was then applied to a Sepharose 2B-CL column (1.6  $\times$  55cm) and 1.60 ml fractions were collected. Otherwise, the protocol was the same as in A.

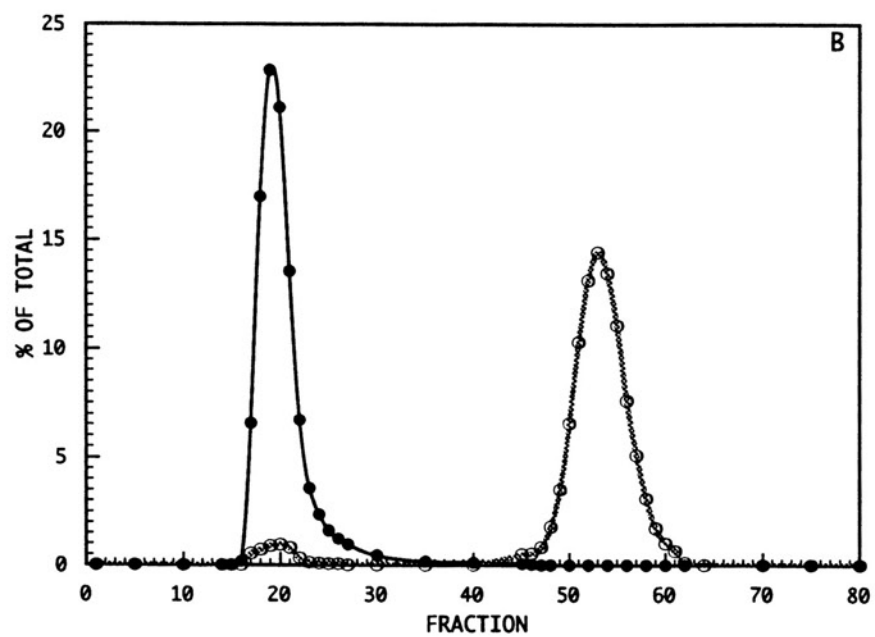
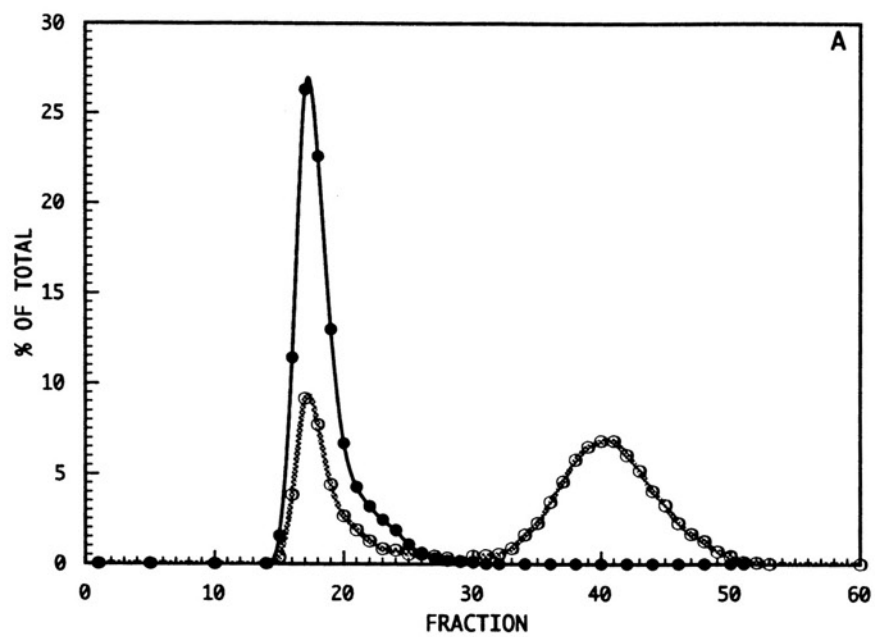


Figure 18.

Effect of cholesterol on the saturation level of cytochrome  $b_5$  binding to PLPC LUVs. (A) 0% cholesterol. Cyt  $b_5$  (0.04  $\mu$ moles) and PLPC liposomes (2  $\mu$ moles PLPC doped with  $6.6 \times 10^4$  dpm [ $^{14}$ C]-POPC/ $\mu$ mole PLPC) were incubated in a total volume of 649  $\mu$ l Tris-acetate buffer for 24 h at 30°C under argon. 610  $\mu$ l of the incubation mixture was then applied to a Sepharose 2B-CL column (0.9  $\times$  28.5cm) equilibrated in Tris-acetate buffer, pH 8.1 and thermostatted at 25°C. Aliquots of 320  $\mu$ l fractions were assayed for PLPC (●) from the dpm of  $^{14}$ C and cyt  $b_5$  (○) from the absorption spectra as described in Experimental Procedures. (B) 50% cholesterol. Cyt  $b_5$  (0.024  $\mu$ moles) was incubated with liposomes containing 10  $\mu$ moles each of PLPC and cholesterol (doped with  $1.2 \times 10^5$  dpm [ $^{14}$ C]-POPC/ $\mu$ mole PLPC) in a total volume of 1.88 ml. 1.74 ml of the incubation mixture was then applied to a Sepharose 2B-CL column (1.6  $\times$  55cm) and 1.60 ml fractions were collected. Otherwise, the protocol was the same as in A.

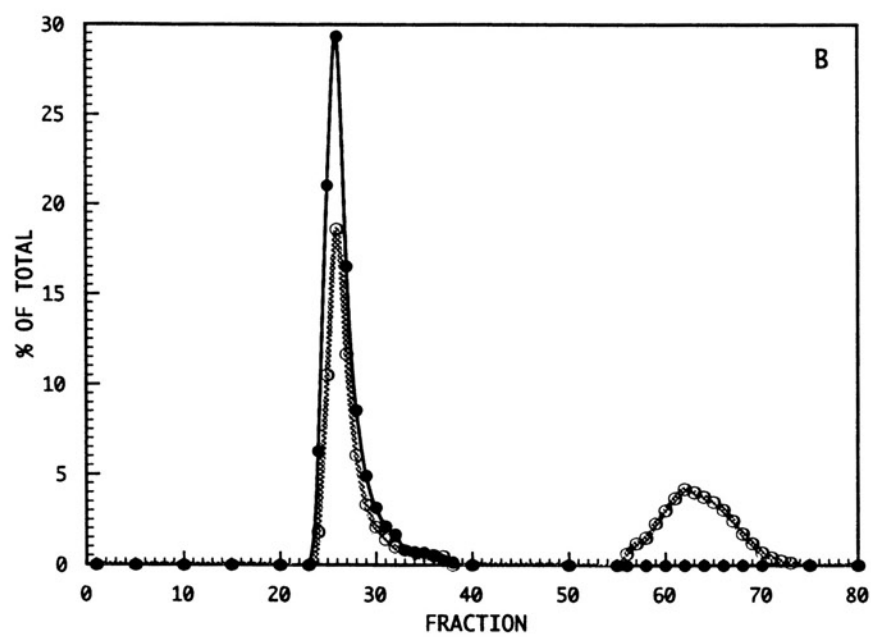
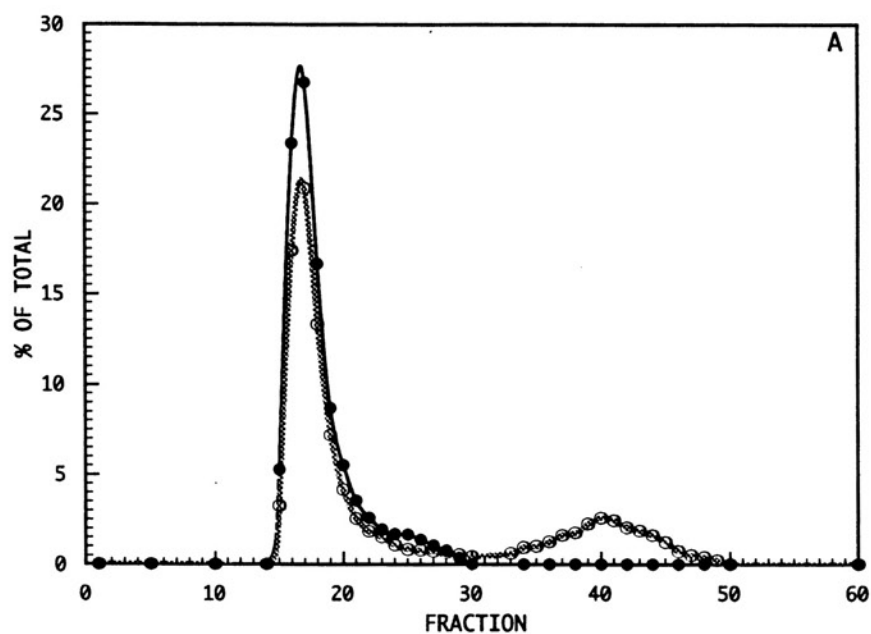




Figure 19.

Effect of cholesterol on the saturation level of cytochrome  $b_5$  binding to egg PC LUVs. (A) 0% cholesterol. Cyt  $b_5$  (0.1  $\mu$ moles) and egg PC liposomes (5  $\mu$ moles egg PC doped with  $9.6 \times 10^4$  dpm [ $^{14}$ C]-POPC/ $\mu$ mole egg PC) were incubated in a total volume of 1.53 ml Tris-acetate buffer for 24 h at 30°C under argon. 1.43 ml of the incubation mixture was then applied to a Sepharose 2B-CL column (1.6  $\times$  55cm) equilibrated in Tris-acetate buffer and thermostatted at 25°C. Aliquots of 1.53 ml fractions were assayed for egg PC (●) from the dpm of  $^{14}$ C and cyt  $b_5$  (○) from the absorption spectra as described in Experimental Procedures. (B) 50% cholesterol. Cyt  $b_5$  (0.024  $\mu$ moles) was incubated with liposomes containing 10  $\mu$ moles each of egg PC and cholesterol (doped with  $9.9 \times 10^4$  dpm [ $^{14}$ C]-POPC/ $\mu$ mole egg PC) in a total volume of 1.72 ml. 1.55 ml of the incubation mixture was then applied to the Sepharose 2B-CL column and 1.60 ml fractions were collected. Otherwise, the protocol was the same as in A.

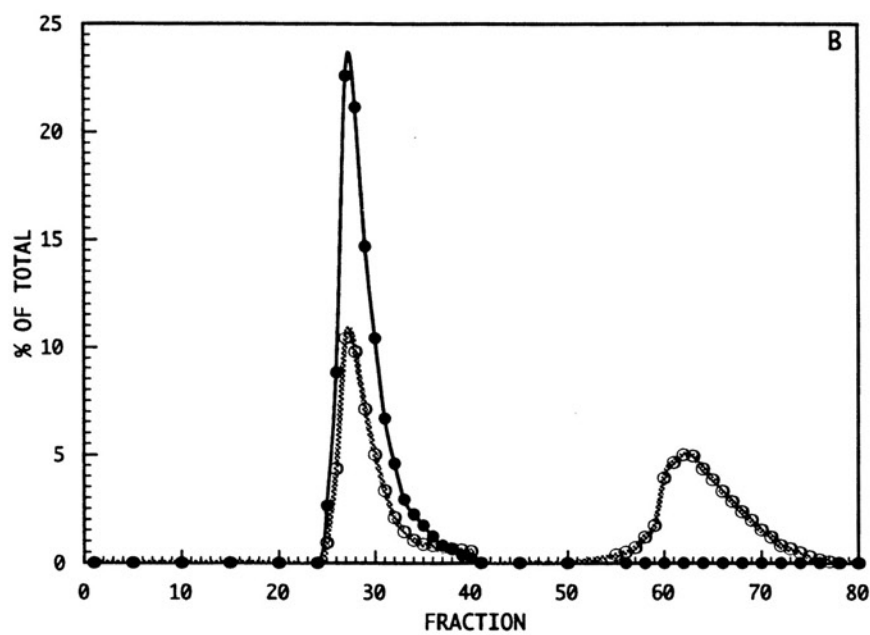
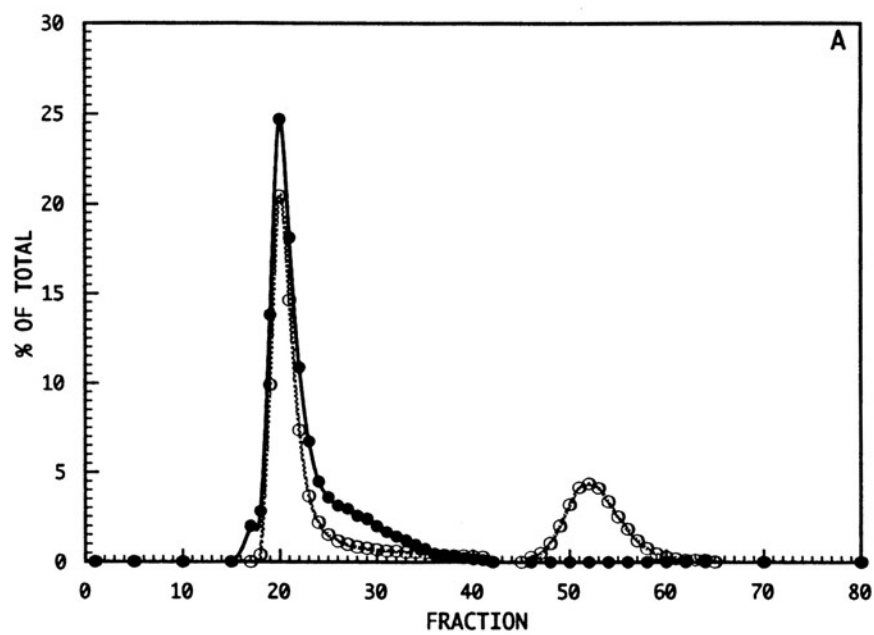


Table II: Effect of Cholesterol on the Saturation Levels of Cytochrome  $b_5$  Binding to Phosphatidylcholine Reverse-phase Liposomes<sup>a</sup>

phospholipid	cytochrome b <sub>5</sub> /1000 phospholipids				ϕ <sup>d</sup>
	0% cholesterol		50% cholesterol		
	observed <sup>b</sup>	corrected <sup>c</sup>	observed	corrected	
DMPC	12.7	12.7	<0.1	<0.1	>127.0
DOPC	10.1	11.5	7.9	9.4	1.2
DLPC	17.2	17.2	16.3	16.7	1.0
POPC	6.8	9.0	0.1	0.1	90.0
SOPC	6.9	10.3	0.1	0.2	51.5
PLPC	16.6	21.9	1.4	1.8	12.2
SLPC	15.1	20.0	1.5	2.3	8.7
egg PC	13.9	19.4	1.2	1.6	12.1
liver PC	15.1	17.9	1.1	1.2	14.9
PC/SPH (1:1)	16.2	17.6	1.4	1.5	11.7

<sup>a</sup>Cyt  $b_5$  and [ $^{14}\text{C}$ ]-labelled reverse-phase liposomes were incubated for 24 hrs at 30-37°C under argon. Initial binding ratios, varied from 1:40 to 1:417 cyt  $b_5$  to phospholipid, that resulted in  $\leq 75\%$  of complete binding were assumed to be saturating cyt  $b_5$  concentrations. <sup>b</sup>The extent of binding was determined from the percentage of cyt  $b_5$  eluting with liposomes from a Sepharose 2B-CL column in the void volume (See Experimental Procedures).

<sup>c</sup>Cyt  $b_5$ :phospholipid at saturation corrected for lamellarity of liposomes.

<sup>d</sup>cholesterol inhibitory parameter,  $\phi = (\text{cyt } b_5 \text{ saturation in liposomes without cholesterol})/(\text{cyt } b_5 \text{ saturation in liposomes with 50\% cholesterol})$ .  $\phi$  is calculated from the corrected values. Selected experiments were repeated (DMPC  $\pm$  50% cholesterol, POPC  $\pm$  50% cholesterol, and liver PC  $\pm$  50% cholesterol) and indicated that the results are accurate to  $\pm 4\%$  of reported values.

Substantial  $\phi$  values signify marked cholesterol-mediated reduction of cyt  $b_5$  binding to liposomes whereas cholesterol inhibitory parameter values of approximately 1.0 indicate relatively modest effects. The most significant cholesterol inhibitory effect ( $\phi \approx 100$ ) is observed with the saturated phospholipid, DMPC, and the mixed-chain monoenoic phospholipids, POPC and SOPC. For mixed-chain dienoic phospholipids and the natural mixtures, cholesterol reduces cyt  $b_5$  partitioning into lipid bilayers by approximately 12-fold. Cholesterol has nominal effects ( $\phi \approx 1.0$ ) on cyt  $b_5$  binding to LUVs prepared from the single-chain unsaturated phospholipids, DOPC and DLPC. However, a cholesterol inhibitory parameter value of 1.0 does not mean that cholesterol has no effect on cyt  $b_5$  binding: when expressed as cyt  $b_5$  bound per total moles lipid, the cyt  $b_5$  saturation levels of bilayers with a 1:1 phospholipid/cholesterol ratio are less than a bilayer comprised of the same number of pure phospholipids. The parameter  $\phi$  simply enables convenient comparison among the various phospholipids.

Increasing phospholipid acyl chain unsaturation mitigates the cholesterol effect on cyt  $b_5$  partitioning into the lipid bilayer, as illustrated by a significantly decreased inhibitory parameter,  $\phi$ . A 50 mole percent cholesterol composition in liposomes that are prepared from POPC and SOPC, in which each phospholipid has a single *cis*- $\Delta^9$  double bond in the *sn*-2 hydrocarbon chain, reduces cyt  $b_5$  binding by an average of approximately 70-fold. In comparison, the cyt  $b_5$  saturation level of PLPC and SLPC (*sn*-2,  $\Delta^{9,12}$ ) liposomes is decreased by an average factor of about 10.5. The presence of a second double bond in the *sn*-2 acyl chain notably diminishes the inhibitory effect by approximately 7-fold. However, for the single-chain unsaturated phospholipids DOPC (*di*- $\Delta^9$ ) and DLPC (*di*- $\Delta^{9,12}$ )  $\phi$

is reduced by a factor of 59 relative to the extent of cholesterol inhibition that is observed with POPC and SOPC.

These studies demonstrate that lipid composition profoundly affects cyt  $b_5$  binding to preformed reverse-phase liposomes, and further suggests that the physical chemistry of membranes may directly facilitate or hinder protein incorporation. If the disordering effects of phospholipid unsaturation promotes cyt  $b_5$  partitioning, then the mechanism by which cholesterol prevents cyt  $b_5$  from binding to liposomes may involve counteracting such bilayer destabilization by its direct interaction with phospholipids.

***Effect of Cholesterol on the Binding of Cytochrome  $b_5$  to Small Unilamellar Vesicles (SUVs) prepared from various Phosphatidylcholines.***

Biological membranes often contain regions of significant curvature. These prominently curved surfaces are normally associated with membrane biogenesis and protein sorting. Since bilayer curvature likely affects the physical properties of lipid molecules, the effect of cholesterol on cyt  $b_5$  partitioning into small unilamellar vesicles (SUVs) was also similarly investigated.

Limit-size vesicles that are prepared by ultrasonication average 200-250 Å in diameter and cannot be resolved from unbound cyt  $b_5$  on a conventional Sepharose 2B-CL gel-filtration column. Therefore, the saturation limits of PC SUVs were determined from the enhancement of intrinsic tryptophan fluorescence when cyt  $b_5$  binds to liposomes (Figure 20). With this experimental approach, individual samples containing a fixed concentration of cyt  $b_5$  were incubated with variable amounts of SUVs.

At low phospholipid:cyt  $b_5$  mole ratios, when cyt  $b_5$  levels are above the liposome saturation limit, fluorescence increases with phospholipid concentration as greater total bilayer surface areas enable more cyt  $b_5$  to become membrane bound. At high phospholipid:cyt  $b_5$  ratios, cyt  $b_5$  fluorescence intensity remains unchanged, indicating complete binding.

Cyt  $b_5$  exhibited an approximately 1.5 to 3.9 fold enhancement in fluorescence intensity when completely bound to SUVs. The extent of the enhancement depended upon which phospholipid was used and upon the cholesterol composition (not shown). No significant light scattering was evident in the fluorescence spectra when cyt  $b_5$  was in the presence of an excess of cholesterol-free liposomes (up to 1:250 cyt  $b_5$ :phospholipid) (Figure 20). However, light scattering was significant when making fluorescence measurements in the presence of SUVs containing 50 mole percent cholesterol, as manifested by a skewed spectrum baseline (Figure 21, Panel A). Since increasing the lipid concentration elevates the baselines of emission spectra, which affects fluorescence intensities, light scattering was corrected by scanning samples of liposomes alone, and then subtracting these scattering intensities from the spectra of samples containing both SUVs and cyt  $b_5$  (Figure 21, Panel A). The baseline-adjusted spectrum (Figure 21, Panel B) could then be corrected for photomultiplier response to yield the processed fluorescence spectrum of cyt  $b_5$  in the presence of 1:1 PC/cholesterol SUVs (Figure 21, Panel C). The maximum intensities of processed fluorescence spectra were then used to quantitate the percentage of bound cyt  $b_5$  at various phospholipid/cyt  $b_5$  mole ratios.

**Figure 20.**

**Fluorescence of cytochrome  $b_5$ .** (A) 1.56  $\mu\text{M}$  cyt  $b_5$  in Tris-acetate buffer. (B) 1.56  $\mu\text{M}$  cyt  $b_5$  in the presence of POPC-SUVs (0.31 mM POPC). (C) Light-scattering of POPC-SUVs (0.66 mM POPC). Excitation is at 280 nm; with excitation and emission bandpass widths adjusted to 2.5 and 5 nm, respectively. Fluorescence spectra have been corrected for photomultiplier response.

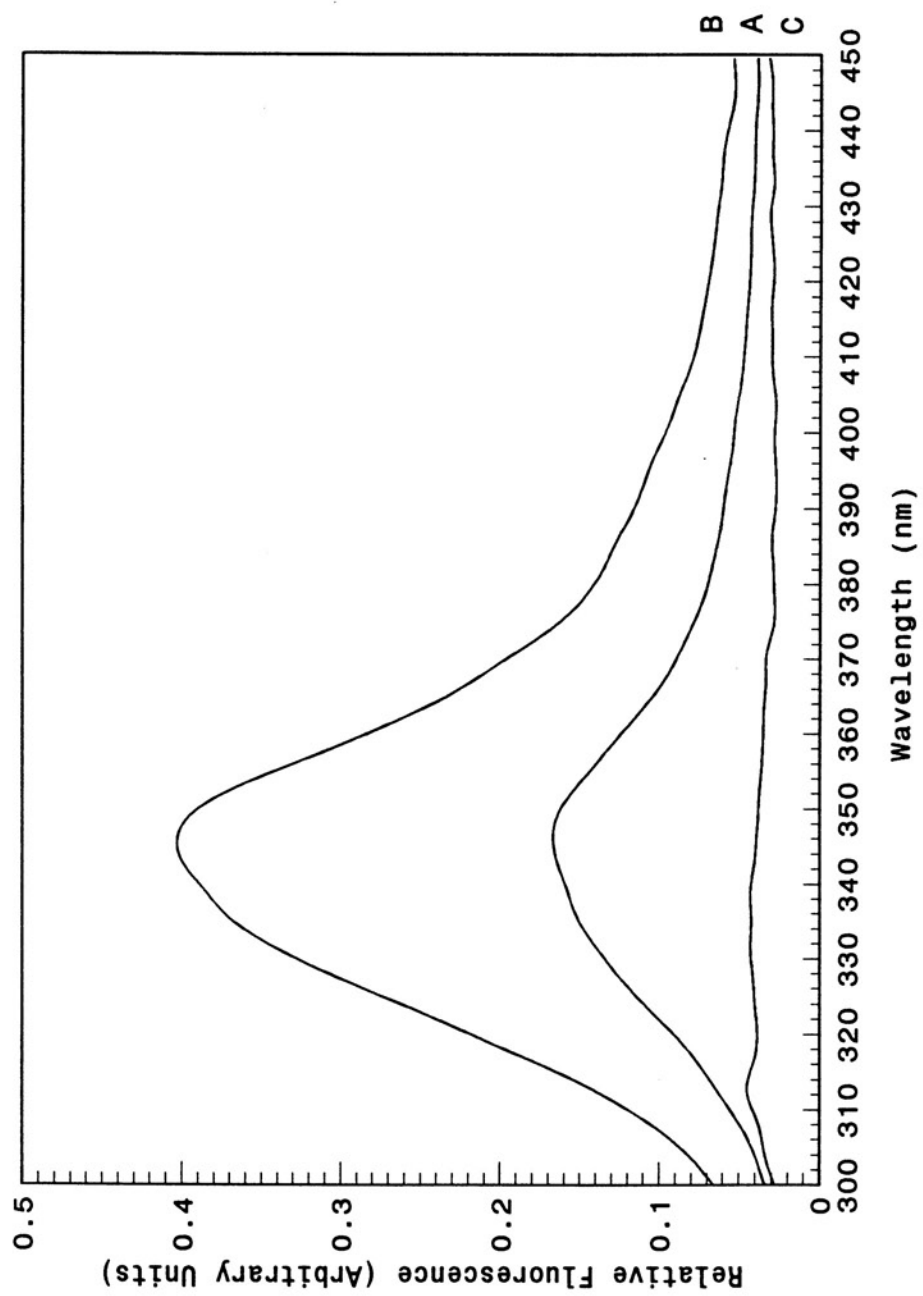
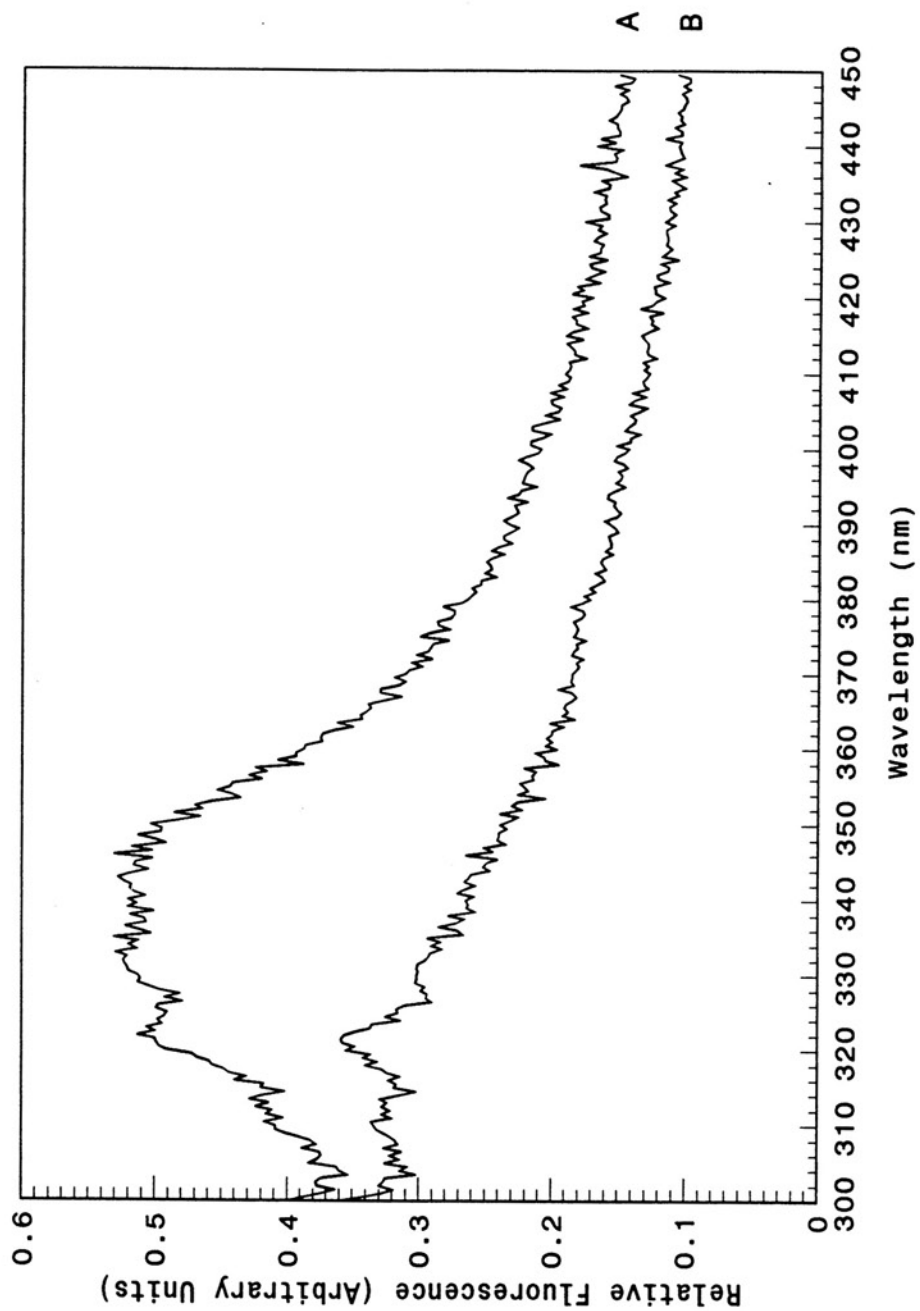
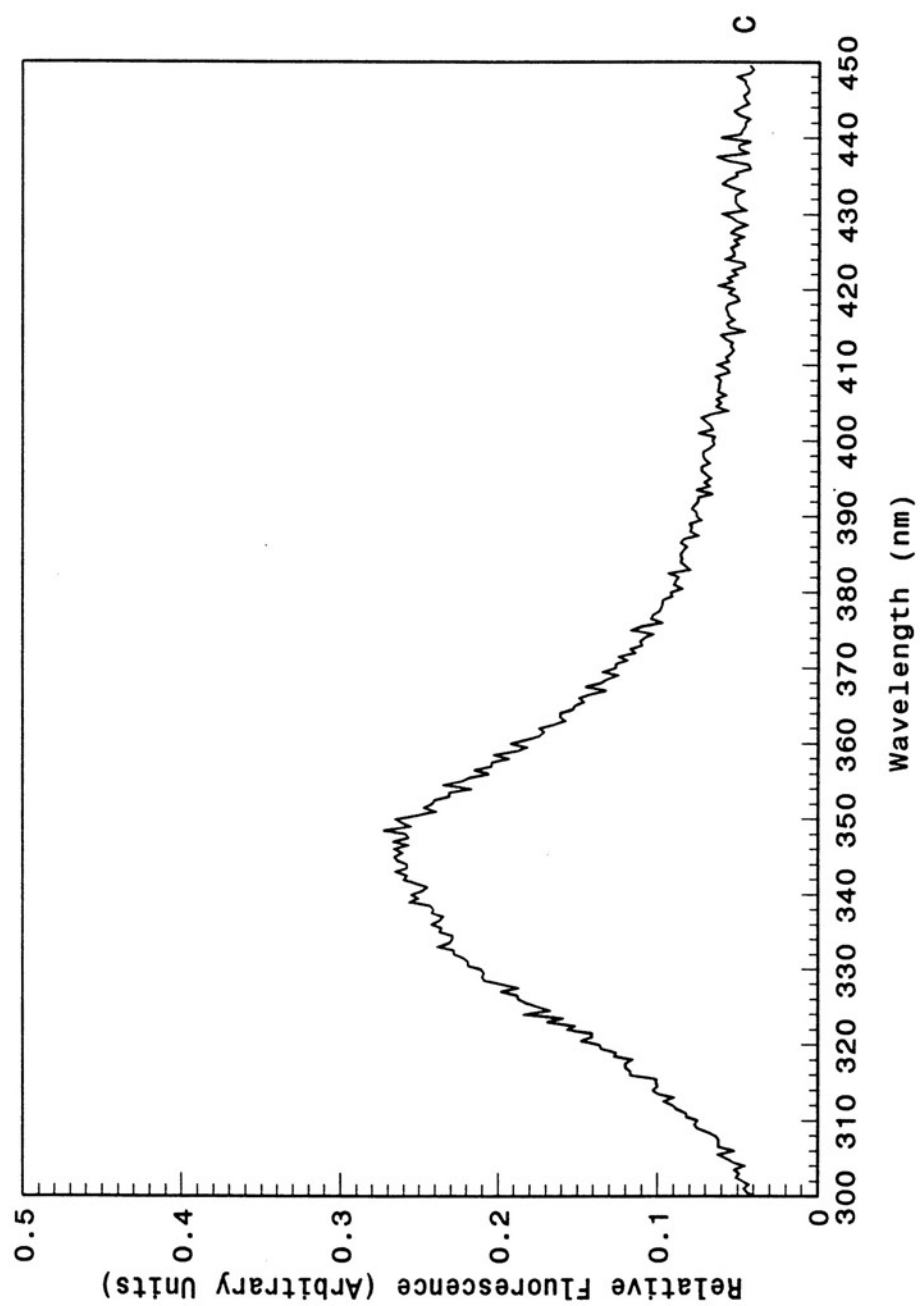


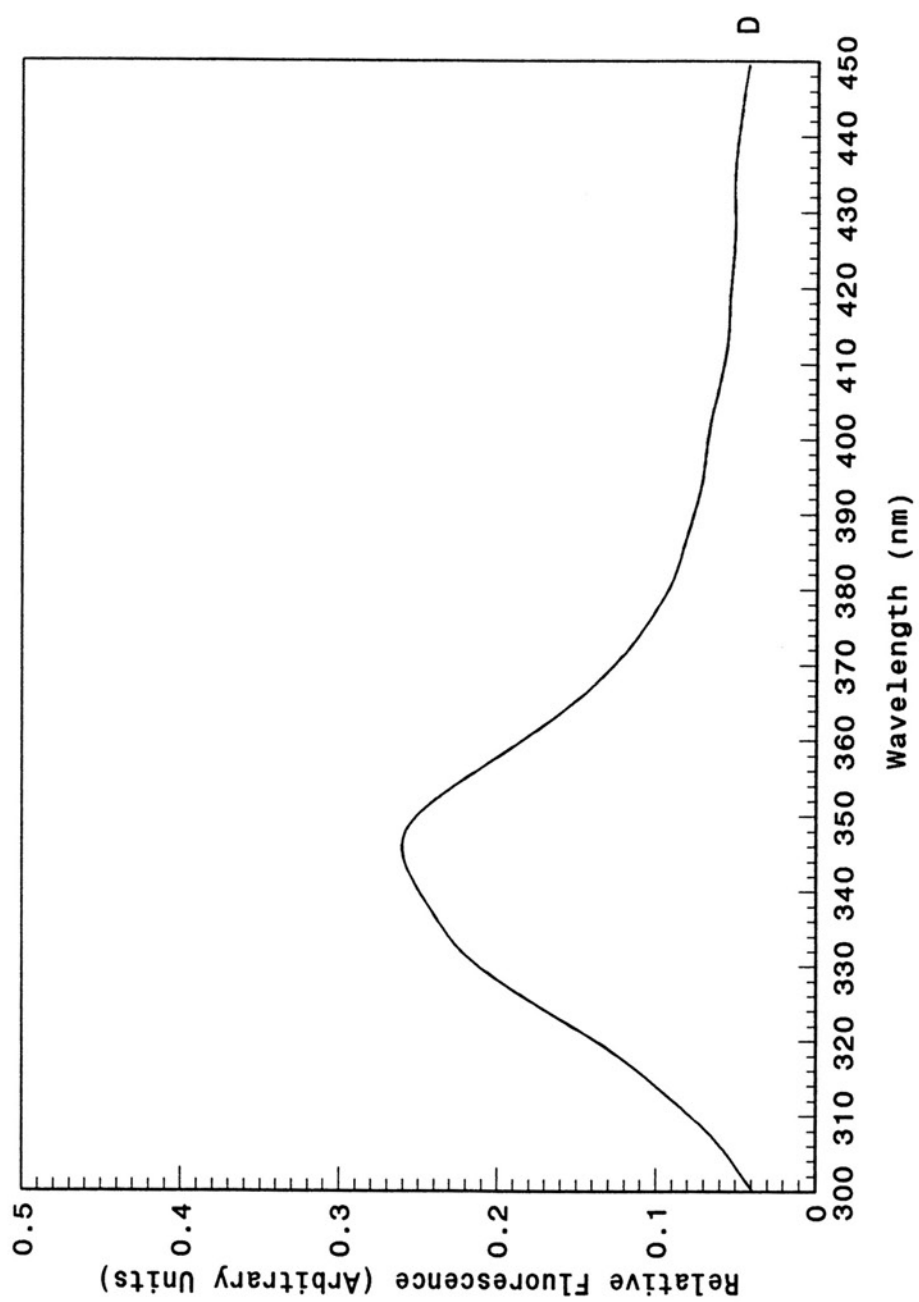


Figure 21.

Treatment of cytochrome  $b_5$  fluorescence spectra. (A) Raw fluorescence spectrum of cyt  $b_5$  in the presence of an excess of POPC SUVs containing 50% cholesterol. Cyt  $b_5$  (1.56  $\mu$ M) was incubated with POPC liposomes (0.62 mM POPC) in 2 ml Tris-acetate buffer for 2 h at 25°C prior to spectrum recording. (B) Light scattering from POPC SUVs; 50% cholesterol. The scan is of liposomes (0.62 mM POPC) in the absence of cyt  $b_5$ . (C) Baseline adjusted fluorescence spectrum of cyt  $b_5$  in the presence of POPC SUVs with 50% cholesterol. The spectrum is the difference of subtracting the light scattering scan of SUVs (B) from the top scan of cyt  $b_5$  and SUVs (A). (D) Processed cyt  $b_5$  fluorescence spectrum. The fluorescence spectrum in (C) has been corrected for photomultiplier response. The maximum cyt  $b_5$  fluorescence intensity of the processed spectrum was used in calculating the amount of liposome-associated cyt  $b_5$  for the binding isotherm.







Representative binding isotherms of cyt  $b_5$  interaction with SUVs prepared from the various phosphatidylcholines with and without 50 mole percent cholesterol are shown in Figures 22-35.

The most apparent difference among the binding isotherms occurs with cholesterol-free sonicated vesicles prepared from the natural phospholipid mixtures (egg PC, liver PC, and 1:1 PC/SPH). The extent of cyt  $b_5$  binding increases linearly with the phospholipid content until complete binding occurs (Figures 22 and 23). A defined breakpoint is observed at a mole ratio of approximately 20 phospholipids:cyt  $b_5$ . Although this result conveniently permits determination of the saturation level of cyt  $b_5$  in an SUV, it also suggests a very high affinity constant, or that cyt  $b_5$  binds irreversibly to liposomes prepared from these natural phospholipid mixtures. The result is consistent with the previous observation of Leto and Holloway (1979) in which cyt  $b_5$  saturation of egg PC SUVs occurs at a similarly distinct phospholipid/cyt  $b_5$  mole ratio. In contrast, with SUVs that are prepared from either synthetic phospholipids or that contain cholesterol, the binding isotherms exhibit a definite curvature (Figures 24-35), suggesting a dynamic equilibrium of bound and free cyt  $b_5$  with liposome surfaces.

When replotted according to the conventional Scatchard method the binding data was not linear, but concave upward instead, indicating that cyt  $b_5$  adsorption to a liposome surface does not simply involve independent sites. Consequently a more sophisticated analysis was required, as discussed in Experimental Procedures (Eqn. 2). This general expression, which is a 2-dimensional analog of the analysis developed for protein binding to DNA, similarly assumes the membrane surface to be a lattice and

**Figure 22.**

Cytochrome  $b_5$  binding to egg PC SUVs; 0% cholesterol. Separate samples containing cyt  $b_5$  (3.12 nmoles) with variable amounts of egg PC liposomes (0-0.624  $\mu$ moles egg PC) were incubated in a total volume of 2 ml Tris-acetate buffer for 2 h at 25°C. The extent of binding was determined from cyt  $b_5$  fluorescence spectra using Eqn. 1. Excitation and emission wavelengths were 280 nm and 338 nm; bandwidths were 2.5 and 5 nm. See Experimental Procedures for additional details.

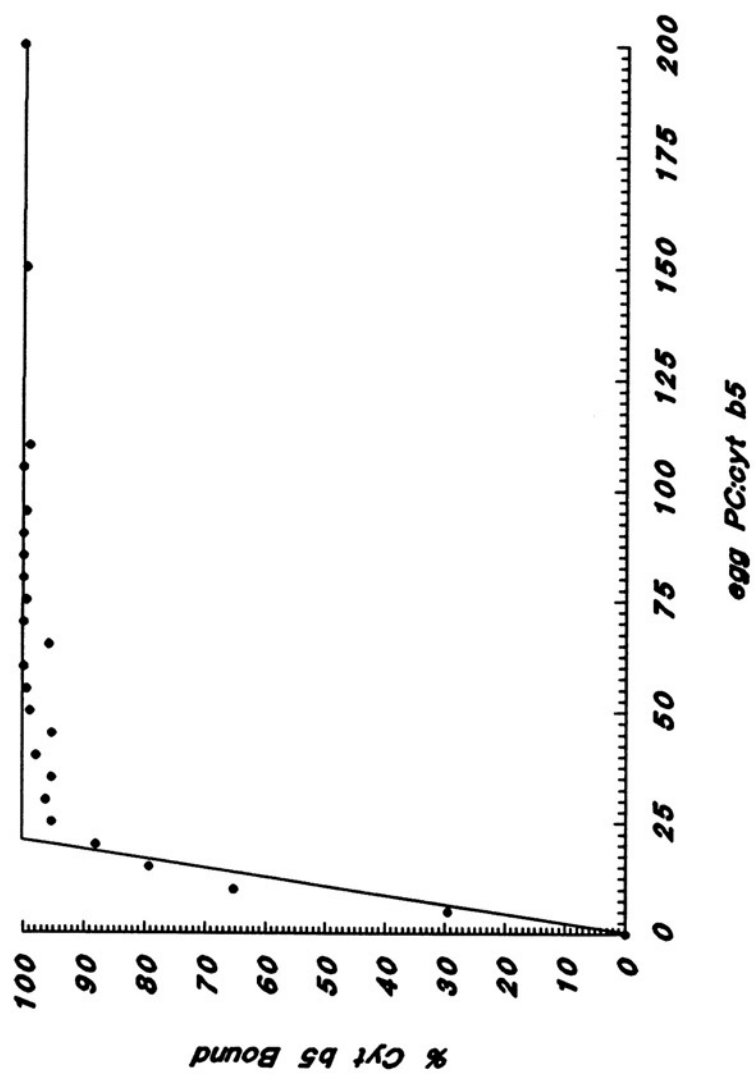


**Figure 23.**

Cytochrome  $b_5$  binding to bovine liver PC/bovine brain SPH (1:1) SUVs; 0% cholesterol. Separate samples containing cyt  $b_5$  (3.12 nmoles) with variable amounts of PC/SPH liposomes (0-0.624  $\mu$ moles PL) were incubated in a total volume of 2 ml Tris-acetate buffer for 2 h at 25°C. The extent of binding was determined from cyt  $b_5$  fluorescence spectra using Eqn. 1. Excitation and emission wavelengths were 280 nm and 338 nm; bandwidths were 2.5 and 5 nm. See Experimental Procedures for additional details.



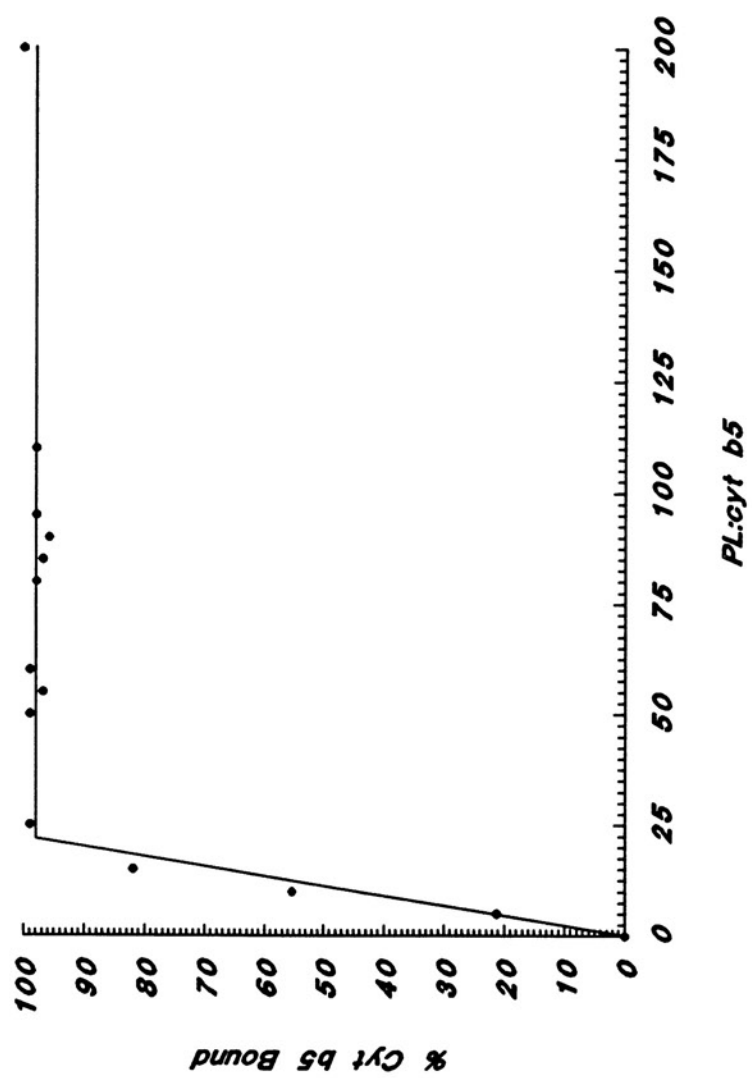
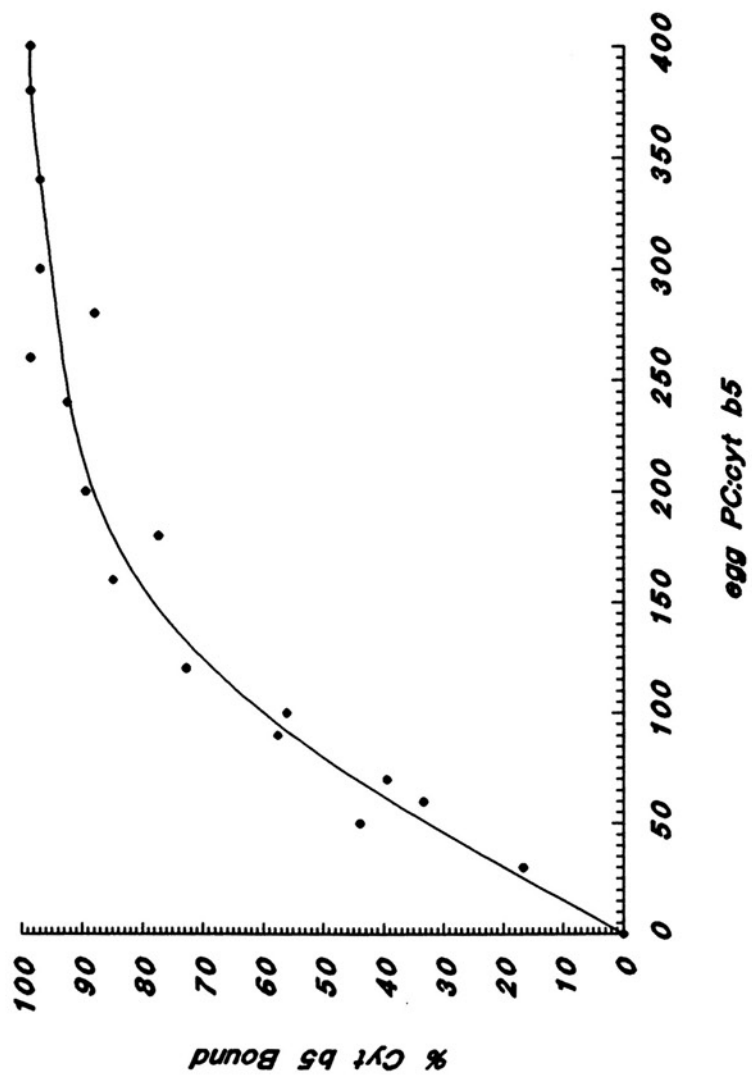


Figure 24.

Cytochrome  $b_5$  binding to egg PC SUVs; 50% cholesterol. Separate samples containing cyt  $b_5$  (3.12 nmoles) with variable amounts of egg PC liposomes (0-1.248  $\mu$ moles each of egg PC and cholesterol) were incubated in a total volume of 2 ml Tris-acetate buffer for 2 h at 25°C. The extent of binding was determined from cyt  $b_5$  fluorescence spectra that have been corrected for light scattering using Eqn. 1. Excitation and emission wavelengths were 280 nm and 338 nm; bandwidths were 2.5 and 5 nm. See Experimental Procedures for additional details.



**Figure 25.**

Cytochrome  $b_5$  binding to bovine liver PC/bovine brain SPH (1:1) SUVs; 50% cholesterol. Separate samples containing cyt  $b_5$  (3.12 nmoles) with variable amounts of liposomes (0-1.248  $\mu$ moles each of phospholipid and cholesterol) were incubated in a total volume of 2 ml Tris-acetate buffer for 2 h at 25°C. The extent of binding was determined from cyt  $b_5$  fluorescence spectra that have been corrected for light scattering using Eqn. 1. Excitation and emission wavelengths were 280 nm and 338 nm; bandwidths were 2.5 and 5 nm. See Experimental Procedures for additional details.

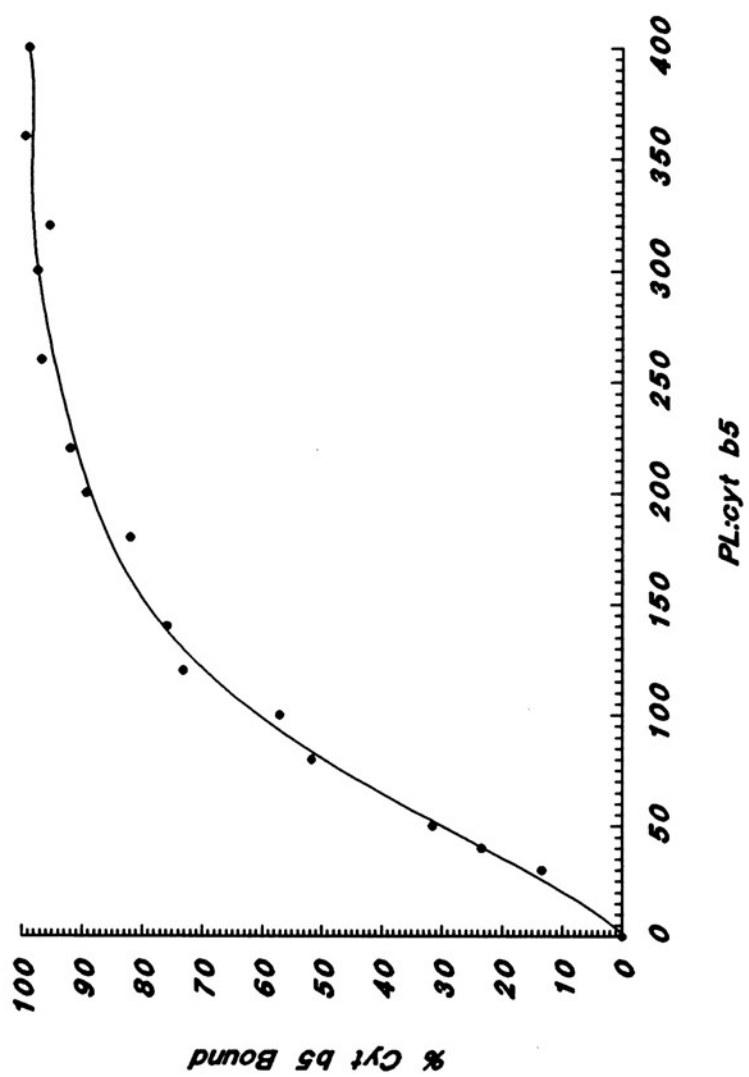


Figure 26.

Cytochrome  $b_5$  binding to DMPC SUVs; 0% cholesterol. Separate samples containing cyt  $b_5$  (3.12 nmoles) with variable amounts of DMPC liposomes (0-0.624  $\mu$ moles DMPC) were incubated in a total volume of 2 ml Tris-acetate buffer for 2 h at 25°C. The extent of binding was determined from cyt  $b_5$  fluorescence spectra using Eqn. 1. Excitation and emission wavelengths were 280 nm and 338 nm; bandwidths were 2.5 and 5 nm. See Experimental Procedures for additional details.

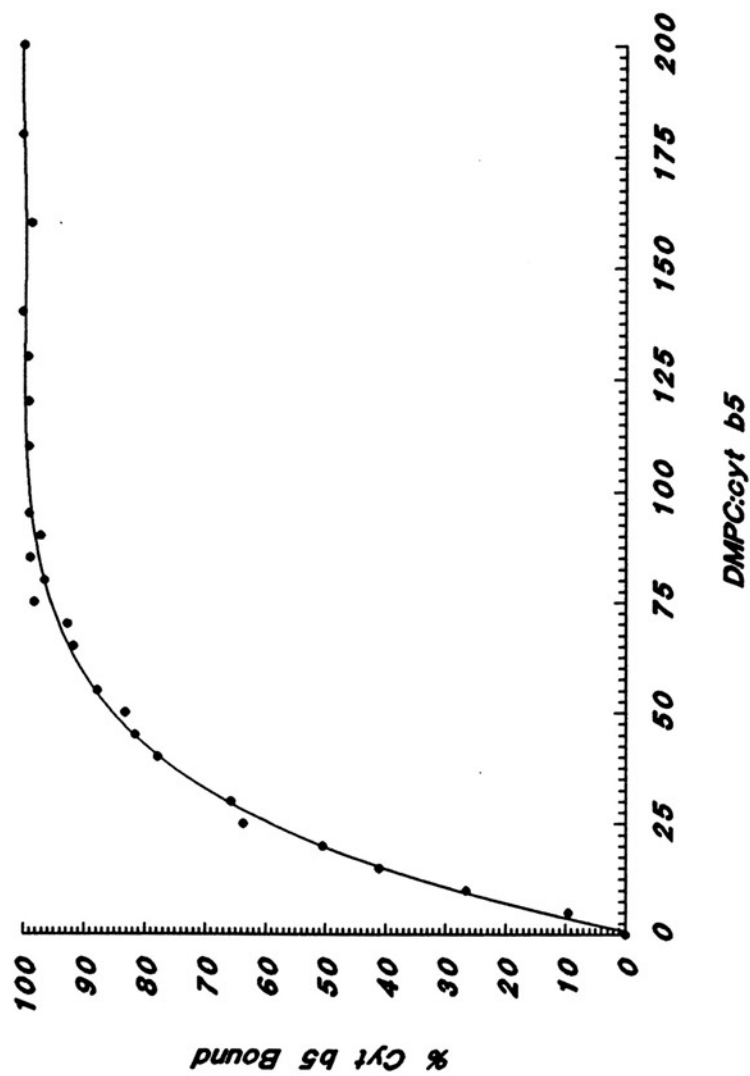


Figure 27.

Cytochrome  $b_5$  binding to DMPC SUVs; 50% cholesterol. Separate samples containing cyt  $b_5$  (3.12 nmoles) with variable amounts of liposomes (0-1.248  $\mu$ moles each of DMPC and cholesterol) were incubated in a total volume of 2 ml Tris-acetate buffer for 2 h at 25°C. The extent of binding was determined from cyt  $b_5$  fluorescence spectra that have been corrected for light scattering using Eqn. 1. Excitation and emission wavelengths were 280 nm and 338 nm; bandwidths were 2.5 and 5 nm. See Experimental Procedures for additional details.



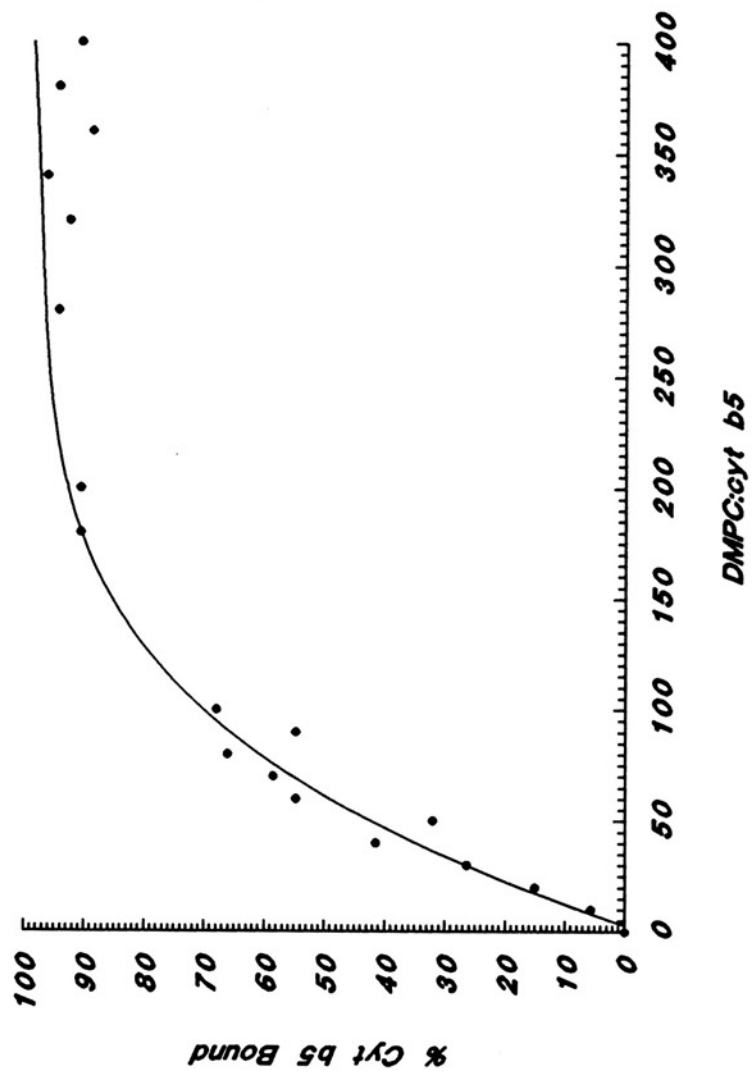


Figure 28.

Cytochrome  $b_5$  binding to DOPC SUVs; 0% cholesterol. Separate samples containing cyt  $b_5$  (3.12 nmoles) with variable amounts of DOPC liposomes (0-0.624  $\mu$ moles DOPC) were incubated in a total volume of 2 ml Tris-acetate buffer for 2 h at 25°C. The extent of binding was determined from measurements cyt  $b_5$  fluorescence spectra using Eqn. 1. Excitation and emission wavelengths were 280 nm and 338 nm; bandwidths were 2.5 and 5 nm. See Experimental Procedures for additional details.

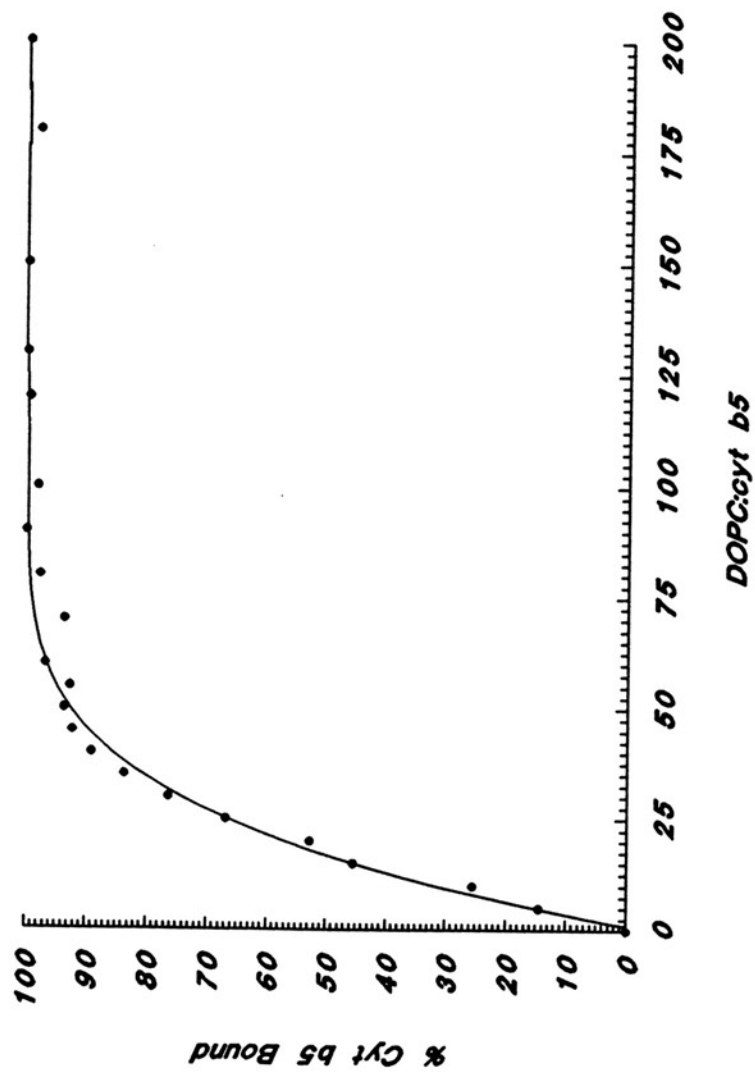


Figure 29.

Cytochrome  $b_5$  binding to DOPC SUVs; 50% cholesterol. Separate samples containing cyt  $b_5$  (3.12 nmoles) with variable amounts of liposomes (0-0.624  $\mu$ moles each of DOPC and cholesterol) were incubated in a total volume of 2 ml Tris-acetate buffer for 2 h at 25°C. The extent of binding was determined from cyt  $b_5$  fluorescence spectra that have been corrected for light scattering using Eqn. 1. Excitation and emission wavelengths were 280 nm and 338 nm; bandwidths were 2.5 and 5 nm. See Experimental Procedures for additional details.

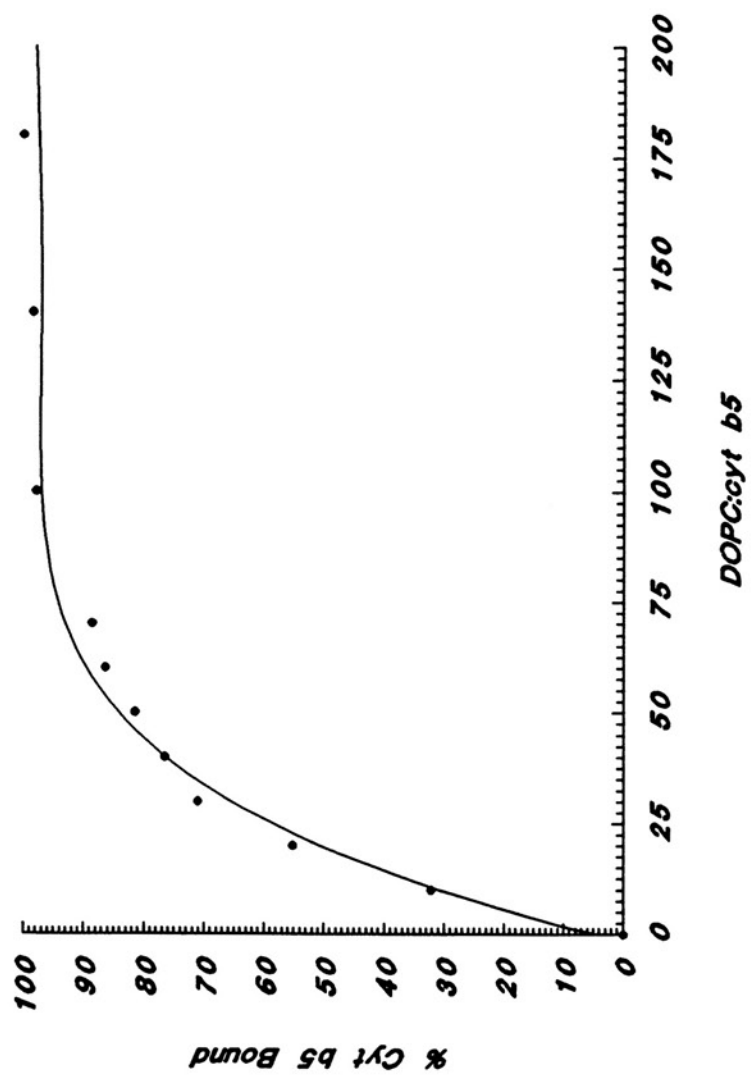


Figure 30.

Cytochrome  $b_5$  binding to POPC SUVs; 0% cholesterol. Separate samples containing cyt  $b_5$  (3.12 nmoles) with variable amounts of POPC liposomes (0-0.624  $\mu$ moles POPC) were incubated in a total volume of 2 ml Tris-acetate buffer for 2 h at 25°C. The extent of binding was determined from cyt  $b_5$  fluorescence spectra using Eqn. 1. Excitation and emission wavelengths were 280 nm and 338 nm; bandwidths were 2.5 and 5 nm. See Experimental Procedures for additional details.

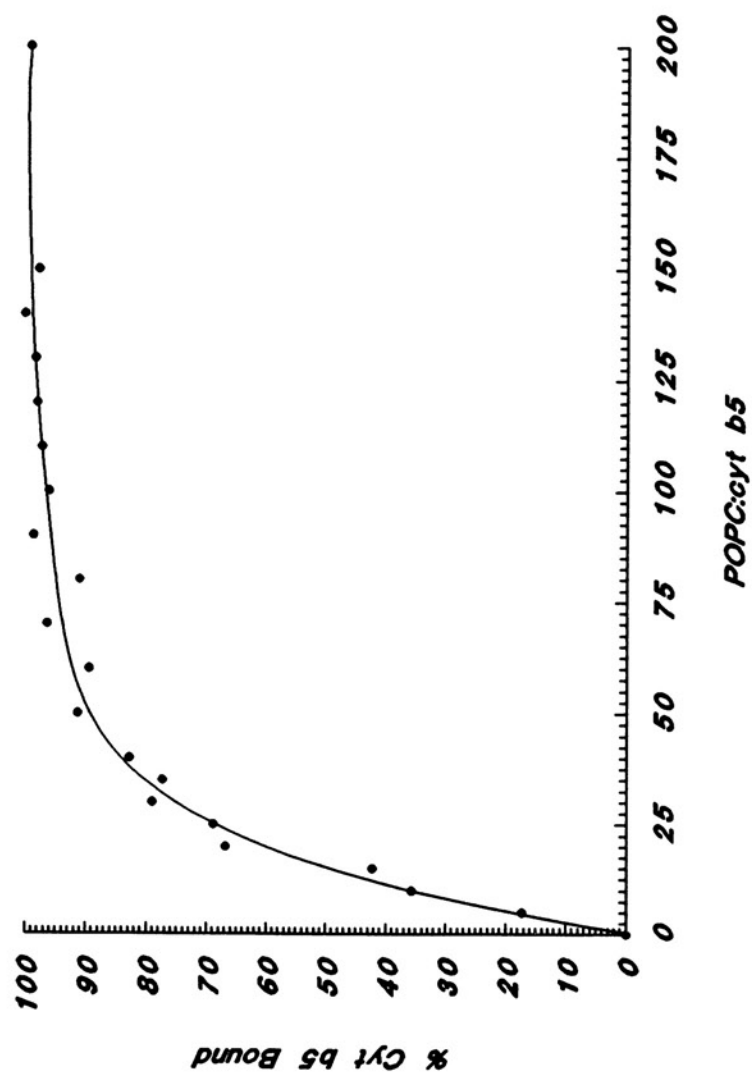
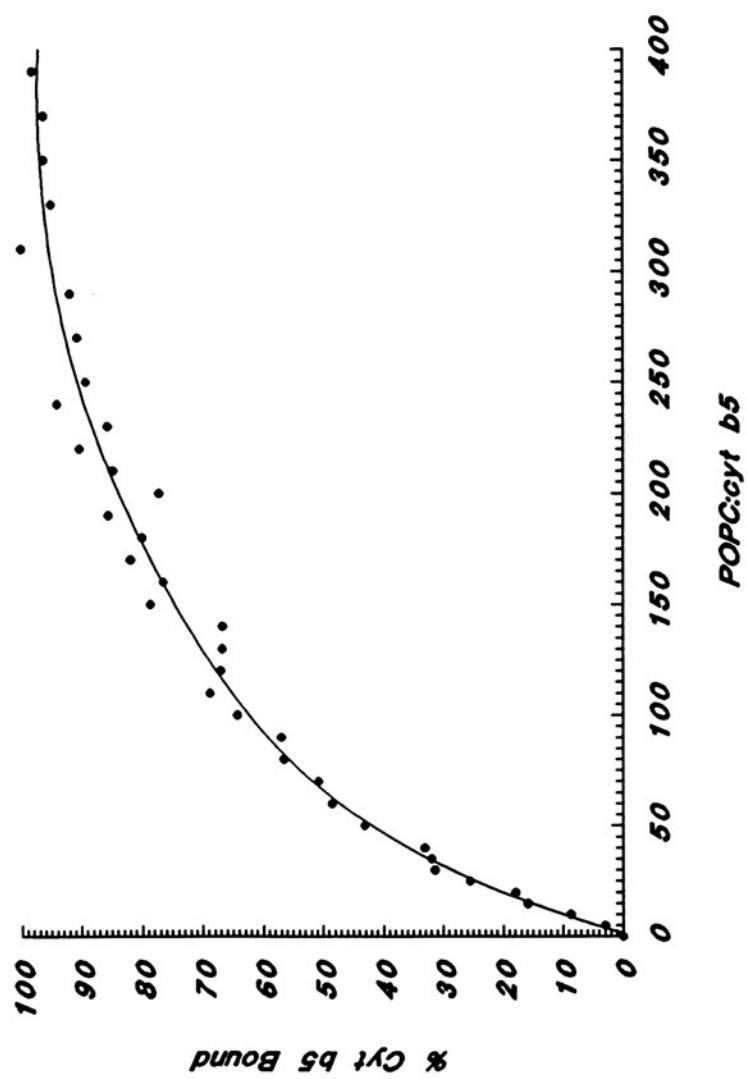


Figure 31.

Cytochrome  $b_5$  binding to POPC SUVs; 50% cholesterol. Separate samples containing cyt  $b_5$  (3.12 nmoles) with variable amounts of liposomes (0-1.248  $\mu$ moles each of POPC and cholesterol) were incubated in a total volume of 2 ml Tris-acetate buffer for 2 h at 25°C. The extent of binding was determined from cyt  $b_5$  fluorescence spectra that have been corrected for light scattering using Eqn. 1. Excitation and emission wavelengths were 280 nm and 338 nm; bandwidths were 2.5 and 5 nm. See Experimental Procedures for additional details.





**Figure 32.**

Cytochrome  $b_5$  binding to SOPC SUVs; 0% cholesterol. Separate samples containing cyt  $b_5$  (3.12 nmoles) with variable amounts of SOPC liposomes (0-0.624  $\mu$ moles SOPC) were incubated in a total volume of 2 ml Tris-acetate buffer for 2 h at 25°C. The extent of binding was determined from cyt  $b_5$  fluorescence spectra using Eqn. 1. Excitation and emission wavelengths were 280 nm and 338 nm; bandwidths were 2.5 and 5 nm. See Experimental Procedures for additional details.

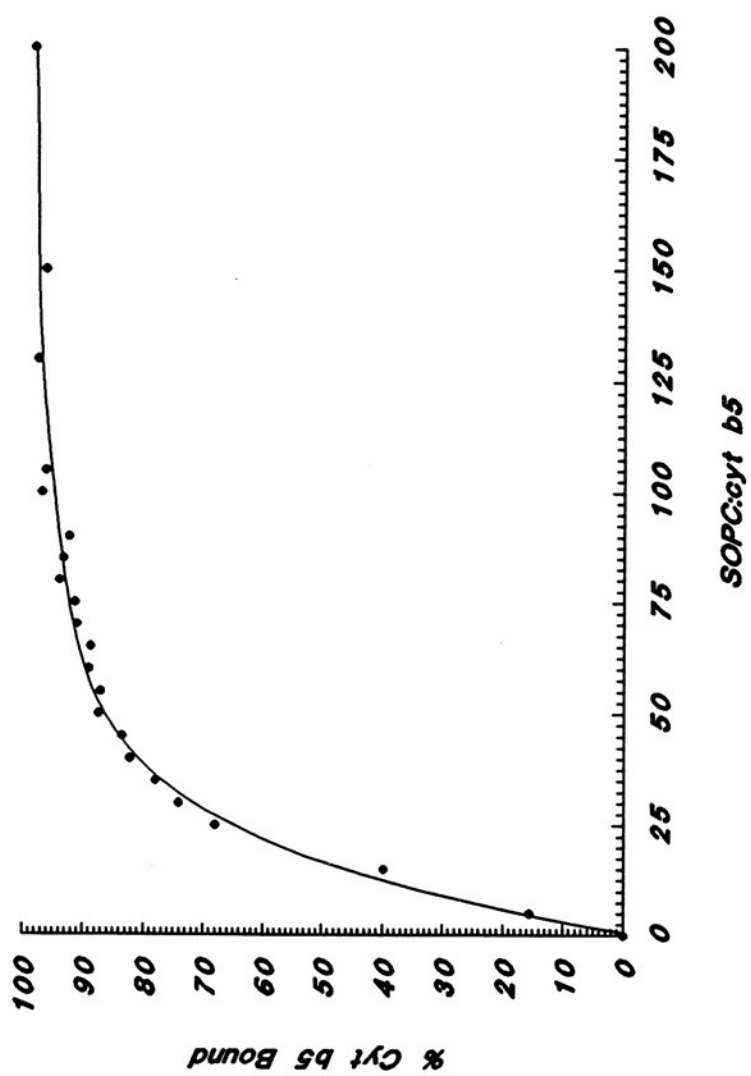
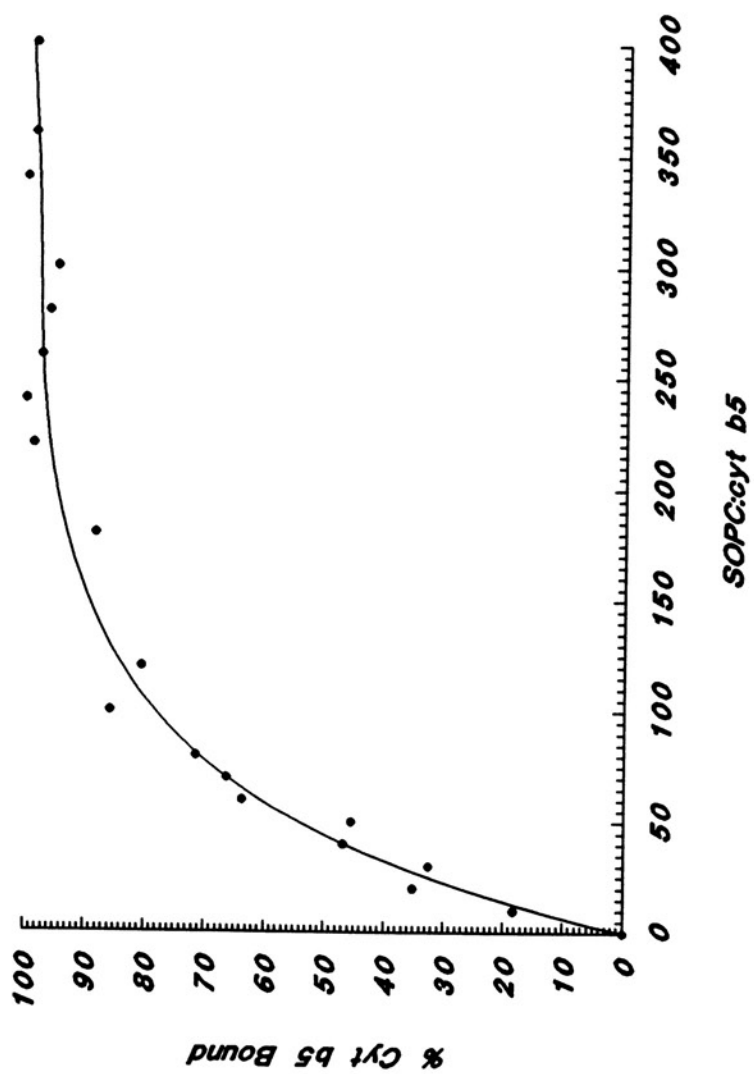


Figure 33.

Cytochrome  $b_5$  binding to SOPC SUVs; 50% cholesterol. Separate samples containing cyt  $b_5$  (3.12 nmoles) with variable amounts of liposomes (0-1.248  $\mu$ moles each of SOPC and cholesterol) were incubated in a total volume of 2 ml Tris-acetate buffer for 2 h at 25°C. The extent of binding was determined from cyt  $b_5$  fluorescence spectra that have been corrected for light scattering using Eqn. 1. Excitation and emission wavelengths were 280 nm and 338 nm; bandwidths were 2.5 and 5 nm. See Experimental Procedures for additional details.



**Figure 34.**

Cytochrome  $b_5$  binding to SLPC SUVs; 0% cholesterol. Separate samples containing cyt  $b_5$  (3.12 nmoles) with variable amounts of SLPC liposomes (0-0.624  $\mu$ moles SLPC) were incubated in a total volume of 2 ml Tris-acetate buffer for 2 h at 25°C. The extent of binding was determined from cyt  $b_5$  fluorescence spectra using Eqn. 1. Excitation and emission wavelengths were 280 nm and 338 nm; bandwidths were 2.5 and 5 nm. See Experimental Procedures for additional details.

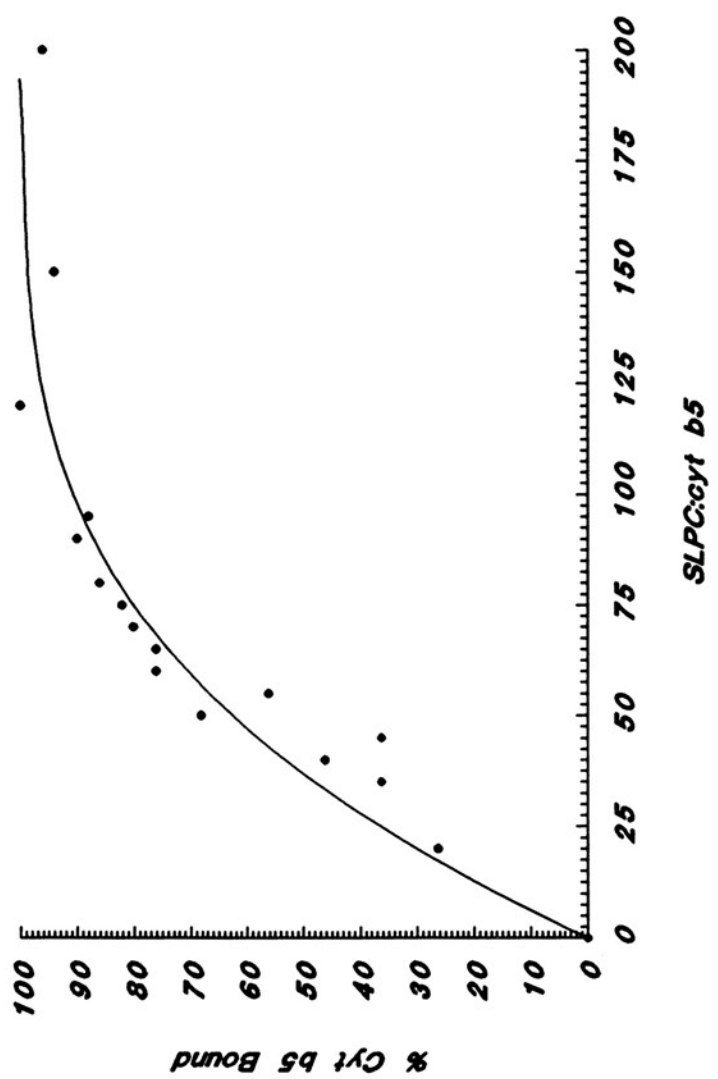
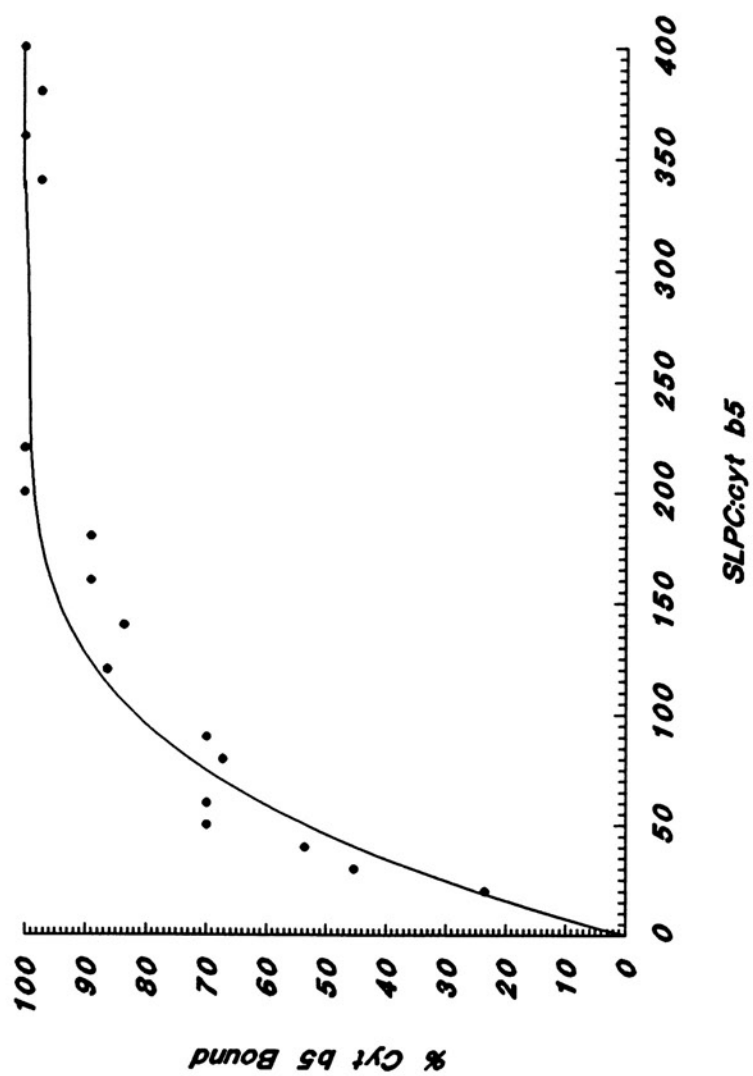


**Figure 35.**

Cytochrome  $b_5$  binding to SLPC SUVs; 50% cholesterol. Separate samples containing cyt  $b_5$  (3.12 nmoles) with variable amounts of liposomes (0-1.248  $\mu$ moles each of SLPC and cholesterol) were incubated in a total volume of 2 ml Tris-acetate buffer for 2 h at 25°C. The extent of binding was determined from cyt  $b_5$  fluorescence spectra that have been corrected for light scattering using Eqn. 1. Excitation and emission wavelengths were 280 nm and 338 nm; bandwidths were 2.5 and 5 nm. See Experimental Procedures for additional details.





accounts for statistical parameters such as surface geometry, excluded area, ligand size, and ligand cooperativity. Based upon the size and shape of the cyt  $b_5$  hydrophilic domain and the average phospholipid areas, a formulation specific to cyt  $b_5$  interaction with liposome surfaces (Eqn. 8) was obtained. Fitting Eqn. 8 to experimental data was accomplished by iteration, in which  $K_{eff}$ , the apparent binding constant,  $n$ , the number of phospholipid molecules per cyt  $b_5$  at saturation, and  $\eta$ , the extent and type of cooperativity among cyt  $b_5$  molecules, were varied independently as free parameters. The effects of  $K_{eff}$ ,  $n$ , and  $\eta$  on the overall appearance of the plotted function were initially ascertained from several theoretical curves of Eqn. 8 that were generated by varying one parameter while the other two parameters remained constant (Figures 36-38).

To determine the best method for applying Eqn. 8 to experimentally obtained data, Scatchard plots of several hypothetical hexagonally-shaped ligands with arbitrarily defined values of  $K_{eff}$ ,  $n$ , and  $\eta$  were used as models. One model ligand was used throughout the comparison as a reference. For illustrative purposes,  $K_{eff}$ ,  $n$ , and  $\eta$  were chosen to be  $8 \times 10^5 \text{ M}^{-1}$ , 24, and 1.0 (no cooperativity), respectively. Using the above parameters in Eqn. 8, the adsorption of this ligand to a membrane surface yields a Scatchard binding isotherm as depicted by the solid curves in Figures 36-38.

Figure 36 shows the effect of binding constant variations on the function of Eqn. 8. Differences in  $K_{eff}$  from the defined value, while  $n$  and  $\eta$  remain constant, changes the ordinate axis intercept of the plotted function. Since increasing  $K_{eff}$  tends to result in an elevated ordinate axis intercept, the function exhibits a larger downward slope. Smaller  $K_{eff}$

values lower ordinate intercepts, which reduces the overall downward curvature.

A similar approach has been taken to understanding how the number of lipid molecules comprising an adsorption site ( $n$ ) affects the curve-fitting routine. When  $K_{\text{eff}}$  and  $\eta$  are the invariable parameters, varying  $n$  induces deviation in the abscissa intercept (Figure 37). The number of subunits that constitute a binding site affects the extent of negative curvature in Eqn. 8. Recalling that the abscissa intercept of Eqn. 8 is actually  $1/n$ , a greater number of lipid subunits required to form an adsorption site gives an intercept at a smaller  $r$  value. Hence, a larger binding lattice size corresponds with greater upward concavity.

Lastly, the effect of the cooperativity parameter  $\eta$  on the shape of the curve was investigated. Using  $K_{\text{eff}}$  and  $n$  as constants, anticooperativity ( $\eta < 1$ ) increases negative curvature whereas positive cooperativity ( $\eta > 1$ ) has an opposite effect on concavity (Figure 38). The results are consistent with Stankowski's (1984) observations.

The theoretical curves indicate that  $K_{\text{eff}}$ ,  $n$ , and  $\eta$  affect the ordinate intercept, abscissa intercept, and concavity of Eqn. 8, respectively. To fit Eqn. 8 to experimental data,  $K_{\text{eff}}$  and  $n$  were approximated from data points that are nearest to the ordinate and abscissa intercepts. The cooperativity parameter was initially assigned a value of  $\eta = 1.0$ . Modification of  $K_{\text{eff}}$  and  $n$  was useful at improving the fit of Eqn. 8 to data along the ordinate and abscissa axis whereas adjustments to  $\eta$  improved the fit to the experimentally obtained data in the center of the curve.

Figure 36.

Theoretical Scatchard plots for the adsorption of hexagonal ligands with different affinity constants. Full line: reference ligand, using  $K_{\text{eff}}=800 \text{ mM}^{-1}$ ,  $n=24$ , and  $\eta=1.0$  in Eqn. 8; dashed line: same as reference ligand, with  $K_{\text{eff}}=1000 \text{ mM}^{-1}$ ; dotted line: ligand with affinity constant  $K_{\text{eff}}=500 \text{ mM}^{-1}$ .

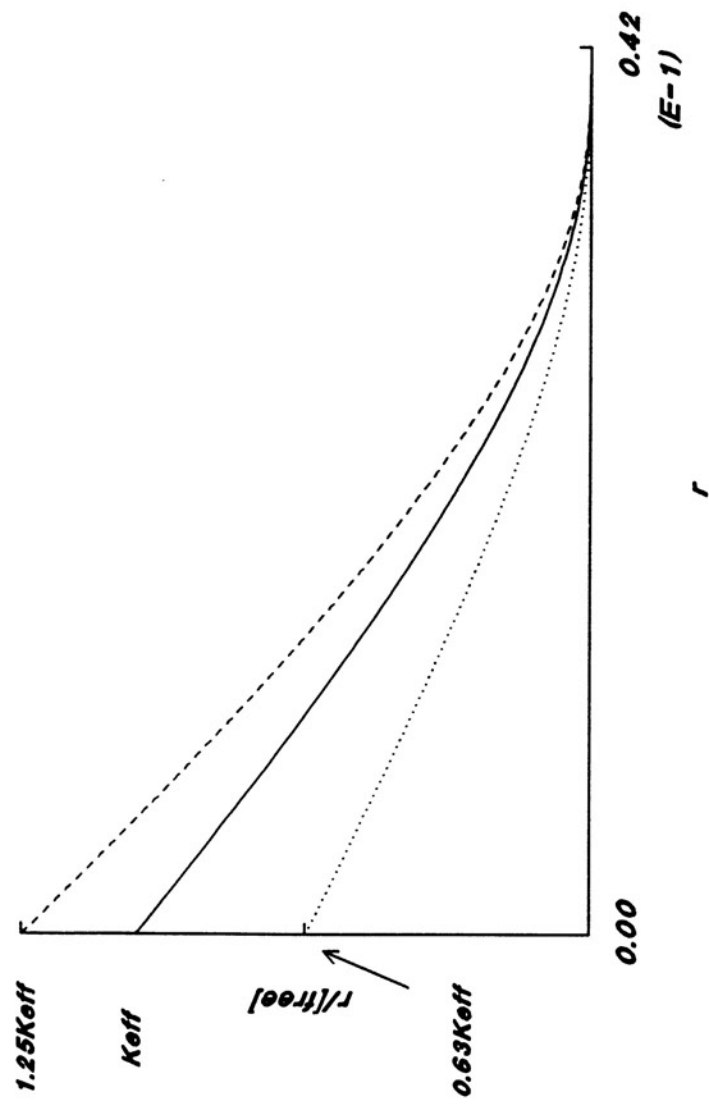


Figure 37.

Theoretical Scatchard plots for the adsorption of hexagonal ligands to membrane lattices of different sizes. Full line: reference ligand, using  $K_{\text{eff}}=800 \text{ mM}^{-1}$ ,  $n=24$ , and  $\eta=1.0$  in Eqn. 8; dashed line: same as reference ligand, except  $n=44$ ; dotted line: ligand of size  $n=10$ .

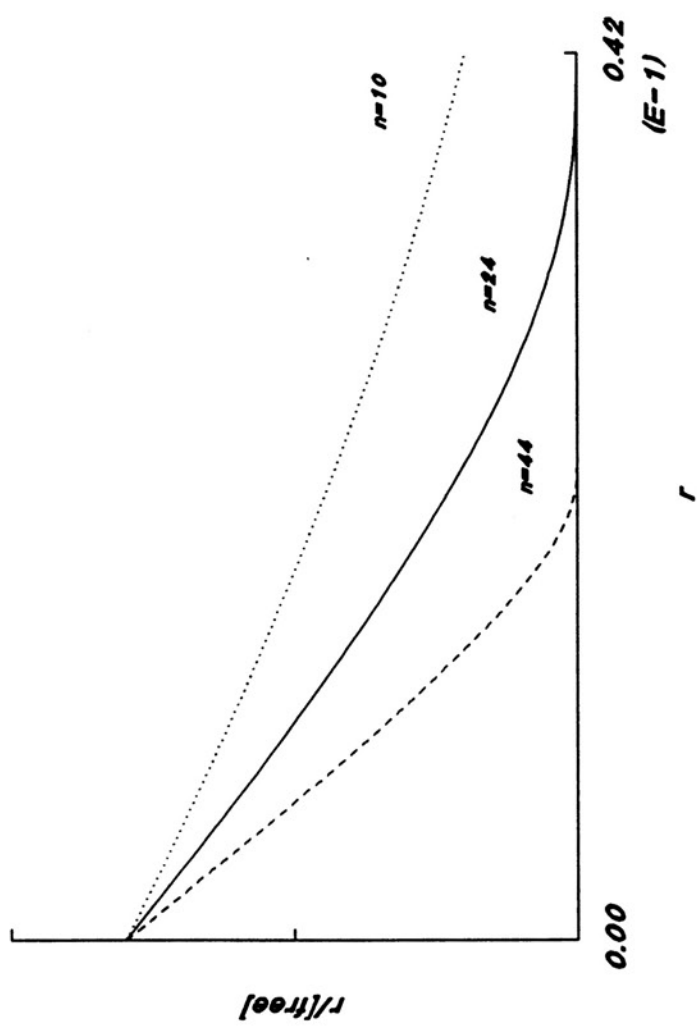
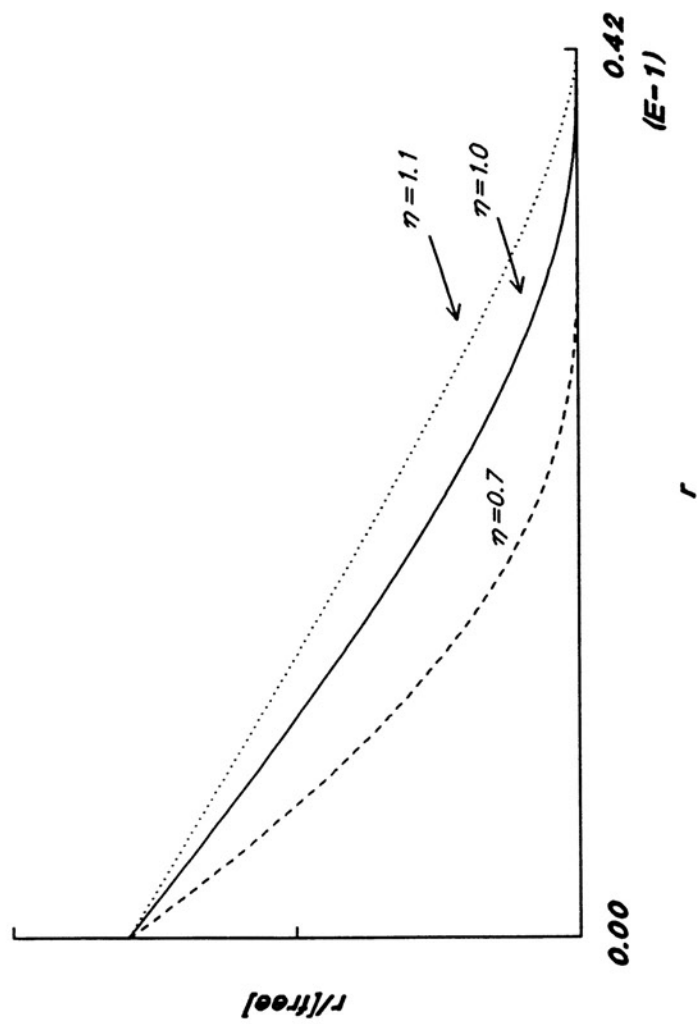


Figure 38.

Theoretical Scatchard plots for the adsorption of hexagonal ligands exhibiting different cooperativities. Full line: reference ligand, using  $K_{\text{eff}}=800 \text{ mM}^{-1}$ ,  $n=24$ , and  $\eta=1.0$  (no cooperativity) in Eqn. 8; dashed line: same ligand with an anticooperativity parameter of  $\eta=0.7$ ; dotted line: ligand with positive cooperativity ( $\eta=1.1$ ).





Figures 39-50 show some representative Scatchard plots in which Eqn. 8 has been fit to experimental binding data. In all cases, data from the initial binding isotherms (Figures 24-35) exhibited significant upward concavity when replotted as  $r/[\text{unbound cyt } b_5]$  (ordinate axis: moles of bound cyt  $b_5$  per mole PC divided by the concentration of free cyt  $b_5$ ) versus  $r$  (abscissa axis: moles of bound cyt  $b_5$  per mole PC).  $K_{\text{eff}}$  (ordinate intercept) and  $1/n$  (abscissa intercept) for cyt  $b_5$  interaction with SUVs prepared from various phosphatidylcholines was determined from the fitted function of Eqn. 8 (solid curves).

Table III summarizes the Scatchard analysis of cyt  $b_5$  binding data for SUVs with and without 50 mole percent cholesterol. Although at this stage of the analysis the binding data is not in a form that permits easy comparison with the observations made with LUVs, the values obtained for the cooperativity parameter,  $\eta$  are noteworthy. For all of the SUV binding studies evaluated by a Scatchard analytical method, the cooperativity parameter was found to be less than 1. This suggests that cyt  $b_5$  insertion into sonicated liposomes is an anticooperative process, where the binding of each cyt  $b_5$  to the vesicle surface increases the difficulty of subsequent ligand adsorption. With binding of additional cyt  $b_5$  molecules, the overall affinity that unbound cyt  $b_5$  has for a proteoliposome decreases. Although the parameter  $\eta$  does not ascribe anticooperativity to a specific cause(s), several possibilities can include electrostatic repulsion among the anionic catalytic domains, steric effects, and cyt  $b_5$ -induced liposomal strain across the bilayer matrix.

Figure 39.

Scatchard plot of cytochrome  $b_5$  binding to egg PC SUVs containing 50 mole percent cholesterol. Cyt  $b_5$  binding data from Figure 24 was replotted as  $r/[\text{unbound cyt } b_5]$  ( $\text{mM}^{-1}$ ) vs.  $r$ , where  $r$  is the molar solution concentration ratio of bound cyt  $b_5$  per phospholipid ( $[\text{bound cyt } b_5]/[\text{PL}]$ ). The fitted curve was obtained using  $K_{\text{eff}}=296 \text{ mM}^{-1}$  (y-axis intercept),  $n=105$  (reciprocal of x-axis intercept), and  $\eta=0.60$  in Eqn. 8. See text for additional details.

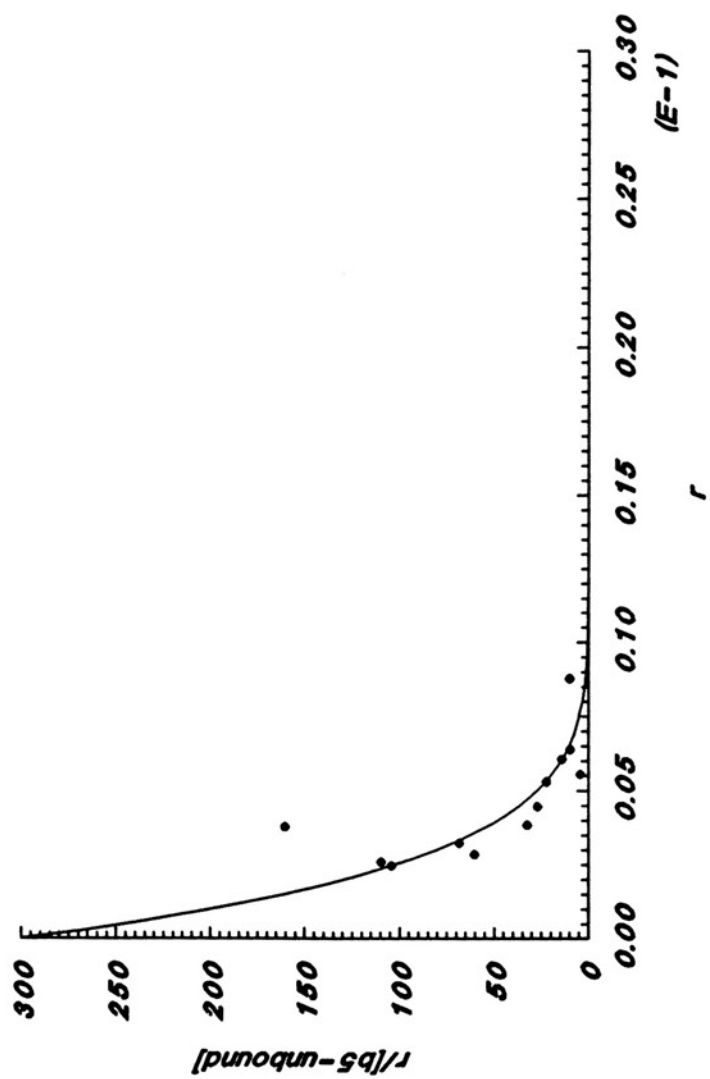


Figure 40.

Scatchard plot of cytochrome  $b_5$  binding to bovine liver PC/bovine brain SPH (1:1) SUVs containing 50 mole percent cholesterol. Cyt  $b_5$  binding data from Figure 25 was replotted as  $r/[\text{unbound cyt } b_5] \text{ (mM}^{-1}\text{)}$  vs.  $r$ , where  $r$  is the molar solution concentration ratio of bound cyt  $b_5$  per phospholipid ( $[\text{bound cyt } b_5]/[\text{PL}]$ ). The fitted curve was obtained using  $K_{\text{eff}}=246 \text{ mM}^{-1}$  (y-axis intercept),  $n=106$  (reciprocal of x-axis intercept), and  $\eta=0.60$  in Eqn. 8.

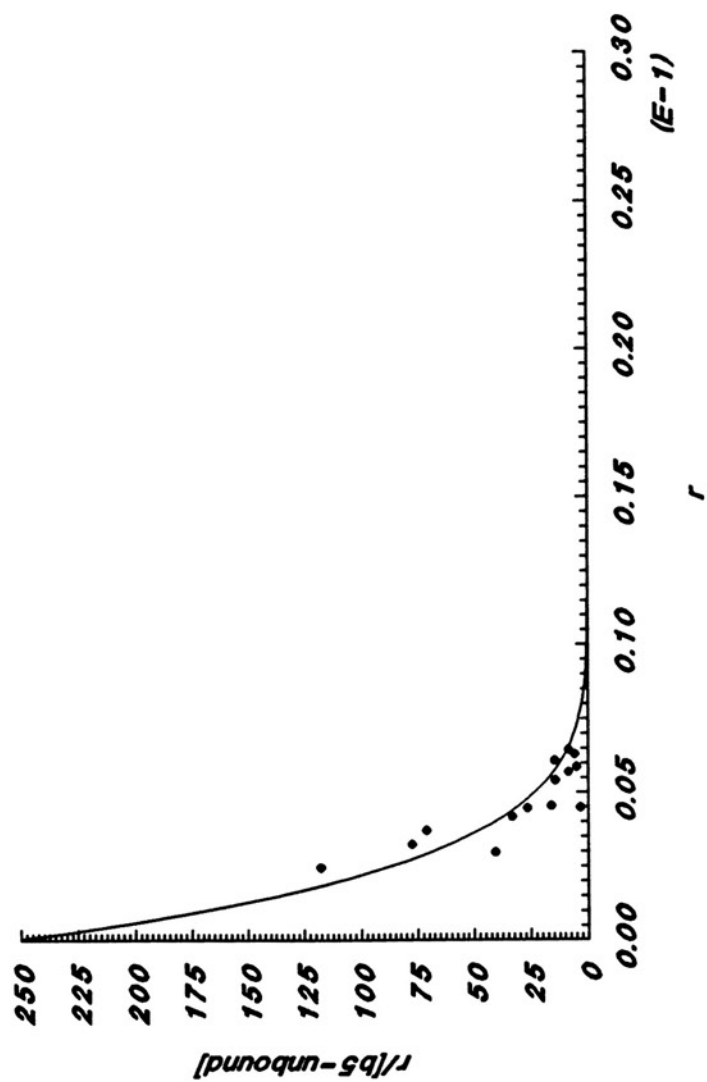


Figure 41.

Scatchard plot of cytochrome  $b_5$  binding to DMPC SUVs. Cyt  $b_5$  binding data from Figure 26 was replotted as  $r/[\text{unbound cyt } b_5]$  ( $\text{mM}^{-1}$ ) vs.  $r$ , where  $r$  is the molar solution concentration ratio of bound cyt  $b_5$  per phospholipid ( $[\text{bound cyt } b_5]/[\text{PL}]$ ). The fitted curve was obtained using  $K_{\text{eff}}=2200 \text{ mM}^{-1}$  (y-axis intercept),  $n=29$  (reciprocal of x-axis intercept), and  $\eta=0.56$  in Eqn. 8.

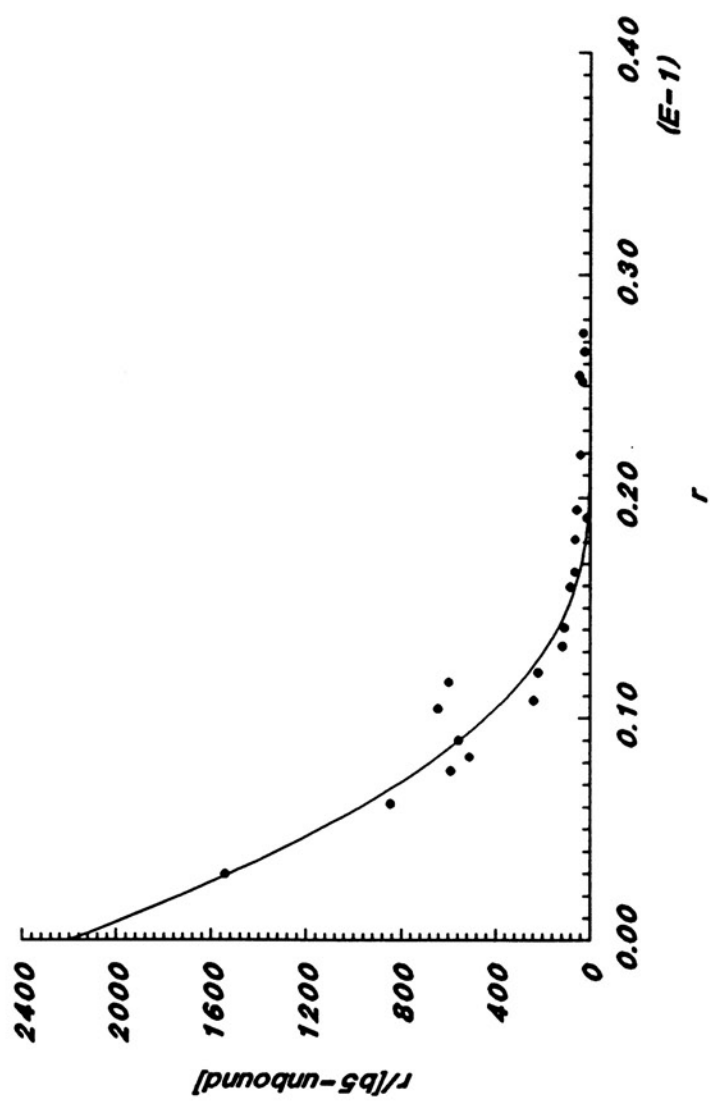




Figure 42.

Scatchard plot of cytochrome  $b_5$  binding to DMPC SUVs containing 50 mole percent cholesterol. Cyt  $b_5$  binding data from Figure 27 was replotted as  $r/[\text{unbound cyt } b_5] \text{ (mM}^{-1}\text{)}$  vs.  $r$ , where  $r$  is the molar solution concentration ratio of bound cyt  $b_5$  per phospholipid ( $[\text{bound cyt } b_5]/[\text{PL}]$ ). The fitted curve was obtained using  $K_{\text{eff}}=70 \text{ mM}^{-1}$  (y-axis intercept),  $n=30$  (reciprocal of x-axis intercept), and  $\eta=0.66$  in Eqn. 8.

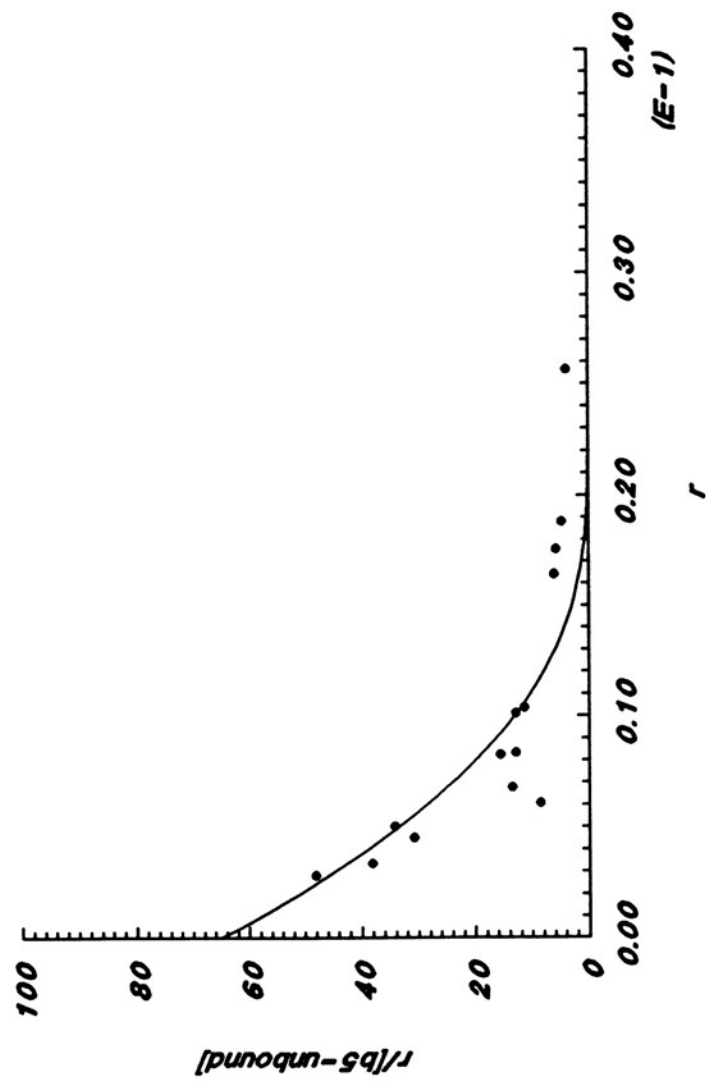


Figure 43.

Scatchard plot of cytochrome  $b_5$  binding to DOPC SUVs. Cyt  $b_5$  binding data from Figure 28 was replotted as  $r/[\text{unbound cyt } b_5]$  ( $\text{mM}^{-1}$ ) vs.  $r$ , where  $r$  is the molar solution concentration ratio of bound cyt  $b_5$  per phospholipid ( $[\text{bound cyt } b_5]/[\text{PL}]$ ). The fitted curve was obtained using  $K_{\text{eff}}=900 \text{ mM}^{-1}$  (y-axis intercept),  $n=16.7$  (reciprocal of x-axis intercept), and  $\eta=0.60$  in Eqn. 8.

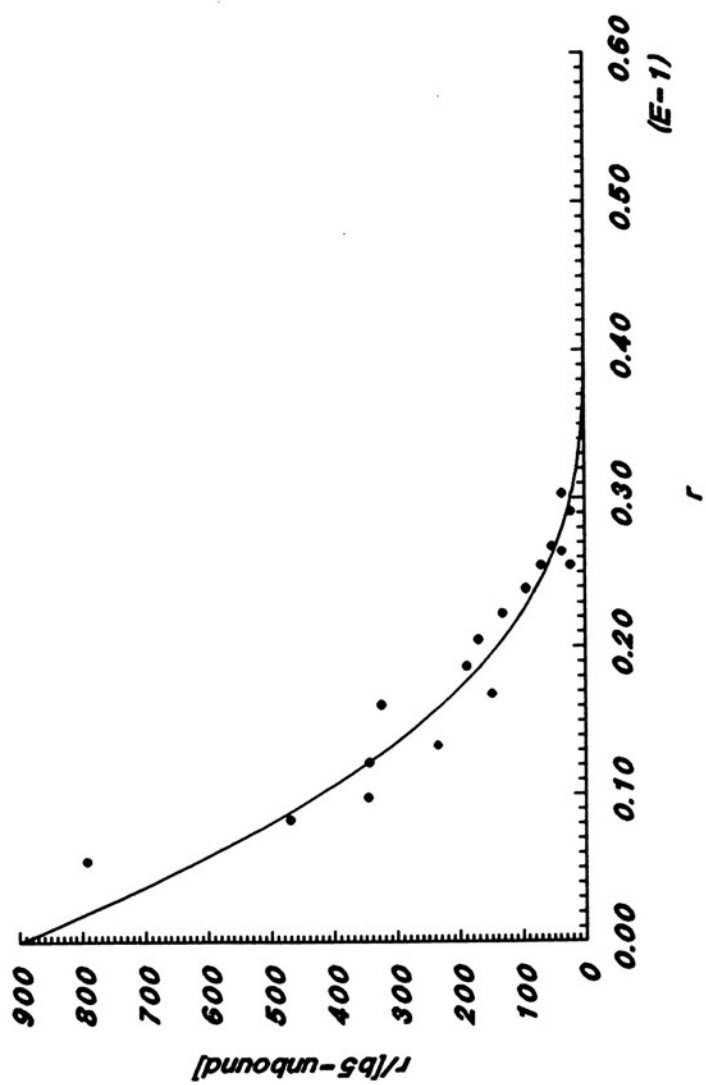


Figure 44.

Scatchard plot of cytochrome  $b_5$  binding to DOPC SUVs containing 50 mole percent cholesterol. Cyt  $b_5$  binding data from Figure 29 was replotted as  $r/[\text{unbound cyt } b_5] \text{ (mM}^{-1}\text{)}$  vs.  $r$ , where  $r$  is the molar solution concentration ratio of bound cyt  $b_5$  per phospholipid ( $[\text{bound cyt } b_5]/[\text{PL}]$ ). The fitted curve was obtained using  $K_{\text{eff}}=600 \text{ mM}^{-1}$  (y-axis intercept),  $n=17.9$  (reciprocal of x-axis intercept), and  $\eta=0.61$  in Eqn. 8.

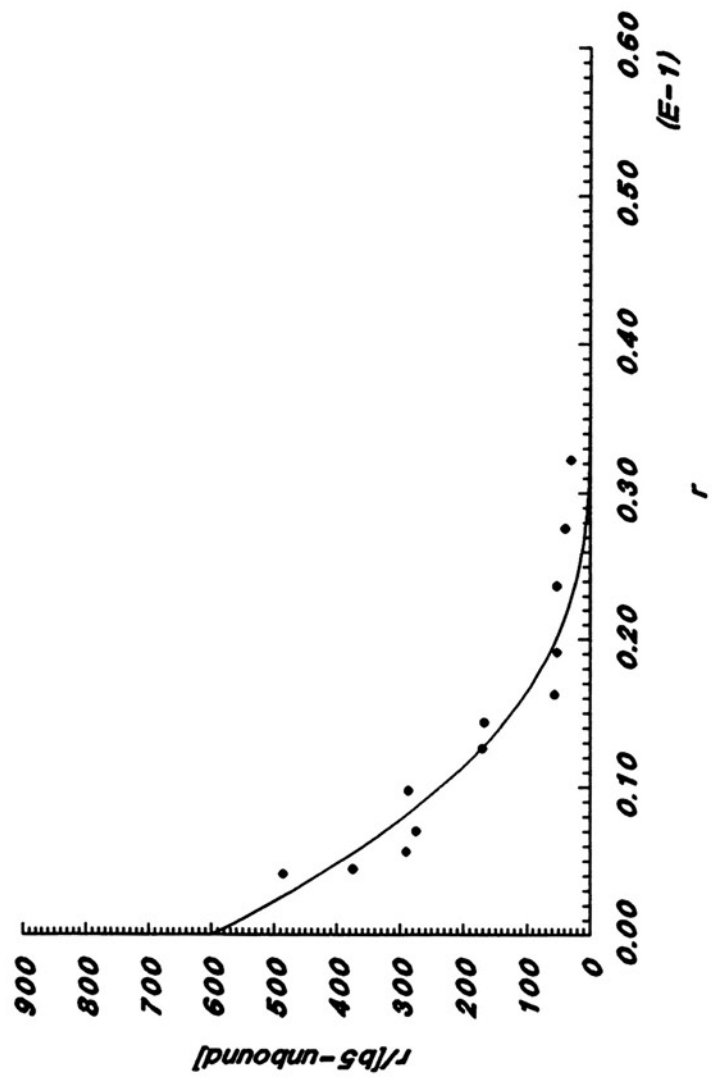


Figure 45.

Scatchard plot of cytochrome  $b_5$  binding to POPC SUVs. Cyt  $b_5$  binding data from Figure 30 was replotted as  $r/[\text{unbound cyt } b_5]$  ( $\text{mM}^{-1}$ ) vs.  $r$ , where  $r$  is the molar solution concentration ratio of bound cyt  $b_5$  per phospholipid ( $[\text{bound cyt } b_5]/[\text{PL}]$ ). The fitted curve was obtained using  $K_{\text{eff}}=362 \text{ mM}^{-1}$  (y-axis intercept),  $n=16.7$  (reciprocal of x-axis intercept), and  $\eta=0.63$  in Eqn. 8.

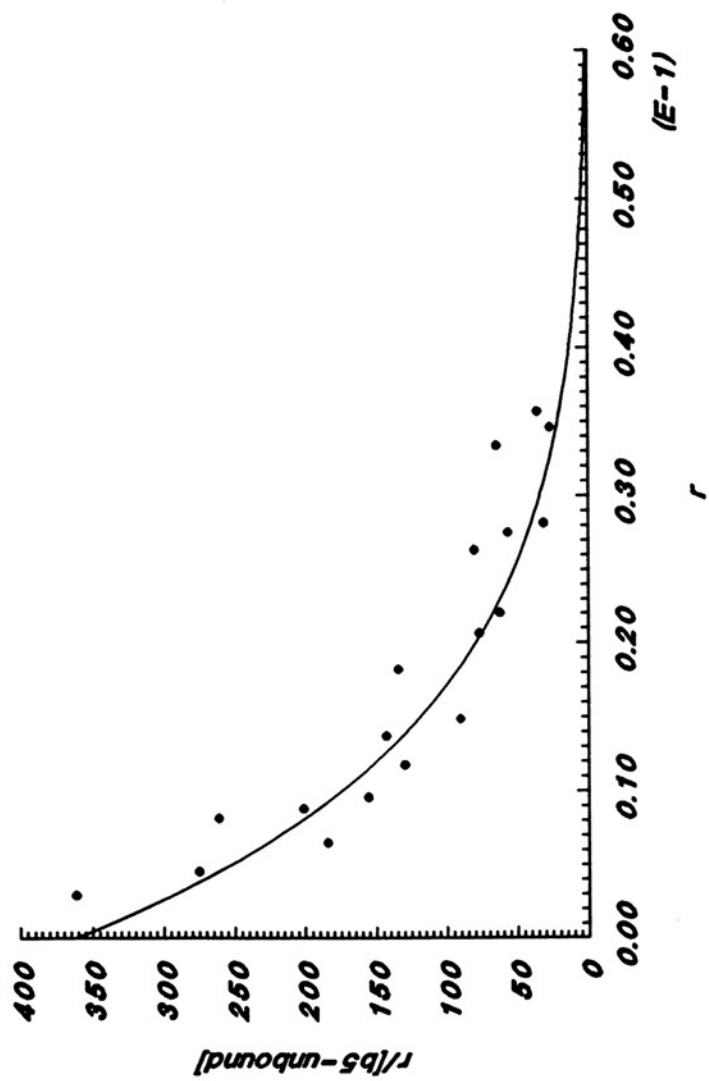




Figure 46.

Scatchard plot of cytochrome  $b_5$  binding to POPC SUVs containing 50 mole percent cholesterol. Cyt  $b_5$  binding data from Figure 31 was replotted as  $r/[\text{unbound cyt } b_5]$  ( $\text{mM}^{-1}$ ) vs.  $r$ , where  $r$  is the molar solution concentration ratio of bound cyt  $b_5$  per phospholipid ( $[\text{bound cyt } b_5]/[\text{PL}]$ ). The fitted curve was obtained using  $K_{\text{eff}}=81 \text{ mM}^{-1}$  (y-axis intercept),  $n=77$  (reciprocal of x-axis intercept), and  $\eta=0.64$  in Eqn. 8.

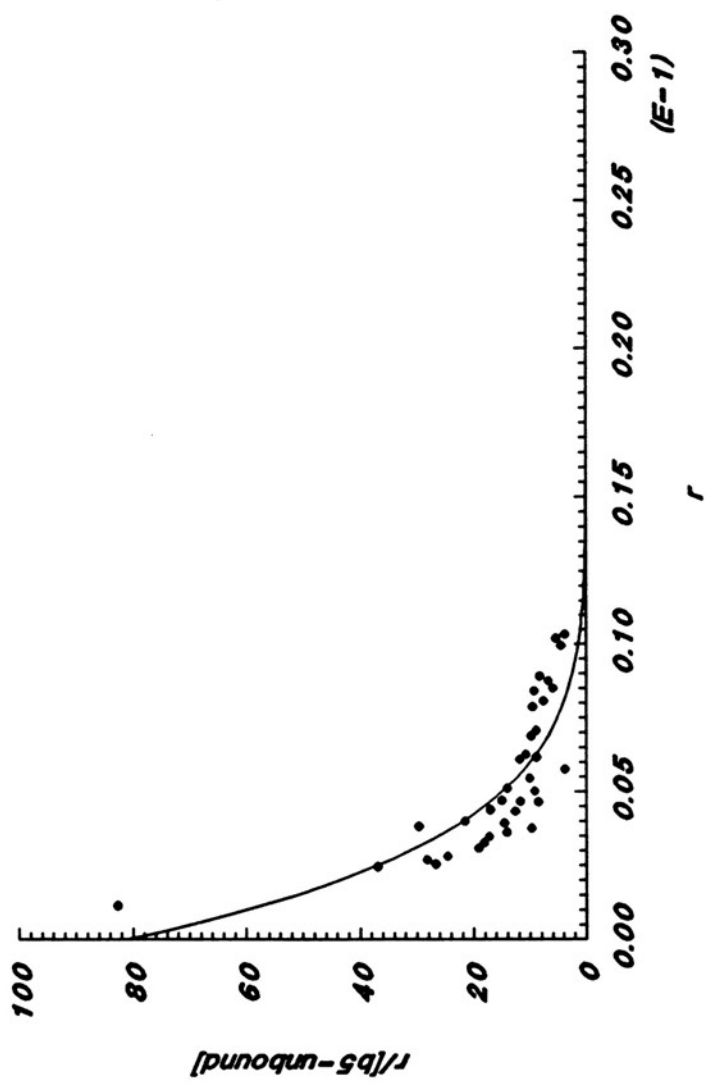


Figure 47.

Scatchard plot of cytochrome  $b_5$  binding to SOPC SUVs. Cyt  $b_5$  binding data from Figure 32 was replotted as  $r/[\text{unbound cyt } b_5]$  ( $\text{mM}^{-1}$ ) vs.  $r$ , where  $r$  is the molar solution concentration ratio of bound cyt  $b_5$  per phospholipid ( $[\text{bound cyt } b_5]/[\text{PL}]$ ). The fitted curve was obtained using  $K_{\text{eff}}=228 \text{ mM}^{-1}$  (y-axis intercept),  $n=16.7$  (reciprocal of x-axis intercept), and  $\eta=0.63$  in Eqn. 8.

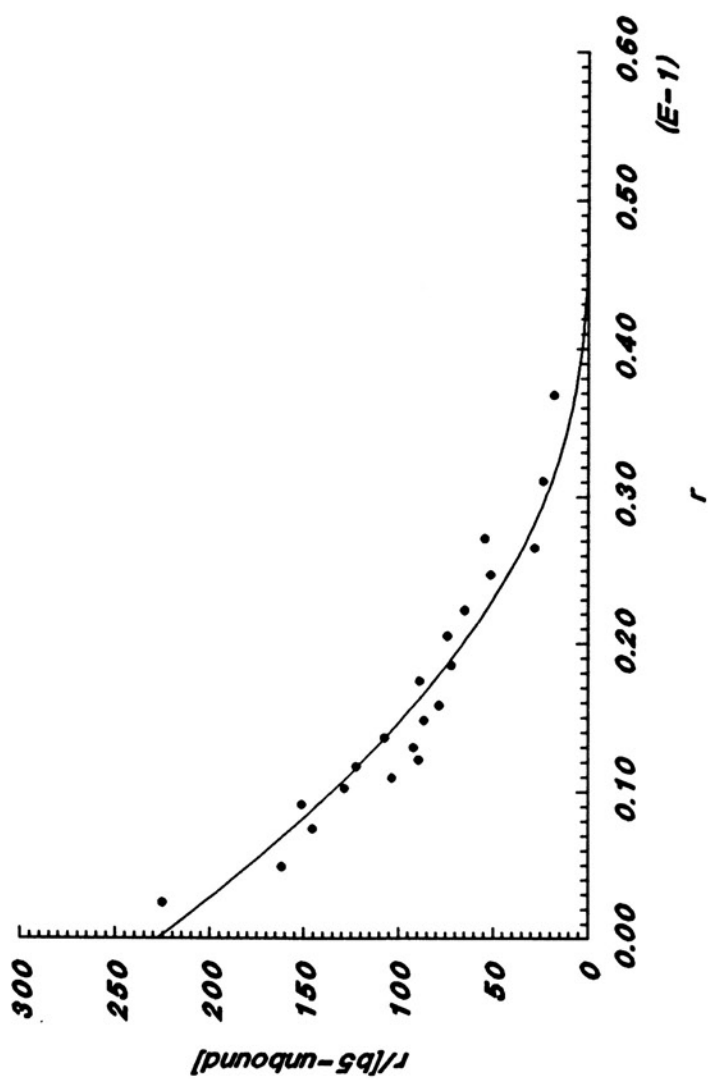


Figure 48.

Scatchard plot of cytochrome  $b_5$  binding to SOPC SUVs containing 50 mole percent cholesterol. Cyt  $b_5$  binding data from Figure 33 was replotted as  $r/[\text{unbound cyt } b_5]$  ( $\text{mM}^{-1}$ ) vs.  $r$ , where  $r$  is the molar solution concentration ratio of bound cyt  $b_5$  per phospholipid ( $[\text{bound cyt } b_5]/[\text{PL}]$ ). The fitted curve was obtained using  $K_{\text{eff}}=164 \text{ mM}^{-1}$  (y-axis intercept),  $n=53$  (reciprocal of x-axis intercept), and  $\eta=0.64$  in Eqn. 8.

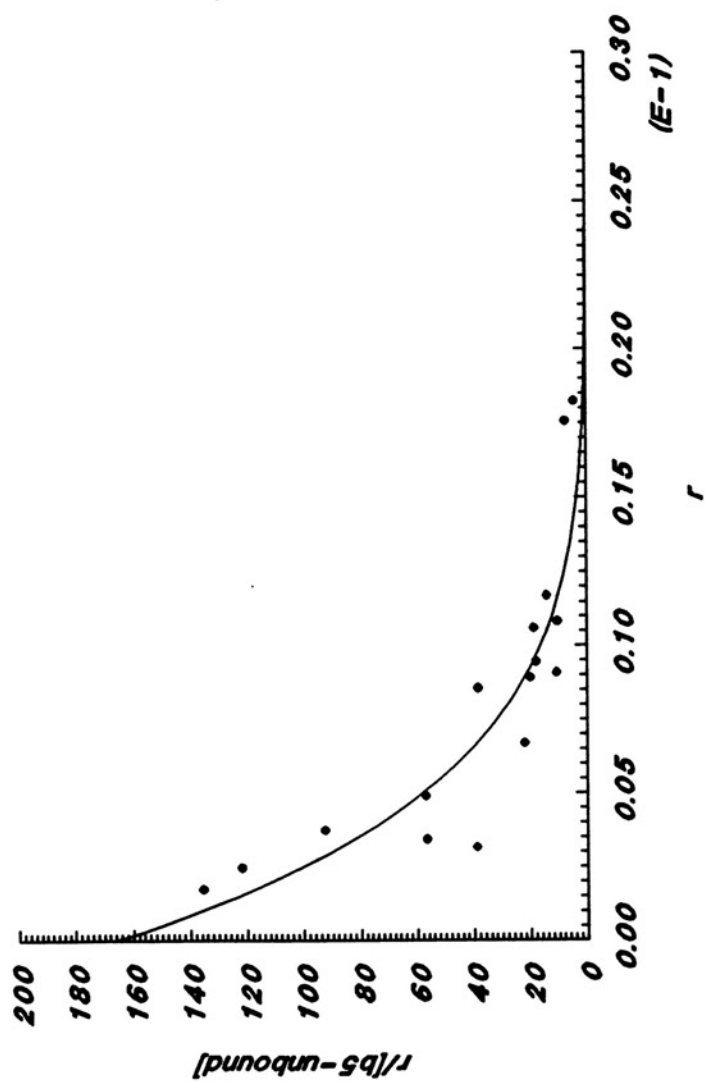


Figure 49.

Scatchard plot of cytochrome  $b_5$  binding to SLPC SUVs. Cyt  $b_5$  binding data from Figure 34 was replotted as  $r/[\text{unbound cyt } b_5]$  ( $\text{mM}^{-1}$ ) vs.  $r$ , where  $r$  is the molar solution concentration ratio of bound cyt  $b_5$  per phospholipid ( $[\text{bound cyt } b_5]/[\text{PL}]$ ). The fitted curve was obtained using  $K_{\text{eff}}=94 \text{ mM}^{-1}$  (y-axis intercept),  $n=18$  (reciprocal of x-axis intercept), and  $\eta=0.66$  in Eqn. 8.

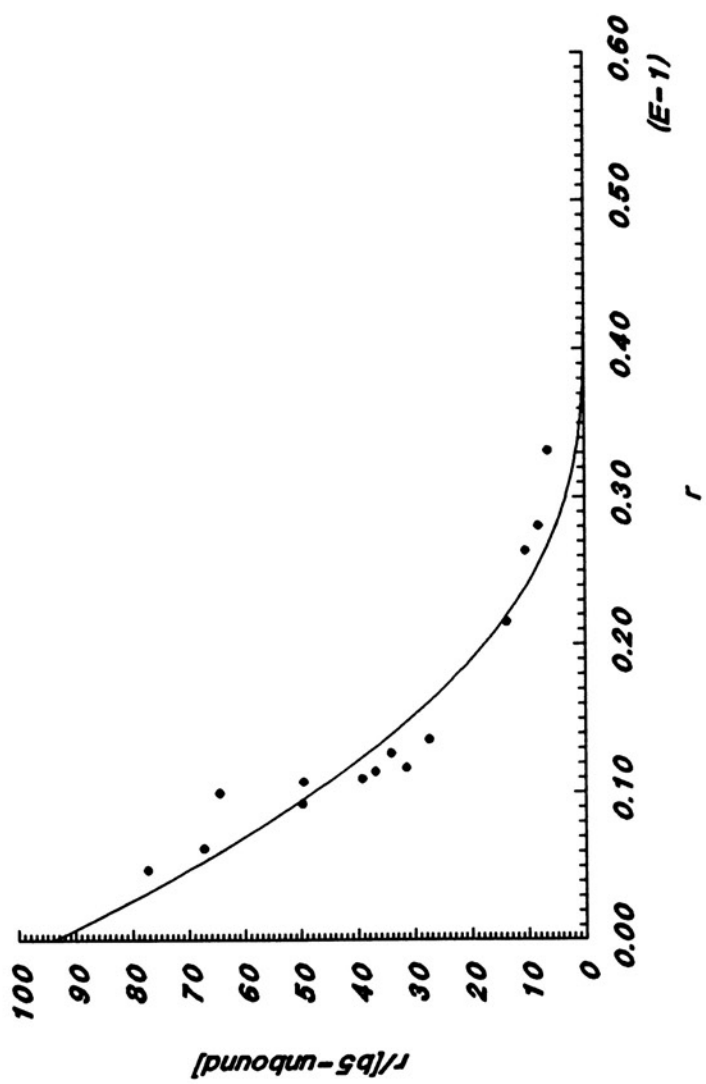




Figure 50.

Scatchard plot of cytochrome  $b_5$  binding to SLPC SUVs containing 50 mole percent cholesterol. Cyt  $b_5$  binding data from Figure 35 was replotted as  $r/[\text{unbound cyt } b_5] \text{ (mM}^{-1}\text{)}$  vs.  $r$ , where  $r$  is the molar solution concentration ratio of bound cyt  $b_5$  per phospholipid ( $[\text{bound cyt } b_5]/[\text{PL}]$ ). The fitted curve was obtained using  $K_{\text{eff}}=110 \text{ mM}^{-1}$  (y-axis intercept),  $n=30$  (reciprocal of x-axis intercept), and  $\eta=0.68$  in Eqn. 8.

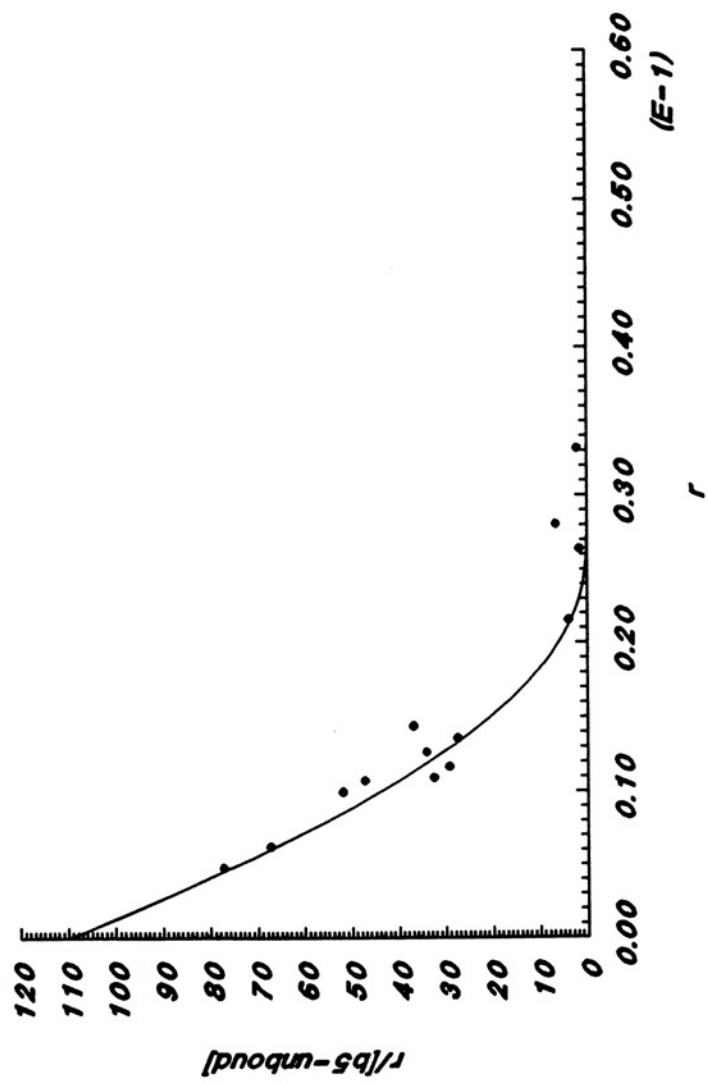


Table III: Scatchard Analysis Summary of Cytochrome  $b_5$  Binding to Small Unilamellar Vesicles prepared from various Phosphatidylcholines and Cholesterol<sup>a</sup>

phospholipid	$K_{\text{eff}}$ ( $\text{mM}^{-1}$ ) <sup>b</sup>	$n^c$	$\eta^d$
DMPC			
0% cholesterol	2200 $\pm$ 190	29.4 $\pm$ 0.9	0.56 $\pm$ 0.03
50% cholesterol	70 $\pm$ 6	30.3 $\pm$ 1.1	0.66 $\pm$ 0.04
DOPC			
0% cholesterol	900 $\pm$ 91	16.7 $\pm$ 0.9	0.60 $\pm$ 0.02
50% cholesterol	600 $\pm$ 46	17.9 $\pm$ 0.6	0.61 $\pm$ 0.03
DLPC			
0% cholesterol	114 $\pm$ 9	17.5 $\pm$ 0.7	0.66 $\pm$ 0.03
50% cholesterol	126 $\pm$ 10	17.5 $\pm$ 0.8	0.67 $\pm$ 0.03
POPC			
0% cholesterol	362 $\pm$ 29	16.7 $\pm$ 1.3	0.63 $\pm$ 0.04
50% cholesterol	81 $\pm$ 9	76.9 $\pm$ 3.2	0.64 $\pm$ 0.03
SOPC			
0% cholesterol	228 $\pm$ 16	16.7 $\pm$ 1.0	0.63 $\pm$ 0.02
50% cholesterol	164 $\pm$ 12	52.6 $\pm$ 1.2	0.64 $\pm$ 0.04
PLPC			
0% cholesterol	107 $\pm$ 11	16.7 $\pm$ 0.6	0.65 $\pm$ 0.02
50% cholesterol	98 $\pm$ 9	32.3 $\pm$ 1.1	0.66 $\pm$ 0.04
SLPC			
0% cholesterol	94 $\pm$ 7	17.9 $\pm$ 0.9	0.66 $\pm$ 0.02
50% cholesterol	110 $\pm$ 9	30.3 $\pm$ 1.0	0.68 $\pm$ 0.02
egg PC			
0% cholesterol	-	(21.3)	-
50% cholesterol	296 $\pm$ 40	105.3 $\pm$ 2.9	0.60 $\pm$ 0.02
liver PC			
0% cholesterol	-	(20.0)	-
50% cholesterol	257 $\pm$ 31	108.7 $\pm$ 3.4	0.60 $\pm$ 0.03
PC/SPH (1:1)			
0% cholesterol	-	(20.0)	-
50% cholesterol	246 $\pm$ 31	106.4 $\pm$ 6.2	0.60 $\pm$ 0.03

<sup>a</sup>Cyt  $b_5$  binding data was plotted as [bound cyt  $b_5$ ]/[PL][free cyt  $b_5$ ] vs. [bound cyt  $b_5$ ]/[PL]. The Scatchard plots were evaluated by fitting Eqn. 8 to the experimental data (See text for additional details). <sup>b</sup>Effective binding constant, which corresponds to the y-axis intercept of the fitted curve. <sup>c</sup>minimum stoichiometric number of PL:cyt  $b_5$ , which is the reciprocal of the x-axis intercept of the fitted curve. The "()" denote values that were obtained directly from the binding isotherms. <sup>d</sup>cooperativity parameter.

Table IV indicates the observed cyt  $b_5$  saturation levels of sonicated, limit-size liposomes of the various natural and synthetic phosphatidylcholines with and without 50 mole percent cholesterol. In each instance, the extent of cyt  $b_5$  binding to SUVs is always significantly greater than the binding to LUVs. Among cholesterol free liposomes, the amount of cyt  $b_5$  per 1000 phospholipids is up to 7-fold greater in SUVs than in LUVs. For liposomes that contain 50 mole percent cholesterol, the saturation limits of SUVs can be up to a factor of 130 greater than those observed with LUVs. Additionally, unsaturation in phospholipid acyl chains does not appear to enhance the extent of cyt  $b_5$  binding in SUVs as it does in LUVs.

The cholesterol inhibitory parameter indicates that cholesterol reduces cyt  $b_5$  binding to all preformed SUVs (in terms of the overall surface area or the number of total lipid molecules that are required for cyt  $b_5$  binding) and that the extent of cyt  $b_5$  binding inhibition differs among the various phosphatidylcholines. As similarly observed with LUVs, unsaturation of phospholipid fatty acyl chains apparently lessens the cholesterol inhibitory effect on cyt  $b_5$  binding into SUVs. Cholesterol most significantly inhibits cyt  $b_5$  binding to SUVs that are prepared from mixed-chain monoenoic (POPC and SOPC) and natural phospholipid mixtures (egg PC, liver PC, and PC/SPH): A 50 mole percent cholesterol composition notably reduces the cyt  $b_5$  saturation level by approximately 5-fold. To a lesser extent, cholesterol inhibits cyt  $b_5$  from binding to SUVs that are prepared with the mixed-chain, dienoic phospholipids PLPC and SLPC ( $\phi \approx 1.8$ ), and has relatively diminished effects on the cyt  $b_5$  saturation point in DOPC and DLPC SUVs ( $\phi \approx 1.0$ ).

**Table IV: Effect of Cholesterol on the Saturation Levels of Cytochrome  $b_5$  Binding to Phosphatidylcholine Small Unilamellar Liposomes<sup>a</sup>**

phospholipid	cytochrome $b_5$ /1000 phospholipids		$\phi^b$
	0% cholesterol	50% cholesterol	
DMPC	34 $\pm$ 1	33 $\pm$ 1	1.0
DOPC	60 $\pm$ 3	56 $\pm$ 2	1.1 $\pm$ 0.1
DLPC	57 $\pm$ 3	57 $\pm$ 3	1.0 $\pm$ 0.1
POPC	60 $\pm$ 5	13 $\pm$ 1	4.6 $\pm$ 0.7
SOPC	60 $\pm$ 4	19 $\pm$ 1	3.2 $\pm$ 0.4
PLPC	60 $\pm$ 2	31 $\pm$ 1	1.9 $\pm$ 0.1
SLPC	56 $\pm$ 3	33 $\pm$ 1	1.7 $\pm$ 0.1
egg PC	47	9.5 $\pm$ 0.3	4.9 $\pm$ 0.2
liver PC	50	9.2 $\pm$ 0.3	5.4 $\pm$ 0.2
PC/SPH (1:1)	50	9.4 $\pm$ 0.6	5.3 $\pm$ 0.3

<sup>a</sup>Cyt  $b_5$  (1.56  $\mu$ M) and SUVs (0-0.624 mM PL) were incubated for 2 h at 25 or 37°C. The extent of binding was determined by fluorometry. Scatchard plots of binding data were evaluated by an iterative fit of Eqn. 8 (See Experimental Procedures). <sup>b</sup>cholesterol inhibitory parameter,  $\phi$  = (cyt  $b_5$  saturation in liposomes without cholesterol)/(cyt  $b_5$  saturation in liposomes with cholesterol). The standard error of the liposome saturation levels and cholesterol inhibitory parameter were obtained from the curve-fitting analysis.

The only exception to fatty acyl unsaturation reducing the cholesterol inhibitory effect is observed with the fully saturated phospholipid, DMPC. Unlike the rather significant inhibition of cyt  $b_5$  binding observed with DMPC LUVs ( $\phi > 127.0$ ), cholesterol nominally affects the saturation level in DMPC SUVs ( $\phi = 1.0$ ).

Although the cholesterol-mediated inhibition of cyt  $b_5$  binding to phosphatidylcholine SUVs essentially parallels the pattern observed with LUVs, the extent is significantly reduced in SUVs. The pronounced surface curvature of SUVs apparently interferes with the inhibitory effect.

In addition to the effect of cholesterol on the cyt  $b_5$  saturation levels of SUVs, the relative intrinsic binding affinities were obtained from the nonlinear Scatchard plots. The apparent or observed affinity constants that cyt  $b_5$  exhibits for phospholipids are on the order of  $10^5 \text{ M}^{-1}$  (Table V). These results appear inconsistent with previous kinetic data which indicate that cyt  $b_5$  monomers bind to preformed vesicles with an affinity constant of approximately  $10^{10} \text{ M}^{-1}$  (Leto and Holloway, 1979). In the present investigation, the experiments were performed in Tris-acetate buffer at a greater ionic strength so that unbound cyt  $b_5$  was mostly self-aggregated as octomers that were in equilibrium with a small amount of cyt  $b_5$  monomers. Therefore, unlike the kinetic study, the observed association constants do not correspond to a simple equilibrium of cyt  $b_5$  monomers with liposomes, but to a more complex pathway with coupled steps instead.

The following reaction scheme suggests a simplified pathway for the binding of cyt  $b_5$  to preformed liposomes under the experimental conditions in the present study:



As shown, cyt  $b_5$  binding to a liposome involves at least 2 individual steps: the dissociation of octomer aggregates into monomers and the partitioning of the monomers into liposomes. A free cyt  $b_5$  monomer may bind to a liposome or, alternatively, it may aggregate with other monomers to make octomers. In other words, the above scheme shows that octomer and proteoliposome formation are competitive. Since the experiments were designed to measure the *total* amounts of liposome-bound and free cyt  $b_5$ , the observed association constants must be composites of separate equilibria among individual reaction steps. The net equilibrium between total free  $b_5$  and total membrane-bound  $b_5$  may be expressed as:

$$K = \frac{[\text{cyt } b_5\text{-liposome}]}{(8[b_5(\text{octomer})] + [b_5(\text{monomer})])[phospholipid]}$$

where  $[\text{cyt } b_5\text{-liposome}]$  is the total concentration of cyt  $b_5$  bound to liposomes and  $8[b_5(\text{octomer})] + [b_5(\text{monomer})]$  is the sum total concentration of free cyt  $b_5$  in solution. Although the association constants that have been observed in this study do not readily indicate the affinity of cyt  $b_5$  monomers for cholesterol-containing liposomes, they do signify that cholesterol may affect the overall equilibrium between membrane-bound and unbound cyt  $b_5$ .

Table V indicates the cyt  $b_5$  binding equilibria for the different phosphatidylcholine SUVs with and without 50 mole percent cholesterol. To more accurately estimate the effect of cholesterol on the affinity of cyt

$b_5$  for a liposome, the experimentally observed equilibrium constants for cholesterol-containing SUVs are also expressed in terms of the total effective lipid concentration. The total effective lipid concentration, which does not account for the condensing effect of cholesterol, is rather simply defined as:  $[\text{phospholipid}] + 1/2[\text{cholesterol}]$ , since cholesterol has approximately one-half the surface area of phospholipids (Jain, 1988f). This parameter more appropriately corresponds to the amount of required lipid to provide sufficient surface areas for cyt  $b_5$  binding.

On a per mole of total effective lipid basis, there is a modest, but detectable reduction of the overall equilibrium constant of cyt  $b_5$  binding to 1:1 phospholipid/cholesterol mixtures for many of the phospholipid systems (Table V). The cyt  $b_5(\text{bound})/\text{cyt } b_5(\text{free})$  equilibria with SUVs containing 50 mole percent cholesterol range from approximately 2-60 -fold less than with liposomes of pure phospholipid. The rather limited reduction in the equilibrium constants observed with most the phospholipids does not readily indicate if cyt  $b_5$  has less affinity for bilayers containing cholesterol, especially since the obtained values are composites of a complex equilibrium scheme. Yet the results with DMPC and the natural phospholipid mixtures are of interest: The relative cyt  $b_5$  equilibrium binding constants are reduced approximately 50-fold when the SUVs contain 50 mole percent cholesterol. Since the cyt  $b_5(\text{octomer}) \rightleftharpoons \text{cyt } b_5(\text{monomer})$  equilibrium constant is probably unaffected from the binding of monomers to liposomes, the observed net decrease in the overall equilibrium between bound and free cyt  $b_5$  suggests that cyt  $b_5$  has less affinity for 1:1 cholesterol/phospholipid mixtures than for the pure phospholipids.



**Table V: Effect of Cholesterol on Cytochrome  $b_5$  Binding Equilibrium for Phosphatidylcholine Small Unilamellar Vesicles<sup>a</sup>**

phospholipid	0% cholesterol	50% cholesterol		$K_{0\%}:K_{c+p}$
	$K_{\text{eff}} \text{ (M}^{-1}\text{)}^b$	$K_{\text{eff}} \text{ (M}^{-1}\text{)}^c$	$K_{\text{eff}(c+p)} \text{ (M}^{-1}\text{)}^d$	
DMPC	$2.2 \times 10^6$	$7.0 \times 10^4$	$4.7 \times 10^4$	47
DOPC	$9.0 \times 10^5$	$6.0 \times 10^5$	$4.0 \times 10^5$	2
DLPC	$1.1 \times 10^5$	$1.3 \times 10^5$	$8.7 \times 10^4$	1
POPC	$3.6 \times 10^5$	$8.1 \times 10^4$	$5.4 \times 10^4$	7
SOPC	$2.3 \times 10^5$	$1.6 \times 10^5$	$1.1 \times 10^5$	2
PLPC	$1.1 \times 10^5$	$9.8 \times 10^4$	$6.5 \times 10^4$	2
SLPC	$9.4 \times 10^4$	$1.1 \times 10^5$	$7.3 \times 10^4$	1
egg PC	(> $10^7$ )	$3.0 \times 10^5$	$2.0 \times 10^5$	>50
liver PC	(> $10^7$ )	$2.6 \times 10^5$	$1.7 \times 10^5$	>59
PC/SPH (1:1)	(> $10^7$ )	$2.5 \times 10^5$	$1.7 \times 10^5$	>59

<sup>a</sup>The equilibrium data has been adapted from the curve-fitting results of Eqn. 8 (Table III). <sup>b</sup>observed cyt  $b_5$  binding equilibrium constant for SUVs; 0% cholesterol. The "( )" denote estimations of the constants: The defined saturation points in the binding isotherms suggests very high cyt  $b_5$  binding affinity to SUVs prepared from natural phospholipid mixtures. <sup>c</sup>observed cyt  $b_5$  binding constant for SUVs; 50% cholesterol. <sup>d</sup>corrected cyt  $b_5$  binding equilibrium constant for 1:1 phospholipid/cholesterol liposome. The binding equilibrium is calculated by expressing observed  $K_{\text{eff}}$  for 50% cholesterol SUVs in terms of effective total lipid, where effective total lipid = [phospholipid] + 1/2[cholesterol].

The results of the curve-fitting analysis (Table III) indicate that the reported cyt  $b_5$  binding equilibrium constants have a standard error of 9.3%.

The significant decrease in the binding affinities observed with DMPC and the natural phospholipid mixtures suggests that cholesterol most likely affects the insertion of the protein. Recalling that cyt  $b_5$  binds tightly to DMPC SUVs (Enoch *et al.*, 1979), a 1:1 DMPC/cholesterol composition may reduce or actually prevent tight insertion, which is manifested by significantly weaker cyt  $b_5$  association (i.e. lower affinity constant) with the liposome. Likewise, the estimated binding equilibrium constants (as the absence of curvature in the binding isotherms indicates) suggest essentially irreversible cyt  $b_5$  binding to cholesterol-free, natural PC SUVs. However, because the evaluated binding affinities for natural PC SUVs containing 50 mole percent cholesterol are probably significantly less than the binding constants for the cholesterol-free liposomes, cyt  $b_5$  probably cannot interact as favorably with the cholesterol containing liposomes.

In summary, a 50 mole percent composition of bilayer cholesterol inhibits cyt  $b_5$  partitioning into limit-size, sonicated phosphatidylcholine liposomes. The extent of binding inhibition is phospholipid dependent: The most significant overall reduction in the cyt  $b_5$  saturation levels occurs with SUVs prepared from the natural phospholipid mixtures or mixed-chain monoenoic phospholipids. Unsaturation in phospholipids diminishes the cholesterol inhibitory effect on cyt  $b_5$  binding. The results are generally consistent with those observed for LUVs, except that the effect is more pronounced in LUVs than in SUVs. Additionally, a 50 mole percent cholesterol composition appears to decrease the relative cyt  $b_5$  binding equilibrium for some SUVs, suggesting that cyt  $b_5$  exhibits weaker association with these liposomes. Therefore, not only does cholesterol

reduce the number of sites available for cyt  $b_5$  interaction with some SUVs, but whatever binding that does occur is less favorable than binding to a pure phospholipid bilayer. The cholesterol-mediated reduction in both the saturation level of SUVs and the cyt  $b_5$  affinity for PC SUVs indicates that cyt  $b_5$  preferentially partitions into pure phospholipid bilayers rather than bilayers that contain cholesterol.

*The Effect of Cholesterol on Cytochrome  $b_5$  binding and insertion into 1-palmitoyl-2-oleoyl-sn-glycero-3-phosphorylcholine LUVs.*

The previous observations indicate that cholesterol significantly reduces the amount of cyt  $b_5$  that can bind to preformed liposomes. However, the extent of inhibition significantly depends upon the bilayer phospholipid composition and curvature. To further characterize and explain this phenomenon in terms of a physico-chemical model, the effect of cholesterol on cyt  $b_5$  binding and insertion into POPC LUVs was examined in detail over the 0-50 mole percent range of cholesterol compositions. This particular liposome system was chosen because of the dramatic effect of cholesterol on spontaneous cyt  $b_5$  partitioning into the lipid bilayer. In particular, LUVs are not affected by curvature-induced strain unlike limit-size liposomes. The previous observations demonstrate that significant bilayer curvature reduces the cholesterol inhibitory effect. The lateral packing of lipid molecules in LUVs also resembles the predominant packing in biological membranes, even though significantly curved surfaces do occur natural bilayers. Not only should the effects of cholesterol be predominantly manifested with this phospholipid system, but POPC actually represents most commonly occurring phospholipids; it is a mixed-chain phospholipid with saturated and unsaturated hydrocarbon chains esterified at the *sn*-1 and *sn*-2 positions of the glycerol base, respectively. In fact, POPC is the predominant component of egg PC, but lacks many of the peroxidation problems associated with the natural mixture.

*(A) Effect of Cholesterol on Cytochrome  $b_5$  Binding to POPC-LUVs.*

The initial approach in this investigation was to determine the cyt  $b_5$  saturation levels of POPC reverse-phase liposomes at various cholesterol/phospholipid ratios. As formerly observed, cholesterol inhibits cyt  $b_5$  binding by up to approximately 90-fold in direct binding mixtures containing saturating cyt  $b_5$  levels and POPC liposomes (See Table II). However, Figure 51 indicates that the reduction in cyt  $b_5$  binding is a complex function of cholesterol composition. The saturation binding curve appears triphasic, with a sharp decrease from 0-20% cholesterol, a plateau between 20-33%, and finally a linear decrease from 33-50% cholesterol. The cholesterol inhibition of cyt  $b_5$  binding to POPC LUVs, which resembles a titration curve, suggests two cholesterol-associated events: one at 20 and possibly another at 33 mole percent cholesterol.

Although the saturation curve exhibits the complex cholesterol-mediated reduction in cyt  $b_5$  binding to POPC LUVs, it does not readily delineate the extent of this inhibition at different cholesterol compositions. Therefore, the data was also evaluated in terms of the cholesterol inhibitory parameter,  $\phi$ , as a function of mole percent cholesterol (Figure 52). The cyt  $b_5$  saturation level of POPC LUVs from 0-20 mole percent cholesterol is reduced by only a factor of 3.6. Likewise, there is also a modest 1.4-fold decrease in cyt  $b_5$  binding to POPC LUVs between 20-33% cholesterol. The most significant inhibitory effect occurs between 33 and 50 mole percent cholesterol, in which cholesterol reduces the cyt  $b_5$  saturation level of the liposomes 17-fold.

The significant inhibitory effect on cyt  $b_5$  binding to POPC-LUVs as cholesterol content increases from 0 to 50 mole percent could be the result of a cholesterol-mediated reduction in the number of sites

**Figure 51.**

Cytochrome  $b_5$  binding to POPC LUVs containing cholesterol. Cytochrome  $b_5$  (0.048-0.08  $\mu$ moles  $b_5$ ) was incubated with POPC LUVs (4-20  $\mu$ moles POPC doped with  $8.0 \times 10^4$  -  $1.9 \times 10^5$  dpm [ $^3$ H] triolein/ $\mu$ mole POPC) under argon in Tris-acetate buffer, pH 8.1 for 24 h at 30°C. The initial cyt  $b_5$ :POPC mole ratio was varied between 1:50 and 1:417. Proteoliposomes were separated from unbound protein on Sepharose 2B-CL columns (0.9  $\times$  28.5 cm or 1.6  $\times$  55 cm) thermostatted at 25°C. The elution profiles of cyt  $b_5$  and POPC-LUVs were determined from the  $A_{413}$  and [ $^3$ H] dpm, respectively. The extent of binding was calculated from the percentage of cyt  $b_5$  eluting with LUVs in the column void volume fractions. Initial binding ratios which resulted in less than 75% of complete protein binding were assumed to be above the saturation level of the liposomes. The saturation levels have been corrected for the lamellarity of liposomes as determined from TNBS labelling experiments. Selected experiments (0%, 10%, 25%, 33%, and 50% cholesterol) were repeated; the reported values are accurate to within  $\pm$  3.5%.

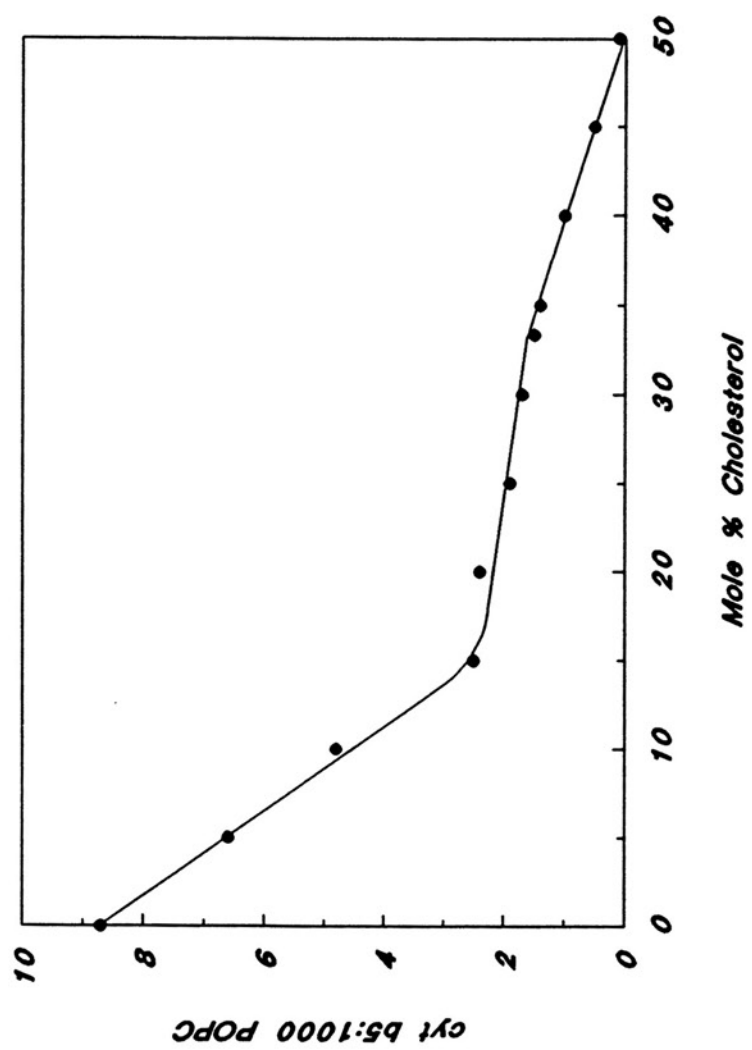
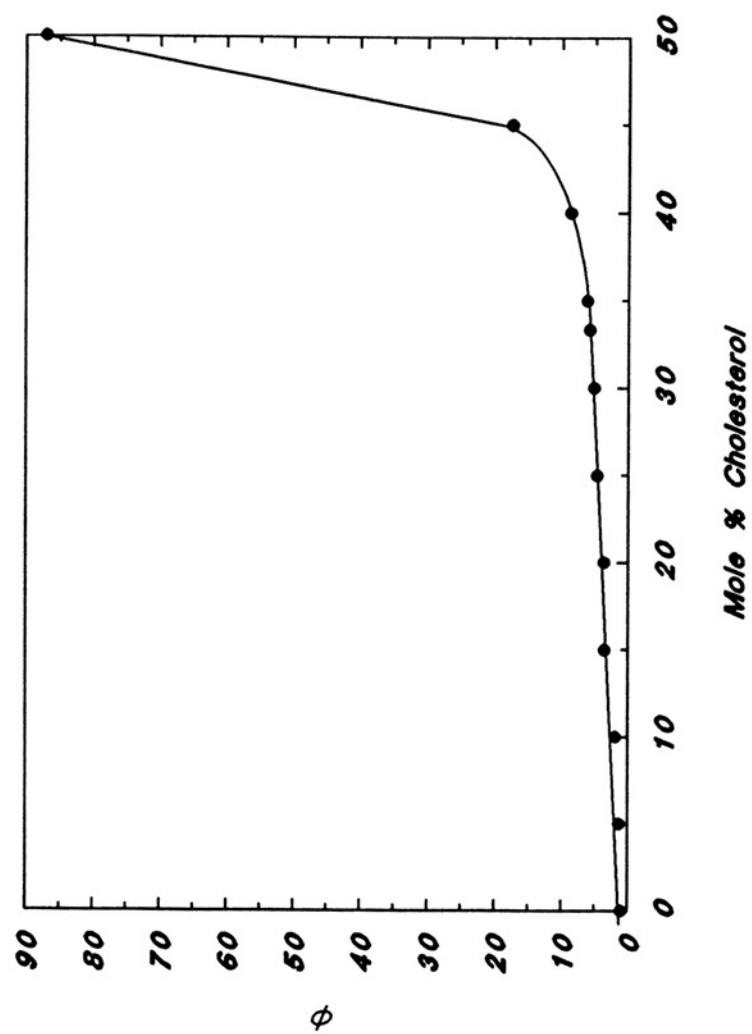


Figure 52.

Inhibition of cyt  $b_5$  binding to POPC LUVs as a function of cholesterol mole percent. The reduction in cyt  $b_5$  binding is expressed in terms of the cholesterol inhibitory parameter,  $\phi$ , using the data from Figure 51.  $\phi = (\text{cyt } b_5 / 1000 \text{ POPC of LUVs without cholesterol}) / (\text{cyt } b_5 / 1000 \text{ POPC of LUVs with cholesterol})$ .





available for cyt  $b_5$  insertion or a decrease in the overall affinity that cyt  $b_5$  has for a liposome, through interaction with phospholipid molecules.

To interpret the cholesterol effect in terms of a physico-chemical model, additional studies were performed to ascertain if cholesterol affects the affinity constant of cyt  $b_5$  for LUVs. The approach was similar to that taken to determine the saturation level of cyt  $b_5$  in SUVs: analysis of binding isotherms of the fraction of bound cyt  $b_5$  as a function of the liposome to cyt  $b_5$  concentration ratio within the 0-40% cholesterol compositional range. Complete cyt  $b_5$  binding isotherms for POPC LUVs with cholesterol compositions that are greater than 40 mole percent could not be obtained due to the very low saturation level of these liposomes. Figures 53, 54, 55, and 56 show the respective binding isotherms of cyt  $b_5$  interaction with POPC LUVs comprised of 0, 10, 20, and 40 mole percent cholesterol. As the cholesterol composition increases, the concentration of liposomes that is required to achieve complete binding of cyt  $b_5$  also concomitantly increases.

Cyt  $b_5$ /LUV binding data was evaluated by replotting in Scatchard form and then using an iterative curve-fitting routine for specifically applied cases of the general expression for cooperative ligand absorption to bilayer surfaces (Eqn. 2). For each POPC-LUV system that had cholesterol compositions of 0, 10, 20, and 40 mole percent, respective cyt  $b_5$  binding sites were modeled based upon the known saturation ratios of cyt  $b_5$ :1000 POPC in cholesterol-containing LUVs (Figure 51), together with the prolate elliptical shape of the cyt  $b_5$  catalytic domain. In POPC reverse-phase liposomes containing 0, 10, 20, and 40 mole percent cholesterol, the saturation levels of 9.0, 4.8, 2.4, and 1.0 cyt  $b_5$ :1000 POPC imply the

Figure 53.

Cytochrome  $b_5$  binding to POPC LUVs; 0% Cholesterol. Separate samples containing cyt  $b_5$  (3.12 nmoles) and POPC liposomes (0-1.248  $\mu$ moles POPC) were incubated in 2 ml total volume of Tris-acetate buffer for 2 h at 30°C. The extent of binding was determined from cyt  $b_5$  fluorescence measurements, using Eqn. 1. Excitation and emission wavelengths were 280 nm and 338 nm; bandwidths were 2.5 and 5 nm. Fluorescence spectra were corrected for light scattering and excitation beam attenuation. See Experimental Procedures for additional details.

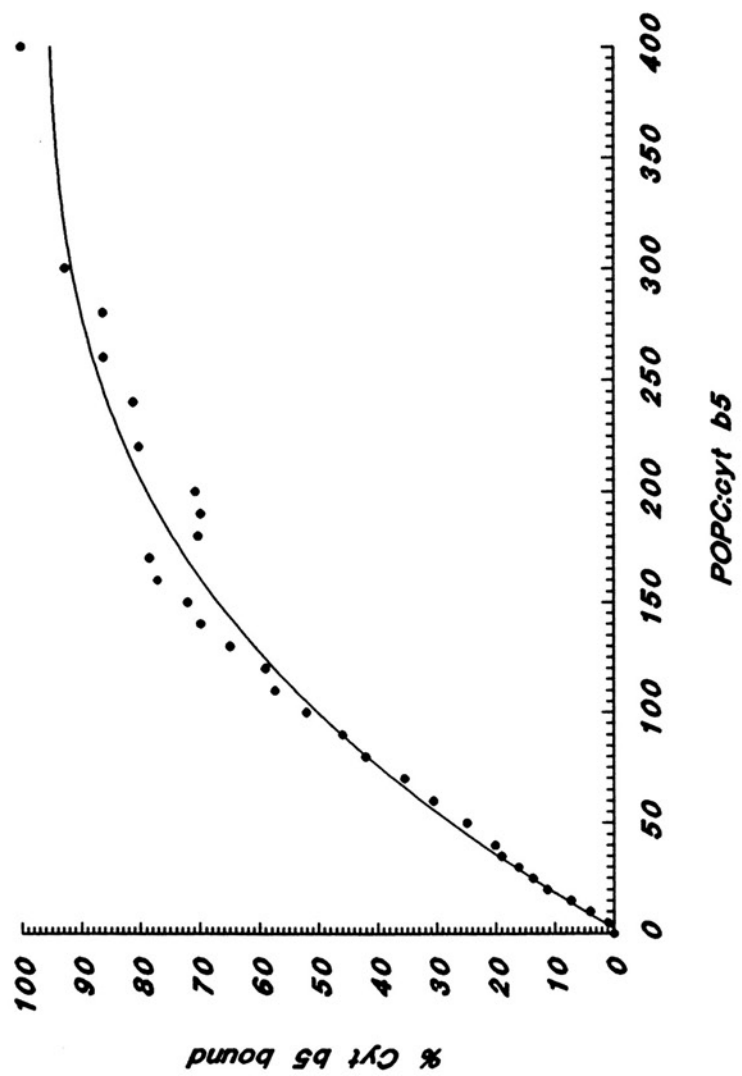


Figure 54.

Cytochrome  $b_5$  binding to POPC LUVs; 10% Cholesterol. Separate samples containing cyt  $b_5$  (3.12 nmoles) and POPC liposomes (0-1.560  $\mu$ moles POPC and 0-0.173  $\mu$ moles cholesterol; 9:1 POPC:cholesterol) were incubated in 2 ml total volume of Tris-acetate buffer for 2 h at 30°C. The extent of binding was determined from cyt  $b_5$  fluorescence measurements, using Eqn. 1. Excitation and emission wavelengths were 280 nm and 338 nm; bandwidths were 2.5 and 5 nm. Fluorescence spectra were corrected for light scattering and excitation beam attenuation. See Experimental Procedures for additional details.

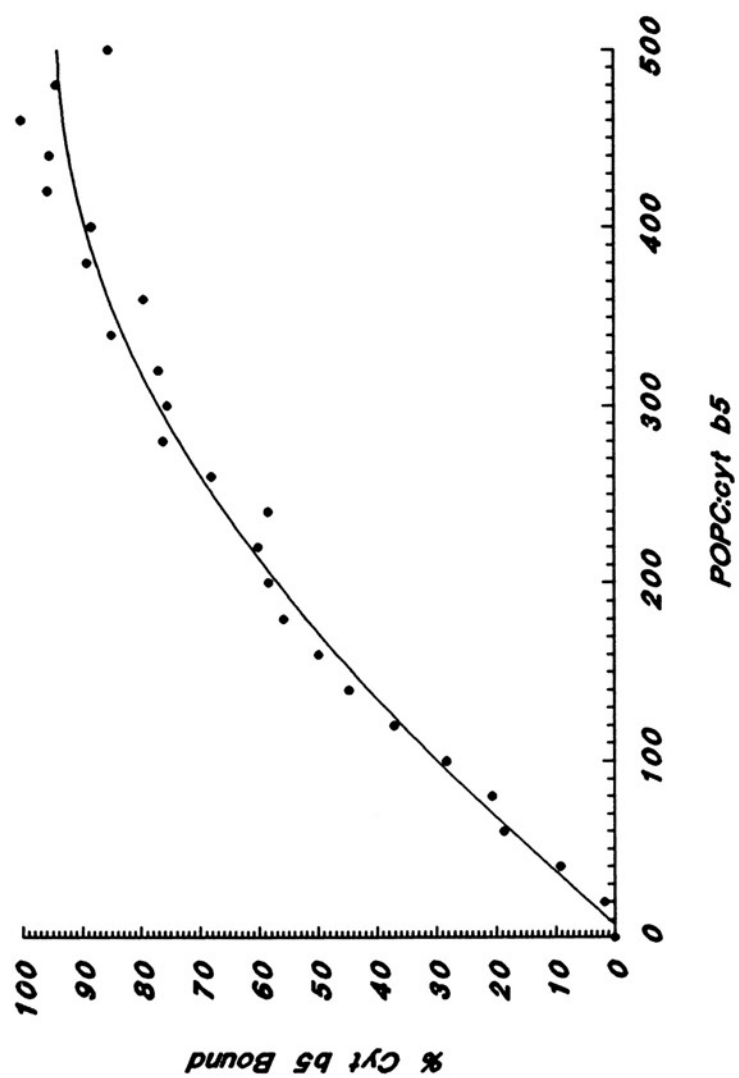
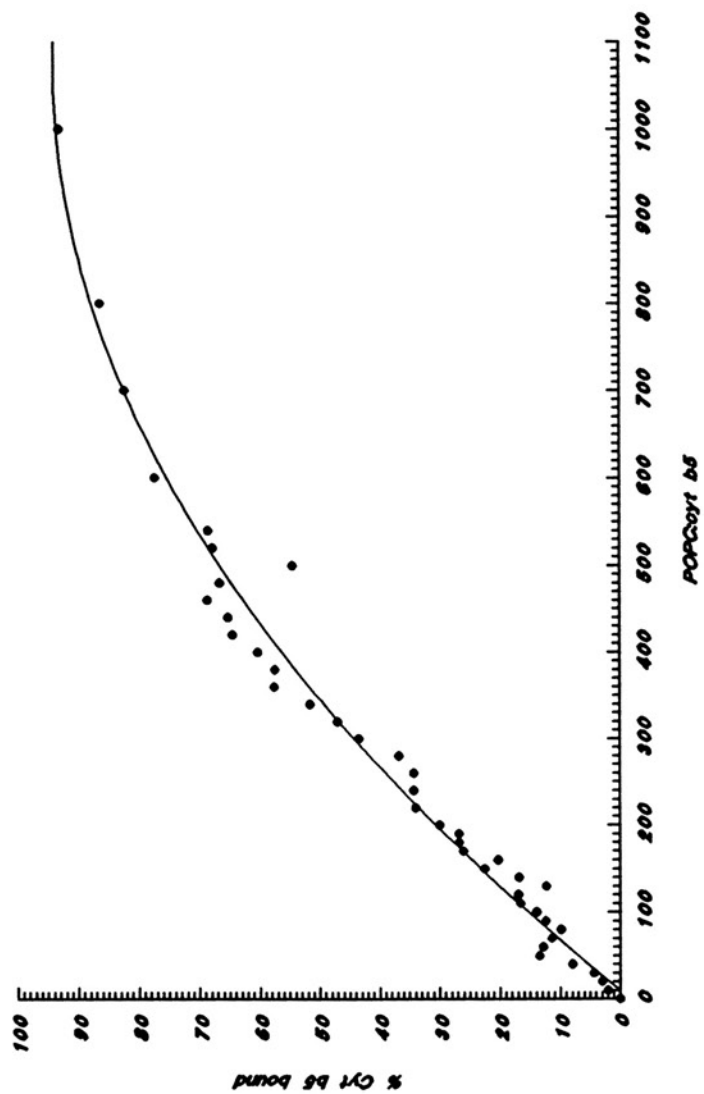


Figure 55.

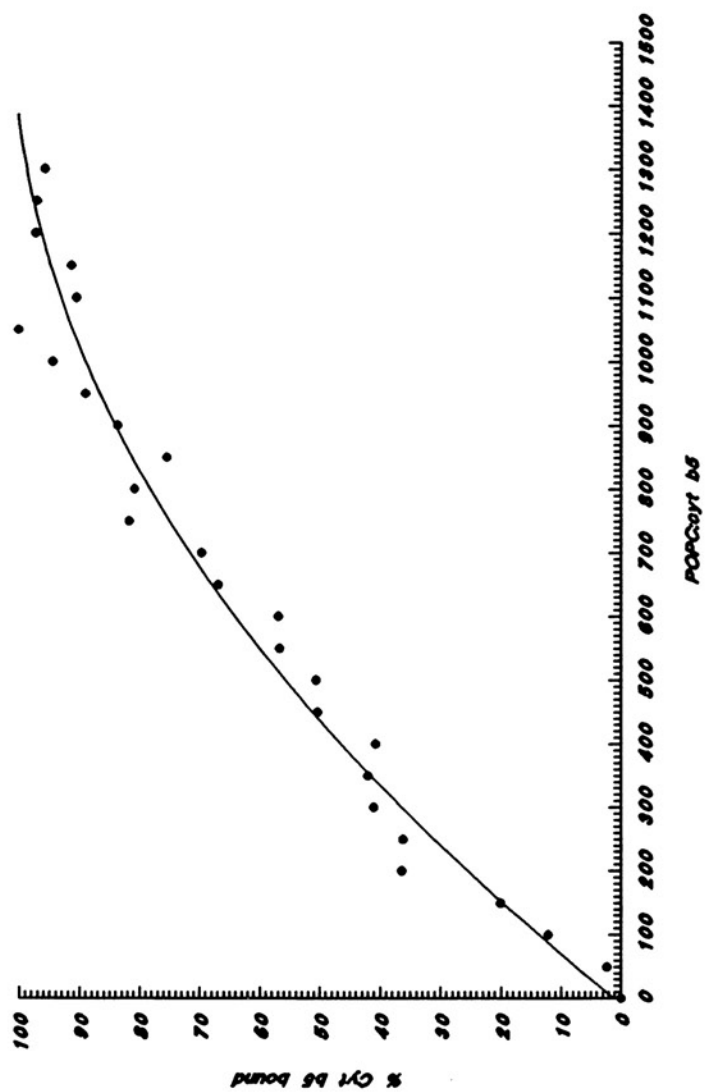
Cytochrome  $b_5$  binding to POPC LUVs; 20% Cholesterol. Separate samples containing cyt  $b_5$  (3.12 nmoles) and POPC liposomes (0-3.12  $\mu$ moles POPC and 0-0.780  $\mu$ moles cholesterol; 4:1 POPC:cholesterol) were incubated in 2 ml total volume of Tris-acetate buffer for 2 h at 30°C. The extent of binding was determined from cyt  $b_5$  fluorescence measurements, using Eqn. 1. Excitation and emission wavelengths were 280 nm and 338 nm; bandwidths were 2.5 and 5 nm. Fluorescence spectra were corrected for light scattering and excitation beam attenuation. See Experimental Procedures for additional details.





**Figure 56.**

Cytochrome  $b_5$  binding to POPC LUVs; 40% Cholesterol. Separate samples containing cyt  $b_5$  (3.12 nmoles) and POPC liposomes (0-4.056  $\mu$ moles POPC and 0-2.704  $\mu$ moles cholesterol; 3:2 POPC:cholesterol) were incubated in 2 ml total volume of Tris-acetate buffer for 2 h at 30°C. The extent of binding was determined from cyt  $b_5$  fluorescence measurements, using Eqn. 1. Excitation and emission wavelengths were 280 nm and 338 nm; bandwidths were 2.5 and 5 nm. Fluorescence spectra were corrected for light scattering and excitation beam attenuation. See Experimental Procedures for additional details.



stoichiometric ratios of exterior monolayer POPC:cyt  $b_5$  to be 56, 104, 208, and 500 respectively. Therefore, the relative area or lattice size that is required for cyt  $b_5$  adsorption in a POPC-LUV increases with cholesterol composition.

As previously determined for the SUV binding studies, the elliptically shaped cyt  $b_5$  catalytic domain covers a minimum area of a single contour shell of eight phospholipids that surrounds a linear sequence of two additional molecules (Figure 11). However, the significantly greater surface areas that are required for cyt  $b_5$  binding in LUVs suggest stretched-hexagonal binding sites with multiple contour shells. For POPC liposomes with 0, 10, 20, and 40% cholesterol, the different adsorption surfaces were modeled to have 4, 5, 8, and 12 concentric phospholipid shells, respectively (Figures 57, 58, 59, and 60). For these particular stretched-hexagonal binding lattices, the number of that comprises each successive contour shell increases by 6 phospholipids. According to this algorithm, the binding sites for cyt  $b_5$  binding to POPC-LUVs with 0, 10, 20, and 40 mole percent cholesterol consist of 70, 102, 234, and 494 phospholipid molecules, respectively. These values, which are consistent with the saturation studies, were used for determining the geometrical parameters  $\lambda$ ,  $\alpha$ , and  $\gamma$ .

Figure 57.

Model of cytochrome  $b_5$  binding lattice for POPC LUVs without cholesterol. The liposome surface was modeled as a stretched-hexagonal lattice with 4 phospholipid contour shells; based upon the saturation ratio of 9.0 cyt  $b_5$ :1000 POPC. The shaded hexagon represents the first contour shell or the actual bilayer surface that the cyt  $b_5$  catalytic domain covers. The contour shells, from the inner most to the exterior shell, each consist of 8, 14, 20, and 26 phospholipid subunits. The geometrical parameters for this lattice were calculated to be  $\lambda=9.7/n$ ,  $\alpha=181.7/n$ , and  $\gamma=18.7$  as described in Experimental Procedures.

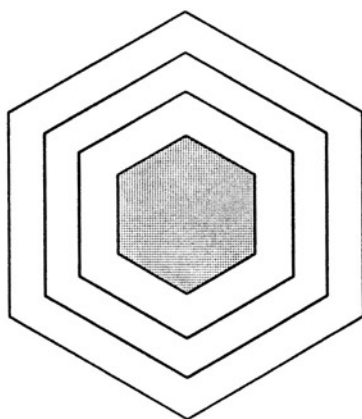


Figure 58.

Model of cytochrome  $b_5$  binding lattice for POPC LUVs with 10% cholesterol. The liposome surface was modeled as a stretched-hexagonal lattice with 5 phospholipid contour shells; based upon the saturation ratio of 4.8 cyt  $b_5$ :1000 POPC. The shaded hexagon represents the first contour shell or the actual bilayer surface that the cyt  $b_5$  catalytic domain covers. The contour shells, from the inner most to the exterior shell, each consist of 8, 14, 20, 26, and 32 phospholipid subunits. The geometrical parameters for this lattice were calculated to be  $\lambda=11.7/n$ ,  $\alpha=271.7/n$ , and  $\gamma=23.2$  as described in Experimental Procedures.

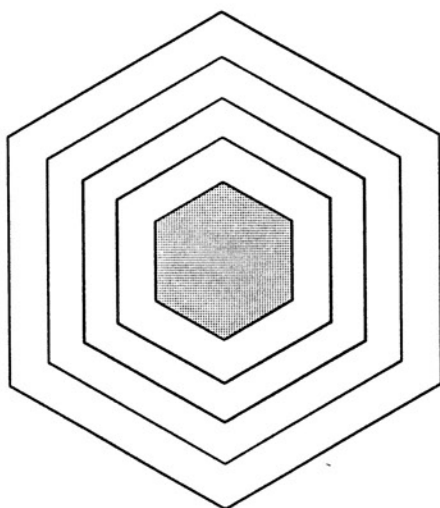


Figure 59.

Model of cytochrome  $b_5$  binding lattice for POPC LUVs with 20% cholesterol. The liposome surface was modeled as a stretched-hexagonal lattice with 8 phospholipid contour shells; based upon the saturation ratio of 2.4 cyt  $b_5$ :1000 POPC. The shaded hexagon represents the first contour shell or the actual bilayer surface that the cyt  $b_5$  catalytic domain covers. The contour shells, from the inner most to the exterior shell, each consist of 8, 14, 20, 26, 32, 38, 44, and 50 phospholipid subunits. The geometrical parameters for this lattice were calculated to be  $\lambda=17.7/n$ ,  $\alpha=649.7/n$ , and  $\gamma=36.7$  as described in Experimental Procedures.



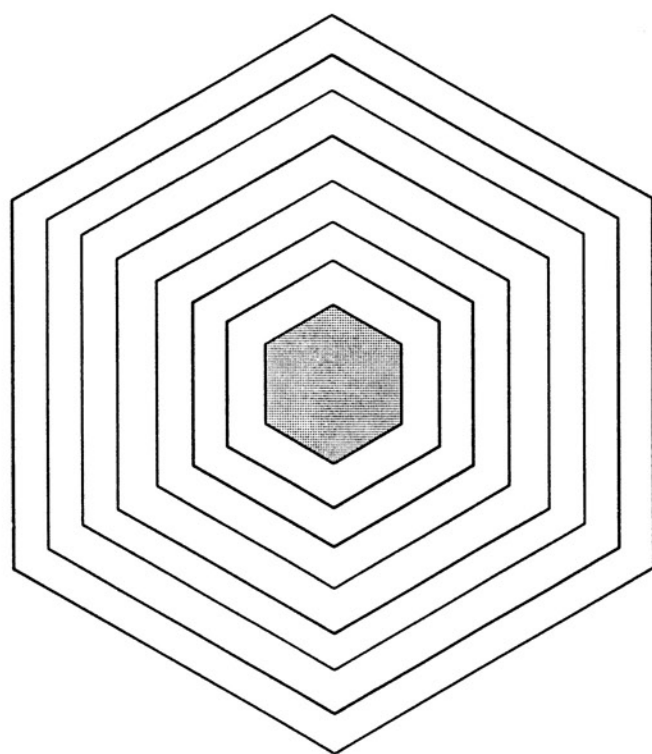
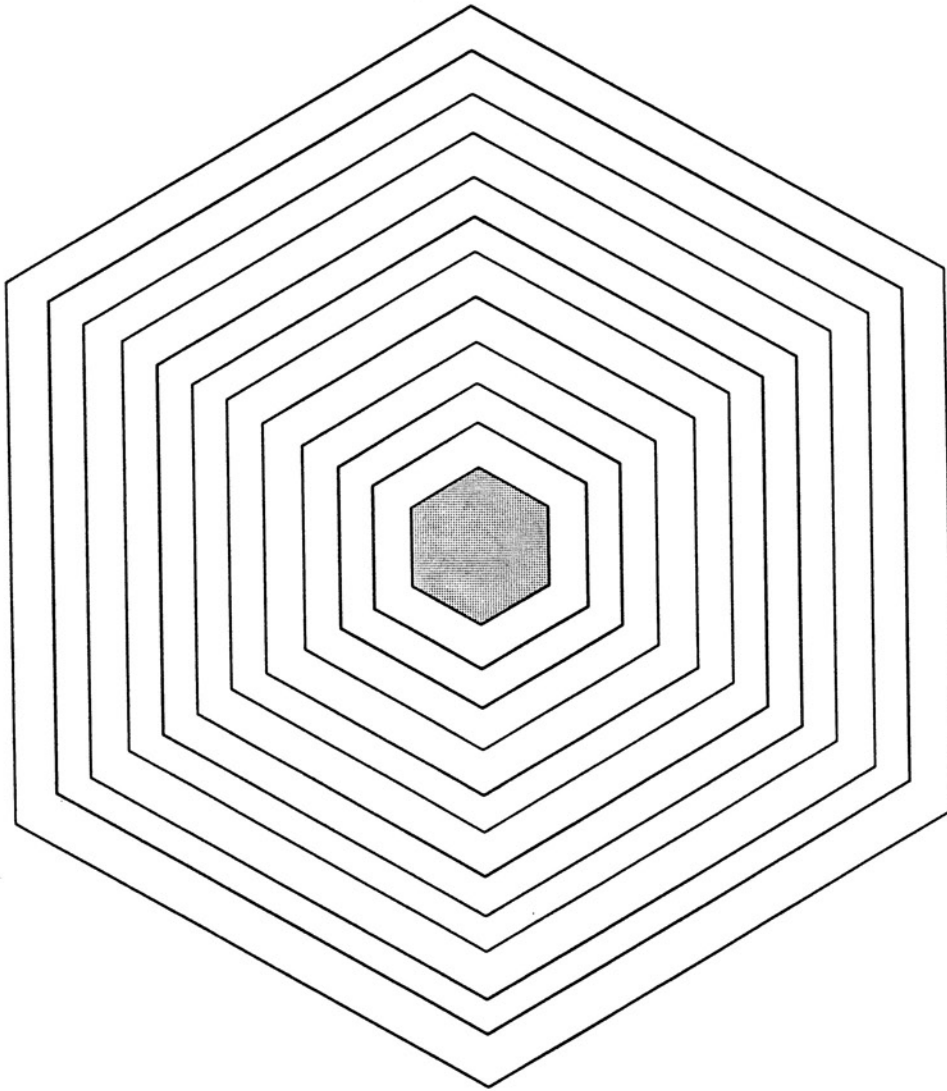


Figure 60.

Model of cytochrome  $b_5$  binding lattice for POPC LUVs with 40% cholesterol. The liposome surface was modeled as a stretched-hexagonal lattice with 12 phospholipid contour shells; based upon the saturation ratio of 1.0 cyt  $b_5$ :1000 POPC. The shaded hexagon represents the first contour shell or the actual bilayer surface that the cyt  $b_5$  catalytic domain covers. The contour shells, from the inner most to the exterior shell, each consist of 8, 14, 20, 26, 32, 38, 44, 50, 56, 62, 68, and 74 phospholipid subunits. The geometrical parameters for this lattice were calculated to be  $\lambda=25.7/n$ ,  $\alpha=1405.7/n$ , and  $\gamma=54.7$  as described in Experimental Procedures.



The various binding lattice models for cyt  $b_5$  interaction with POPC-LUVs permitted obtaining very good curve-fits of Eqn. 2 to experimental data (Figures 61, 62, 63, and 64). The Scatchard plots show that upward concavity increases as cholesterol composition in a liposome increases. Among the four Scatchard plots, only the x-axis intercept, or the saturation ratios of cyt  $b_5$  to POPC appears to significantly change. The apparent binding equilibrium constants (ordinate intercepts) remain essentially identical.

The results of the binding data analysis for cyt  $b_5$  interaction with POPC-LUVs containing cholesterol are summarized in Table VI. As noted above, the observed binding affinity of cyt  $b_5$  for POPC remains essentially unchanged with increasing cholesterol content. At composition that are not greater than 40 mole percent, cholesterol does not appear to affect the binding equilibrium of cyt  $b_5$  to POPC. Additionally, the cooperativity parameter  $\eta$  in LUVs is approximately 0.93, which is significantly greater than in SUVs, where  $\eta=0.63$ . This experimental observation is intuitively consistent: the lower cyt  $b_5$  to POPC saturation ratios in LUVs correlate with greater distances among protein molecules. With SUVs, the greater packing density of cyt  $b_5$  molecules results in greater anticooperativity effects. In fact, anticooperativity effects are almost negligible in LUVs; the cooperativity parameter approaches unity, which indicates no cooperativity among adsorbed ligands (Stankowski, 1984).

As similarly indicated for the SUVs, the equilibrium constants that are directly obtained from the Scatchard plots essentially pertain to the affinity of unbound cyt  $b_5$  for phospholipid. Although these constants may signify if cholesterol affects cyt  $b_5$  interaction with phospholipids, they

Figure 61.

Scatchard plot of cytochrome  $b_5$  binding to POPC LUVs; 0% cholesterol. Cyt  $b_5$  binding data from Figure 53 was replotted as  $r/[\text{unbound cyt } b_5]$  ( $\text{mM}^{-1}$ ) vs.  $r$ , where  $r$  is the molar solution concentration ratio of bound cyt  $b_5$  to phospholipid ( $[\text{bound cyt } b_5]/[\text{PL}]$ ). The fitted curve was obtained using  $K_{\text{eff}}=94 \text{ mM}^{-1}$  (y-axis intercept),  $n=161$  (reciprocal of x-axis intercept), and  $\eta=0.90$  in the following equation:

$$r/C_A = K_{\text{eff}}(1-nr) \left[ 1 - \frac{9.7r}{1+9.7r-nr} \cdot \frac{2}{l+1} \right]^{18.7}$$

with

$$l = [1 + 38.8r(\eta - 1)(1 - nr) / (1 + 9.7r - nr)^2]^{1/2}$$

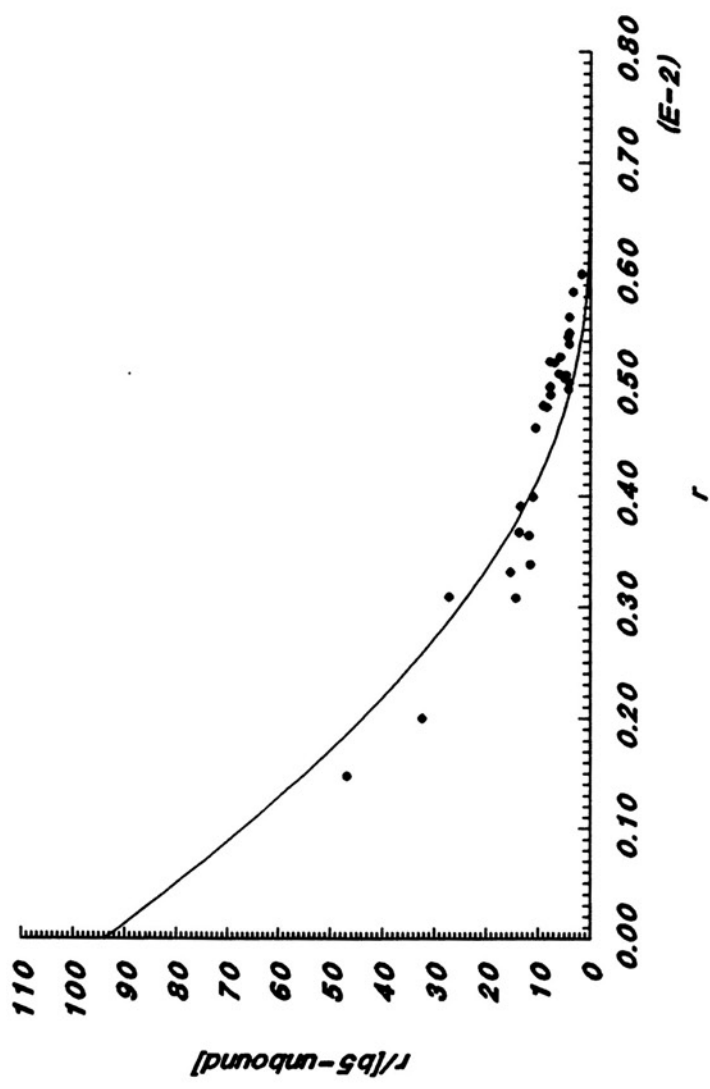


Figure 62.

Scatchard plot of cytochrome  $b_5$  binding to POPC LUVs; 10% cholesterol. Cyt  $b_5$  binding data from Figure 54 was replotted as  $r/[\text{unbound cyt } b_5]$  ( $\text{mM}^{-1}$ ) vs.  $r$ , where  $r$  is the molar solution concentration ratio of bound cyt  $b_5$  to phospholipid ( $[\text{bound cyt } b_5]/[\text{PL}]$ ). The fitted curve was obtained using  $K_{\text{eff}}=91 \text{ mM}^{-1}$  (y-axis intercept),  $n=278$  (reciprocal of x-axis intercept), and  $\eta=0.91$  in the following equation:

$$r/C_A = K_{\text{eff}}(1-nr) \left[ 1 - \frac{11.7r}{1+11.7r-nr} \cdot \frac{2}{J+1} \right]^{23.2}$$

with

$$J = [1 + 46.8r(\eta-1)(1-nr) / (1+11.7r-nr)^2]^{1/2}$$

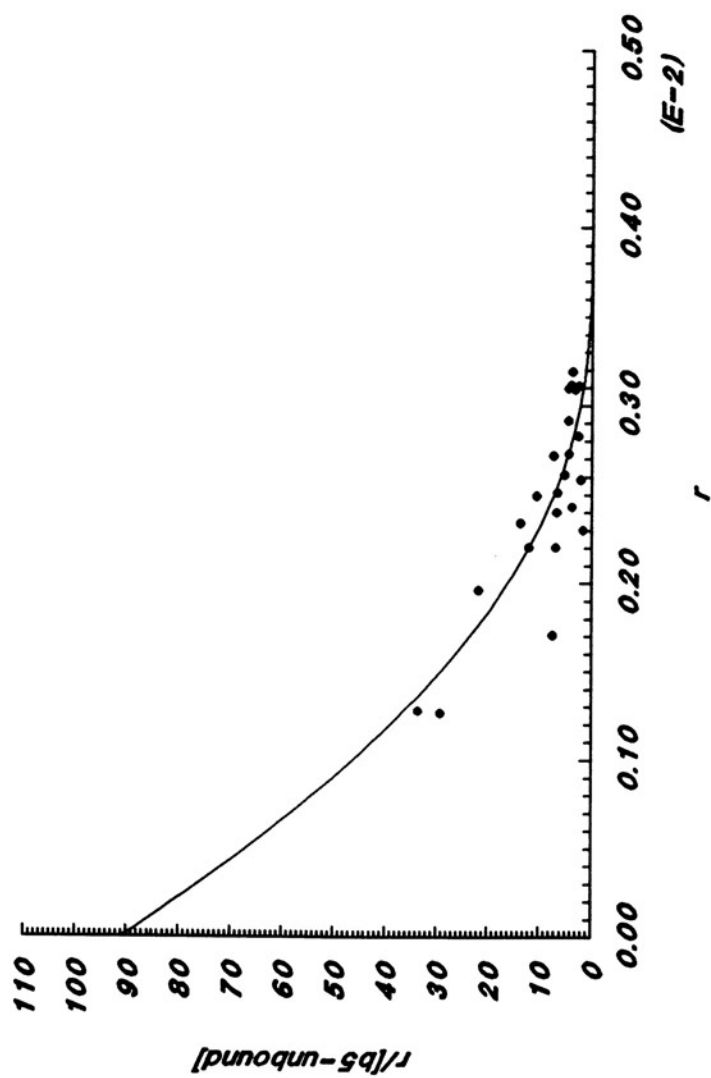




Figure 63.

Scatchard plot of cytochrome  $b_5$  binding to POPC LUVs; 20% cholesterol. Cyt  $b_5$  binding data from Figure 55 was replotted as  $r/[\text{unbound cyt } b_5]$  ( $\text{mM}^{-1}$ ) vs.  $r$ , where  $r$  is the molar solution concentration ratio of bound cyt  $b_5$  to phospholipid ( $[\text{bound cyt } b_5]/[\text{PL}]$ ). The fitted curve was obtained using  $K_{\text{eff}}=85 \text{ mM}^{-1}$  (y-axis intercept),  $n=588$  (reciprocal of x-axis intercept), and  $\eta=0.93$  in the following equation:

$$r/C_A = K_{\text{eff}}(1-nr) \left[ 1 - \frac{17.7r}{1+17.7r-nr} \cdot \frac{2}{I+1} \right]^{36.7}$$

with

$$I = [1 + 70.8r(\eta-1)(1-nr) / (1+17.7r-nr)^2]^{1/2}$$

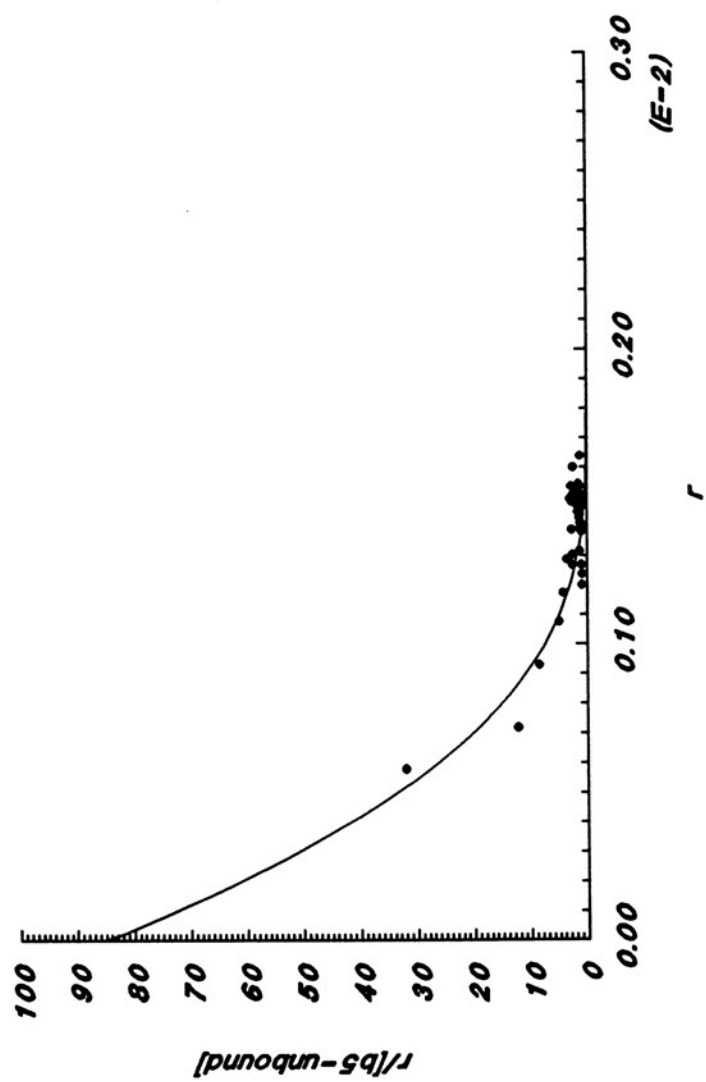


Figure 64.

Scatchard plot of cytochrome  $b_5$  binding to POPC LUVs; 40% cholesterol. Cyt  $b_5$  binding data from Figure 56 was replotted as  $r/[\text{unbound cyt } b_5]$  ( $\text{mM}^{-1}$ ) vs.  $r$ , where  $r$  is the molar solution concentration ratio of bound cyt  $b_5$  to phospholipid ( $[\text{bound cyt } b_5]/[\text{PL}]$ ). The fitted curve was obtained using  $K_{\text{eff}}=94 \text{ mM}^{-1}$  (y-axis intercept),  $n=667$  (reciprocal of x-axis intercept), and  $\eta=0.96$  in the following equation:

$$r/C_A = K_{\text{eff}}(1-nr) \left[ 1 - \frac{25.7r}{1+25.7r-nr} \cdot \frac{2}{l+1} \right]^{54.7}$$

with

$$l = [1 + 102.8r(\eta-1)(1-nr) / (1+25.7r-nr)^2]^{1/2}$$

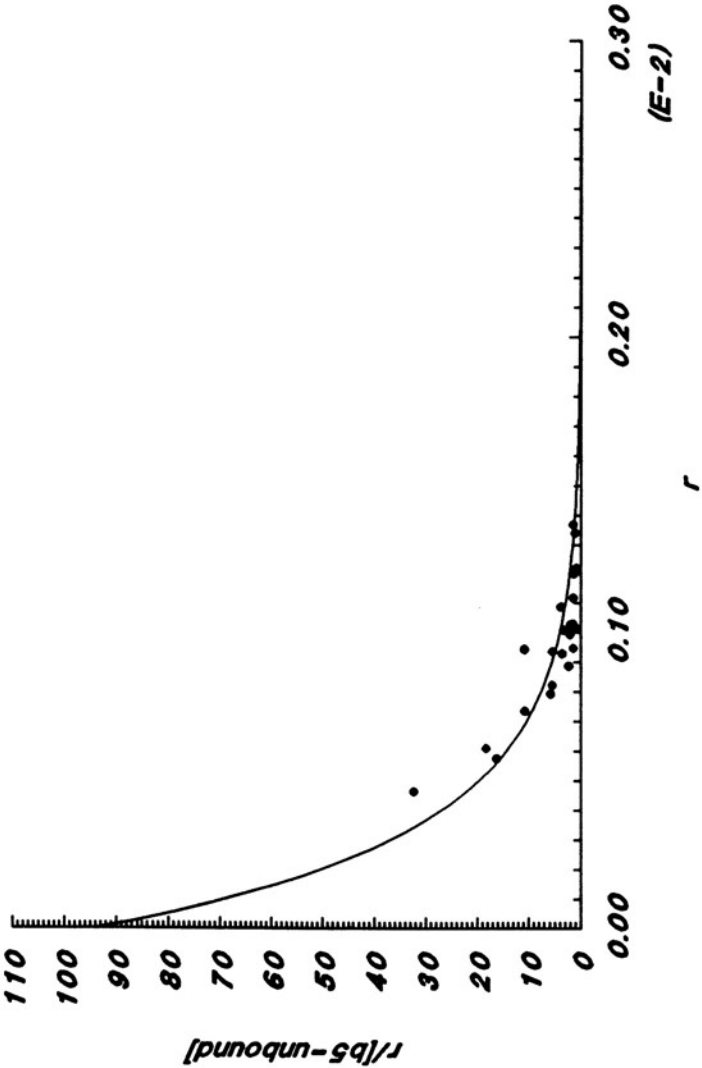


Table VI: Effect of Cholesterol on Cytochrome  $b_5$  Binding to POPC LUVs<sup>a</sup>

% cholesterol	$K_{\text{eff}}$ ( $M^{-1}$ ) <sup>b</sup>	$1/n^c$	$\eta^d$	$K_{c+p}$ ( $M^{-1}$ ) <sup>e</sup>	cyt $b_5$ :1000 POPC
0	$9.4 \times 10^4$	0.0062	0.90	$9.4 \times 10^4$	6.2
10	$9.1 \times 10^4$	0.0036	0.91	$8.6 \times 10^4$	3.6
20	$8.5 \times 10^4$	0.0017	0.93	$7.6 \times 10^4$	1.7
40	$9.4 \times 10^4$	0.0015	0.96	$7.1 \times 10^4$	1.5

<sup>a</sup>Cyt  $b_5$  binding data was plotted as [bound cyt  $b_5$ ]/[POPC][free cyt  $b_5$ ] vs. [bound cyt  $b_5$ ]/[POPC]. The Scatchard plots were evaluated by fitting Eqn. 8 to the experimental data (See text for additional details). <sup>b</sup>Effective binding constant, which corresponds to the y-axis intercept of the fitted curve. The mean standard error from the curve-fitting analysis is  $\pm 14.4\%$  of the reported values. <sup>c</sup>maximum (i.e. saturating) stoichiometric number of cyt  $b_5$ /PL, which occurs at the x-axis intercept of the fitted curve. The inverse is the minimum number of PL per cyt  $b_5$ . The results are accurate to within  $\pm 4.2\%$ . <sup>d</sup>cooperativity parameter. The mean standard error is  $\pm 4.1\%$ . <sup>e</sup>Equilibrium of cyt  $b_5$  binding for a liposome. The binding equilibrium is calculated by expressing  $K_{\text{eff}}$  in terms of effective total lipid. Since cholesterol has approximately one-half the surface area of phospholipids, the concentration of effective total lipid is assumed to be [phospholipid] + 1/2[cholesterol].

fail to readily show the effect of cholesterol on the binding affinity for the bilayer. Therefore, these experimentally observed equilibrium constants are evaluated in terms of the concentration of total effective lipid. Table VI shows a nominal reduction of 1.3-fold in the  $\text{cyt } b_5(\text{bound})/\text{cyt } b_5(\text{free})$  equilibrium with POPC LUVs as the cholesterol content increases. Since the overall  $\text{cyt } b_5$  binding equilibrium constants for both POPC molecules and the liposomes remain essentially unaffected within the composition range of 0-40 mole percent cholesterol, the reduction in the  $\text{cyt } b_5$  saturation level of the liposomes appears to result from the reduction in the number of sites (or phospholipids) that are available for  $\text{cyt } b_5$  insertion into the bilayer.

The saturation levels of  $\text{cyt } b_5$  in POPC-LUVs containing cholesterol obtained from the binding isotherm analyses (Table VI) are consistent with the uncorrected results obtained when excess  $\text{cyt } b_5$  and preformed liposomes are incubated for prolonged periods and the extent of binding is determined by gel-filtration (Table II). Multiplying the  $\text{cyt } b_5$  to 1000 POPC ratios in Table VI by a factor of 1.3 (to correct for vesicle lamellarity) gives the corrected saturation levels of 8.1, 4.7, 2.2, and 1.9  $\text{cyt } b_5$ :1000 POPC in LUVs of 0, 10, 20, and 40 mole percent cholesterol. Since these results are comparable to those in Figure 51, they are internal controls that confirm the validity of the assumptions and protocol used in the Scatchard analysis of binding data.

*(B) Effect of Cholesterol on the Tight Insertion of Cytochrome  $b_5$  into POPC-LUVs.*

Perhaps the most significant discovery in this investigation is

that, while inhibiting cyt  $b_5$  binding, cholesterol accelerates the rate at which bound cyt  $b_5$  is converted from the "loose" to the "tight" configuration. This observation is especially relevant because the tight configuration is the physiological binding form of cyt  $b_5$ .

These experiments were actually initiated as controls because cyt  $b_5$  binds to bilayers in two forms and the saturation studies and curve-fitting model consider only the "loose" binding form. Therefore, it became necessary to determine if cholesterol affects the type of insertion of cyt  $b_5$  into liposomes. The extent of tight insertion was determined by measuring the amount of cyt  $b_5$  that can undergo spontaneous transfer to a population of acceptor vesicles. Donor LUVs and acceptor SUVs had identical cholesterol/phospholipid ratios in order to prevent any net redistribution of cholesterol between liposome populations. SUVs were chosen as acceptors because cyt  $b_5$  has been previously demonstrated to have a >200-fold greater affinity for SUVs over LUVs (Greenhut *et al.*, 1986). Additionally, SUVs can quickly and completely be resolved from a population of large reverse-phase liposomes, by either gel-filtration or sedimentation. Figures 65, 66, and 67 show typical results of the transfer experiments for 0 & 10%, 20 & 25%, and 35 & 40% cholesterol, respectively. Tightly inserted cyt  $b_5$  elutes with the LUVs in the column void volume fractions whereas the transferable cyt  $b_5$  elutes with the SUV acceptors in the included fractions. Figure 68 shows the amount of cyt  $b_5$  that inserts in the tight configuration into POPC reverse-phase liposomes at cholesterol compositions from 0-50 mole percent. During a prolonged 24 h incubation period with POPC-LUVs, the amount of bound cyt  $b_5$  that spontaneously inserts in the tight configuration increases from

Figure 65.

Cytochrome  $b_5$  transfer from donor POPC LUVs to acceptor POPC SUVs. (A) Liposomes with 0% cholesterol. Cyt  $b_5$  (0.08  $\mu$ moles) was incubated with POPC LUVs (4  $\mu$ moles POPC doped with  $9.7 \times 10^4$  dpm [ $^3\text{H}$ ]-triolein/ $\mu$ mole POPC) in Tris-acetate buffer for 24 h at 30°C under argon. Unbound protein was removed by gel-filtration on a Sepharose 2B-CL column (0.9 x 28.5 cm), equilibrated in Tris-acetate buffer and thermostatted at 25°C. Aliquots of 320  $\mu$ l fractions were assayed for  $^3\text{H}$  and the  $A_{413}$ . The peak void volume fractions were pooled and then incubated with an excess of POPC SUVs (doped with  $8.7 \times 10^4$  dpm [ $^{14}\text{C}$ ]-POPC/ $\mu$ mole POPC) [4:1, POPC<sub>SUV</sub>:POPC<sub>LUV</sub>] for 2 h, 30°C, under argon. The transfer mixture was then reapplied to the washed Sepharose 2B-CL column. Fractions were assayed for LUVs (●), SUVs (○), and cyt  $b_5$  (▲) by  $^3\text{H}$ ,  $^{14}\text{C}$  dpm, and  $A_{413}$  respectively. Nontransferable cyt  $b_5$  remains with the LUVs following incubation with SUV acceptors. (B) Liposomes with 10% cholesterol. The protocol was the same as in (A), except that donor and accpetor liposomes contained 10 mole percent cholesterol.



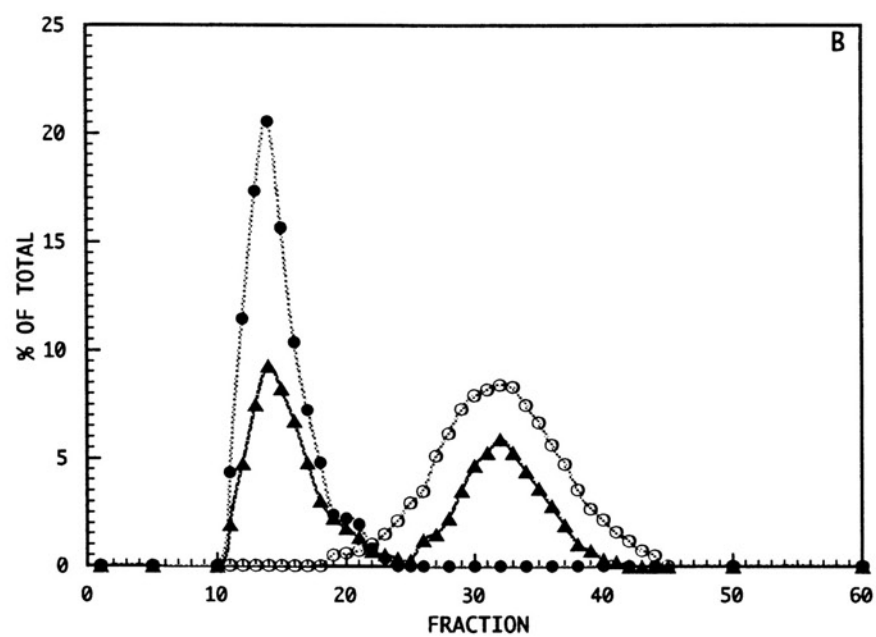
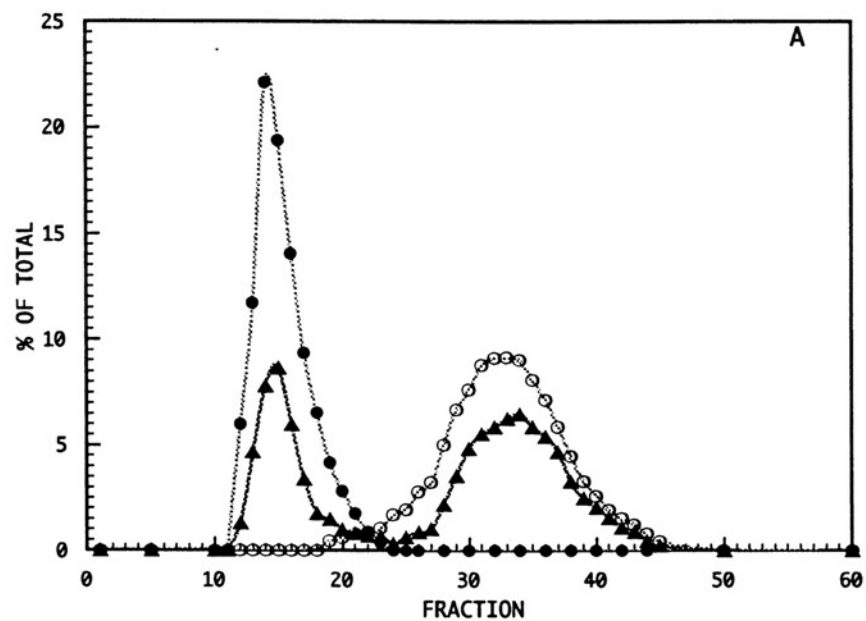


Figure 66.

Cytochrome  $b_5$  transfer from donor POPC LUVs to acceptor POPC SUVs. (A) Liposomes with 20% cholesterol. Cyt  $b_5$  (0.048  $\mu$ moles) was incubated with POPC LUVs (20  $\mu$ moles POPC doped with  $1.9 \times 10^5$  dpm [ $^3$ H]-triolein/ $\mu$ mole POPC) in Tris-acetate buffer for 24 h at 30°C under argon. Unbound protein was removed by gel-filtration on a Sepharose 2B-CL column (1.6 x 55 cm), equilibrated in Tris-acetate buffer and thermostatted at 25°C. Aliquots of 1.5 ml fractions were assayed for  $^3$ H and the  $A_{413}$ . The peak void volume fractions were pooled and then incubated with an excess of POPC SUVs (doped with  $2.9 \times 10^4$  dpm [ $^{14}$ C]-POPC/ $\mu$ mole POPC) [4:1 POPC<sub>SUV</sub>:POPC<sub>LUV</sub>] for 2 h, 30°C, under argon. The transfer mixture was then reapplied to a washed Sepharose 2B-CL column. Fractions were assayed for LUVs (●), SUVs (○), and cyt  $b_5$  (▲) by  $^3$ H,  $^{14}$ C dpm, and  $A_{413}$  respectively. Nontransferable cyt  $b_5$  remains with the LUVs following incubation with SUV acceptors. (B) Liposomes with 25% cholesterol. The protocol was the same as in (A), except that donor and acceptor liposomes contained 25 mole percent cholesterol.

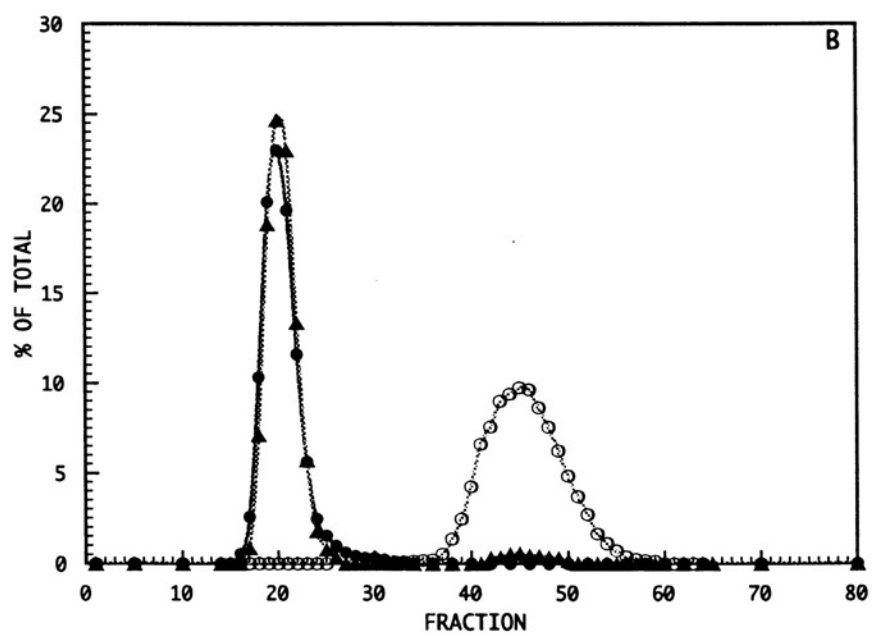
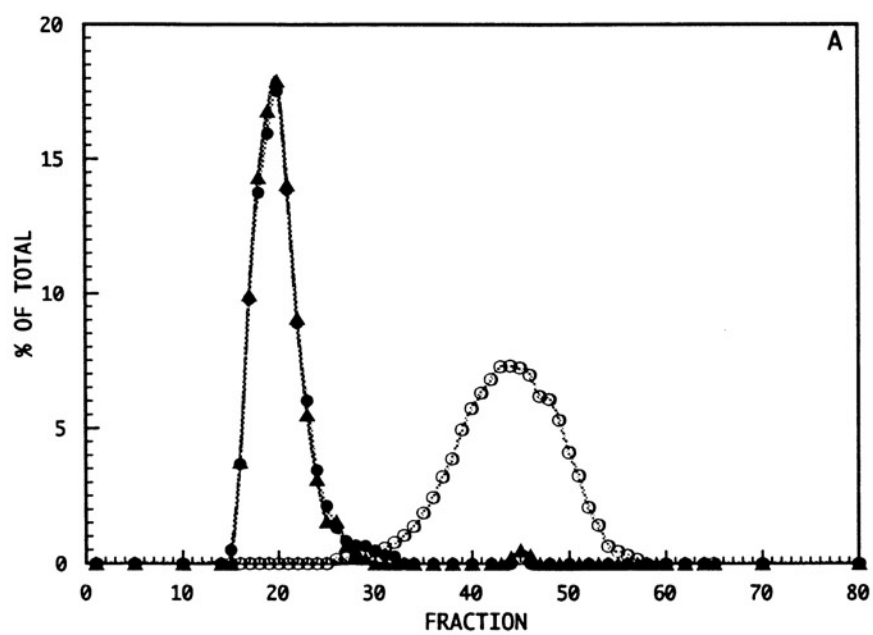


Figure 67.

Cytochrome  $b_5$  transfer from donor POPC LUVs to acceptor POPC SUVs. (A) Liposomes with 35% cholesterol. Cyt  $b_5$  (0.048  $\mu$ moles) was incubated with POPC LUVs (20  $\mu$ moles POPC doped with  $8.3 \times 10^4$  dpm [ $^3\text{H}$ ]-triolein/ $\mu$ mole POPC) in Tris-acetate buffer for 24 h at 30°C under argon. Unbound protein was removed by gel-filtration on a Sepharose 2B-CL column (1.6 x 55 cm), equilibrated in Tris-acetate buffer and thermostatted at 25°C. Aliquots of 1.74 ml fractions were assayed for  $^3\text{H}$  and the  $A_{413}$ . The peak void volume fractions were pooled and then incubated with an excess of POPC SUVs (doped with  $2.6 \times 10^4$  dpm [ $^{14}\text{C}$ ]-POPC/ $\mu$ mole POPC) [4:1 POPC<sub>SUV</sub>:POPC<sub>LUV</sub>] for 2 h, 30°C, under argon. The transfer mixture was then reapplied to a washed Sepharose 2B-CL column. Fractions were assayed for LUVs (●), SUVs (○), and cyt  $b_5$  (▲) by  $^3\text{H}$ ,  $^{14}\text{C}$  dpm, and  $A_{413}$  respectively. Nontransferable cyt  $b_5$  remains with the LUVs following incubation with SUV acceptors. (B) Liposomes with 40% cholesterol. The protocol was the same as in (A), except that donor and acceptor liposomes contained 40 mole percent cholesterol.

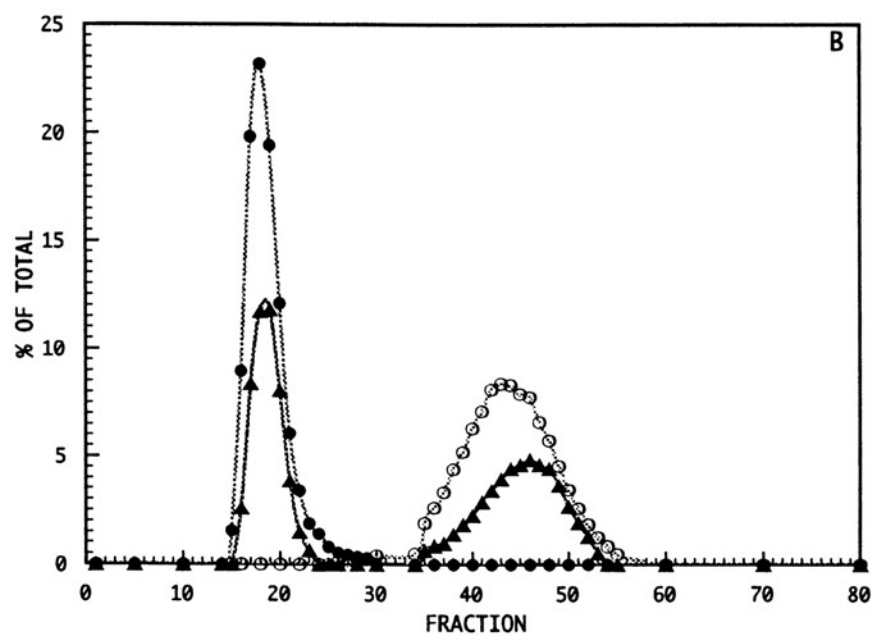
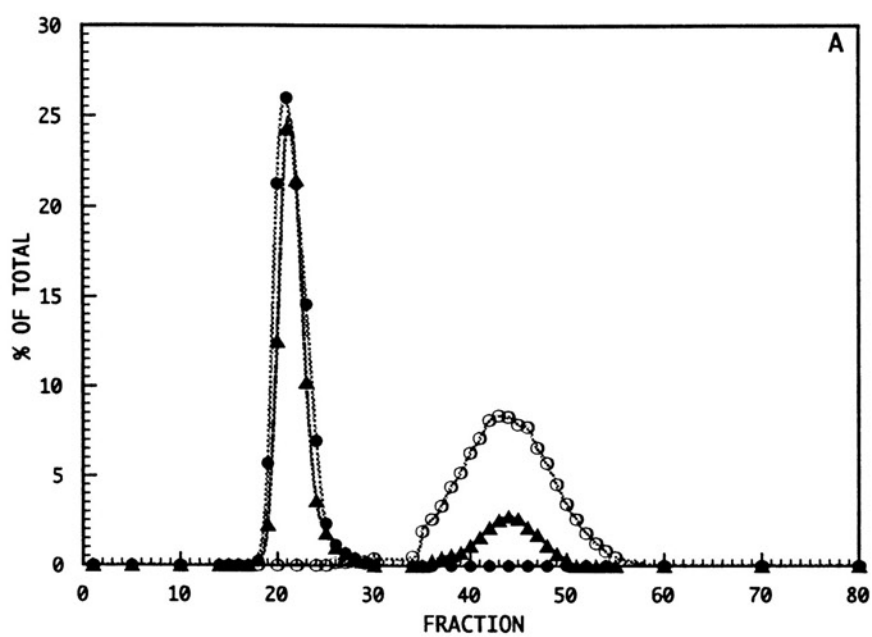
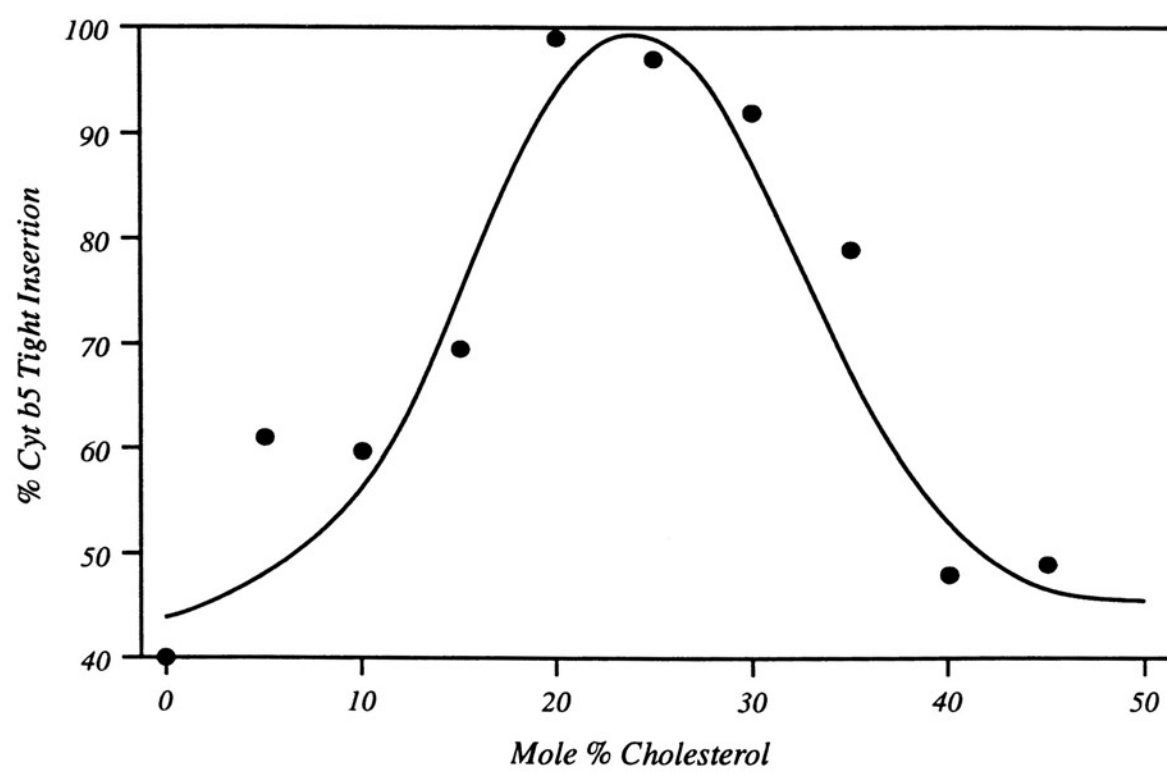


Figure 68.

Cytochrome  $b_5$  tight insertion into POPC LUVs within 24 hours as a function of cholesterol mole percent. Cyt  $b_5$ -liposome complexes from Figure 51 were pooled and then incubated with a 4-fold molar excess of POPC SUV lipid for 2 h at 30°C under argon to deplete the LUVs of transferable protein. Donor and acceptor populations were separated on a Sepharose 2B-CL column (0.9 x 28.5 cm or 1.6 x 55 cm) and fractions were assayed for cyt  $b_5$ , POPC LUVs, and POPC SUVs. The extent of tight insertion was determined from the amount of nontransferable cyt  $b_5$  remaining with LUVs.



approximately 40% at 0 mole percent cholesterol, to nearly 100% at 20-25 mole percent cholesterol, and then decreases to near baseline at 50 mole percent.

Recent studies in this laboratory have shown that prolonged incubation of cyt  $b_5$  with reverse-phase liposomes of POPC results in slow conversion of the loose to the tight binding form, with a half-time of approximately 9 days (Greenhut *et al.*, 1993). However, this transformation is a complex process in which the tightly inserted cyt  $b_5$  is concentrated in a sub-population of "insertion-active" liposomes.

Because there appears to be a complex rearrangement of the cyt  $b_5$ /liposome system during prolonged incubation periods, the effect of cholesterol on the rate of tight insertion was further examined within a 2 hour time interval. For these studies, subsaturating cyt  $b_5$ :POPC ratios were used to eliminate the additional step of separating unassociated protein that may potentially interfere with transferral. An initial ratio of 1 cyt  $b_5$  per 1,302 POPC was found to result in >90% cyt  $b_5$  binding to all reverse-phase liposomes over a 0-40% cholesterol compositional range within 2 hours. The extent of tight insertion could then be readily determined as before, via intervesicle transfer to an excess of SUVs, and then separating the liposome populations by sedimentation through glycerol step gradients.

Although sedimentation through glycerol gradients was used to quantitate the extent of cyt  $b_5$  tight insertion into cholesterol-containing reverse-phase vesicles within 2 hours, the method also indicated that tight insertion may be a surprisingly complex process. Figure 69 shows the results of cyt  $b_5$  transfer between large and small liposomes of various



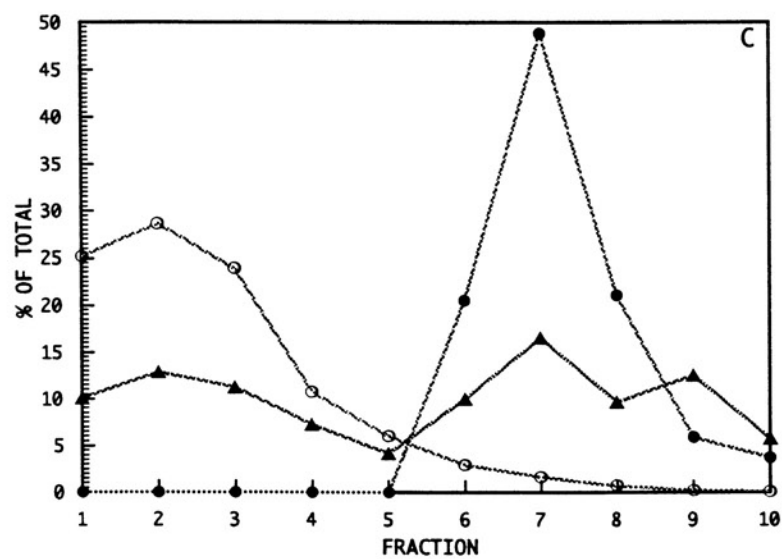
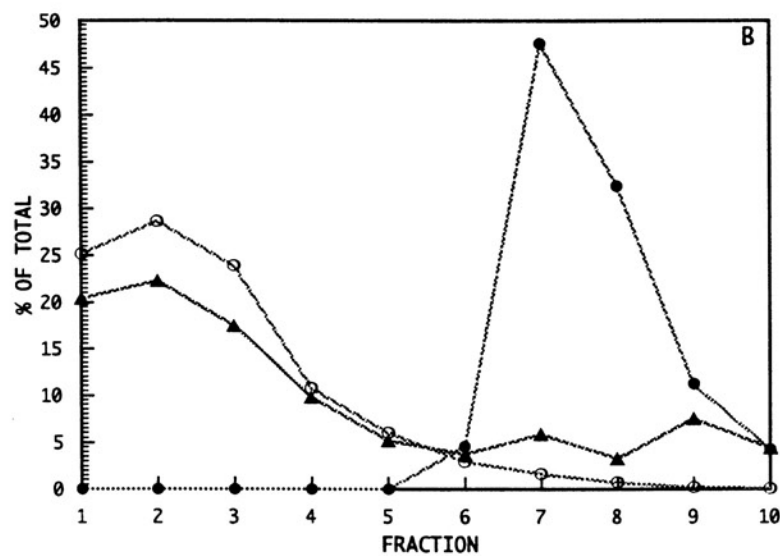
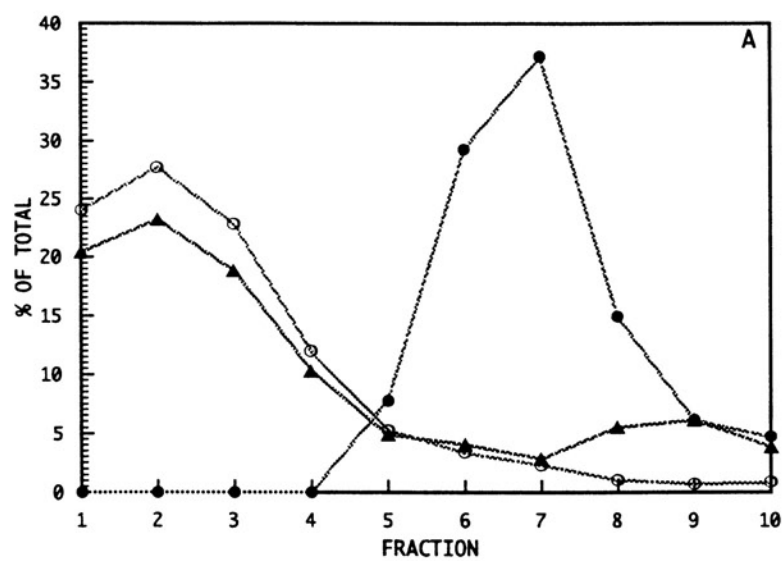
cholesterol compositions. At 0% cholesterol (Panel A), all but 10-20% of the cyt  $b_5$  readily transfers from the large to the small liposome population, indicating that this smaller fraction which sediments is tightly inserted into reverse-phase liposomes after 2 hours. However, as shown by the gradient profile, tightly bound cyt  $b_5$  is not uniformly distributed among reverse-phase liposomes but concentrated in a relatively small percentage of the vesicles towards the bottom of the gradient. This laboratory has suggested that this tight insertion is due to the formation of "insertion-active" vesicles (Greenhut *et al.*, 1993).

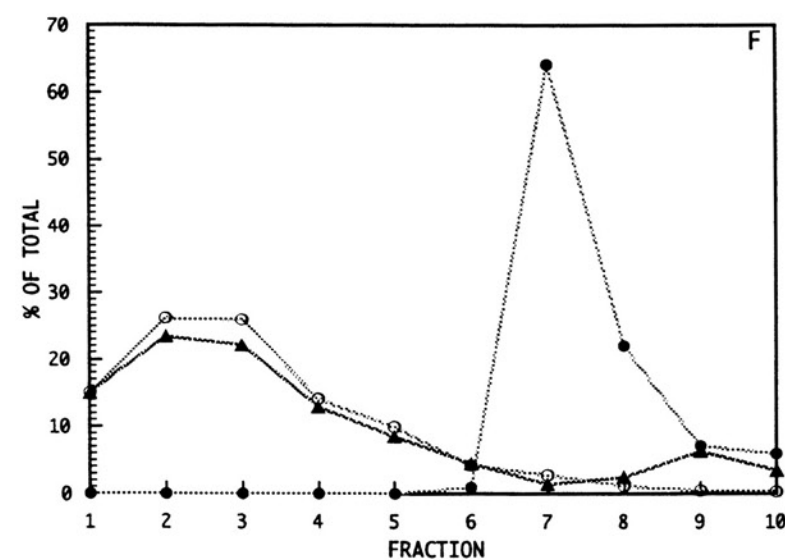
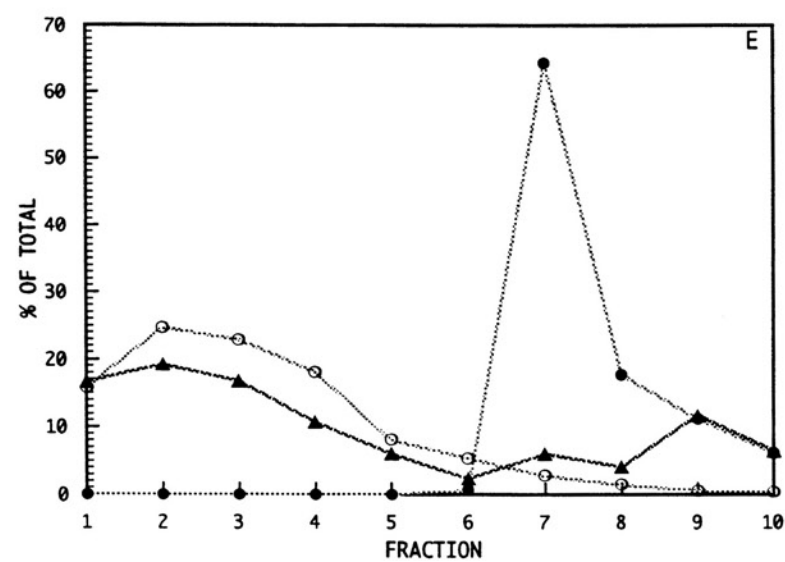
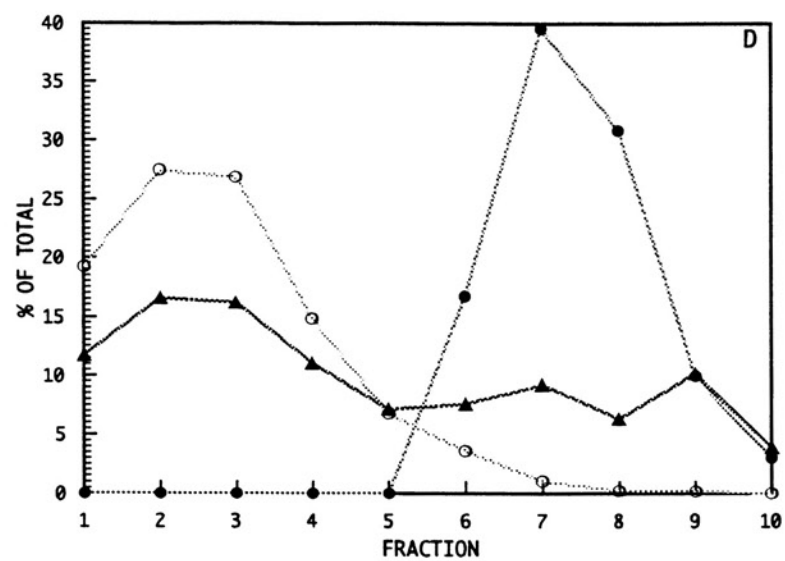
As the cholesterol content increases from 0 to 25 mole percent, the amount of cyt  $b_5$  that inserts in the tight configuration sharply rises. However, from the complex glycerol gradient profiles, there appear to be separate fractions of tightly inserted cyt  $b_5$ . As shown for liposomes containing 10 and 25 mole percent cholesterol, two migratory bands of cyt  $b_5$  become evident (Panels B and C, respectively): one that is essentially coincident with the sedimenting liposomes and the second toward the gradient base. Although both bands increase concomitantly with cholesterol content, the co-migrating cyt  $b_5$  band becomes predominant at approximately 25% cholesterol. Above 25 mole percent cholesterol, this band decreases (Panels D and E) and disappears completely at 40% (Panel F). Similarly, the fast-sedimenting noncoincident fraction also decreases beyond 25% cholesterol, and eventually becomes the only gradient location of tightly inserted cyt  $b_5$  at 40%.

The following explanation for these results is suggested: At 0% cholesterol, cyt  $b_5$  tight insertion results solely from the formation of a subpopulation of destabilized, "insertion-active" vesicles. In liposomes

Figure 69.

Cyt  $b_5$  transfer from POPC reverse-phase donor liposomes to acceptor POPC SUVs. (A) 0% cholesterol, (B) 10% cholesterol, (C) 25% cholesterol, (D) 30% cholesterol, (E) 35% cholesterol, and (F) 40% cholesterol. [ $^3\text{H}$ ]-labelled POPC LUVs and [ $^{14}\text{C}$ ]-labelled POPC SUVs were prepared from common chloroform stock solutions of POPC and cholesterol (See Experimental Procedures). Cyt  $b_5$  (3.84 nmoles) was incubated with POPC LUVs (5  $\mu\text{moles}$  POPC) in Tris-acetate buffer for 2 h, 30°C, under argon. POPC SUV acceptors (15  $\mu\text{moles}$  POPC) were then added and the mixture was incubated for an additional 2 h as before to deplete LUVs of loose protein. 0.6 ml aliquots of the transfer mixtures were then applied to glycerol step gradients of 1.3 ml 1% glycerol, Tris-acetate buffer and 0.1 ml 60% glycerol pad. The gradients were centrifuged in a 50-Ti fixed-angle rotor at 45,000 rpm, 25°C, for 1 h. Fractions of 0.2 ml were collected and assayed for LUVs ( $\bullet$ ), and SUVs ( $\circ$ ), and cyt  $b_5$  ( $\blacktriangle$ ) by  $^3\text{H}$ ,  $^{14}\text{C}$  dpm, and  $A_{413}$  respectively. Nontransferable cyt  $b_5$  remains with the LUVs following incubation with SUV acceptors.





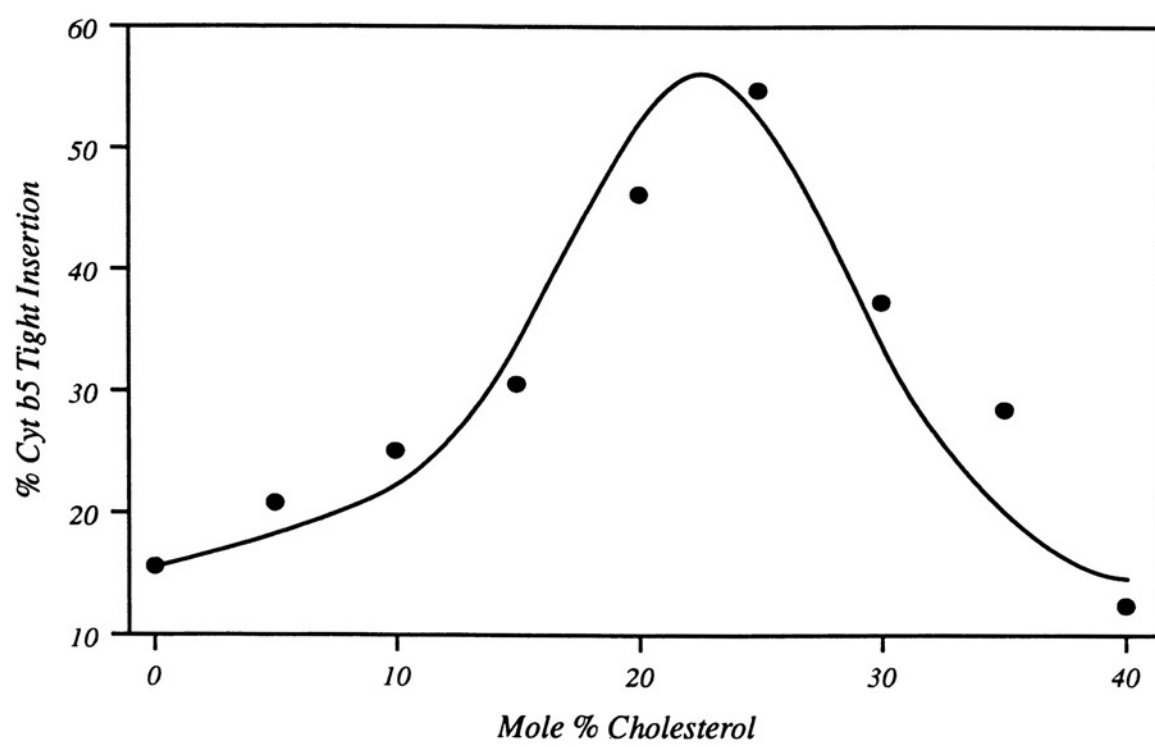
that have compositions up to about 33-35 mole percent cholesterol, tight insertion arises from bilayer cholesterol content (the cyt  $b_5$  band coincident with liposomes) and from a combination of the cholesterol effect and "insertion-active" vesicle formation (noncoincident band toward the gradient bottom). There is no method to experimentally characterize the vesicle sub-populations for determining the percentage of cyt  $b_5$  tight insertion due to cholesterol or protein-induced liposome destabilization in these lower fractions. Above 35 mole percent cholesterol, the tightly inserted cyt  $b_5$  again becomes localized in liposomes toward the gradient base, indicating that this tight insertion probably is not cholesterol-mediated.

Figure 70 shows cyt  $b_5$  tight insertion into POPC LUVs containing cholesterol within 2 h. The amount of cyt  $b_5$  that becomes nontransferable increases from approximately 15% at 0% cholesterol, to a maximum of 50-55% between 20-25% cholesterol; further increase in cholesterol composition causes a decrease in the percentage of cyt  $b_5$  tight insertion, which descends to baseline at 40 mole percent. The extent of tight insertion within 2 hours is approximately one-half of that observed for 24 hours. The greater percentage of bound cyt  $b_5$  that becomes nontransferable during prolonged 24 hour incubations probably is not solely cholesterol-related, but also a manifestation from a complex system transformation of "insertion-active" liposome formation. Together, Figures 68 and 70 provide evidence of a significant cholesterol-associated effect at 20-25 mole percent.

In these studies, tight insertion is defined operationally as the amount of nontransferable cyt  $b_5$  remaining with large vesicles following

**Figure 70.**

Cytochrome  $b_5$  tight insertion into POPC LUVs within 2 hours as a function of cholesterol mole percent. The extent of tight insertion was determined from the amount of nontransferable cyt  $b_5$  remaining with POPC donor liposomes following incubation with acceptor POPC SUVs as described in Figure 69.



a 2 hour incubation with an excess of SUV acceptors. However, an alternative possibility was that the rate of cyt  $b_5$  transfer from cholesterol-containing liposome populations is significantly slower, i.e. "loose" cyt  $b_5$  transfers more slowly from liposomes containing cholesterol. However, this seems unlikely for several reasons. First, a certain fraction of the cyt  $b_5$  always transfers to acceptor vesicles for essentially all of the liposome preparations, which suggests comparable cyt  $b_5$  transfer rates from liposomes with and without cholesterol. Second, although cholesterol stimulates tight insertion as the composition increases to 20-25 mole percent, it then reduces tight insertion at higher compositions. If cholesterol is indeed reducing the transfer rate, then nontransferrability should increase proportionately with cholesterol content. Figures 68 and 70 indicate otherwise. Third, when a large excess of SUVs that are devoid of cholesterol are used as the acceptor population, the extent of cyt  $b_5$  transfer following 24 h incubations with LUVs is indistinguishable from studies using cholesterol-containing SUV acceptors (data not shown). Since cholesterol spontaneously transfers between liposome populations with a half-time of approximately 2 hours, the transfer rate should increase from the cholesterol-depleted liposomes if the cyt  $b_5$  is simply in a slower transferable form. The fact that the transfer rate is unaffected by the presence or absence of cholesterol in the acceptor vesicles suggests that the rate of cyt  $b_5$  transfer from cholesterol-containing vesicles is unchanged. Finally, the extent of cyt  $b_5$  transfer appears to be unaffected by the incubation time of donor liposomes with SUV acceptors. The transfer rate was directly examined using liposomes comprised of 25 mole percent cholesterol, which

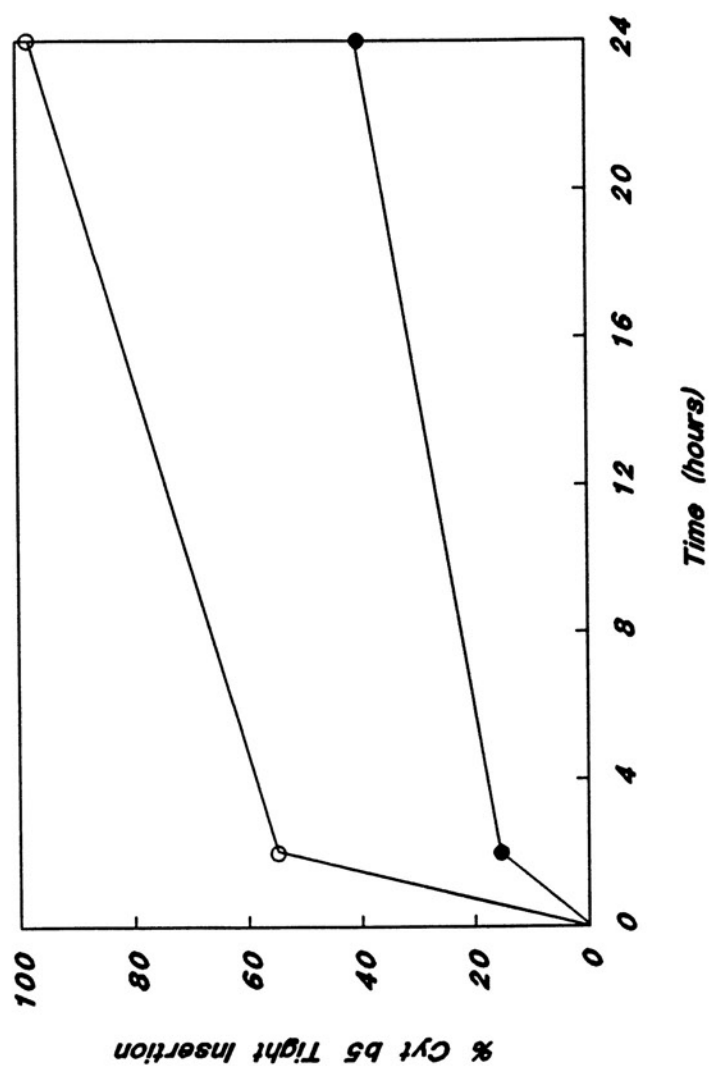


demonstrate the most significant decrease in cyt  $b_5$  transfer. In 2 hour transfer experiments, approximately 50% of the cyt  $b_5$  becomes tightly inserted into large vesicles of 25% cholesterol within 2 hours (Figure 69). If tight insertion is indeed due to a slower rate of cyt  $b_5$  desorption from cholesterol-containing vesicles, then this can imply a potential 2 hour half-time for transfer from POPC-LUVs comprised of 25% cholesterol. A prolonged incubation with SUV acceptors should then further deplete the donors of any loose protein. Since a 2 hour transfer depletes the large vesicles of about 50% of the cyt  $b_5$ , an 8 hour incubation with SUV acceptors should deplete the donors of approximately 94% of the protein (6% remaining with donors) if cholesterol does affect the transfer rate. However, a 4-fold extended transfer period gives essentially identical results, within experimental error, as a 2-hour transfer. Approximately 50% and 52% cyt  $b_5$  remains with donor vesicles containing 25% cholesterol following 2 and 8 hour incubations with SUV acceptors, respectively. These results are evidence that the observed tight insertion is not due to a decreased transfer rate of loose cyt  $b_5$  from cholesterol-containing liposomes.

Determination of the extent of cyt  $b_5$  tight insertion into cholesterol-containing vesicles following short and prolonged (2 and 24 hours, respectively) incubation periods permits estimating the effect of cholesterol on the kinetics of tight insertion (Figure 71). The rate of tight insertion shows biphasic kinetics: where a fraction of the cyt  $b_5$  inserts rapidly in the tight configuration within 2 hours, followed by a slower phase. Since there is no way to experimentally determine the rate of tight insertion occurring within 2 hours, the half-times of only the

Figure 71.

Kinetics of cyt  $b_5$  tight insertion into POPC reverse-phase liposomes. A.)  
No cholesterol. (●)  $T_{1/2} \approx 2$  days. B.) 25% cholesterol (○)  $T_{1/2} \approx 7$  hours.



slow phase can be determined. For simplicity, the half-time of tight insertion into LUVs containing 20-25% cholesterol (where cholesterol most significantly increases the tight insertion rate) is compared with the half-time for liposomes without cholesterol: The half-time of cyt  $b_5$  tight insertion into POPC-LUVs that are devoid of cholesterol is approximately 2 days, whereas for liposomes containing 25% cholesterol it decreases to approximately 7 hours.

To summarize, the effect of cholesterol on cyt  $b_5$  partitioning into POPC LUVs is to simultaneously inhibit the overall binding and facilitate insertion into the tight or physiological configuration into the lipid bilayer. The saturation curve resembles a titration curve, with inflection points occurring at approximately 20 and 33 mole percent cholesterol. The affinity that cyt  $b_5$  has for an LUV seems to be unaffected by the cholesterol composition. This suggests that cholesterol reduces the number of phospholipids that are available for cyt  $b_5$  binding. Maximum tight insertion occurs at approximately 20-25 mole percent cholesterol. Cholesterol increases the rate constant for cyt  $b_5$  tight insertion, from  $k \approx 1 \times 10^{-2} \text{ h}^{-1}$  at 0% cholesterol to  $k \approx 1 \times 10^{-1} \text{ h}^{-1}$  at 20-25% cholesterol.

#### *Effect of Cytochrome $b_5$ Tight Insertion on the Saturation Level of Liposomes.*

A concern in these studies was that, since cyt  $b_5$  binds to preformed liposomes in two possible configurations, the fraction of bound cyt  $b_5$  that is subsequently converted from the loose to the tight binding form could potentially elevate the actual cyt  $b_5$  saturation levels in liposomes. If so, the diminished inhibition of cyt  $b_5$  binding that is observed with

some liposome systems may not necessarily be the result of ineffective phospholipid/cholesterol interactions. Instead, binding may simply be enhanced in some cholesterol containing liposomes because tightly inserted cyt  $b_5$  promotes insertion of additional protein by affecting the dynamic equilibrium between bound and unbound cyt  $b_5$ .

To examine if conversion from the loose to the tight form affects cyt  $b_5$  saturation levels, a control experiment was performed in which the extent of cyt  $b_5$  binding to POPC LUVs with 25 mole percent cholesterol at various time intervals was determined. This particular liposome system was chosen because cyt  $b_5$  becomes completely inserted in the tight configuration within 24 hr. In direct binding studies in which the initial ratio is 2.4 cyt  $b_5$ :1000 POPC, the saturation level of binding to POPC LUVs; 25% cholesterol at 2, 24, and 48 hr is 1.21, 1.29, and 1.29 cyt  $b_5$ :1000 POPC, respectively. Cyt  $b_5$  binding is essentially complete within the first 2 h of incubation. Since the extent of cyt  $b_5$  tight insertion is 50% and 100% within 2 and 24 h, respectively (Figure 71) these results indicate that conversion from the loose to the tight configuration does not elevate the cyt  $b_5$  saturation level of liposomes. Since the extent of binding and loose-to-tight conversion appear to be independent processes, it can be assumed that the fractions of loosely and tightly associated protein may be disregarded in the interpretation of results. Therefore, the extent to which cholesterol inhibits cyt  $b_5$  partitioning into lipid bilayers must depend upon the effective interactions, or condensed lateral packing, of phospholipids and cholesterol.

## DISCUSSION

A model system investigation of the binding and insertion of cyt  $b_5$  into phosphatidylcholine/cholesterol liposomes has been conducted with the intention that the results would be propitious to infer the effect of cholesterol on the solubility/affinity of integral proteins in lipid bilayers. The following observations have been made in the present study:

(i) The saturation levels of SUVs are significantly greater than those of LUVs. The saturation limits of LUVs are so low that there appear to be many vacant interactive sites for the binding of additional protein.

(ii) The overall cyt  $b_5$  binding equilibria with SUVs that are prepared from natural phospholipid mixtures are greater than the equilibria with SUVs of a single component.

(iii) In terms of overall surface area, cholesterol reduces cyt  $b_5$  binding to all liposomes, including those that are prepared with noncondensable phospholipids. The efficacy of inhibition dramatically increases with the condensability of the phospholipids.

(iv) Cholesterol inhibition is much more pronounced in LUVs than in SUVs.

(v) The saturation level of cyt  $b_5$  binding to POPC LUVs as a function of cholesterol concentration appears triphasic, similar to a titration curve, with inflection points at 20 and 33 mole percent cholesterol.

(vi) The rate of cyt  $b_5$  tight insertion is maximal at 20-25 mole percent cholesterol.

These results may be accounted for in terms of a unifying model on the basis of two assumptions: (1) Annular lipid, and lipid extending beyond the first shell, must have sufficient segmental freedom in order to

form a complimentary fit to the irregular shape of the the cyt  $b_5$  membrane anchoring tail. (2) The "bimolecular mesomorphic model" (Hyslop *et al.*, 1990) for the lateral organization of cholesterol and phosphatidylcholine in bilayers is essentially correct.

The ability of phospholipids to adopt complimentary configurations to the asymmetric shape of the membrane anchoring domain probably determines the extent of cyt  $b_5$  solubility in bilayers. Figure 72 depicts that the irregular conformation of the cyt  $b_5$  tail disrupts phospholipid packing in membranes. To maintain bilayer integrity (i.e. to prevent a net increase in water and small molecule permeation through the hydrophobic core) the annular phospholipids must assume different shapes to effectively pack against the protein. Similarly, any bilayer defects that may be introduced from the altered shapes of the annular phospholipids must also be compensated by conformational changes in phospholipids beyond the first shell. Therefore an intrinsic characteristic and/or extrinsic agent that hinders phospholipid motional freedom will reduce the overall bilayer capacitance for accomodating cyt  $b_5$ .

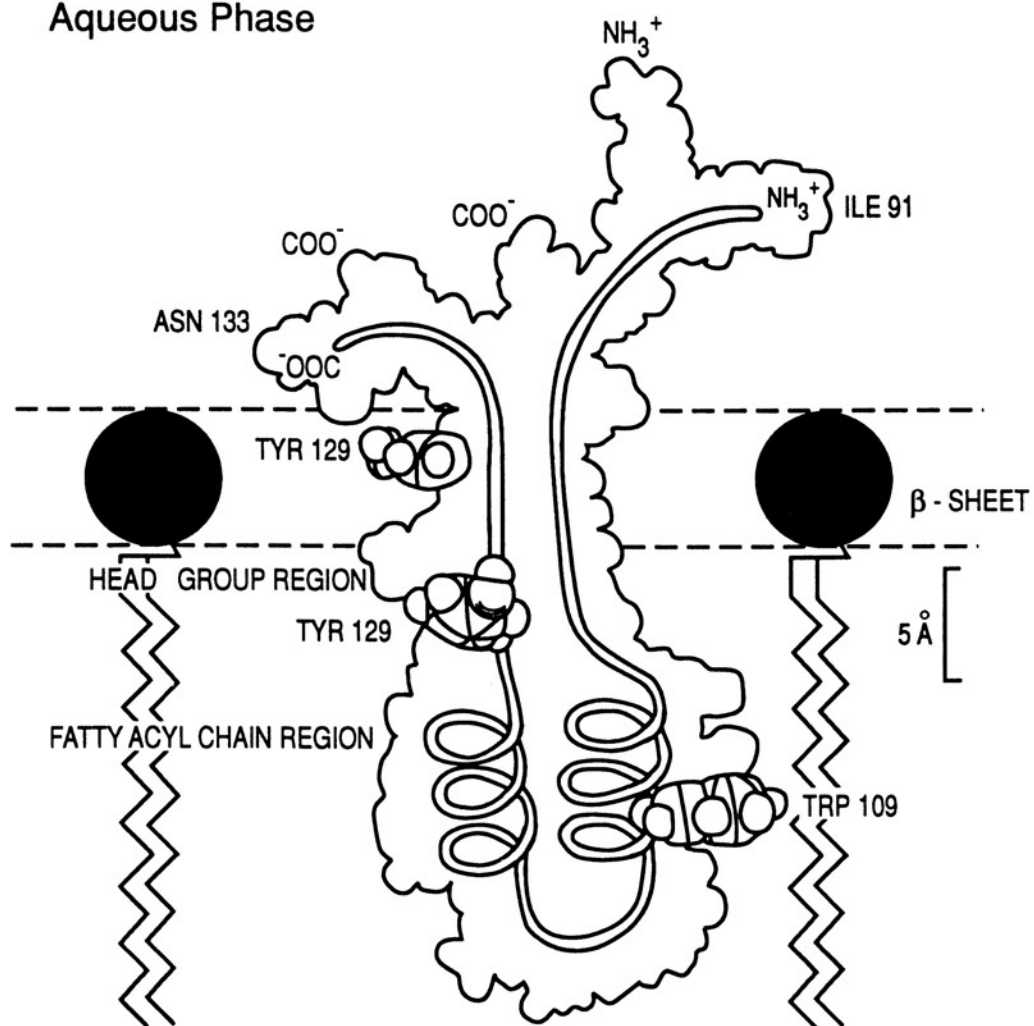
With cholesterol-free liposomes, bilayer curvature significantly affects the overall amount of cyt  $b_5$  that can bind per unit of surface area. The cyt  $b_5$ :PL ratios at the liposome saturation points are as much as 7 fold greater in an SUV than an LUV. Some representative examples for the spacing of cyt  $b_5$  molecules on liposome surfaces are considered to demonstrate the significance of curvature effects on cyt  $b_5$  binding. For most of the cholesterol-free SUVs the average saturation level of binding was found to be approximately 56 cyt  $b_5$ :1000 PL, or about 18 PC per cyt  $b_5$ . TNBS-labelling of selected liposome preparations showed that approximately

Figure 72.

Structure of the cytochrome  $b_5$  membrane binding domain in a bilayer. The outline is a profile of the CPK space-filling model. The topology of the cyt  $b_5$  tail is based upon the membrane inserted configuration that has been previously proposed by Strittmatter and Dailey (1982).



## Aqueous Phase



62% of the total phospholipid (out:in = 1.6) is located in the exterior monolayers, so that a binding site for a cyt  $b_5$  molecule actually consists of 11 phospholipids. These experimental results are consistent with the assumptions for the binding lattice model on an SUV. Using the molecular areas of the individual phosphatidylcholines (Jain, 1988f) and the simplifying assumption that the radius for a perfectly spherical, cyt  $b_5$  catalytic domain is 14.6 Å (Visser *et al.*, 1975), the distances among cyt  $b_5$  molecules on the surface of an SUV vary from only about 2-11 Å (Figure 73). As shown, at the saturation level of an SUV, bound cyt  $b_5$  molecules are so congested that there is no area for any additional protein. The rather close proximities of cyt  $b_5$  molecules are consistent with the  $\eta$  values that indicate anticooperativity from curve-fitting routine. In contrast, the distances among cyt  $b_5$  molecules are significantly greater in a saturated LUV: cyt  $b_5$  molecules are separated by distances extending from 20 Å (PLPC, egg PC) to as much as 45 Å (POPC) in cholesterol-free LUVs (Figure 73). Even at the saturation level of LUVs, these liposomes appear to have sufficient capacity for additional cyt  $b_5$  interaction. Unlike SUVs, with LUVs a considerable amount of the overall liposome surface area remains excluded from participating in cyt  $b_5$  binding.

These observed results with different liposomes may be explained in terms of the phospholipid motional freedom model that has been suggested herein. The profound surface curvature of SUVs results in a strained packing of phospholipid molecules. Because phospholipids are unable to align parallel with each other, their considerable motional freedom permits cyt  $b_5$  to readily partition into the bilayer. In contrast, phospholipids are more restricted in LUVs to undergo conformational

**Figure 73.**

**Proximity of cytochrome  $b_5$  molecules in LUVs and SUVs. (A) SUVs, (B) LUVs (PLPC, egg PC), and (C) LUVs (POPC).**

## Proximity of Cytochrome $b_5$ Molecules in Liposomes

Scale

1.5 cm = 20Å

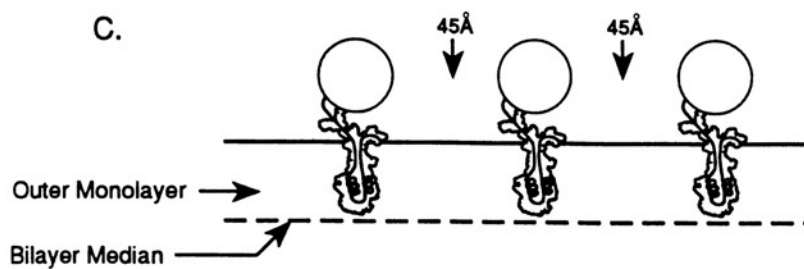
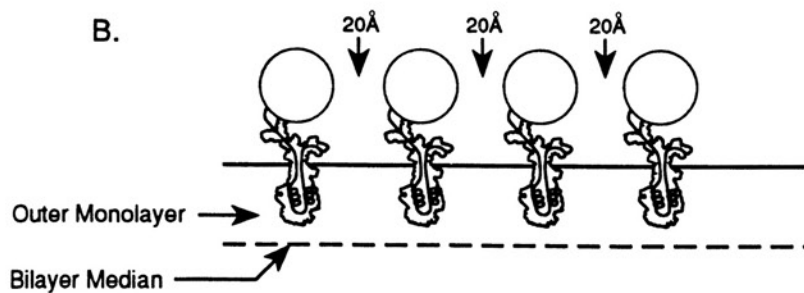
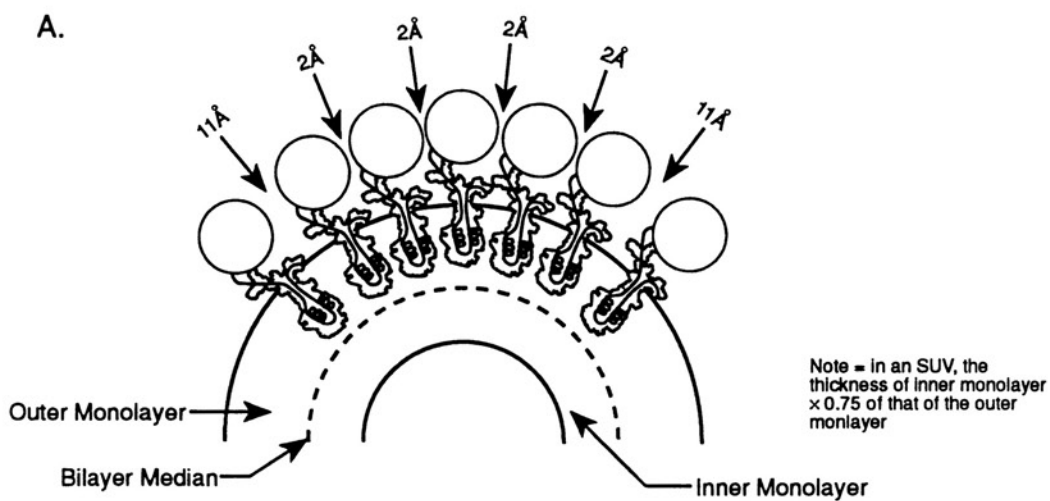
Cytochrome  $b_5$

Tail 20Å → 1 cm

Hydrophilic Domain 29.2Å → 1.5 cm

SUV

Diameter = 200Å → ~ 10 cm



changes because of the effective intermolecular packing. Because fewer phospholipids in LUVs cannot accommodate the irregular shape of the tail, cyt  $b_5$  molecules require more surface area for binding. However, the restrictions of phospholipid motional freedom in LUVs may be offset by unsaturation in the fatty acyl chains. As noted previously, double bonds disrupt cooperative interactions among phospholipid molecules and lower the free energy of adjacent *trans-gauche* isomerizations from +3.5 to +2 Kcal mole<sup>-1</sup> (Huang, 1977). Therefore, highly unsaturated phospholipids should more readily adopt complimentary configurations to the irregular shape of the cyt  $b_5$  membrane binding domain. Accordingly, the required surface area per cyt  $b_5$  molecule is less in LUVs prepared from more unsaturated phospholipids such as egg PC and PLPC (Figure 73, Panel B) than in LUVs that are composed of POPC (Figure 73, Panel C).

Similar to the differences in the cyt  $b_5$  saturation levels among various liposomes, the greater affinity that cyt  $b_5$  exhibits for cholesterol-free SUVs that are prepared from natural PC mixtures relative to the affinity for SUVs of a single synthetic PC are also consistent with the annular phospholipid model. Cyt  $b_5$  essentially binds irreversibly to egg PC, liver PC, and PC/SPH (1:1) SUVs because these natural mixtures have a diversified composition of phospholipid fatty acyl chains from which to form a stable, complimentary protein annulus while simultaneously maintaining bilayer integrity. In contrast, the number of possible configurations in SUVs that only have a single phospholipid component are very limited. As a result, forming a stable interaction between a cyt  $b_5$  molecule and the bilayer becomes increasingly difficult.

The extent of cyt  $b_5$  binding to a liposome appears to be directly

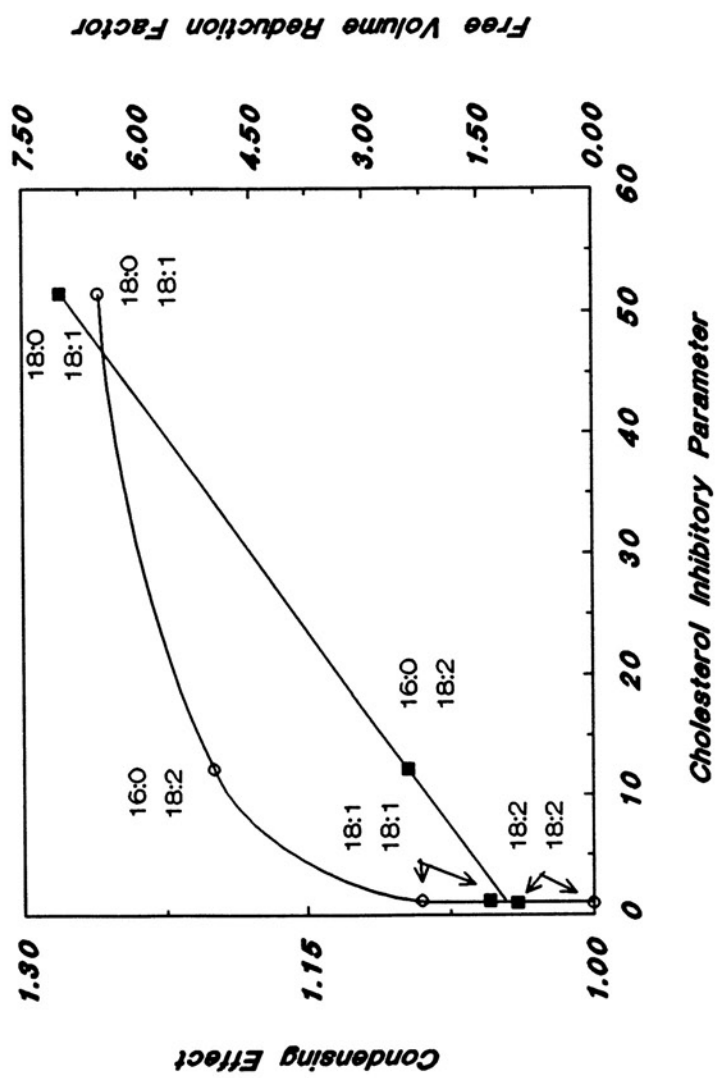
related to the ability of phospholipids to adapt into geometries that compliment the asymmetrically shaped membrane anchoring tail. Therefore, cholesterol probably inhibits cyt  $b_5$  from binding to liposomes by restricting the motional freedom of phospholipids. In terms of overall cyt  $b_5$  per total surface area, the solubility of cyt  $b_5$  in a bilayer containing cholesterol is always reduced relative to a bilayer of pure phospholipid. However, the extent of cyt  $b_5$  binding inhibition depends upon the effective lateral interaction of cholesterol with phospholipids.

The effect of cholesterol on reducing the cyt  $b_5$  saturation levels of preformed liposomes is more pronounced in LUVs than in SUVs. Due to the significant curvature of SUVs, poor alignment between cholesterol and phospholipids results in a rather ineffective restriction of the phospholipid motional freedom. Accordingly, cholesterol has only a slight inhibitory effect on cyt  $b_5$  binding to SUVs. In contrast, LUVs do not have any curvature induced strain so that cholesterol effectively aligns parallel with phospholipids. As a result, the restricted segmental motion of phospholipids causes a more definitive extent of cyt  $b_5$  binding inhibition.

The concept that the inhibitory effect is a manifestation of synergistic interactions between cholesterol and phospholipids is additionally supported by the observation that the extent of reduction in cyt  $b_5$  binding depends upon phospholipid type. With the exception of DMPC, unsaturation in the phospholipid fatty acyl chains tends to decrease the cholesterol-mediated inhibition in preformed liposomes in a manner that correlates with the condensing effect (Figure 74) (Demel *et al.*, 1967; Demel *et al.*, 1972b). As indicated by the deviations from ideal molecular

Figure 74.

Correlation of cholesterol-mediated inhibition of cyt  $b_5$  binding to LUVs with the Condensing Effect and Free Volume. The data for the condensing effect (O) and free volume reduction factor (■) has been adapted from Demel *et al.*, 1967 and Demel *et al.*, 1972b. Data for relative cyt  $b_5$  binding inhibition has been taken from Table II.





areas, cholesterol most effectively interacts with mixed-chain monoenoic (*sn*-2  $\Delta 9$ ) and dienoic (*sn*-2  $\Delta 9,12$ ) phospholipids. Accordingly, cholesterol has the most pronounced inhibitory effect on cyt  $b_5$  binding to liposomes that are prepared from these phospholipids. In contrast, the condensing effect shows that cholesterol interacts less favorably with the di-unsaturated phospholipids (DOPC and DLPC). Although cholesterol reduces the amount of cyt  $b_5$  binding per unit surface area to liposomes prepared from DOPC and DLPC, the extent of inhibition is significantly less than what is observed with the condensible phospholipids.

The extent of cyt  $b_5$  binding inhibition depends upon the effective interaction of cholesterol with phospholipids. But the reduction in phospholipid surface areas actually originates from cholesterol occupying (i.e. decreasing) the available bilayer free volume (Straume and Litman, 1987; Almeida *et al.*, 1992). A decrease in free volume restricts the motional freedom of phospholipids. Among various phospholipids, relative free volume reductions may be compared in terms of the factor,  $\Delta f_v$ :

$$\Delta f_v = \left( \frac{A_{ideal} - A_{min}}{A_{obs} - A_{min}} \right)$$

where  $A_{ideal}$  is the ideal mean molecular area based upon the additivity rule,  $A_{obs}$  is the actually observed mean molecular area, and  $A_{min}$  is the minimum area of the specific phospholipid. Figure 74 indicates a linear correlation between the  $f_v$  and the cholesterol inhibitory parameter  $\phi$ . The extent of cyt  $b_5$  binding inhibition is consistent with the cholesterol-mediated reduction in free volume, which corresponds to restrictions in the motional freedom of phospholipids.

In addition to the cholesterol-related reduction in cyt  $b_5$  saturation

levels of PC liposomes, the decrease in the overall equilibrium of bound to unbound cyt  $b_5$  is similarly consistent with the proposal that cholesterol causes phospholipid bilayers to be less effective solvents for intrinsic proteins. Any mismatch between the cyt  $b_5$  surface and an annulus with motionally restricted phospholipids results in reduced binding affinity for the membrane.

Although cholesterol inhibits cyt  $b_5$  binding to phosphatidylcholine liposomes, the triphasic reduction of the cyt  $b_5$  saturation levels in POPC LUVs (Figure 51) indicates that the inhibitory effect is a complex function of cholesterol composition. While the saturation curve does not explicitly delineate the cholesterol inhibitory effect, the inflection points do suggest cholesterol-associated events at 20 and 33 mole percent cholesterol. Comparison of the relative cyt  $b_5$  binding to POPC LUVs containing cholesterol (Figure 52) reveals that the cyt  $b_5$  saturation levels of POPC LUVs from 0-20 mole percent cholesterol is reduced by only a factor of 3.6. Likewise, there is also a modest 1.4-fold decrease in cyt  $b_5$  binding to POPC LUVs between 20-33% cholesterol. The most significant reduction in relative cyt  $b_5$  binding per mole cholesterol occurs between 33 and 50 mole percent cholesterol, where the cyt  $b_5$  saturation level of the liposomes decreases 17-fold.

The analysis of binding data indicates that the relative cyt  $b_5$  binding equilibrium with POPC LUVs remains essentially unaffected within a compositional range of 0-40 mole percent cholesterol. Therefore, at cholesterol compositions less than 50 mole percent, the inhibition of cyt  $b_5$  binding likely is a manifestation of a cholesterol-mediated reduction in the number of available interactive sites (or phospholipids that have

sufficient motional freedom) on the liposome surface. If so, then only at 1:1 phospholipid/cholesterol compositions should cholesterol reduce the overall cyt  $b_5$  binding equilibrium, when phospholipids are maximally restricted in their motional freedom.

The effect of cholesterol on cyt  $b_5$  interaction with POPC LUVs becomes additionally complicated because, while inhibiting partitioning into the bilayer matrix, cholesterol simultaneously can facilitate cyt  $b_5$  tight insertion. The maximum rate of cyt  $b_5$  tight insertion occurs in POPC LUVs with a cholesterol composition of 20-25 mole percent. Accordingly, it seems unclear why the cyt  $b_5$  binding equilibrium remains essentially constant while the tight insertion rate changes. As previously noted, the measured binding equilibrium is a complex constant of several independent reactions. With LUVs, the conversion from loose to tight binding probably affects the overall measured binding equilibrium constant so that any differences in the actual affinity of cyt  $b_5$  monomers for the liposomes are not readily apparent. However, since the cyt  $b_5$  tight insertion rates for both POPC LUVs with 0% and 40% cholesterol (approximately 12-15% tight insertion within 2 h) are comparable, the original interpretation that cholesterol does not reduce the affinity of cyt  $b_5$  for POPC LUVs within the compositional range of 0-40 mole percent still seems valid.

The kinetics indicate that tight insertion most likely results from a permanently destabilized state of the vesicle, as opposed to a transient bilayer destabilization upon the initial interaction of cyt  $b_5$  with the liposome. To be the result of a transient bilayer destabilization, tight insertion should be at least a time-independent process. In other words, the extent of cyt  $b_5$  tight insertion into a liposome with a given

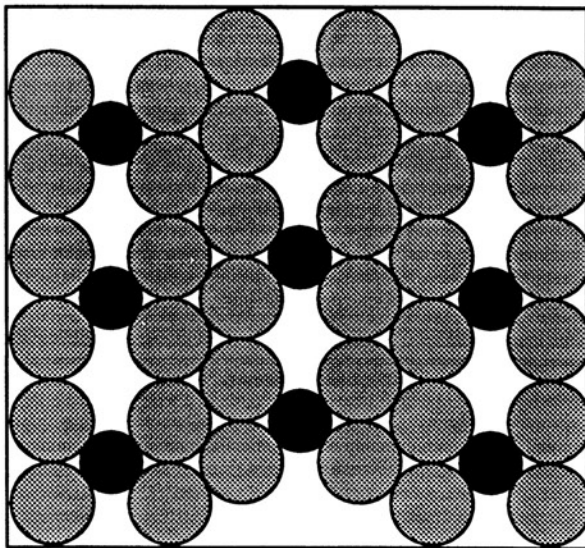
cholesterol composition must be the same at 2 and 24 h. However, the kinetics show that tight insertion is a time-dependent process.

Cholesterol accelerates the rate at which bound cyt  $b_5$  is converted from the "loose" to the "tight" configuration. The slow phase rate constant increases from  $k \approx 1 \times 10^{-2} \text{ h}^{-1}$  at 0% cholesterol to a maximum of  $k \approx 1 \times 10^{-1} \text{ h}^{-1}$  at 20-25%, suggesting that the liposomes are in a permanently destabilized state.

The complex effect of cholesterol on inhibiting cyt  $b_5$  binding while simultaneously accelerating the rate of tight insertion may be understood in terms of the physico-chemical model that has been proposed for cholesterol organization in liquid-crystalline POPC liposomes. The "ordered bimolecular mesomorphic lattice" model, which is based upon steady-state fluorescence depolarization in 1:1 cholesterol/POPC bilayers, proposes that in liquid-crystalline bilayers infrequent cholesterol-cholesterol contacts require that each cholesterol molecule has four phospholipid molecules as nearest-neighbors (Hyslop *et al.*, 1990). According to these constraints, the model indicates that: (1) each phospholipid contacts 1 cholesterol molecule at 20 mole percent cholesterol (Figure 75); (2) there are 2 cholesterol contacts per phospholipid at 33% cholesterol (Figure 76); and (3) at 50% cholesterol each phospholipid contacts 4 cholesterol molecules (Figure 77). The model suggests that cholesterol decreases phospholipid-phospholipid interactions by inducing the formation of 4:1 phospholipid-cholesterol clusters. However, at 20 mole percent cholesterol (Figure 75), these 4:1 assemblies do not interact as effectively as pure phospholipids and therefore may disrupt lateral packing in the bilayer. As the bilayer cholesterol

Figure 75.

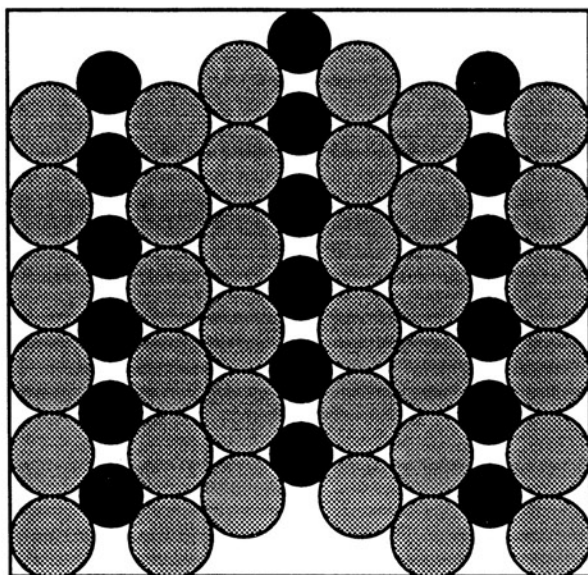
"Bimolecular mesomorphic lattice" model at 20 mole percent cholesterol. The ratio of phospholipids (gray circles) and cholesterol (filled circles) is 4:1. Each phospholipid has 1 cholesterol contact. Cholesterol molecules have 4 phospholipid as nearest neighbors. [Adapted from Hyslop *et al.*, 1990.]



20% cholesterol:  
1 cholesterol contact/PC

Figure 76.

"Bimolecular mesomorphic lattice" model at 33 mole percent cholesterol. The ratio of phospholipids (gray circles) and cholesterol (filled circles) is 2:1. Each phospholipid has 2 cholesterol contacts. Cholesterol molecules have 4 phospholipid as nearest neighbors. [Adapted from Hyslop *et al.*, 1990.]

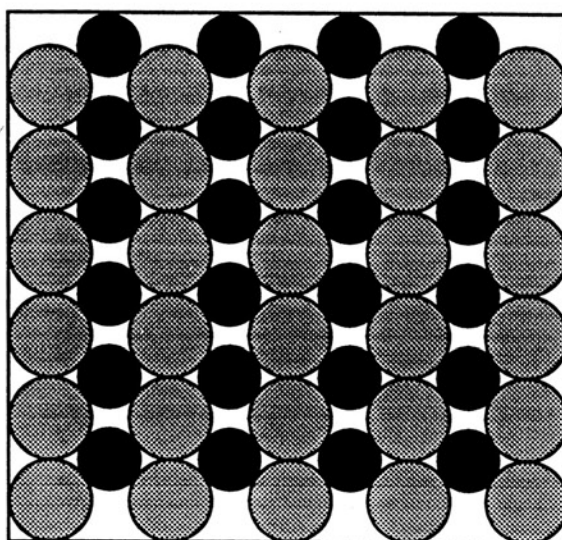


33% cholesterol:  
2 cholesterol contacts/PC



Figure 77.

"Bimolecular mesomorphic lattice" model at 50 mole percent cholesterol. The ratio of phospholipids (gray circles) and cholesterol (filled circles) is 1:1. Each phospholipid has 4 cholesterol contacts. Cholesterol molecules have 4 phospholipid as nearest neighbors. [From Hyslop *et al.*, 1990.]



50% cholesterol:  
4 cholesterol contacts/PC

concentration increases beyond 20 mole percent, cholesterol initially "fills" the defective packing areas, but does not reduce the number of phospholipid-phospholipid contacts up to 33 mole percent. The amount of phospholipid-phospholipid interactions then continues to decrease from 33 to 50 mole percent cholesterol. Additionally, the model indicates that no cholesterol-phase inhomogeneity occurs in the bilayer. This particular model can be used to account for cyt  $b_5$  interactions with cholesterol containing POPC LUVs, as follows.

The cholesterol-mediated reduction in the saturation level of POPC LUVs indicates that cyt  $b_5$  probably requires a pure phospholipid annulus to partition into POPC LUVs, and therefore the extent of cyt  $b_5$  binding is proportional to the number of phospholipid-phospholipid contacts. The "inflection" points in the cyt  $b_5$  saturation curve at 20 and 33 mole percent cholesterol relate to the number of phospholipid-cholesterol contacts as the liposome cholesterol content increases.

The initial decrease in cyt  $b_5$  binding to POPC LUVs from 0 to 20 mole percent cholesterol corresponds with the increased number of individual phospholipids that contact cholesterol. Liposomes consisting of 20 mole percent cholesterol have only 25% of the phospholipid-phospholipid contacts of liposomes without cholesterol. The 3.6-fold difference in the cyt  $b_5$  saturation level of the liposomes is consistent with cholesterol reducing the number of binding sites (i.e. phospholipid-phospholipid contacts) by a factor of 4 between 0 and 20 mole percent.

In contrast to the distinct inhibition of cyt  $b_5$  binding that occurs at less than 20 mole percent cholesterol, the plateau region of the saturation curve indicates a relatively nominal decrease in the saturation

level of POPC LUVs with increasing cholesterol content. Within the composition range of 20-33 mole percent cholesterol, the saturation limit of the liposomes is only reduced an additional 1.4-fold. This minimal inhibitory effect on cyt  $b_5$  partitioning binding correlates with the quantity of phospholipid-phospholipid contacts remaining unaffected by further increase in cholesterol content. According to the model, cholesterol does not decrease these interactions, but instead it may improve the lateral packing among the 4:1 clusters (Figures 75 and 76).

The most significant inhibition of cyt  $b_5$  binding occurs at 33-50 mole percent cholesterol. Within this composition range, phospholipid-phospholipid contacts must again be disrupted to accommodate any additional bilayer cholesterol. The increased amount of phospholipid-cholesterol contacts corresponds to the significant additional 17-fold reduction in cyt  $b_5$  binding to POPC LUVs. As Figures 76 and 77 indicate, each additional cholesterol molecule disrupts 2 additional phospholipid-phospholipid contacts at compositions greater than 33 mole percent. But individual phospholipids that contact 4 cholesterol molecules are probably totally excluded from forming a cyt  $b_5$  annulus as the extremely low saturation level of 1:1 POPC/cholesterol LUVs (1 cyt  $b_5$ :10,000 POPC) indicates. If so, then the most significant inhibitory effect on cyt  $b_5$  binding occurs at compositions above 33 mole percent cholesterol because, on a *per mole* basis, a cholesterol molecule completely restricts 4 POPC molecules from interacting with cyt  $b_5$ . Since cholesterol requires an annulus of 4 phospholipids, it probably inhibits cyt  $b_5$  binding by "competing" for available phospholipids. However, a phospholipid is only completely removed from possible interaction with cyt  $b_5$  only if itself contacts 4

cholesterol molecules.

Although cholesterol apparently inhibits cyt  $b_5$  from partitioning into POPC LUVs by restricting phospholipids from forming favorable interactive sites, it can facilitate tight insertion because certain binding sites may have intrinsic defects. As previously determined in this investigation, a minimum of approximately 11 phospholipid molecules comprise a cyt  $b_5$  annulus. In liposomes without cholesterol, the phospholipids have optimal entropy to readily assume configurations that compliment the structure of cyt  $b_5$ . As a result, the phospholipids can form a rather stable annulus around the protein. In the presence of cholesterol, however, phospholipids are restricted in their sequential motion (Stockton and Smith, 1976; McIntosh, 1978; Scott and Kalaskar, 1989). Consequently, the nearest neighbor phospholipid molecules that contact cholesterol in the 4:1 clusters have reduced flexibility to match protein conformation. As indicated from the cyt  $b_5$  saturation curve, instead of forming a protein annulus with individual phospholipid subunits, cyt  $b_5$  binding sites must be formed from the 4:1 phospholipid/cholesterol clusters. The 4-fold reduction in cyt  $b_5$  binding at a 4:1 POPC/cholesterol ratio is consistent with binding sites that require a 4-fold increase in the number of phospholipids. However, the 4:1 phospholipid/cholesterol clusters cannot adapt to the irregular shape of the protein because of the restricted motional freedom. Hence, annular sites formed with 4:1 clusters probably have defective lipid packing. As a result, these destabilized sites facilitate tight insertion of cyt  $b_5$ .

The formation of 4:1 phospholipid/cholesterol complexes can account for the kinetics of tight insertion as a function of cholesterol

concentration. As the cholesterol content of an LUV increases from 0 to 20 mole percent, the quantity of the 4:1 clusters, and therefore the number of destabilized annuli, increases. An increase in the number of destabilized annuli corresponds with the increase in rate of cyt  $b_5$  tight insertion. However, this assumption does not distinguish whether a destabilized annulus consists solely of 4:1 complexes, or a mixture of unrestricted phospholipid molecules and phospholipid/cholesterol clusters at liposome compositions that are less than 20 mole percent cholesterol. In either instance, a 4:1 cluster in an annulus may introduce sufficient packing deficiencies that promote tight insertion. At approximately 20 mole percent, the maximum rate of cyt  $b_5$  tight insertion is consistent with a maximum amount of destabilized sites; annuli can only be formed from the 4:1 phospholipid/cholesterol clusters at 20 mole percent cholesterol. At cholesterol compositions greater than 20-25 mole percent, cyt  $b_5$  tight insertion decreases because cholesterol improves the lateral packing of the 4:1 complexes. The restriction of the 4:1 cluster re-orientational movement reduces the frequency of forming destabilized annuli.

In summary, the studies herein signify the effects of cholesterol on cyt  $b_5$  partitioning into phosphatidylcholine bilayers. Cholesterol predominantly reduces the cyt  $b_5$  saturation level of liposomes. However, the extent of binding inhibition depends upon effective interactions between cholesterol and phospholipids. Phospholipid unsaturation, bilayer curvature, and the relative cholesterol/phospholipid mole ratios affect the lateral packing of cholesterol and phospholipid molecules in a manner which correlates with reductions in bilayer free volume. Essentially, cholesterol reduces the solvent efficacy of phosphatidylcholine bilayers

for cyt  $b_5$  by restricting phospholipid motional freedom. At relatively low concentrations, cholesterol facilitates cyt  $b_5$  tight insertion because its partial restriction of phospholipids may actually introduce defects into the bilayer.

In conclusion, cyt  $b_5$  has reduced solubility in preformed liposomes that contain a mixture of phospholipids and cholesterol because phospholipids cannot form a complimentary annulus. As a result, cyt  $b_5$  preferentially partitions into pure phospholipid bilayers. The results of this investigation may signify an important function of cholesterol for lipid-protein interactions in biological membranes. If cyt  $b_5$  is an archetypical intrinsic membrane protein, then other membrane associated proteins may similarly prefer a pure phospholipid milieu rather than a mixture of phospholipids and cholesterol. Therefore, as a membrane component cholesterol may be an important determinant of the overall protein/lipid composition in biological membranes. Additionally, cholesterol may function as a regulatory mechanism for the lateral distribution of intrinsic proteins within biological membranes. Further studies with other integral membrane proteins and more complex lipid systems will be required to further characterize if cholesterol modulates these effects.

## REFERENCES

- Almeida, P. F. F., Vaz, W. L. C., and Thompson, T. E., (1992) *Biochemistry*, 31, 6739-6747.
- Anderson, D. J., Mostov, K. E., and Blobel, G., (1983) *Proceedings of the National Academy of Sciences, U. S. A.*, 80, 7249-7253.
- Arinc, E., Rzepecki, L. M., and Strittmatter, P., (1987) *Journal of Biological Chemistry*, 262, 15563-15567.
- Ayanoglu, E., Chiche, B. H., Beatty, M., Djerassi, C., and Düzgünes, N., (1990) *Biochemistry*, 29, 3466-3471.
- Barenholz, Y., Gibbes, D., Litman, B. J., Goll, J., Thompson, T. E., and Carlson, F. D., (1977) *Biochemistry*, 16, 2806-2810.
- Bartlett, G. R., (1959) *Journal of Biological Chemistry*, 234, 466-468.
- Bendzko, P., Prehn, S., Pfeil, W., and Rapoport, T., (1982) *European Journal of Biochemistry*, 123, 121-126.
- Bloch, K. (1976) in *Reflections on Biochemistry*, Kornberg, A., Horecker, B. L., Cornudella, L., and Oró, J., Pergamon Press, Oxford, pp. 143-150.
- Blok, M. C., Van Deenen, L. L. M., and De Gier, J., (1977) *Biochimica et Biophysica Acta*, 464, 509-518.
- Calabro, M. A., Katz, J. T., and Holloway, P. W., (1976) *Journal of Biological Chemistry*, 251, 2113-2118.
- Calhoun, W. I. and Shipley, G. G., (1979) *Biochemistry*, 18, 1717-1722.
- Chatterjee, N. and Brockerhoff, H., (1978) *Biochimica et Biophysica Acta*, 511, 116-119.
- Cherry, R. J., Müller, U., Holenstein, C., and Heyn, M. P., (1980) *Biochimica et Biophysica Acta*, 596, 145-151.
- Christiansen, K. and Carlsen, J., (1986) *Biochimica et Biophysica Acta*, 860, 503-509.
- Copeland, B. R. and McConnell, H. M., (1980) *Biochimica et Biophysica Acta*, 599, 95-109.
- Davis, P. J. and Keough, K. M. W., (1983) *Biochemistry*, 22, 6334-6340.
- De Kruyff, B., Demel, R. A., Slotboom, A. J., Van Deenen, L. L. M., and Rosenthal, A. F., (1973) *Biochimica et Biophysica Acta*, 307, 1-19.



- De Kruyff, Van Dijck, P. W. M., Demel, R. A., Schuijff, A., Brants, F., and Van Deenen, L. L. M., (1974) *Biochimica et Biophysica Acta*, **356**, 1-7.
- Demel, R. A., Van Deenen, L. L. M., and Pethica, B. A., (1967) *Biochimica et Biophysica Acta*, **135**, 11-19.
- Demel, R. A., Bruckdorfer, K. R., and Van Deenen, L. L. M., (1972a) *Biochimica et Biophysica Acta*, **255**, 321-330.
- Demel, R. A., Geurts Van Kessel, W. S. M., and Van Deenen, L. L. M., (1972b) *Biochimica et Biophysica Acta*, **266**, 26-40.
- Demel, R. A., Jansen, J. W. C. M., Van Dijck, P. W. M., and Van Deenen, L. L. M., (1977) *Biochimica et Biophysica Acta*, **465**, 1-10.
- Dufourcq, J., Bernon, R., and Lussan, C., (1974) *Académie de Science, Series D*, **278**, 2565-2568.
- Dufourcq, J., Faucon, J. F., Lussan, C., and Bernon, R., (1975) *FEBS Letters*, **57**, 112-116.
- Düzgünes, N., Wilschut, J., Hong, K., Fraley, R., Perry, C., Friend, D. S., James, T. L., and Papahadjopoulos, D., (1983) *Biochimica et Biophysica Acta*, **732**, 289-299.
- El-Sayed, M. Y., Guion, T. A., and Fayer, M. D., (1986) *Biochemistry*, **25**, 4825-4832.
- Engelman, D. M. and Rothman, J. E., (1972) *Journal of Biological Chemistry*, **247**, 3694-3697.
- Enoch, H. G., Fleming, P. J., and Strittmatter, P., (1979) *Journal of Biological Chemistry*, **254**, 6483-6488.
- Enomoto, K. and Sato, R., (1973) *Biochemical and Biophysical Research Communications*, **51**, 1-7.
- Enomoto, K. and Sato, R., (1977) *Biochimica et Biophysica Acta*, **466**, 136-147.
- Estep, T. N., Mountcastle, D. B., Biltonen, R. L., and Thompson, T. E., (1978) *Biochemistry*, **17**, 1984-1989.
- Gennis, R. B., (1989a) *Biomembranes Molecular Structure and Function*, pp. 20-23, Springer-Verlag, New York.
- Gennis, R. B., (1989b) *Biomembranes Molecular Structure and Function*, p. 31, Springer-Verlag, New York.
- Gennis, R. B., (1989c) *Biomembranes Molecular Structure and Function*, pp. 48-49, Springer-Verlag, New York.

- George, S. K., Najera, L., Countryman, C., Sandoval, R. P., Benson, L., and Ihler, G. M., (1989a) *Biochemical Society Transactions*, 17, 545-546.
- George, S. K., Najera, L., Sandoval, R. P., Countryman, C., Davis, R. W., and Ihler, G. M., (1989b) *Journal of Bacteriology*, 171, 4569-4576.
- George, S. K., Najera, L., Sandoval, R., and Ihler, G. M., (1990) *Biochimica et Biophysica Acta*, 1061, 26-32.
- Gogol, E. P. and Engelman, D. M., (1984) *Biophysical Journal*, 46, 491-495.
- Greenhut, S. F. and Roseman, M. A., (1985) *Biochemistry*, 24, 1252-1260.
- Greenhut, S. F., Bourgeois, V. R., and Roseman, M. A., (1986) *Journal of Biological Chemistry*, 261, 3670-3675.
- Greenhut, S. F., Taylor, K. M. P., and Roseman, M. A., (1993) *Biochimica et Biophysica Acta*, 1149, 1-9.
- Hochli, (1980) *Federation Proceedings*, 39, 1632.
- Holloway, P. W., and Katz, J. T., (1975) *Journal of Biological Chemistry*, 250, 9002-9007.
- Huang, C.-H., (1977) *Lipids*, 12, 348-356.
- Humphries, G. M. K., and Lovejoy, J. P., (1983) *Biophysical Journal*, 42, 307-310.
- Hyslop, P. A., Morel, B., and Sauerheber, R. D., (1990) *Biochemistry*, 29, 1025-1038.
- Jain, M. K., (1988a) *Introduction to Biological Membranes*, 2ed., p. 29, John Wiley & Sons, Inc., New York.
- Jain, M. K., (1988b) *Introduction to Biological Membranes*, 2ed., pp. 29-30, John Wiley & Sons, Inc., New York.
- Jain, M. K., (1988c) *Introduction to Biological Membranes*, 2ed., p. 141, John Wiley & Sons, Inc., New York.
- Jain, M. K., (1988d) *Introduction to Biological Membranes*, 2ed., p. 7, John Wiley & Sons, Inc., New York.
- Jain, M. K., (1988e) *Introduction to Biological Membranes*, 2ed., p. 144, John Wiley & Sons, Inc., New York.
- Jain, M. K., (1988f) *Introduction to Biological Membranes*, 2ed., p. 64, John Wiley & Sons, Inc., New York.
- Jain, M. K. and Zakim, D., (1987) *Biochimica et Biophysica Acta*, 906, 33-68.

- Johannsson, A., Keightley, C. A., Smith, G. A., and Metcalfe, J. C., (1981) *Biochemistry Journal*, 196, 505-511.
- Kariel, N., Davidson, E., and Keough, K. M. W., (1991) *Biochimica et Biophysica Acta*, 1062, 70-76.
- Keough, K. M. W., Giffin, B., and Matthews, P. L. J. (1989) *Biochimica et Biophysica Acta*, 983, 51-55.
- Kleinfeld, A. M. and Lukacovic, M. F., (1985) *Biochemistry*, 24, 1883-1890.
- Ladbrooke, B. D., Williams, R. M., and Chapman, D., (1968) *Biochimica et Biophysica Acta*, 150, 333-340.
- Leto, T. L., and Holloway, P. W., (1979) *Journal of Biological Chemistry*, 254, 5015-5019.
- Lichtenberg, D. and Barenholz, Y. (1988) *Methods of Biochemical Analysis*, 33, 337-462.
- Mabrey, S., Mateo, P. L., and Sturtevant, J. M., (1978) *Biochemistry*, 17, 2464-2468.
- Madden, T. D., King, M. D., and Quinn, P. J., (1979) *Nature*, 279, 538-541.
- Madden, T. D., King, M. D., and Quinn, P. J., (1981) *Biochimica et Biophysica Acta*, 641, 265-269.
- Mathews, F. S., Argos, P., and Levine, M., (1971) *Cold Spring Harbor Symposium on Quantitative Biology*, 35, 387-395.
- Mathews, F. S., Levine, M., and Argos, P., (1972) *Journal of Molecular Biology*, 64, 449-464.
- McIntosh, T. J., (1978) *Biochimica et Biophysica Acta*, 513, 43-58.
- Melchior, D. L., Scavitto, F. J., and Steim, J. M., (1980) *Biochemistry*, 19, 4828-4834.
- Merk Index, 10<sup>th</sup> Edition, (1983), M. Windholz, Editor, pp. 480 & 611, Merk and Company, Incorporated, Rahway, New Jersey.
- Michelangeli, F., East, J. M., and Lee, A. G., (1990) *Biochimica et Biophysica Acta*, 1025, 99-108.
- Mitchell, D. C., Straume, M., Miller, J. L., and Litman, B. J., (1990) *Biochemistry*, 29, 9143-9149.
- Okada, Y., Sabatini, D. D., and Kreibich, G., (1979) *Journal of Cell Biology*, 83, 437a.

- Ozols, J., (1989) *Biochimica et Biophysica Acta*, **997**, 121-130.
- Papahadjopoulos, D., Nir, S., and Ohki, S., (1971) *Biochimica et Biophysica Acta*, **266**, 561-583.
- Poensgen, J., and Ullrich, V., (1980) *Biochimica et Biophysica Acta*, **596**, 248-263.
- Presti, F. T., Pace, R. J., and Chan, S. I., (1982) *Biochemistry*, **21**, 3831-3835.
- Rachubinski, R. A., Verma, D. P. S., and Bergeron, J. J. M., (1978) *Journal of Cell Biology*, 362a.
- Reid, L. S., Lim, A. R., and Mauk, A. G., (1986) *Journal of the American Chemical Society*, **108**, 8197-8201.
- Reid, L. S., Mauk, M. R., and Mauk, A. G., (1984) *Journal of the American Chemical Society*, **106**, 2182-2185.
- Remacle, J., (1978) *Journal of Cell Biology*, **79**, 291-313.
- Rogers, M. J. and Strittmatter, P., (1975) *Journal of Biological Chemistry*, **250**, 5713-5718.
- Roseman, M. A., Holloway, P. W., and Calabro, M. A., (1978) *Biochimica et Biophysica Acta*, **507**, 552-556.
- Roseman, M. A., Holloway, P. W., Calabro, M. A., and Thompson, T. E. (1977) *Journal of Biological Chemistry*, **252**, 4842-4849.
- Roseman, M. A., Litman, B. J., and Thompson, T. E., (1975) *Biochemistry*, **14**, 4826-4830.
- Rubenstein, J. L. R., Smith, B. A., and McConnell, H. M., (1979) *Proceedings of the National Academy of Sciences, USA*, **76**, 15-18.
- Sankaram, M. B. and Thompson, T. E., (1991) *Proceedings of the National Academy of Sciences, USA*, **88**, 8686-8690.
- Scott, H. L. and Kalaskar, S., (1989) *Biochemistry*, **28**, 3687-3691.
- Silvius, J. R., McMillen, D. A., Saley, N. D., Jost, P. C., and Griffith, O. H., (1984) *Biochemistry*, **23**, 538-547.
- Simmonds, A. C., East, J. M., Jones, O. T., Rooney, E. K., McWhirter, J., and Lee, A. G., (1982) *Biochimica et Biophysica Acta*, **693**, 398-406.
- Smith, L. M., Rubenstein, J. L. R., Parce, J. W., and McConnell, H. M., (1980) *Biochemistry*, **19**, 5907-5911.

- Spatz, L. and Strittmatter, P., (1971) *Proceedings of the National Academy of Sciences, USA*, **68**, 1042-1046.
- Stankowski, S., (1983a) *Biochimica et Biophysica Acta*, **735**, 341-351.
- Stankowski, S., (1983b) *Biochimica et Biophysica Acta*, **735**, 352-360.
- Stankowski, S., (1984) *Biochimica et Biophysica Acta*, **777**, 167-182.
- Stockton, G. W. and Smith, I. C. P., (1976) *Chemistry and Physics of Lipids*, **17**, 251-263.
- Straume, M. and Litman, B. J., (1987) *Biochemistry*, **26**, 5121-5126.
- Strittmatter, P., Rogers, M. J., and Spatz, L., (1972) *Journal of Biological Chemistry*, **247**, 7188-7194.
- Strittmatter, P. and Dailey, H. A., in *Membranes and Transport* (1982) Vol. 1 (A. N. Martinosi, Ed.), p. 71, Plenum Press, New York.
- Sullivan, M. R. and Holloway, P. W., (1974) *Biochemical and Biophysical Research Communications*, **54**, 808-815.
- Tajima, K. and Gershfeld, N. L., (1978) *Biophysical Journal*, **22**, 489-500.
- Tajima, S. and Sato, R., (1979) *Biochimica et Biophysica Acta*, **550**, 357-361.
- Takagaki, Y., Radhakrishnan, R., Gupta, C. M., and Khorana, H. G., (1983a) *Journal of Biological Chemistry*, **258**, 9128-9136.
- Takagaki, Y., Radhakrishnan, R., Writz, W. A., and Khorana, H. G., (1983b) *Journal of Biological Chemistry*, **258**, 9136-9142.
- Taylor, K. M. P. and Roseman, M. A., (1990) *Biophysical Journal*, **57**, 476a.
- Taylor, K. M. P. and Roseman, M. A., (1993) *Biophysical Journal*, **64**, A58.
- Taylor, R. P., Huang, C.-H., Broccoli, A. V., and Leake, L., (1977) *Archives of Biochemistry and Biophysics*, **183**, 83-89.
- Tennyson, J. and Holloway, P. W., (1986) *Journal of Biological Chemistry*, **261**, 14196-14200.
- Tsong, T. Y., (1975) *Biochemistry*, **14**, 5415-5417.
- van Blitterswijk, W. J., van der Meer, B. W., and Hilkmann, H., (1987) *Biochemistry*, **26**, 1746-1756.
- van Meer, G., (1989) *Annual Reviews in Cell Biology*, **5**, 247-275.

Visser, L., Robinson, N. C., and Tanford, C. (1975) *Biochemistry*, **14**, 1194-1199.

Vist, M. R. and Davis, J. H., (1990) *Biochemistry*, **29**, 451-464.

Warren, G. B., Houslay, M. D., Metcalfe, J. C., and Birdsall, N. J. M., (1975) *Nature*, **255**, 684

Wattenberg and Silbert, (1983) *Journal of Biological Chemistry*, **258**, 2284-

Worcester, D. L. and Franks, N. P., (1976) *Journal of Molecular Biology*, **100**, 359-378.

Yeagle, P. L., (1981) *Biochimica et Biophysica Acta*, **640**, 263-273.

Yeagle, P. L., (1984) *The Journal of Membrane Biology*, **78**, 201-210.

Yeagle, P. L., (1985) *Biochimica et Biophysica Acta*, **822**, 267-287.

Yeagle, P. L., Martin, R. B., Lala, A. K., Lin, H.-K., and Bloch, K., (1977) *Proceedings of the National Academy of Sciences, U. S. A.*, **74**, 4924-4926.

Zatz, J. L., (1974) *Journal of Pharmaceutical Sciences*, **63**, 858-861.